58p

(NASA TT F-8842)

[redacted]

WAR MINISTRY (AIR)
TECHNICAL AND INDUSTRIAL DIRECTION
FLIGHT TEST CENTER

Object of Study: Breguet 941

T Breguet 941 Identification, Performance, Flight Qualities

N66 38360 (ACCESSION NUMBER)
185 (PAGES)
(NASA CR OR TMX OR AD NUMBER)
(THRU) 1
(CODE) 09
(CATEGORY)
FACILITY FORM 602

Translation of: "Avion Breguet 941. Identification - Performances - Qualites de vol". Ministère des Armees (Air). Direction Technique et Industrielle. Centre d'Essais en Vol, Report No. 1, 1963

NATIONAL AERONAUTICS AND SPACE ADMINISTRATION,
WASHINGTON, D.C. March 1964 58p

NASA TT F-8842

[redacted]

Transl. into ENGLISH from Paris, Min. des Armees 1963

NASA TT F-8842

BREGUET 941. IDENTIFICATION, PERFORMANCE, FLIGHT QUALITIES

Translation of "Avion Bréguet 941. Identification, Performances, Qualités en vol"
Ministère des Armées, Paris,
Report No. 1, 1963

NATIONAL AERONAUTICS AND SPACE ADMINISTRATION
WASHINGTON SEPTEMBER 1966

WAR MINISTRY (AIR)
TECHNICAL AND INDUSTRIAL DIRECTION
FLIGHT TEST CENTER

Object of Study: Breguet 941.

Report No. 1

Object of Report: Identification, Performance, Flight Qualities

Registry Number: 7

Date: 22 March 1963

References: Technical Specifications of Breguet 941-01
Letter 353/CEV, Dated 15 November 1961
Requests for Tests STA/A1 No. 38026, dated 18 July 1962

CONTENTS

LIST OF ILLUSTRATIONS

Figures

Figures

Figures

Figures

1. GENERAL REMARKS

/1

The Breguet 941-01 made its first flight in June 1961. A first preliminary evaluation of the airplane by the CEV (flight Test Center) was made during October 1961 in Toulouse. The results were forwarded in Letter No. 553/CEV[1] of 15 November 1961.

Since, that time technological improvements of the airplane have been carried out and flight tests performed at the contractor's plant. As a result, the following changes have been made:

1. the wing leading edges were fixed,

2. the maximum flap deflection was increased from 60° to 97° for the inside flaps and 72° for the outside flaps, and

3. dynamic pitch and roll response were improved by increasing the corresponding control surfaces.

This report presents the CEV test results obtained during the last three phases of the tests of the present airplane configuration.

The schedule of these phases is as follows:

1. from 7-19-62 to 9-21-62, 11 flights,

2. from 11-8-62 to 12-4-62, 23 flights, and

3. from 1-2-63 to 1-11-63, 12 flights.

The first phase was interrupted between 8-21 and 9-18, following damage to an inside flap actuator, which resulted in a stopping of the flight test and a modification.

The program included the following:

1. a study of the flying qualities for the main configurations,

2. measurement of performance,

3. a statistical study of the reproducibility of short landings,

---

[1] No. 353 given on original title page.

4. a short study of the possible use of a mixing linkage making it possible to control the differential by means of the stick or the rudder pedals and to design the controls for the production airplane, and

5. the verification of guaranteed contractual performance.

Next, the airplane was shipped back to the Breguet plant for installation of the new propeller transmission with couplings, built by Hispano and auxiliary test equipment to permit its evaluation by C.E.A.M.

2. DESCRIPTION OF THE AIRPLANE /3

2.1 Fuselage

It is characterized by:

1. A pilot cockpit with a windshield having a great amount of visibility,

2. A cargo compartment with a rectangular useful section, and

3. A rear section through which the cargo can be loaded, by means of a ramp integral to the structure, operated by hydraulic actuators. Side loading hatches permit completely free access to the ramp.

Dimensions of the cargo compartment:

width: 2.45 m	height: 2.25 m
floor length: 10.90 m	overall length: 13.0 m
floor area: 26.5 m^2	volume: 60 m^3

The height of the ramp is adjustable to facilitate loading and unloading (see photographs).

2.2 Wing

It is characterized by two spars with a continuous flange and a third spar with wire netting to insure "fail safe" features of the structure. Honeycomb sandwich structure is used for the skin.

Inside the wing, there are four integral fuel tanks. The wing has two pairs of double flaps. The rear part of the outer flaps is also used as an aileron. On the upper surface of the wing there are spoilers, controlled by the stick. In the leading edge the transmission shaft is installed, held by about twenty bearings. /4

Wing span: 23.20 m

Reference area: 82.60 m^2

2.3 Tail

The horizontal tail has a span of 10 m with an adjustable stabilizer and an elevator.

The single vertical tail has a fixed part and two rudder surfaces. The motion of the second rudder is twice that of the first. At speeds larger than 100 knots, the first surface is locked in neutral position and only the second one can move.

2.4 Flight Controls

2.4.1 Elevator

The two sticks actuate two double irreversible servocontrols S.A.M.M. type 7080, each one controlling one elevator surface. The control linkages are rigid and also control a Messier "Oscar" actuator which can be disconnected if desired, and a Breguet spring box (see schematic on Figure 8).

The law of displacement of the controls is given in Figure 19.

The stick forces are shown on Figures 20 and 21.

2.4.2 Lateral Control

The two sticks are connected to a rigid linkage which controls:

1. two irreversible double servocontrols SAMM type 7090 acting on the ailerons,

2. two irreversible servocontrols SAMM type 7050 acting on the spoilers,

3. a Breguet spring box, and

4. a hydraulic actuator installed on the central propeller shaft casing, controlling the differential pitch of the outer propellers.

Control forces and displacements are given in Figures 22 and 23. /5

2.4.3 Directional Control

Each rudder surface is actuated by a double servocontrol, Model 7080. Both servos are hooked to the control system for V < 100 knots.

A mechanical device allows the nulling of the control rod of the first rudder, or the mechanical locking of the first rudder at flight speeds above 100 knots. Control lights in the cockpit show the sequence, and a spring box is inserted in the control linkage. Control forces and displacements are shown on Figures 24 and 25.

2.4.4 Stabilizer

Two trim levers in the cockpit are mounted on SAMM 103 handles and control the position of the stabilizer by means of two independent circuits, through an electrical actuator driving a double irreversible servocontrol SAMM, Type 7100.

2.4.5 Flaps

A Hispano hydraulic motor, equipped with a detector of position and torque asymmetry, drives a torsion shaft, linked directly to an Aviac screw actuator for the inner flaps and indirectly, through various mechanical devices, to an Aviac screw actuator for the outer flaps. The actual gearing ratio gives a maximum flap deflection of 72° for the outer flaps and 97° for the inner flaps.

The Hispano hydraulic motor is driven electrically:

1. by the controls of the first pilot between flap deflection angles of 0° and 97°. The circuits are hooked through the detectors of position and torque asymmetry and are shut off by the microswitches indicating that maximum flap deflection has been reached, and

2. by a lever mounted on the single engine control, insuring flap control between 75° and 97°. This lever incorporates the same security features as the control of the first pilot. /6

3. an alternate control "second pilot," mounted on the central console, and therefore accessible to the first pilot, for which maximum flap deflection is shown by a revolution counter, mechanically linked to the Hispano motors. The circuit is not linked to the asymmetry detector or the microswitch, and is used only in an emergency.

A sketch of inner and outer flaps is shown in Figure 6.

2.5 Landing Gears

2.5.1 Nose Gear

The nose gear consists of two tandem wheels mounted at the extremity of an oleo strut. It can be retracted under the floor of the cockpit. A wheel under the left panel allows, through a hydraulic actuator, the orientation of the nose gear through a range of $\pm 65^{\circ}$.

2.5.2 Main Landing Gear

The main landing gear is of the Messier "Jockey" type. Each side can be retracted into a nacelle located along the fuselage, and consists of two wheels in tandem, with a common oleo. It is equipped with low-pressure tires, and the wheels have hydraulic brakes. The oleo can also be used to vary the length of the strut, and therefore to modify the attack angle of the airplane on the ground. Distance between nose and main gear is 6.960 m; the track width is 3.594 m. A sketch of the main landing gear is shown in Figure 12.

2.6 Engines /7

The Breguet 941-01 incorporates four G.T.P. Turbomeca Turmo III-D gas turbines, with free turbines. The power is first extracted through a shaft (called the 6,000 rpm shaft) driving the main Breguet transmission, which is located in the wing leading edge and supported by the nose spar, and then through a front shaft driving the propeller directly (called the 1200 rmp shaft). A schematic diagram of the safety devices incorporated in the power train is shown in Figures 4 and 5. Power curves are shown in Figures 42, 47, and 49. Normal rated power on the ground is 4 x 1,165 hp (4 x 860 = 3,440 kw). No provisions are made for deicing of the engines or of the wings.

2.7 Propellers

The airplane has four propellers, designed by Breguet and built by Ratier Figeac. Propeller diameter is 4.5 m. The two outer propellers are canted outboard; the inner ones are canted inboard, in order to reduce induced drag. The pitch of the four propellers is controlled by four torsion shafts originating from a common casing located in the fuselage, each acting on a screw actuator and a servocontrol on the shaft. A hydraulically-controlled mechanical stop is mounted on the propeller shaft. The central casing fulfills the following functions:

1. automatic or manual rpm regulation, through pitch equalization of the four propellers,

2. thrust reversal by means of a change to "small pitch," with simultaneous removal of the shaft stops, and

3. differential pitch on the outer propellers, limited to 3.5°, with maximum of 3° on lateral control and 1.5° on directional control. The corresponding actuator is controlled either from the rudder pedals or from the stick.

It would be desirable to be able to decrease the pitch of the outer propellers (hence the blowing over the wing tips), and create a dip in the lift curve, thus increasing the induced drag (this is called the "transparency function"). However, this could not be tested, since it would require the removal in flight of the mechanical stops (such movable stops are presently under study by the Contractor). /8

On the other hand, the propellers can be feathered by first declutching the transmission, which is achieved by a hydraulic actuator and by presurizing the "high pitch" chamber of the servomechanism in the propeller shaft. The reverse maneuver is impossible in flight.

2.8 Fuel System

The wing contains four tanks with a total capacity of 7300 liters. Each reservoir feeds the corresponding engine, but all are interconnected. Refueling can be accomplished simultaneously or separately, under pressure, through two openings on each side of the fuselage, forward of the landing gear nacelles. It can also be performed by gravity, one reservoir at a time.

Each reservoir contains 1800 liters and has a fuel gage, two immersed pumps B.P., and a mechanically-actuated fire block valve.

2.9 Hydraulic System

Pressurization is insured by two hydraulic pumps driven by the main gear train, and therefore by any one of the four engines. The pickup is mounted on gear boxes 2 and 3. A hydraulic electrical pump is started by a manometric contact sensing any pressure drop.

2.10 Electrical System

Power is furnished by four generators, one mounted on each engine, and two alternators driven by the main gear train with pickup at gear boxes 2 and 3.

2.11 Miscellaneous Equipment: Radio, Air Conditioning /9

Equipment is standard, and includes standard cockpit instrumentation. In particular, the engines are monitored. Special instrumentation includes a continuous-reading angle of attack indicator with a weathervane and a B.I.P.; sideslip is also measured by a weathervane.

The airplane is equipped with two transmitter-receivers V.H.F. SARAM and a two-frequency radio compass with frame. Operation of the latter is not very reliable, and the radiation pattern of the V.H.F. antennas must contain some dead regions. A device indicating a 7-meter altitude is temporarily installed. It is manufactured by SNECMA under the trade name of Lumisol. Its operation is based on the reflection of an infrared beam, but the device is not reliable. The cockpit is heated by a gasoline heater; however when the flaps are deflected, the cockpit rapidly fills with the burnt gases, and the tightness is not satisfactory.

2.12 Emergency Provisions

An emergency hatch is provided behind the pilots' seats. Each nacelle is equipped with a fire extinguisher, and one can, if necessary, use the fire extinguisher of the neighboring nacelle.

2.13 Access

Some access provisions are good (engine nacelles); others are not (for example, the landing gear). However, improvements should be easy.

2.14 Test Equipment

The test installation was made by Breguet, it includes 10 A13 and 1 A20, a closed-circuit television system which allows observation of the flow on the tail areas from the location of the second pilot, torque meters on gear boxes 1 and 3, a visual vibration indicator for the gas turbines, and a visual vibration indicator for the propellers. The recorded test parameters are shown in Annex 3.

2.15 Pilot Controls

The configuration of the Breguet 941-01 airplane is not conventional, /10 but it has been possible to use only conventional flight controls, as shown by the following list:

1. stick, with a SAMM 103 hand grip, on which are mounted the stabilizer trim lever and the radio switch,

2. rudder pedals, each pedal being equipped with a braking device acting on the corresponding landing gear wheel,

3. three-position lever (down, stop, up) with automatic return when the aircraft is stopped, continuously controlling the position of the high-lift flaps,

4. three switches to reset the zeros of the three artificial feel boxes,

5. lever controlling the locking of the first rudder,

6. two landing gear retraction levers, one for normal use, one for emergency,

7. wheel to maneuver the front wheel,

8. parking brakes,

9. four throttles controlling engine power, mounted on the central console, each with a lock so that they can be moved simultaneously using a single lever mounted on the left console,

10. lever on the central console, controlling the automatic regulation of the rpm of the transmission and of the four propellers. It is possible to disconnect the automatic regulation and control the propellers manually,

11. reverse thrust is obtained by raising and "breaking" the power throttle on the left console (a maneuver similar to the "PC" control of fighter airplanes). The maneuver is only possible when a small lock is first released. The passage back from reverse thrust to normal thrust can be made by pushing the pitch lever back up for the inner propellers. For the outer propellers, it is accomplished with a lever mounted on the engine throttle. Temporarily, this lever also controls the flaps between 75° and 97°,

12. four large knobs are used for propeller feathering, and /11

13. several levers and switches for such maneuvers as the disconnecting of the spoilers or of the thrust differential, which would be eliminated in a production model. On the other thand, some controls are for the exclusive use of the second pilot or of the flight engineer, such as circuit-breakers, interconnecting fuel tank valves, cabin heat control, etc.

2.16 Weight and Balance

2.16.1 Weight and center of gravity breakdown is shown in Figures 26 and 27.

The prototype is actually tail-heavy due to recent control surface modifications. This requires a large amount of ballast in the pilot cockpit and water ballast in a forward tank.

The CEV tests were made for a series of weights in accordance with the contractual specifications. Three water tanks, containing, respectively, 1700, 1700 and 1200 liters, make possible changes in airplane weight and c.g. location.

2.16.2 Weight Breakdown

During the CEV tests, the weight breakdown was as follows:

1. airplane, empty weight + oil + residual fuel		12,000 kg
2. load:		
ballast, pilot cockpit	214 kg	
ballast, station 11	100 kg	
test equipment	1182 kg	
3 empty ballasts	588 kg	
Lumisol	12 kg	
I.L.S.	12 kg	
	2111 kg	
		2,111 kg
3. fuel: 7200 liters		5,760 kg
	Total	19,871 kg

At a maximum takeoff weight of 20,800 kg, by distributing the load properly, a useful load of 3,100 kg can be attained. The fuel load corresponds to about 6 hours of high-speed cruise, and the payload can obviously be increased by decreasing the range (see Chapter 4, Performance). /12

2.17 Flight Regimes and Limitations

For the first two test phases, V_i was limited to 100 knots.

After modifications to the prototype, it was necessary to make new vibration tests.

During the last test phase, the CEV was limited to V_i = 225 knots[1].

The results of the tests, together with calculations, showed that there was no flutter limit, under the reservation of locking the first rudder.

1. anemometric speeds: V_i first pilot (upper pitot tube)

   V_i < 225 knots, landing gear up, first rudder locked

   V_i < 100 knots, first rudder unlocked

   V_i < 130 knots, V_s 0 to 30°, landing gear extended

   V_i < 100 knots, V_s 45°

   V_i < 85 knots, V_s 70°

   V_i < 75 knots, V_s 98°

2. airplane angle of attack: first pilot (weathervane)

   - 10° < i < 30°

   i < 4°, beginning of the flare (to limit the loads on the landing gear).

3. angle of attack of horizontal tail: dp i_e (probe PH)

   dp i_e < 10 mB. This value cannot be reached during any maneuver.

4. sideslip: Jg copilot (weathervane on upper part of fuselage)

   Jg < 20° for V_i 100 knots

   Jg < 25° for V_i 85 knots

   Jg < 30° for V_i 60 knots

5. load factor: n g, 1st pilot /13

   0 < n < 2.5 g (provisional, waiting the results of additional tests by Breguet, with various fuel distributions among the wing tanks). (So far, Breguet has flown at 2.8 g.)

---

[1]The aviation company has since reached the speed V_c of 253 knots above V_d.

6. vertical speeds: Vz, 1st pilot. Velocities specified to limit landing gear stresses during landing.

final approach: $Vz < 800$ ft/min

calculated impact: $Vz < 600$ ft/min limit load at 18,700 kg

500 ft/min < safe load at 18,700 kg

800 ft/min < limit load at 17,800 kg

650 ft/min < safe load at 17,800 kg

7. weights

	Expected	Actual (manufacturer)
hard runway, takeoff:	$M < 20{,}500$ kg overload	20,805 kg[1]
grass runway, takeoff:	$M < 18{,}715$ kg normal	18,800 kg
landing		
grass runway:	$M < 18{,}700$ kg exceptional	18,600 kg[1]
	$M < 17{,}800$ kg normal	

These weights are for the case of a runway landing.

8. c.g. location

$25\% < C < 35\%$ for all configurations

9. wind

head wind < 40 knots (mean turbulence)

cross wind < 30 knots (manufacturer's tests)

10. range of calculations

Figures 28 to 32 show the domains and the particular points for which performance was calculated. As far as ailerons are concerned, the CEV used the following rule:

---

[1] Weights since reached: 21,100 kg on takeoff and more than 19,000 kg on landing on a grass runway.

1/2 deflection at $V_i < 150$ knots

since all the cases of Figure 31 are thus covered; allowance being made for the temporary limitation of the load factor.

3. CALIBRATION OF THE ANEMOCLINOMETRIC INSTALLATION /15

3.1 Low-Speed Calibration

3.1.1 Calibration of the Anemometer

During the first phase of the tests, an attempt was made to make the calibration for the STOL landing configuration, with flaps deflected 98°, the landing gear extended, by the method recommended in Report CEV 627/SM, using cinetheodolites. As was anticipated in the report: "The reader will be able to judge the difficulty of meeting all the necessary meteorological conditions." Actually, these conditions are very difficult to obtain simultaneously. This is due to the method:

1. either, the wind is weak, but its fluctuations are relatively large, and reduce the accuracy of velocity measurements, or

2. the wind is strong, and in spite of a good relative accuracy, the absolute error is still too large in comparison with the speed of the airplane.

As long as the means to measure instantaneously the wind velocity at an altitude of 150 or 200 meters are not available, it will be impossible to obtain accurately the anemometric speed of an STOL airplane in a configuration for which level flight is not possible. For 97° flap deflection, with the blowing of the landing condition, the airplane loses altitude.

However, an accurate calibration would only be useful to draw powered flight polars. In view of the low speed of the airplane, an error of 1 or 2 knots on the velocity results in a relatively large error on $\overline{C_z}$.

The accuracy is sufficient for the normal use of the airplane, since the velocity meter is not the instrument which the pilot uses for flying. Since the slope of the curves $\overline{C_z} = \overline{C_z}(i)$ is small (therefore the velocity differences are small for large differences in incidence), and since the range of incidences which the airplane can normally use is narrow, it is better to use for an STOL configuration either a continuous angle of attack meter or a paravisual instrument of the B.I.P. type.

The calibration of the anemometer in the landing configuration is shown in Figure 33. The "width" of the band was explained above, and the /16

effect of blowing is to increase the dispersion. In the takeoff configuration, the calibration could not be made because of lack of time.

3.1.2 Angle of Attack Calibration

The angle of attack is obtained from the formula:

$$\text{attitude} = \text{slope} + \text{angle of attack}$$

It can be seen that the inaccuracy on the windspeed is felt on the value of the slope. On the other hand, the attitude can only be measured by a vertical gyroscope, the precession of which is cut during the accelerated flight phases. Although the instrument is reset after landing by an artillery level, the parasite precession spoils the measurements. For the weathervane angle of attack meter, the wind-tunnel result is used:

$$i_{true} = 2/3\ i_{weathervane}[1]$$

The calibration of the pressure probe is shown in Figure 34. The inaccuracy is also due to wind fluctuations and in variations due to blowing.

3.2 High-Speed Calibration

3.2.1 Anemometry

The anemometric calibration was made by simultaneously using passages in front of fixed locations and in front of the tower, in order to confirm the accuracy of the total pressure readings at high speeds.

Correlation is excellent. Pressure probes located in the nose probe and those on the Gerbier antenna at the top of the vertical tail were calibrated simultaneously, to make an eventual elimination of the nose probe possible.

The results are in Figures 35 to 38.

3.2.2 Angle of Attack

/17

During the transits in front of fixed bases, advantage was taken of the zones with extensive level flight to obtain the angle of attack calibration from:

---

[1] The exact law is given in the paper "Data reduction" furnished to NASA.

$$A = i_{true}$$

A was measured with a vertical gyroscope; the forward weathervane was calibrated, and then the dp_i of the B.I.P. pressure probe was measured. A high-speed powered polar was drawn simultaneously, and it was possible to calculate a Δp for all points of the polar curve.

The results are shown in Figures 39, 40, and 41. It can be seen that the slope of the calibration curve of the forward weathervane effectively has the value 2/3.

4. PERFORMANCE

/19

4.1 General Remarks

As part of the first two test phases, when the airplane was always restricted to $V_i < 100$ knots, we endeavored to obtain an accurate evaluation of the takeoff and landing performance of the airplane. It was noted that takeoff performance could be very precisely reproduced by using the following procedure: stick all the way back at 45 knots, allow the airplane to take off, and stabilize at $i_{\text{front probe}} = 5^\circ$.

For landing, the performance depended upon the landing procedure; therefore, it was necessary to define, (1) maximum performance and, (2) a performance that could easily be reproduced in the V.M.C. condition by a pilot properly checked out on the prototype. The measurement of the performance accounts for the actual flying qualities of the airplane.

During the last test phase, it was possible to rapidly evaluate the "cruise" condition of the airplane. Though the basic parameter is the power level of the engines, instantaneous full consumption meters were installed, and the results are presented in terms of fuel flow.

4.2 Takeoff

A few takeoffs performed with the above procedure were tracked by theodolites up to the passage of the 10.5 meter obstacle. The measured distances first had to be reduced to a zero axial component. The method that was used is discussed in Annex 1 and Figures 44 and 45. Conversely, this method permits calculation of the performance for any axial component. It was then necessary to transcribe the performance for other weights and other atmospheric conditions. The method used is discussed in Annex 2.

During the tests, the torque meters were not operating. The power ratings shown were obtained from calculations based on speeds, fuel consumptions and power curves provided by Société Turbomeca, and not from direct measurements (Figures 42 and 43). /20

It should be noted that the takeoff regime actually corresponds to 102 percent power, according to Turbomeca, but takeoff was always made at Ng = 100 percent, corresponding to the stop of the engine throttle adjusted for that test phase. Under those conditions, by resetting the power settings, the performances would probably be slightly larger than those shown in this report. The appearance of the curves of Figure 46 seem to justify the validity of the method of data reduction.

The tests were made in hot weather. For a standard atmosphere, according to the curves of Figures 29 and 30, the shaft power would be 4 x 1175 x 0.736 x 0.974 = 3400 kw; therefore, standard takeoff distances can easily be extrapolated. It can be seen that the airplane satisfies the specifications which require, for the assault mission, a takeoff length between 270 and 300 m. At 19,400 kg, the airplane takes off in 300 meters.

4.3 Landing

Though the airplane could make conventional landings by using only a fraction of the available flap deflections, the CEV wished to verify that the STOL landing was not an exceptional maneuver, but actually corresponded to a normal use of the airplane. Therefore, during all three test phases, all landings were made "with steep gradient," which corresponds to the case of a landing strip surrounded by obstacles.

It now remains to define the landing procedure and the performance on a short terrain without obstacles. The intended landing procedure was as follows:

1. passage of the 50 ft obstacle with the maximum vertical velocity compatible with the landing gear, i.e., 800 ft/min., thus giving the maximum slope (see the limitations: all landings performed at less than 18,700 kg weight),

2. normal flare, for a touch-down on the main landing gear, without attempting to do it too low; thus avoiding a performance that would be difficult to reproduce

3. deceleration until stop; obtained after immediate reverse thrust application at full power and average wheel braking. /21

4.3.1 Passage of the 50-Ft Obstacle

4.3.1.1 Search for Optimum Conditions. Naturally, the best performance is obtained with the highest slope. Stress measurements on the landing gear structure by the manufacturer showed that it was advisable not to exceed the sinking speeds given in paragraph 2.17 (800 ft/min for the current weight), and that it was essential for the incidence to be lower than 4° at the beginning of the flare, in order to be able to take advantage of a decrease of sinking speed during the flare. To avoid rapid changes of incidence, which are undesirable at low altitude, the approach was made with an incidence stabilized around 2° to 3°.

For various flap deflections, it is necessary to use the power which under those conditions gives a descent rate slightly lower than 800 ft/min. Then, it is noticed that the largest slope is obtained by using maximum flap deflection. This is expected, since around maximum deflection flap deflection increments contribute only to drag, and not to lift.

The result is that the pilot will use full flap deflection, maintain the incidence around 3° by trimming the horizontal tail, and will adjust the throttle in order to control the vertical speed, hence the slope. Under those conditions, V_i varies fairly little and stays around 55 knots, depending upon the weight. This number, together with the vertical speed of 800 ft/min gives a slope in quiet air of about 15 percent, i.e., an angle of 8 degrees with the horizontal.

4.3.1.2 Test Conditions. Naturally, it would have been possible to specify a piori the conditions determined above and to film the landings on a runway, but this would not have resolved the problem of the dispersion of the touch-down point, and thus the validity of the performance.

Tests made in small fields surrounded by high trees, have shown that a row of trees allows the pilot to set his course on a correct trajectory and to visualize on the ground a presumed impact point. These approach tests were unfortunately followed by fly-around at very low altitude as the proper landing authorization could not be obtained. Additional tests of this type should be made and the landing completed, since this would add to our knowledge of the behavior of the airplane. /22

As it was difficult to produce a row of trees on the runway a small mirror was used as in a carrier landing. This simple device was only intended to replace the 50-ft obstacle, but it also helped to develop a concept for a possible STOL landing aid. For additional details, see the chapter: Flying Qualities.

The pilot maintained the airplane in the gliding plane defined by the mirror. The landing performance could be measured by determining the

distance between the theoretical point where the bottom of the mirror field was 15 meters away from the ground and the touchdown point of the airplane.

During certain flights, different glide angles were tried. At 6° flying is easier, but performance falls off; above 8°, the sinking speed exceeds the allowable limit. The axial component of the wind decreases the glide slope and therefore makes flying easier.

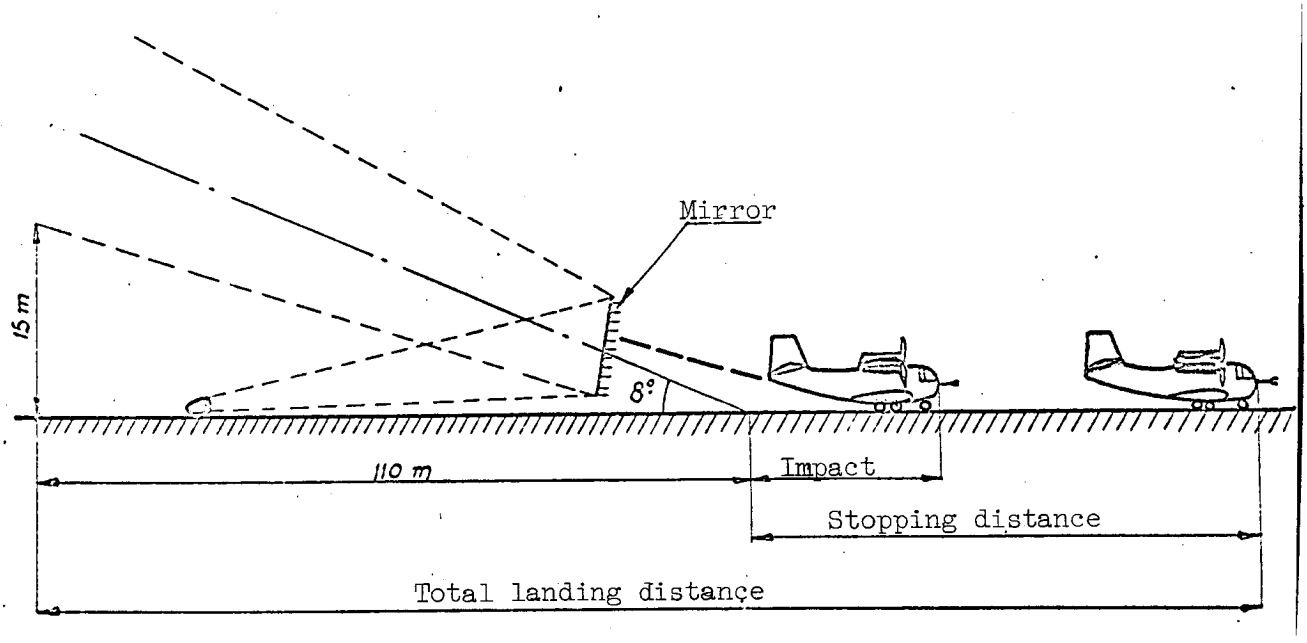

4.3.2 Landing Flare

/23

Since the "Lumisol" device did not function properly, no research on flare procedure was conducted.

Landings could be made without practically any flare; naturally, they correspond to maximum performance: touchdown at the precise intersection of the glide path with the ground. The higher the flare takes place, the further away the touchdown point from the glide path intersection, and the larger the dispersion around the mean value. Naturally, the correct landing attitude is assumed.

The landing flare procedure was left to the initiative of the pilot; two full lines on the runway, one at 15 meters, the other at 25 meters from the trace of the glide path, gave him the optimum touchdown point.

4.3.3 Ground Roll

The deceleration to rest is obtained by gentle braking and, mostly, by reversing the thrust at touchdown with full power. For a given weight,

the deceleration is remarkably constant and does not depend much upon the wind.

4.3.4 Results

The results are presented in the form of tables relating to 8 flights.

The tables show the touchdown point and the stopping point with respect to the trace on the ground of the plane inclined at 8° defined by the mirror. The 50-ft obstacle was passed at $\frac{15}{\tan 8^{\circ}}$ = 110 meters before.

The last number gives the overall landing performance.

FLIGHT 193 /24

18,260 kg C = 33% Slope 8°

Head wind 6 kts
Mean Vz - 550 feet/minute

Mean Ng 91 to 89%

Touchdown	Stop	Total landing distance
62	153	263
24	101	211
35	109	219
30	100	210
31	90	200
21	118	228
45	107	217
35	143	253
80	181	291
60	153	263
35	143	253

FLIGHT 194

17,620 kg C = 33% Slope 8°

Wind 30° to the right 10/12 kts
Mean Vz - 800 feet/minute

Mean Ng = 86%

Touchdown	Stop	Total landing distance
15	103	213
15	104	214
60	-	-
15	82	192
12	71	181
05	64	174
15	-	-
15	57	167
45	-	-

FLIGHT 195 /25

18,240 kg 33% Slope 8°

Head wind 6 to 8 kts
Vz - 700 feet/minute

Ng 87%

12	120	230	
25	140	250	
17	140	250	
23	127	237	
15	115	225	
13	100	210	
24	220	330	reverse pitch
07	102	212	
13	110	220	
35	120	230	

FLIGHT 196

18,240 kg 33% Slope 8°

Head wind 18 kts
Mean Vz - 800 feet/minute

Mean Ng 87%

Touchdown	Stop	Total landing distance
05	Stopping location N was not measured.	
15		
30		
10		
18		

FLIGHT 202 /26

18,620 kg 33% Slope 9.5°

Head wind 18 kts
Mean Vz - 1100 feet/minute

Ng 81%

12	90	180
12	95	185
13	-	-
09	98	188
53	full power applied again	
25	-	
16	135	225
22	full power applied again	
26	123	213
13	113	203
14	80	170

/27

FLIGHT 203

Slope 8°

Wind 60° forward right 10-15 kts
Ng 86% - Vz 800 feet/minute

Touchdown	Stop	Total landing distance
17	-	-
10	112	222
14	117	227
26	134	244
16	107	217
25	111	221
23	126	236

Slope 6°

Ng = 88% - Vz = - 600 feet/minute

25	114	254
48	153	293
35	123	263
30	121	261
20	85	225 (no mirror)

FLIGHT 209

18,600 kg c.g. forward Slope 5°

Wind 60° forward right 16 kts

Only touchdown point was measured

38
15
21
27
31
20

FLIGHT 210

18,260 kg C = 33% Slope 6°

Head wind 4 kts

Touchdown	Stop	Total landing distance
20		
28		
35		
27		
23		

The results of all landing tests are shown in the tables. One can therefore see the effect of pilot error and of pilot proficiency on the dispersion. During flights 202 and following, the pilot was asked to fly around if the approach was judged imperfect. It is therefore from these flights that the landing performance and the dispersion must be judged. Therefore, reproducible performance for a proficient pilot is around 250 meters. /28

This means that, though the airplane is capable of a higher performance, a pilot with average proficiency on this craft can decide with absolute safety, passing the obstacle with a 250-meter terrain in front of him, either to continue the landing if he judges the approach good, or to fly around.

However, it must be noted that the mirror represents the real obstacle only imperfectly and was only a mediocre landing aid. Tests over real obstacles remain to be performed. If properly conducted, this will confirm the above data. The pilots should be trained to this kind of exercise, and one should not limit oneself to the early results. The gain which could come from the use of some form of adaptive guidance remains to be assessed.

4.4 Cruise Performance at 10,000 feet

Level-flight performance was measured for gross weights of 17,500, 18,500 and 20,000 kg. The results are shown in Figure 48. Power was calculated from corrected fuel flow (see Turbomeca Study No. 60,850, July 20, 1962):

$$C_{corr.} = 0.973\ C_{true}$$

using the curves of Figure 47. Allowance was made, as for the takeoff, for the losses in the front reducing gear (Figure 43), but the losses in the 90° gear boxes were neglected.

The maximum continuous rating of the gas turbines is temporarily limited to 97.7 percent. Under those conditions, the airplane flies at 385 km/hour; i.e., 5 km/hour above the minimum guaranteed cruise speed of the specification. At the maximum continuous theoretical power, the airplane flies above 400 km/hour with a fuel consumption of 4 x 253 kg/hour.

4.5 Special Contract Performance Requirements /29

These performance items were measured for verification of the contract requirements.

4.5.1 Climb Speed for the Logistics Mission

The conditions of the technical clauses are: one engine off; takeoff configuration: Zp = 0 - θ = 15°.

This performance was tested at a weight of 20,680 kg, in standard atmosphere -10°.

During the tests, the fuel consumption was Cb = 3 x 337 kg/hour. Corrected consumption was $C_{corr.}$: 0.973 x 337 = 328 kg/hour.

The results from the Turbomeca curves of Figure 49 show that the power was only 1140 shaft HP for each engine at 6,000 rpm, i.e., slightly less than the standard 100 percent power, which is 1165 HP. This was obtained by a very slight reduction of the power of the three remaining engines.

The measured climb speed with the landing gear extended, between 175 ft and 375 ft, is: V = 2.02 m/sec.

The technical clauses required a value between 1.5 and 2.7 m/sec.

4.5.2 Climb Speed for the Assault Mission

In the assault mission with one engine off, takeoff configuration: Z = 0 - θ = 38°.

The theoretical gross weight was supposed to be about 18,715 kg. The test was made by cold weather (standard - 10°) at a weight of 19,800 kg; i.e., one ton above the theoretical weight.

The measured climb speeds are as follows:

1. with the remaining three engines set at Ng = 98.5 percent, i.e., for a power of 3 x 1180 HP between 200 and 800 ft:

Vz = 2.65 m/sec, and

2. with the remaining three engines set at Ng = 95 percent, i.e., for a power of 3 x 960 HP between 300 and 500 ft: /30

Vz = 0.92 m/sec

It suffices to extrapolate the engine power curves up to $\theta = 38^{\circ}$ to deduce with good accuracy the climb speed under these conditions. From Figure 42, at 38°, 3 x 975 HP would result, and the climb must be maintained at 1 m/sec at the theoretical weight.

4.5.3 Ceiling

The conditions of the technical clauses are: Zp ceiling: 10,000 ft with one engine off, at the starting weight for the logistic mission cruise. Maximum continuous power for propeller static thrust for a theoretical weight of about 20,000 kg. The test was performed between 9900 and 10,600 ft in standard atmosphere at 20,200 kg.

The climb speed with three engines at 97.7 percent power was:

Vz = 1.18 m/sec

The airplane has, as required, a practical ceiling of 10,000 ft. The real ceiling is above 12,000 ft.

4.5.4 Basic Mission

Principal Mission: "Assault"

The technical clauses define the following mission:

1. payload: 3 tons (one way) (return empty),

2. distance between base and forward field = 500 km,

3. length of base and forward field = 200 m,

4. flight at low altitude (300 m) compulsory for a distance of 200 km, going to and returning from the forward field,

5. fuel reserves (those of Mil Spec 5011 A),

6. normal takeoff weight, and

7. average cruise speed (no wind) larger than 400 km/hour

At the takeoff weight of 19,400 kg, distributed as follows: /31

Empty weight	12,000
Crew	200
Useful load	3,000
Useful fuel	3,600
Reserves 200 + 400	600
	19,400

the airplane can perform its main mission, but the low-altitude cruise speed must be lower than 400 km/hr, to avoid using the fuel reserves.

Additional performance tests at Zp = 300 m would be required to determine the low-altitude cruise speed.

Logistics Mission

The technical clauses define the following mission:

1. useful load: 4.5 to 5 tons,

2. distance between the two fields: 1200 km,

3. length of field at arrival: 200 m,

4. fuel reserves: those of Mil Spec 5011 A,

5. takeoff weight: overload, and

6. average cruise speed (no wind) larger than 400 km/hr.

With the following weight estimate:

Airplane, empty	12,000
Crew	200
Useful load	4,500
Fuel	3,900
Total	20,600 kg

the airplane can perform the logistics mission at a cruise speed of 385 km/ /32
hr. At a higher cruise speed, the fuel reserves of Mil Spec 5011 A would have to be partially used. These reserves correspond to 5 percent of the

total fuel, plus the fuel weight necessary for a 30-minute flight at low altitude, and at maximum endurance.

4.6 Conclusions

The prototype of the Breguet 941-01 generally meets the desired performance requirements. The only reservation concerns the rearward location of the center of gravity which requires forward ballast that must be included in the payload. Also, recent area increases of the control surfaces led to double-curvature airfoils which are fairly heavy. A slight performance gain can be expected by weight reduction.

5. FLYING QUALITIES /33

5.1 General Remarks

The plan for the study of the flying qualities of the Breguet 941-01 airplane is conventional. However, some difficulties were encountered, because of the particular formula of the airplane.

The aerodynamic coefficients of a conventional airplane do not depend greatly upon propeller slipstream, and the critical analysis necessary for the study of the flying qualities does not require flight tests within excessively restrictive margins of altitude and of power setting. This is not the case for the Breguet 941, for which the wing is entirely immersed in the propeller slipstream. The fundamental flight parameter is the thrust coefficient C_T, defined in the annex, which cannot be measured directly in flight by the pilot. In order to evaluate certain response characteristics of the airplane it was necessary to carefully specify test altitudes and input functions; but, these conditions are hard to combine with the fact that the airplane is capable of important vertical velocities in the STOL configuration. Therefore, flight tests of this airplane are difficult.

Another difficulty in the study of the flying qualities of the Brequet 941-01 results from the fact that an airplane with a blown wing has certain damping terms, for example L_p, which are small. This means that transient effects in control surface response are large, the velocities are practically never stabilized; in particular, in roll, even after a 60° disturbance, the curve $p(t)$ shows no signs of saturation. Therefore, the tests should be made using angle-sensing accelerometers and not gyrometers. Unfortunately, these instruments are not currently used as standard flight-test instrumentation.

Therefore, only a global evaluation of the flying qualities of the airplane will be given here. It will be extensively supported by pilot opinions, since the application either of the classical norms, or of the Agard "recommendations" sometimes require delicate interpretations. The figures will show the most important parameters governing the dynamic stability and control effectiveness of the airplane.

5.2 Taxiing

/34

To obtain a sufficient electrical voltage, it is necessary to bring up at lease one of the engines from the ground idle position to the flight idle position. Under these conditions, the thrust of the four propellers at minimum low pitch is a little too large, which causes the airplane to accelerate and to roll too fast when the parking brake is released. To avoid excessive brake heating due to their continuous application, one must engage the four propellers into reverse thrust, then return the two inner propellers to positive pitch. This maneuver is simple to perform by "breaking" and again applying the throttle control. Taxiing under those conditions is correct, and can even be controlled by changing the propeller pitch.

This maneuver is unusual but after familiarization leads to easy and accurate control of taxiing speed. The many maneuvers in which thrust is reversed cannot be accepted for routine use until the propeller pitch control is redesigned and integrated among the normal flight controls.

The directional control obtained by steering the front landing gear wheels is sufficient in practice even for short turn radii. In addition, it is possible to assist steering by using the brakes or propeller thrust differential.

With cross winds of the order of 25 to 30 knots, taxiing is still possible in spite of the lateral inclination taken by the airplane. It does not seem advisable to make taxiing tests at higher cross wind speeds until spare propellers become available.

5.3 Longitudinal Flying Qualities

5.3.1 Static Stability

C.g. travel limits specified by the Contractor are from 25 to 35 percent. For all c.g. positions, the static margin is positive or zero. In the STOL configuration the results are presented in the form $\beta = f(i)$; the basic parameter being the angle of attack, i.e., control surface position against angle of attack.

Figure 50 shows the takeoff configuration. The slope is correct for a c.g. location of 33 percent, near the most rearward c.g. location.

Figure 51 shows a transient climb condition after takeoff. For a c.g. location of 33 percent, the slope is correct. /35

In cruise configuration, with the c.g. at 33 percent, it can be seen that the position of the elevator only varies by 1.5° (see Figure 52). With the c.g. at 34 percent, there is no change.

In the STOL landing configuration, the airplane is statically stable for all c.g. locations, with a tendency to neutral stability for rear c.g.'s and at high angles of attack (see Figures 53 and 54).

The influence of sideslip is shown in Figure 55. It can be seen that, to hold a constant incidence of 20° with increasing sideslip, it is necessary, for a sidelsip between 0° and 10°, to push the control stick by an amount corresponding to about a 4° displacement of the control surface, i.e., about 40 mm.

The effect of blowing is shown on Figure 56. To hold a constant incidence of 3°, which is the normal incidence at the beginning of the flare in the landing configuration, the position of the elevator is given by the second curve, where one chooses the surface position corresponding to the 3° incidence. It is evident that the effect of increased blowing is definitely a pitch-down moment, and this is related to the dynamic effects discussed later on.

The effect of the ground is a pitch-down moment, as can be seen by approaching the runway with a low sinking speed. For vertical speeds smaller than 2 m/sec and constant incidences of 2°, the airplane stops sinking about 2 or 3 meters from the ground. It is then noticed that the position of static equilibrium of the elevator to maintain the same incidence corresponds to a displacement towards pitch-up moments of about 30 percent of the total available control, for a c.g. located at 33 percent.

5.3.2 Longitudinal Dynamic Stability

In the takeoff configuration, the phugoid motion is slightly diverging, with a forward c.g. and full power, near the ground. This is not disturbing to the pilot, since the airplane climbs fast and only remains a short time in the unstable altitude range. Between 1,000 and 2,000 ft, the phugoid is already only of constant amplitude.

With an aft c.g., in the above configuration, the phugoid has constant amplitude, and, as soon as engine power is reduced to P.M.C. (continuous power), it damps out, as can be seen from Figure 57.

The period is 25 seconds. However, damping remains small. In an intermediary takeoff or approach configuration, with 30° flaps, the period is already longer (30 sec) for the same amount of blowing. Damping remains small (Figure 58). /36

In the landing configuration, with all flaps down and average blowing, the period remains 23 sec and damping remains small (Figure 59).

In the cruise configuration, the static margin being zero, the phugoid motion does not appear. The response of the airplane to a control deflection is aperiodic and diverging.

5.3.3 Elevator Effectiveness

5.3.3.1 Landing Configuration. In this case, the effectiveness is good and there is no tendency to start pitch-up. There is no response lag and the concavity of the curve q (t) is almost immediately directed downwards.

As shown on Figures 60 and 61, control response is practically independent of initial incidence, and remains sufficient at initial incidence angles larger than 10°. Excessive ground impacts that can occur when the incidence at the beginning of the flare is larger than 4° are not due to a lack of effectiveness of the elevator, but must be due to a rapid decrease of ground effect at increasing incidences.

Similarly, whatever the c.g. location, the effect of blowing on the response of the airplane is negligible (Figures 62 and 63) and, referred to the same disturbance amplitude, all response curves can practically be superposed within the usual range of blowing.

5.3.3.2 Cruise Configuration. Displacement per g are given on Figure 64. In addition, control loads and displacements and control adjustments of the Oscar actuator are shown in Figures 19, 20 and 21.

The impression remains that elevator control is too sensitive, which is an inescapable consequence of the large velocity spread of the Breguet 941[1]. The displacements of the stick are small. /37

On the other hand, the Oscar device has an appreciable time lag and there results some rather tricky flying at the boundaries of the flight regime, especially at high speed.

---

[1] The "Ajax" device, now being installed in the airplane, should remedy that situation.

The elevator itself functions correctly, but its adaptation must be improved. In particular, a stiffening of the control loads would be preferable to change in the adjustment of the Oscar device, which would not decrease its response time.

To satisfy Amendment 4b11 of the FAA CAR 4b regulation, concerning the determination of the never-exceed speed, a study was made of recovery from dives corresponding to passages at the cruise altitude, with cruise velocity and cruise power, and with increasingly negative attitudes. For 15°, the throttling and beginning of the recovery were made at a corrected speed of 228 knots. The velocity only begins to decrease 2 seconds after the maneuver, the total duration of the dive being in excess of 10 sec, in accordance with the regulation. The load factor during recovery did not exceed 1.5 g (Figure 65).

5.3.3.3 Takeoff and Climb Configurations. The stick can be pulled all the way back at a speed 10 knots lower than takeoff speed. Unloading of the front wheel precedes takeoff by about two seconds. The front wheel actually leaves the ground at a speed 10 percent lower than takeoff speed, but this 10 percent only correspond to about 5 to 6 knots and, if one accounts for the very important acceleration of the airplane during takeoff, the duration of that phase is very short, and the two phenomena of rotation and of takeoff appear to coincide. As soon as takeoff is finished, a slight stick release is necessary. However, attitude contol of the airplane during climb is easy.

In the intermediary configurations, there exists no problem of elevator effectiveness. Some disturbances are only caused in response to configuration changes.

5.3.4 Response to Configuration Changes /38

Figures 66 to 78 show the main results[1]. The following items are noteworthy:

The initial effect of a power increase in the STOL configuration to decrease incidence and attitude. Conversely, lowering the flaps decreases the indicated incidence, mostly for large flap deflections, gives a pitch-up moment, initially makes the airplane climb, but finally, increases the sinking speed (without any changes in the blowing).

---

[1]Trim changes due to power effects have already been included. Trim changes due to flaps will be incorporated in a program initiated at the beginning of 1964.

There results:

1. an action in the wrong direction on throttle application. However, it is possible, by acting simultaneously and rapidly on the elevator, to reduce the altitude loss to practically nothing (Figure 77). Stick action must be quick, large and mostly immediate; otherwise, the resultant nose-down attitude change causes an appreciable altitude loss, and

2. some difficulty in holding correctly the approach path in the STOL landing when the path angle is equal to or larger than 8°. To hold the incidence requires great pilot attention; otherwise, the airplane easily sideslips. The sideslip causes pitch-up, and its action adds to that of the blowing. A simple mechanical device, now being developed by the Contractor, which changes trim as a function of the power setting, should partially solve the problem.

5.3.5 Conclusion on Longitudinal Flying Qualities

The major deficiency concerning longitudinal flying qualities is the tendency toward important incidence changes in turbulent air in the landing configuration.

Since the difference between usual and extreme incidences is large (3° to 30°), the phenomenon is not dangerous, but requires constant attention from the pilot who must start his flare with an incidence between 0° and 4°.

This phenomenon could only be explained following systematic tests. /39
It can also be found under other circumstances: in paragraph 5.3.1, it was seen that 10° of sideslip corresponded to a 4° elevator deflection, and about 40 mm of stick displacement. Since the elevator is quite effective and, on the other hand, it is easy to accidentally sideslip 10°, it can be seen that, if the stick is not pushed back immediately by an appropriate amount, an appreciable yaw occurs, analogous to the response to a control input.

This phenomenon may be linked to the low damping of the phugoid motion, which does not inconvenience the low-speed flying, but which could explain these variations of incidence. A motion could be started by turbulence, sideslip, or changes in blowing and would only stop if countered with the remaining elevator power. Under those conditions, loss of control is not a problem, but if action is delayed, the stick displacement necessary to stop the motion may become quite large.

Let us also mention that in this special case there is no basic difference between damped and divergent phugoid motion, if one is only interested in the transient motion corresponding to the first "arch," i.e., to the first quarter of period, when the period is larger than 20 seconds.

Another inconvenience comes from the control linkage friction. The threshold of the springs, adjusted to give positive action for all positions have values larger than those recommended by Agard[1].

Since, on the other hand, the slope of the curve of elevator deflection against stick displacement is slightly too low around zero in the STOL configuration, some difficulty can be expected in holding the correct incidence. The airplane is not flown like the usual heavy airplane; stick displacements of 40 to 50 mm around the equilibrium position are frequent, and since the thresholds are large, piloting the craft is fatiguing. Large stick motions also result from the bad flexibility of the slope. Since the response to power setting changes must be made in the wrong direction, large elevator changes must be made[2].

However, it is possible, at the present time, to make accurate approaches, even with appreciable air turbulence. For an approach made on a terrain surrounded by trees, the slope variations can easily be evaluated by judging the perspective of the obstacles on the ground, and the stable slope which corresponds to the optimum sinking speed of the airplane can be located rapidly. The pilot passes 2 meters above the tree tops without difficulty, since the airplane attitude is practically parallel to the slope (i is small, about 3°) on a trajectory which can be established before reaching the tree level. /40

A field, 380 m in length, with 10 to 15 meter high trees on all sides was tested for an approach; powered flight was resumed during the flare and the trees were easily cleared. If necessary, the pilot would not have hesitated to land with touchdown at one-third of the field length and complete stop at two-thirds.

This experience is reproducible. The glide over the obstacle is easy, since the tail of the airplane does not "drag." However, landing with a low and flat approach was not studied systematically.

At the time of the flare, it is essential to have an incidence between 0 and 4°. For lower incidences, one loses slightly on the

---

[1] Recently, these thresholds were reduced, and are now under the recommended Agard limits.

[2] The defects noted in this paragraph have recently been corrected.

performance by increasing the length covered before impact. For higher incidence, though the longitudinal response is the same, the impact becomes harder and the available landing gear stresses may be reached. This is probably due to a decrease in ground effect.

The flare itself is only a change of attitude to make the airplane "touch down" on the main landing gear. When the incidence at the beginning of the flare is right, the flare maneuver presents no difficulties. It must be started low, but the altitude margin is not critical: about 10 to 3 meters.

Elevator performance, acceptable in all other configurations, (see a previous discussion) is unpleasant but not dangerous in the landing configuration. The elevator control is always effective which is the important point. A better adaptation of the control system, mostly a decrease of linkage friction, should be able to decrease the defects noted above and to give good or even comfortable piloting characteristics.

5.4 Lateral Flying Qualities /41

5.4.1 General Remarks

During the last test phase at the CEV, the pitch control of one of the outer propellers (one of those actuated by the differential) had a backlash slightly larger than the allowable specifications. This defect caused a frequent lateral asymmetry, which was detrimental for the correct recording of the transversal response of the airplane. As was mentioned earlier, the propeller pitch control should be a flight control and not the output of a regulating device.

The basic configuration was as follows[1]:

1. the main rudder locked above 100 knots, and is controlled by the rudder pedals under 100 knots,

2. a 26° differential,

3. ailerons operated conventionally, and

4. spoilers operated conventionally.

Other configurations were tested by combination of the following modifications:

---

[1]Present modifications with respect to this configuration are: 3° differential (for roll); ailerons are eliminated; and enlarged spoilers, with a different deflection law.

1. ailerons locked; roll by differential and spoilers,

2. spoilers locked; roll by differential and ailerons,

3. elimination of the roll differential. A differential reduced to 1.5° and controlled by the rudder pedals, and

4. main rudder surface locked under 100 knots. Directional control assured only by the second rudder.

5.4.2 Spiral Stability

The dihedral effect and the yaw stability being weak (the induced action of yaw on roll and of roll on yaw being decreased by action of the propeller slipstream on the wing), the spiral stability is low or even slightly negative depending upon the configurations. Roll and yaw interaction is never important or disturbing.

Tables 79 and 80 show hands-off operation during a coordinated turn. /42
The initial position of the controls gives the direction of the spiral stability, and the evolution of the parameters gives the trend for the airplane. However, errors may stem from propeller asymmetry.

It can be seen that:

1. with 30° flap deflection, for a turn to the right at an inclina-

of about 15°, the stick is in a position corresponding to 1° of left aileron. Hands-off, the airplane slowly increases its lateral inclination by about 1° per second. Similarly the yaw rotation accelerates slowly,

2. with 98° flap deflection and an inclination of about 10°, the phenomenon is analogous; the initiation of roll is even slower, and

3. in cruise (Figure 80), the airplane is spirally stable and levels off slowly hands-off. The spiral instability, when it exists, is never disturbing.

5.4.3 Roll Effectiveness

5.4.3.1 Cruise Configuration. In cruise, for the basic configuration, roll effectiveness is good. The only defect comes from the mechanical design of the control linkage, which has excessive friction[1].

[1]All these features were improved in 1964 over the 1963 tests.

Figures 81 and 82 show the response following roll disturbances at a given speed, for various blowings. The influence of blowing is small. On the other hand, reverse yaw cannot be detected, but the craft sideslips as it has low yaw stability.

Figures 83 and 84 show the response to a similar disturbance at two different speeds without propeller differential and with spoilers and ailerons. The response is similar but slower: the influence of the lag due to the boundary layer of the spoilers when they come out is felt by the pilot through a region of low effectiveness around the zero[1].

Figure 85 shows the response to a roll disturbance with locked ailerons corresponding to one-half of the maximum stick deflection, with only spoilers and differential. The direct action is good. The disadvantage of a region of low effectiveness is serious. A possible remedy /43 is to move the spoilers faster through the boundary layer[2]. The disadvantage is the total absence of opposite yaw. The secondary action is a direct yaw, which may make coordinated turns more difficult. This is a direct consequence of the fact that differential and spoilers obviously create a direct yaw[3].

5.4.3.2 Configuration with Flaps Deflected 30°. In an intermediary configuration of flaps deflected 30° with normal roll, control is effective (Figure 86), opposite yaw negligible, and there is no sideslip. Roll control is very good, the correct coordination at the beginning and at the end of the turn requires some pilot concentration, but acquiring a few degrees of sideslip is neither dangerous nor disturbing in this configuration.

5.4.3.3 Landing Configuration. With maximum flap deflection, a few control response curves are shown in Figure 87. Let us note in particular:

1. a very good roll effectiveness,

2. opposite yaw, and

---

[1] All these features were improved in 1964 over the 1963 tests.
[2] This change was incorporated in the airplane in late 1963.
[3] The differential can be locked in the cruise condition.

3. a sideslip increasing rapidly if the pilot does not coordinate with the rudder pedal.

Another peculiarity rests in the very low roll damping which gives the impression of a very low lag, and then of an absence of saturation. This is more noticeable when the pilot becomes more familiar with the airplane.

Opposite yaw is not disturbing, except possibly at the end of a turn, where the coordination requires pilot concentration.

Figures 88 and 89 show the response to a roll disturbance without spoilers, and with maximum flap deflection. For the same deflection, the roll acceleration is definitely smaller without the spoilers. The influence in yaw and sideslip is small.

The spoilers are excellent, but as discussed earlier, the kinematics /44
of the spoiler controls must be changed to eliminate the zone of low effectiveness felt by the pilot around the zero.

Figure 90 shows the response with the same flap configuration, but with locked ailerons; roll being insured by differential and by spoilers. There is no longer opposite yaw, and sideslip increases more slowly.

Figure 91 gives the response with the same flap configuration, without differential, but with ailerons and spoilers. Except for the low-effectiveness zone, the response to a normal deflection is still nearly sufficient, and one can think of using roll over only one fraction of the available differential propeller pitch.

At the present time, roll control of the airplane is adequate for all configurations. There is a lag in spoiler action, which could be corrected, and does not play a big role in the basic configuration. On the contrary, the limitation of aileron travel in cruise can only temporarily be tolerated. It would be advisable either to eliminate the ailerons if it is found that it is not detrimental to the flying qualities for the other configurations, or to decrease the maximum loads on the aileron servos by decreasing their cross section or by using a pressure-reducer on the hydraulic circuit. On a production airplane, it would be still better to strengthen the wing, since the Contractor claims that it would be done without large weight increases[1].

---

[1] See the preceding discussion.

5.4.4 Yaw Effectiveness

5.4.4.1 Cruise Condition

In cruise above 100 knots, the main rudder surface is locked. The response to a yaw disturbance is shown in Figure 92. The direct action is correct, the secondary action is an induced roll, in the correct direction. The sideslip reaches a maximum and decreases, which is excellent, and allows turning the rudder alone.

With a 1.5° differential in yaw, the response is larger. The secondary action is also larger, and the sideslip is slightly smaller for the same yaw response. Flying in cruise is quite pleasant in this configuration (Figure 93).

5.4.4.2 Intermediary Flap Deflection. With an intermediary flap deflection (Figure 94), a disturbance in yaw excites the yaw oscillation of the airplane, which is little damped. The period is long and does not disturb the pilot. The induced roll is in the correct direction. /45

5.4.4.3 Landing Configuration

5.4.4.3.1 Normal yaw configuration. For maximum flap deflection, Figures 95 and 96 indicate the extreme propeller effect already indicated earlier. For large blowings, i.e., for an important differential action, the roll response is always to the right, whatever the initial direction of the disturbance. However, one can see that, if the initial rudder pedal action is good, the secondary roll reaction is zero or even slightly opposite. This represents the major deficiency of yaw control in this flap configuration: it is impossible to fly the airplane with the rudder only, even if the pilot accepts large amounts of sideslip. For example, this makes impossible a correction of inclination with the rudder alone, when the pilot is otherwise concentrating on holding the airplane incidence. This may seem unusual, but the ability to be able to hold a direction and in particular to be able to stop a turn with the feet alone results in pleasant flying characteristics.

With lower blowing, this phenomenon is less disturbing, since the direct induced roll due to the yaw velocity increases (Figure 97). An opposite roll may occur during 2 or 3 seconds, and it is this transient response which may prove disturbing to the pilot.

5.4.4.3.2 Yaw control with foot rudder and differential. An immediate solution comes to mind. It consists in controlling with the foot not only the rudder, but also a certain amount of the propeller pitch

differential. Figure 98 shows the response of the airplane under those conditions: naturally, the initial yaw response is large, there is no longer an opposite induced roll, even during the transient regime, and the sideslip increases more slowly.

Since one disposes of large yawing moments, an attempt was also made to keep the main rudder locked in the STOL configuration; the pedals acting only on the second rudder. This could only decrease further the poor transient roll response. Results are shown in Figure 99; yaw response is slightly lower, roll response is about the same. The sideslip increase is slower.

In the last two configurations, the main advantage rests in an easier coordination at the beginning and at the end of turns. If the main rudder is kept locked, there is still sufficient response in the usual flight conditions but the minimum critical speed is increased, especially if an outer propeller is feathered. /46

5.4.4.3.3 Yaw control with main rudder locked. The airplane was also tested for comparative purposes, with the main rudder locked in STOL configuration; the differential remaining part of the yaw control system. The response is a little weaker, the minimum speed problem remains, but again the coordination seems to be easier to achieve than in the basic configuration, since the transient roll response was found to be better (Figure 100).

5.4.4.4 Takeoff Configuration - Main Rudder Locked. The configuration discussed last was also tested in the takeoff configuration (Figure 101). The conclusions are the same as above.

5.4.5 Homogeneity of the Controls

The homogeneity was studied by flying at steady increasing sideslip values and recording the corresponding control positions.

5.4.5.1 Cruise Configuration. In cruise configuration (Figure 102) the homogeneity is excellent; the controls are crossed and the coordination presents no problem.

5.4.5.2 Intermediary Flap Deflection. The homogeneity is adequate, for an intermediary flap deflection (Figure 103). The controls are crossed, for a steady sideslip. Figure 104 shows a test made in takeoff configuration with the main rudder locked. In this case, the coordination is correct.

5.4.5.3 Landing Configuration. For maximum flap deflection, the coordination is more difficult. This is well shown on Figure 105, and there is practically no yaw deflection required for counteracting a steady sideslip. The conclusions are the same as for the locked main rudder (Figure 106). /47

With locked ailerons, no benefit stems from opposite yaw (Figure 107). It is still possible to easily stabilize sideslip angles larger than 20°. With some differential pitch control linked to the rudder control, the controls are again crossed for a steady sideslip in the two yaw configurations (Figures 108 and 109).

These last results show that it is possible to find a distribution of the differential between stick and rudder control which can give very pleasant flying characteristics.

It must be remembered at 55 knots a very small inclination is sufficient to turn with a very short radius. The coordination at the beginning and at the end of turns must be made easier, but the airplane is already usable, even with the inconvenience due to the friction in the control linkages.

5.4.6 Minimum Control Speed

On the Breguet 941, the loss of one engine does not stop the corresponding propeller, and the airplane configuration remains symmetrical. The propellers of the airplane can still be feathered, but the case in which this operation must be performed does not correspond to what is usually called "engine failure," but rather to serious damage; projectile impact for example. Declutching and feathering may be forced either by gear box trouble or by abnormal propeller vibrations due to blade damage or to impact.

On a helicopter, damage to the main or to the tail rotor necessarily results in the loss of the machine. On the Breguet 941 the asymmetry resulting from a feathered propeller rules out operation in the STOL configuration. Therefore, one minimum speed in conventional configuration was investigated. The most unfavorable case is when the outer propeller stops. The results are as follows:

1. the propeller can be feathered at cruise speed,

2. in searching for the minimum speed with no roll inclination, maximum rudder deflection is reached around 75 knots. Incidence and sideslip are respectively 10° and 7°, and

3. for a roll inclination of about 5° the rudder pedals are only at 2/3 of maximum deflection, but the stick displacement is larger.

When landing in the above propeller configuration, with 45° flap deflection and a V_i of 82 knots, the symmetrical propeller can be feathered immediately after touchdown to allow use of reverse thrust immediately after impact. Landing distance under these conditions is about 500 meters. If an inner propeller is feathered, the corresponding minimum speed is 10 knots lower.

The only critical case would be feathering at takeoff in STOL configuration, but because of the high acceleration of the airplane, this phase is very short. During the landing maneuver, the situation can be serious only through a very restricted altitude range, since, if the airplane has sufficient altitude, the pilot can reduce thrust, retract the flaps and accelerate rapidly away.

It must be remembered that a gear box failure is not instantaneous. The crew disposes of alarms through a monitoring of oil level and temperature which give an early detection of possible gear failure. Damage to the propeller blade remains the only case requiring immediate propeller feathering, but this phenomenon has a very low probability of occurrence. Besides, it would have to coincide precisely with two very short flight phases to become dangerous.

5.4.7 Conclusions on Lateral Characteristics /49

In cruise, the only important thing to note is that the limitation on aileron deflection can only temporarily be accepted[1].

In the STOL configuration, maneuvering characteristics are always good, but correct coordinated turns are difficult to achieve (recent improvements were discussed in the previous pages). The airplane can be used today, but modification to the flight controls, and if possible, the addition of a mixing device to the differential should result in pleasant flying characteristics.

6. CONCLUSIONS /51

The Breguet 941 No. 01 made its first flight in June 1961 and was accepted in January 1963.

---

[1] With the recent elimination of the ailerons, the problem disappears.

In the meantime, 200 flights have been performed, of which 46 were conducted at the CEV (technical clauses and basic missions are described in the Annex).

The flight domain explored as of this day is as follows[1]:

1. indicated speeds: from about 50 knots (STOL landings) to 225 knots,

2. load factor: up to n = 2.5,

3. incidence: up to $i_g = 30^\circ$; incidences larger than 10° were rarely used under normal flight conditions,

4. sideslip: up to $j_g = 30^\circ$; sideslip angles of 15° were already difficult to obtain, and

5. weights: up to 20,850 kg; i.e., 350 kg above the present limitation.

The only disturbing limitation at the present time (April 1963) concerns aileron[2] deflection at high V_i.

The main performance results are as follows:

Takeoff: with the weight of the assault mission the airplane takes off over a 10.5 meter obstacle with zero wind and standard conditions in 300 meters. This is in accordance with the specifications, and in spite of the handicap due to actual engine adjustment.

Climb speed: with one engine out, and at the logistics mission weight, climb speed at sea level is 2.02 m/sec. This is larger than the required minimum of 1.5 m/sec.

Cruise speed: in spite of the temporary limitation to 97.7 percent of maximum continuous power, the airplane flies at 385 km/hr, i.e.,

---

[1]The domain explored at the beginning of 1964 is as follows: indicated speeds from 38 to 253 knots; $i_g = 33^\circ$, $j_g = 34^\circ$, i_g is the angle of attack of the weathervane, j_g is the sideslip of the weathervane.

[2]In 1964, the ailerons were removed.

5 km/h above the rejection clause of the specifications. At maximum continuous theoretical power the speed will be in excess of 400 km/hr.

Ceiling: for the logistics mission, with one engine out and standard atmosphere, climb speed is 1.18 m/sec at 3000 meter altitude (specification ceiling). Under those conditions absolute ceiling is more than 3500 m. /52

Landing: at normal gross weight the best overall total landing distance (over a 50-ft obstacle) is about 200 meters. A performance of 250 meters is guaranteed to be reproducible. This is due to a good accuracy on the touchdown point. (Specification requirement: 220 m normal, 250 m guaranteed.)

Basic missions: under the reservations of correct payload distribution, which limits the use of the cargo compartment, the airplane can perform the assault and the logistic mission described in the specifications. On a production airplane, a lengthening of the fuselage would eliminate the problems of load distribution.

As far as flying qualities are concerned the takeoff presents no difficulty, and in cruise, the airplane flies satisfactorily. However, the addition of a "V^2 effect," which would stiffen the controls at high V_i, is desirable[1].

For the "landing" configuration, a few reservations must be made. However, control effectiveness is sufficient to allow flight on a given trajectory under all conditions, but at the expense of extreme concentration by the pilot during that short phase of flight. Other items that should be noted are: high control linkage friction, opposite pitch response to power changes, erratic incidence changes under turbulent air conditions, and difficulty in coordinating lateral controls. Comfortable flying could be obtained by the following: modify the flight controls; link stabilizer trim and power changes, distribute the differential action between stick and rudder pedals[2].

From a technological viewpoint the Breguet 941 is a conventional airplane, except for the interconnected propellers, the propeller pitch control and the landing gear.

During the 200 flights which were performed, the Breguet transmission performed normally, but required frequent oil changes. After

---

[1]Such a device (Ajax) is currently (January 1964) being installed.
[2]Note recent improvements (1964) discussed in the text.

installation of the new Hispano transmission, flights should confirm the excellent results obtained from ground tests[1].

The propeller pitch control mechanism, acceptable on the prototype, must be improved for a production airplane, since at the end of the 200 flights, a backlash in the outer propeller pitch has been noted. /53

The landing gear performed well, though all landings were of the STOL type.

During the first phase of the tests, a fragmentary study of flight check and maintenance was made.

Before further progress to a production airplane it will be necessary to make improvements to facilitate maintenance and checking, and in particular improve access to the wing structure and to the power plants.

In summary, the Breguet 941 is no longer an experimental aircraft, like its predecessor, the Breguet 940. It is the prototype of a production transport airplane capable of 3 to 6 ton payloads, depending upon the missions. It has satisfactory STOL performance and cruise speed. The loss of an engine has no influence on the flying of the airplane or on its ability to perform a short landing.

The problems that remain to be solved are similar to those always found on conventional prototypes at an already fairly advanced stage of development.

ISTRES, 18 April 1963

KLOPFSTEIN, Principal Engineer
Airplane Section Engineer

TAMAGNINI, Principal Engineer
Airplane Section Chief

GUENOD, Chief Engineer
Assistant Technical Director

[1]Excellent results obtained on the ground with the new Hispano transmission have recently been verified in flight.

Distribution List omitted in translation.

Translated for the National Aeronautics and Space Administration
by John F. Holman and Co. Inc.

ANNEX 1

Correction for the Influence of the Relative Wind Component on the Takeoff Performance of the BREGUET 941-01

1. PRINCIPLE

The acceleration, upon the release of the brakes, is independent of the relative wind component for values smaller than 20 m/sec. It depends only upon the mass of the airplane, and temperature and pressure conditions. In addition, the velocity curves are practically straight lines until about 20 m/sec. This means that aerodynamic forces remain negligible in comparison with propeller thrust and inertia forces up to such speeds. Similarly, the influence of the lift, which decreases the ground friction, is negligible.

2. CALCULATION

2.1 Ground Roll

For a given weight and a given thrust, (see Transcription in Annex 2), the acceleration is known; therefore, it suffices to calculate the length travelled to reach takeoff speed. The calculation can be made graphically.

2.2 Lift-Off and Climb over a 10.5 m Obstacle

The duration of the maneuver is practically constant. The length travelled is corrected to account for the axial wind component.

3. TYPICAL RESULTS

An example of application of this method is shown on Figures 44 and 45. The two takeoffs were performed a few minutes apart in opposite directions. The results are excellent and conform the validity of the method.

4. AREA OF VALIDITY

This method does not hold when the wind velocity reaches values such that the velocity curve has a curvature, i.e., near the takeoff speed. In that case, there is no problem of takeoff performance for the BREGUET 941. Takeoff occurs with a head wind and the total takeoff length is

ridiculously short. There is no advantage in taking off with tail winds. No tests were performed under these conditions.

ANNEX 2

Note on the Transcription of Takeoff Performance for Airplanes with Blown Wings

Study of the parameters that influence the takeoff distance over an obstacle.

1. BLOWING COEFFICIENT

The propeller thrust coefficient

$$C_T = \frac{T}{qS}$$

and the general incidence of the airplane completely define the global coefficients $\overline{C_Z}$ and $\overline{C_X}$. The coefficient can be written

$$C_T = \frac{T}{\frac{1}{2}\rho_0 \sigma V^2 S}$$

Therefore, it is only a function of the quantity T/σ and of the speed:

$$C_T = f\left(\frac{T}{\sigma}, V\right)$$

2. PROPELLER THRUST--CHARACTERISTIC EQUATION

We can assume that the propeller power remains constant during ground roll, rotation, and climb over the 10.5 m obstacle.

Let us consider the reduced parameters for thrust, power and speed defining propeller operation.

$$\tau = \frac{T}{\rho n^2 D^4} = \frac{T}{\rho_0 \sigma n^2 D^4}$$

$$\chi = \frac{W}{\rho n^2 D^5} = \frac{W}{\rho_0 \sigma n^2 D^5}$$

$$\gamma = \frac{V}{n D}$$

Assuming that the propeller governor changes the pitch α in such a way as to maintain the propeller speed n constant and that the engine power is constant up to the takeoff, the parameter χ is constant during takeoff, and only depends upon temperature and pressure conditions which can modify the ratio W/σ.

The curves showing the variation of the parameters τ and χ as a function of the pitch α and of γ are described in the following sketches:

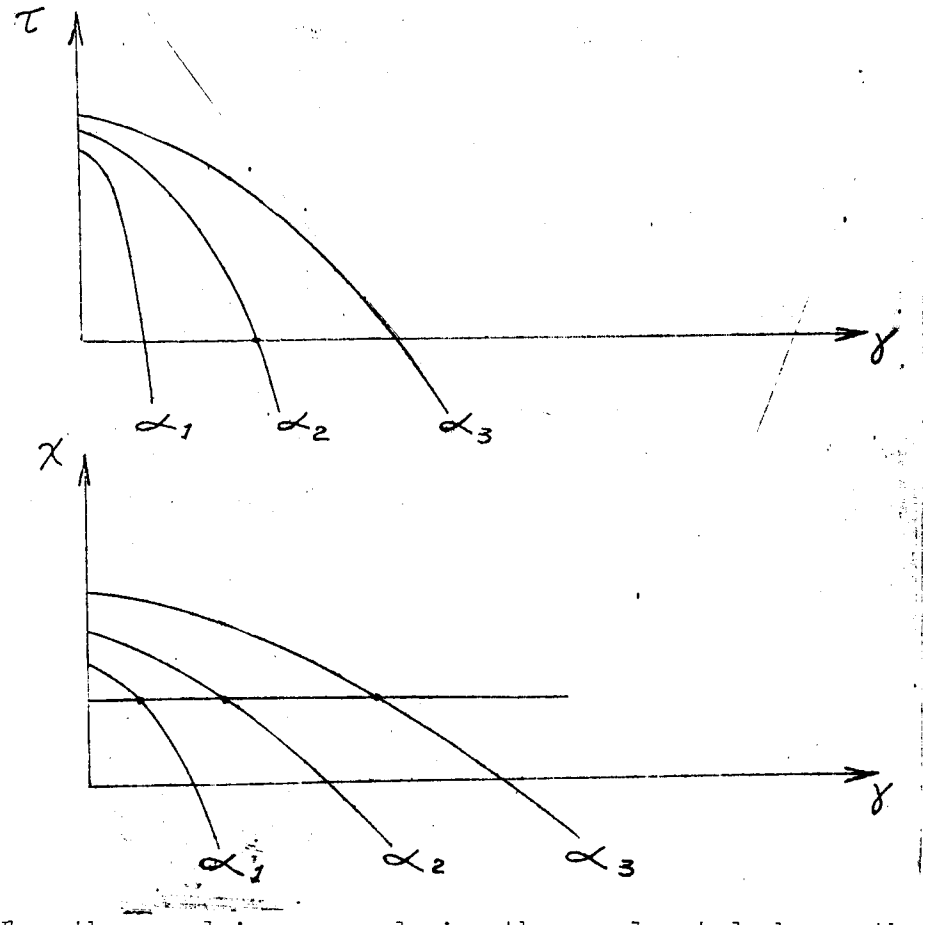

When the speed increases during the accelerated phase, the governor increases the pitch to maintain constant rotational speed and, since χ is constant, there exists a relationship between pitch and speed. Therefore, α between the equations can be eliminated:

$$\tau = j(\gamma,\alpha)$$
$$\chi = g(\gamma,\alpha)$$

Hence:

$$\tau = (\chi,\gamma),$$

which is characteristic of the propeller and of the constant-speed governor. It is not the general characteristic equation of one propeller at a given fixed pitch. The variables are the same and the equation is different, since n is constant.

From which we can deduce the characteristic equation:

$$\frac{T}{\sigma} = f\left(\frac{W}{\sigma}, V\right)$$

Hence, the blowing coefficient C_T only depends upon the parameters W/σ, V.

3. TAKEOFF SPEED

Until publication of precise specifications giving takeoff procedures and speeds for airplanes with blown wings, we shall assume that takeoff can be made at constant incidence when a certain speed V_d, is reached, which varies as a function of gross weight.

When these conditions are reached, we have:

$$\frac{\overline{Rz}}{mg} = 1$$

Hence

$$\frac{\frac{1}{2}\rho S V^2 \overline{C_z}}{mg} = 1$$

multiplying both sides by C_T:

$$\frac{\frac{1}{2}\rho S V^2 \overline{C_z} \times C_T}{mg\ C_T} = \frac{T}{mg}\ \frac{\overline{C_z}}{C_T} = 1$$

But $\overline{C_z}$ only depends upon i and C_T, if we fix the incidence, $\overline{C_z}$ only depends upon C_T. The second ratio only depends upon C_T, hence upon W/σ and V. Since T/σ only depends upon the same parameters, we have:

$$\frac{1}{\frac{mg}{\sigma}} \times \varphi\left(\frac{W}{\sigma}, V\right) = 1$$

The speed V_d only depends upon the parameters mg/σ, V/σ. It can be shown (see note A.A.L.B. DTAé - Gr/JMRd/JL-No. 908) that these conditions correspond to a constant margin with respect to maximum lift.

4. GROUND ROLL (not corrected for wind effects)

A double integration of the acceleration up to speed V_d defined in paragraph 1.3, which only depends upon mg/σ and W/σ, gives:

$$\gamma_x = \frac{T - \overline{R_x}}{mg} - \tau \left(\frac{mg - \overline{R_z}}{mg} \right)$$

$$\gamma_x = \frac{\frac{T}{\sigma} - \frac{\overline{R_x}}{\sigma}}{\frac{mg}{\sigma}} - \tau \left(1 - \frac{\frac{R_z}{\sigma}}{\frac{mg}{\sigma}} \right)$$

Since:

$$\frac{\overline{R_x}}{\sigma} = \frac{1}{2} \rho_o S V^2 \overline{C_x}$$

$$\frac{\overline{R_z}}{\sigma} = \frac{1}{2} \rho_o S V^2 \overline{C_z}$$

and since the coefficients $\overline{C_x}$ and $\overline{C_z}$ at constant incidences, only depend upon C_T hence W/σ and V, the expression of γ_x only depends upon mg/σ, W/σ and V.

$$\gamma_x = \Gamma \left(\frac{mg}{\sigma} \quad \frac{W}{\sigma} \text{ et } V \right)$$

During a takeoff, the only variable is V, but, since V_d depends upon the same parameters exclusively, the variable disappears between the limits of integration and the length is only a function of W/σ and mg/σ

$$\gamma_x = \Gamma (V)$$

the ground roll time t_1 is such that:

$$V_d \left(\frac{mg}{\sigma}, \frac{W}{\sigma} \right) = \int_0^{t_1} \Gamma(V) \, dt$$

therefore, t_1 only depends upon mg/σ and W/σ; hence, also L_1.

5. CLIMB OVER THE OBSTACLE

5.1 Length of Curved Path

Since the radius of the curved path only depends upon V_d:

$$\mathcal{R} = \frac{V_d^2}{(n-1)g}$$

the length travelled until a constant slope is reached, L_2, only depends upon V_d, thus upon W/σ and mg/σ.

5.2 Steady Climb

At constant incidence, the coefficients $\overline{C}_x$ and $\overline{C}_z$ only depend upon C_T, hence upon W/σ and V_d, i.e., W/σ and mg/σ

$$\tan \theta = \overline{C}_z/\overline{C}_x$$

The takeoff length L_3 therefore only depends upon W/σ and mg/σ.

6. CONCLUSION

If we assume:

a) constant propeller speed, and constant power applied to the propellers,
b) the takeoff speed calculated from the equation of paragraph 1.3:

$$\frac{1}{\frac{mg}{\sigma}} \times \varphi\left(\frac{W}{\sigma}, V\right) = 1$$

c) a given constant incidence during climb, independent of the speed calculated in b) above, the total takeoff length $L = L_1 + L_2 + L_3$ is only a function of the weight and power reduced parameters:

$$W/\sigma \qquad\qquad mg/\sigma$$

where W = engine power.

Therefore, films can be made, at maximum gross weight, of the takeoff which will allow construction of the following curves:

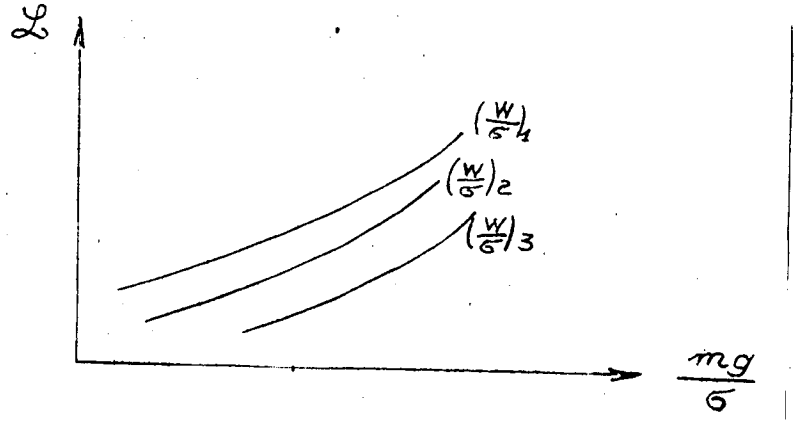

The power can be graduated in altitude for a given atmosphere so that the calculation of takeoff length for any atmosphere is immediate.

ANNEX 3

TEST INSTALLATION EQUIPMENT

HB - A 132 No. 516 - Longitudinal:

Recorded parameter	Instrument	Receiver
Pr	Badin	G. 12
p	Badin	H. 131
A	J 262	E. 511
ql	J 142	E. 511
θi	T 411	E. 601
Jzl	J 42	E 511
Top synchro	X 2011	E 07
dpi plane H		H 232
β left	M 120	E 511
Incidence, fuselage	weathervane	E 512
Incidence, probe	weathervane	E 512
Top Lumisol	Lumisol	E 07

HB - A 132 No. 517 - Roll:

D	M 120	E 511
G	M 120	E 511
D	M 120	E 511
A'	J 26	E 512
ps	J 14	E 511
Stress 13	Gage	E 601
Probe B.J.P.	K 2200	H 232
JX1	J 4211	E 511

HB - A 132 No. 876 - Propulsion:

N gear box M_2	tacho.	P 51
N gear box M_3	tacho.	P 51
Governor lever	M 120	E 511
Pitch, propeller 1	M 120	E 511
Pitch, propeller 2	M 120	E 511
Pitch, propeller 3	M 120	E 511
Pitch, propeller 4	M 120	E 511
Pressure regulator	H 293	E 511
Electric pump pressure	H 293	E 511
Pressure, high pitch	H 293	E 511
Torque meter, engine 1	Cimatic	
Torque meter, engine 3	Cimatic	

HB - A 132 No. 874 - Yaw:

Recorded parameter	Instrument	Receiver
N continuous G.T.P.1	Tacho.	P 51
5 nose gear (1)	M 120	E 511
5 nose gear (2)	M 120	E 511
1	J 143	E 512
d p j	Probe	H 232
j	Weathervane	E 512
JX1 spar, main d	J 42	E 512
D 5	M 120	E 511
θ transmission bearings		E 601
C fuel flow, engine 1	Flow meter	E 07

HB - A 132 No. 755 -

N continuous G.T.P.2.	Tacho.	P 51
βc		E 511
C fuel flow, engine 2		E 507
β right	M 120	E 511
Stress β 65	Gage	E 601
Stress β 68	Gage	E 601
Pr vertical tail	Gerbier	G 12
d Pr	Gerbier	H 230
P hard	Badin	H 1320
total fuselage		H 23
JLS - glide path		E 34
JLS - localizer		E 34

HB - A 132 No. 875 -

N continuous G.T.P.3	Tacho.	P 51
C fuel flow, engine 4		E 07
Spoiler, extreme right	M 120	E 511
Spoiler, extreme left	M 120	E 511
Stress 520		E 60
Stress 521		E 60
Single control	M 120	E 511
P2 engine 3	H 292	E 511
θ kerosene M 3	T 43	E 34

HB - A 132 No. 663 -

N continuous G.T.P.4	Tacho.	P 51
Flap, left	M 120	E 511

HB - A 132 No. 663 -

Recorded parameter	Instrument	Receiver
Flap, right	M 120	E 511
Landing gear stresses p^{al}, nosegear, right		E 60
Landing gear stresses p^{al}, main, right		E 60
C fuel flow, engine 4	E 3	E 07
Vibration fus., front (Y)	J 22	E 60
Vibration fus., rear (Y)	J 22	E 60
Aft fuselage tip	J 22	E 60
Landing gear stresses, nosegear, left	Gage	E 34
Landing gear stresses, main, left	Gage	E 34
Landing gear stresses, nosegear, right	Gage	E 34

HB - A 132 No. 518 - Landing gear:

Displacement TP., nosegear, right	M 120	E 511
Displacement TP., nosegear, left	M 120	E 511
Displacement TP., main, right	M 120	E 511
Displacement TP., main, left	M 120	E 511
T nosegear	M 120	E 511
Stress T nosegear	Gage	E 34
Braking pressure	M 120	E 511

HB - A 132 No. 991 - Vibrations:

βc, main	J 222	E 601
βc, nosegear	J 222	E 601
Tip M4 (2)	J 222	E 23
Ext long., nosegear, right (z)	J 222	E 23

HB - A 132 No. 136 - Vibrations:

1 Nosegear (Y)	J 223	E 601
1 Main (Y)	J 22	E 601

HB - A 132 No. 136 - Vibrations:

Recorded parameter	Instrument	Receiver
2 Nosegear (Y)	J 22	E 601
2 Main (Y)	J 22	E 601

HB - A 21 No. 6630 - Safety (shielding):

Pr	Badin	G 22
P	Badin	M 14
J 2_1	J 53	J 53
β right	M 120	E 521
CT normal		
CT emergency	B 201	E 07

ANNEX 4

CONTRACTUAL PERFORMANCES

	Production model	
	Normal	Guaranteed
Takeoff Assault mission over 10.5 m obstacle Z = 0 $\theta = 15^{\circ}$	270 m	300 m
Landing Assault mission over 15 m obstacle Z = 0 $\theta = 15^{\circ}$	220 m	250 m
Climb speed Logistic mission (overload) one engine off - takeoff configuration Z = 0 $\theta = 15^{\circ}$	2.7 m/s	1.5 m/s
Climb speed Assault mission one engine off - takeoff configuration Z = 0 $\theta = 38^{\circ}$	2.7 m/s	1 m/s
Mean cruise speed At mean cruise weight Z = 3000 m W engine 855 HP	400 km/h	380 km/h
Ceiling One engine off, at weight at beginning of cruise of the logistic mission at maximum continuous power 1040 HP, with static pro- peller	3000 m	3000 m

Conditions:

Standard concrete runway - Standard atmosphere at Z = 0,
No wind - Engines at takeoff power,
Static power: 1165 HP (measured on dynamometer at acceptance test). The basic missions are described in the performance chapter.

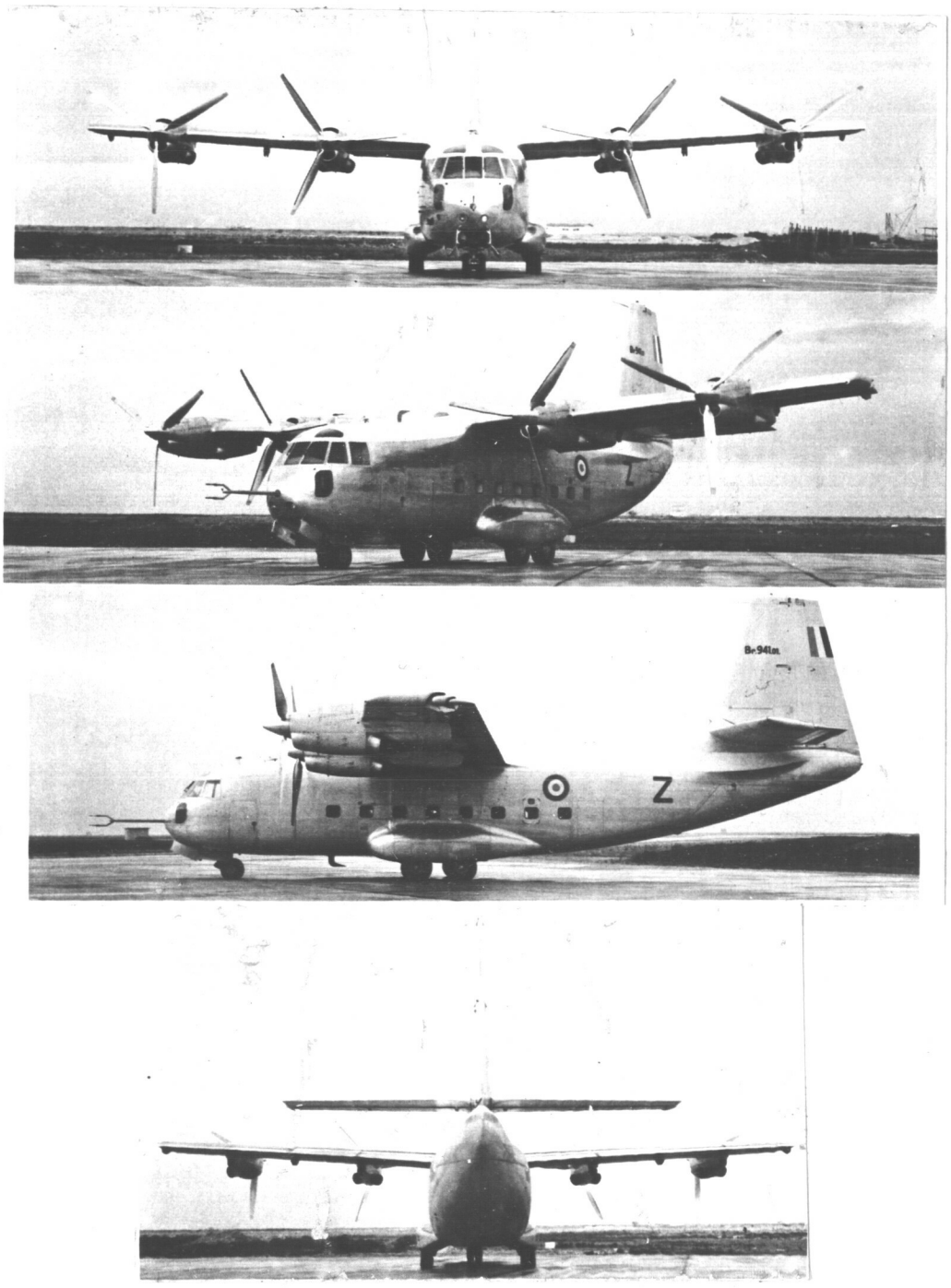

Figure 1. Four views of the airplane.

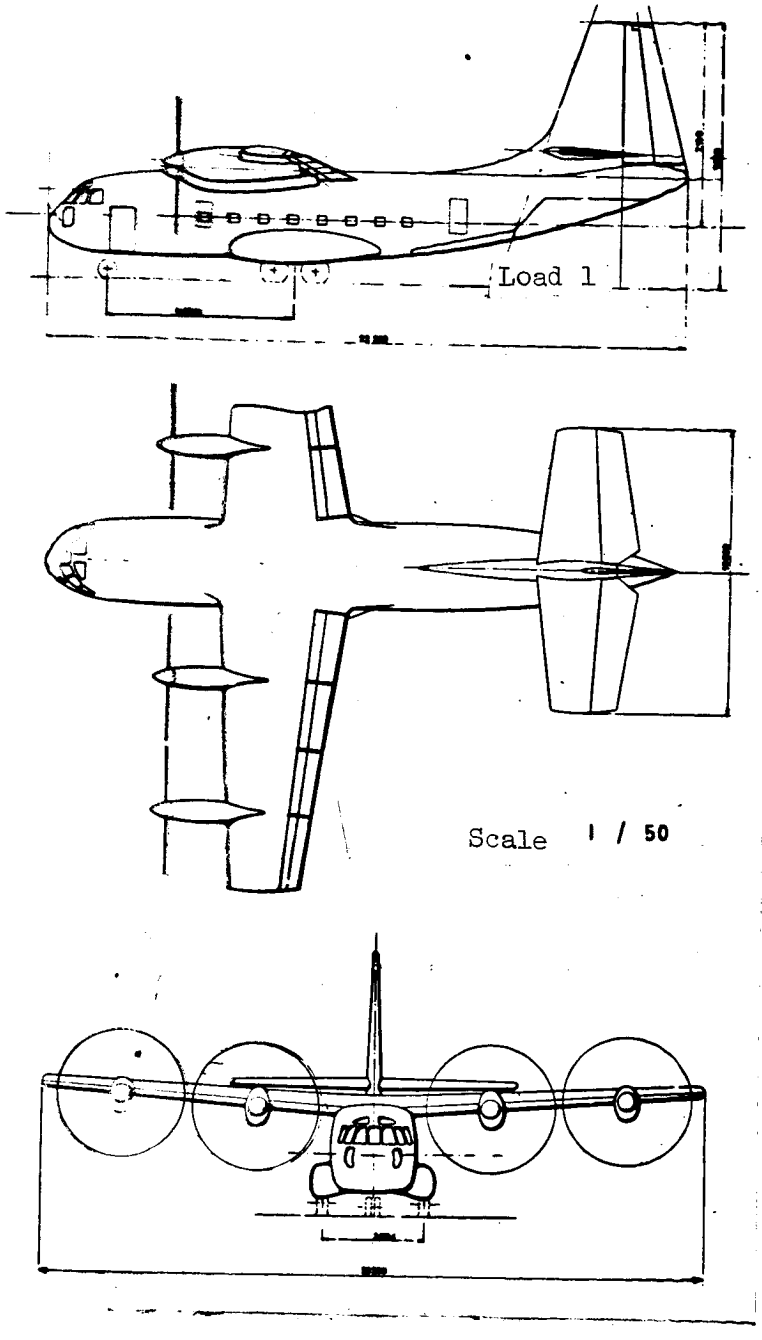

Figure 2. Three-sided view of the airplane.

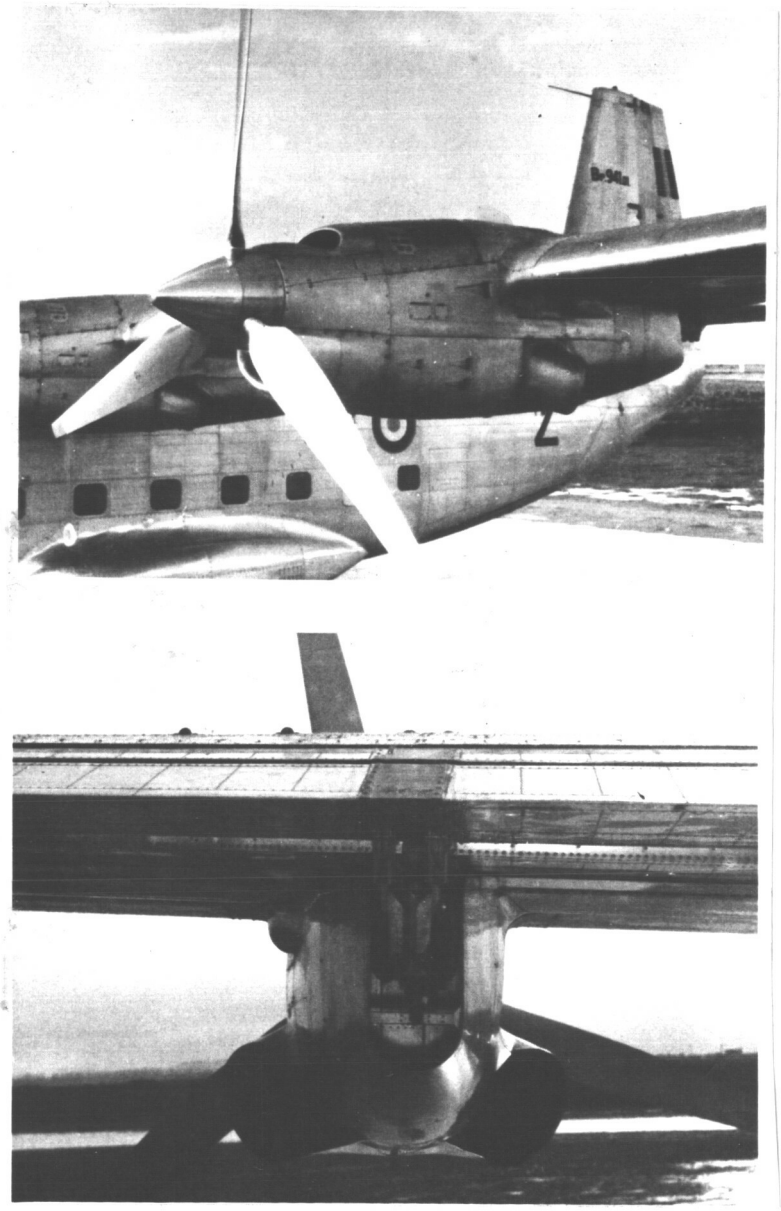

Figure 3. View of the engine assembly.

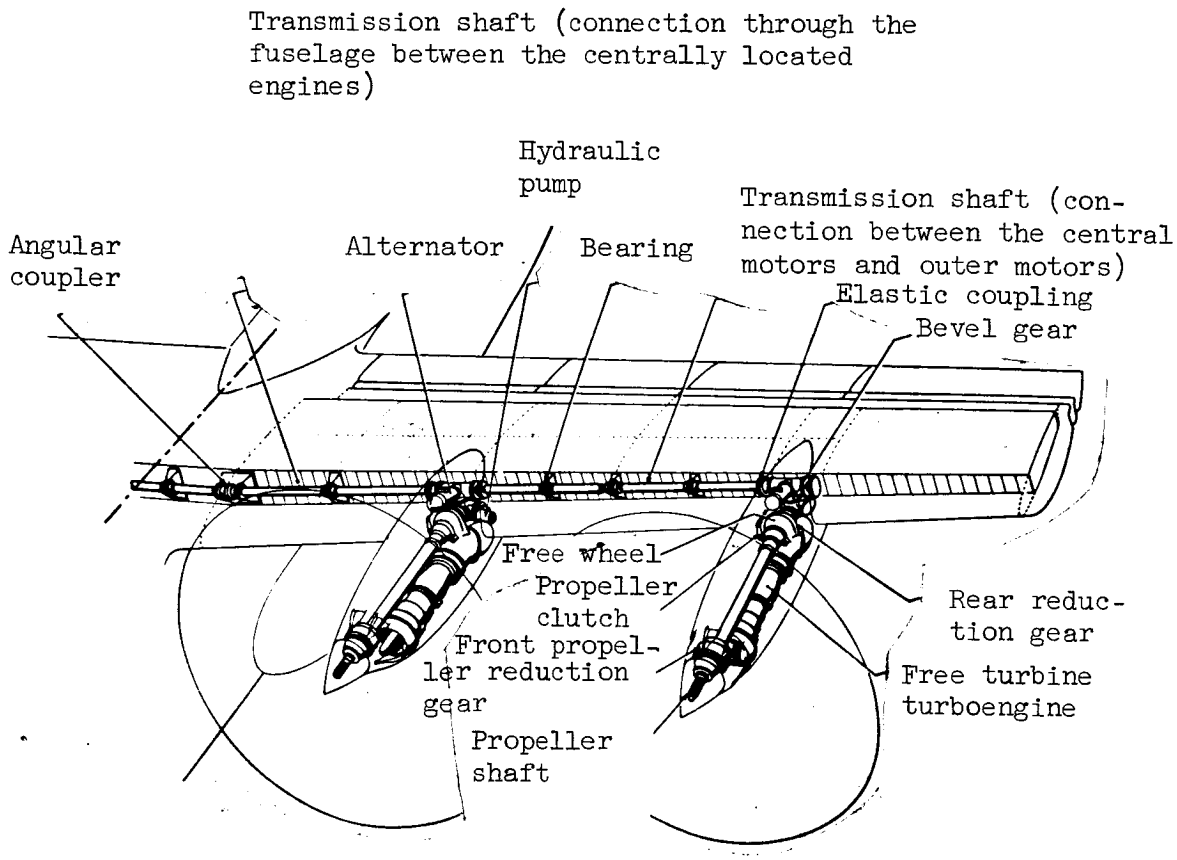

Figure 4. Power plant and transmission system.

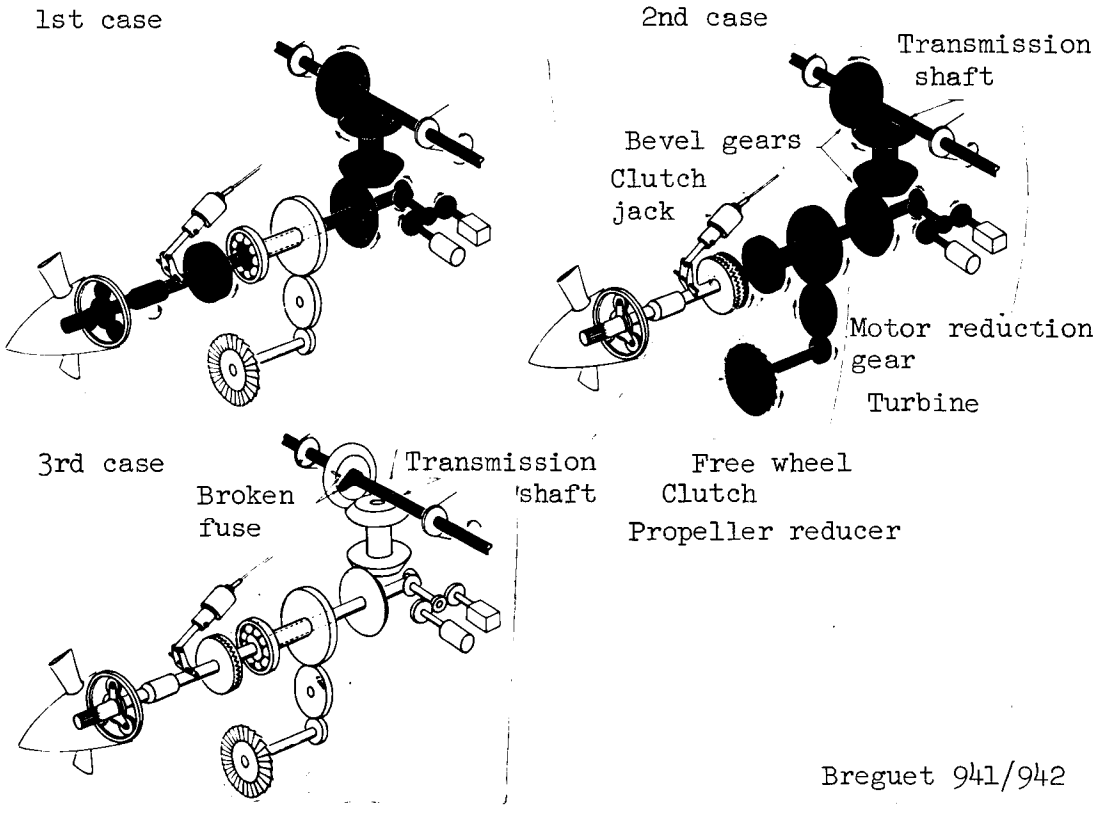

Figure 5. Safety devices used on the transmission.

First Case: Breakdown of the turbine or jamming of the motor reducing gear. The free wheel isolates the parts from the remainder of the transmission. The remaining 3 motors drive the 4 propellers.

Second Case: Jamming of the propeller reducing gear or propeller vibrations: the pilot uses the clutch and increases the propeller pitch to feathering pitch. The 4 motors drive the remaining 3 propellers.

Third Case: Jamming of a motor shaft element or of the bevel gears. The fuse breaks and isolates the motor from the transmission shaft, which continues to drive the 3 other propellers.

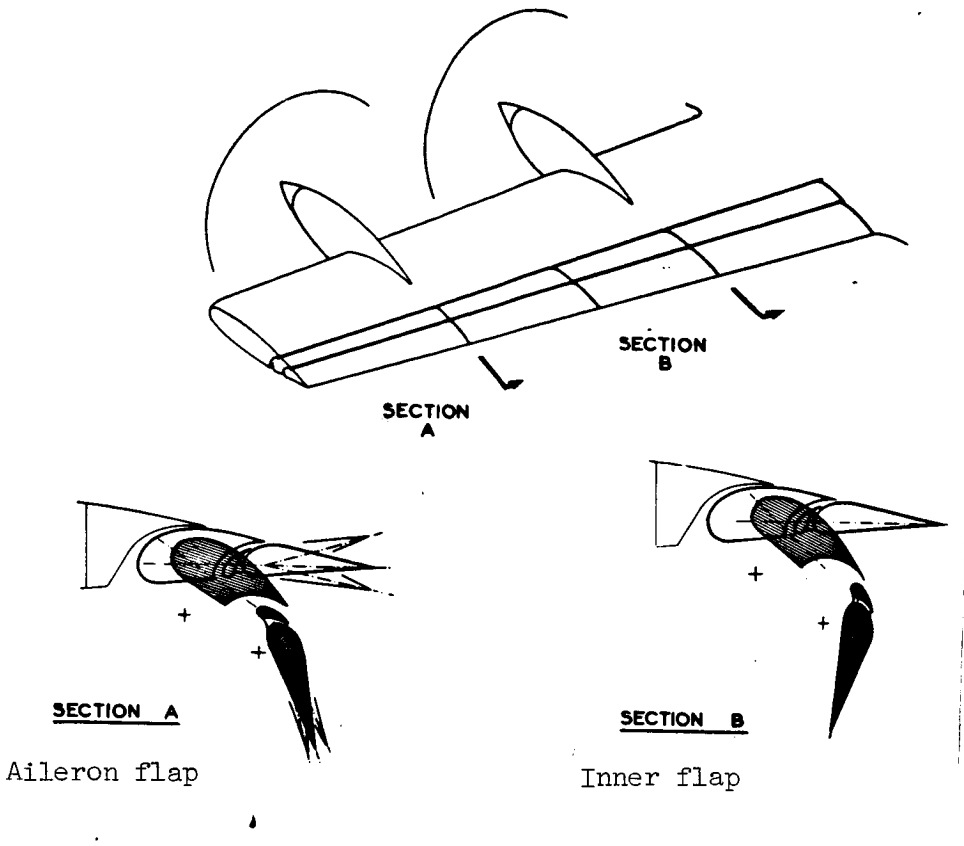

Aileron flap

Inner flap

Figure 6. Schematic views of the flaps and ailerons.

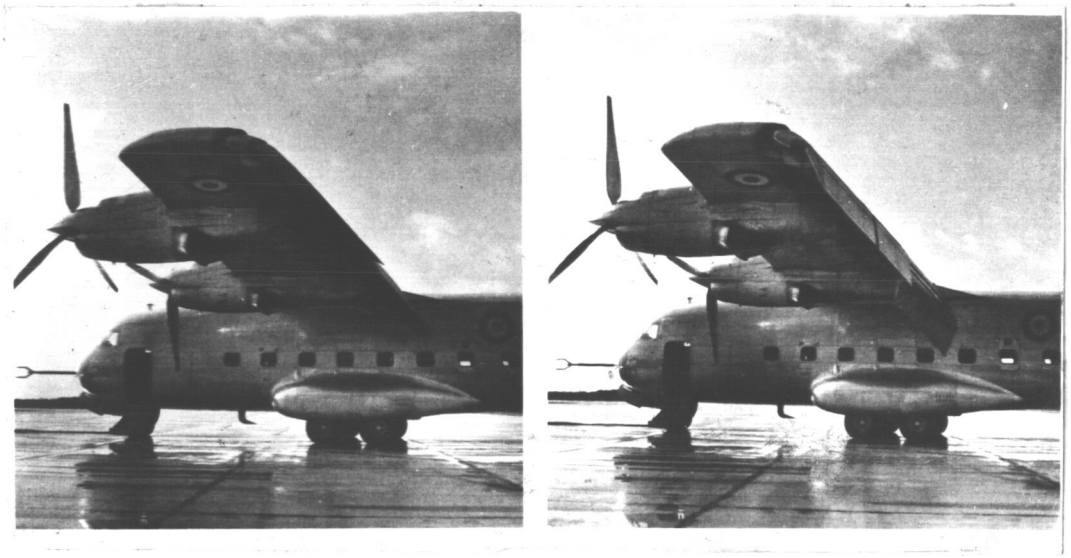

Flaps positioned for take-off

Flaps positioned for landing

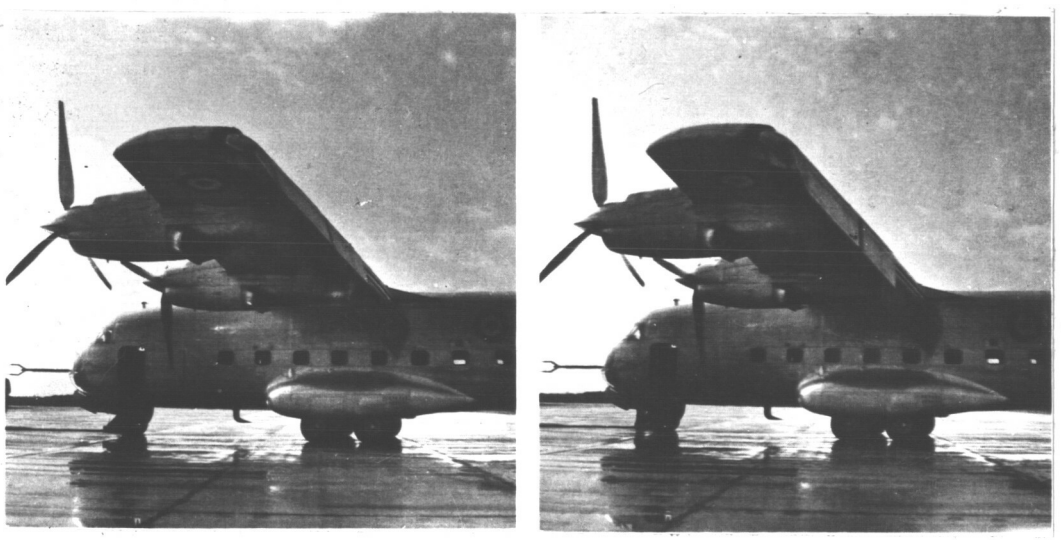

Raised aileron

Lowered aileron

Figure 7. Flap and aileron sets.

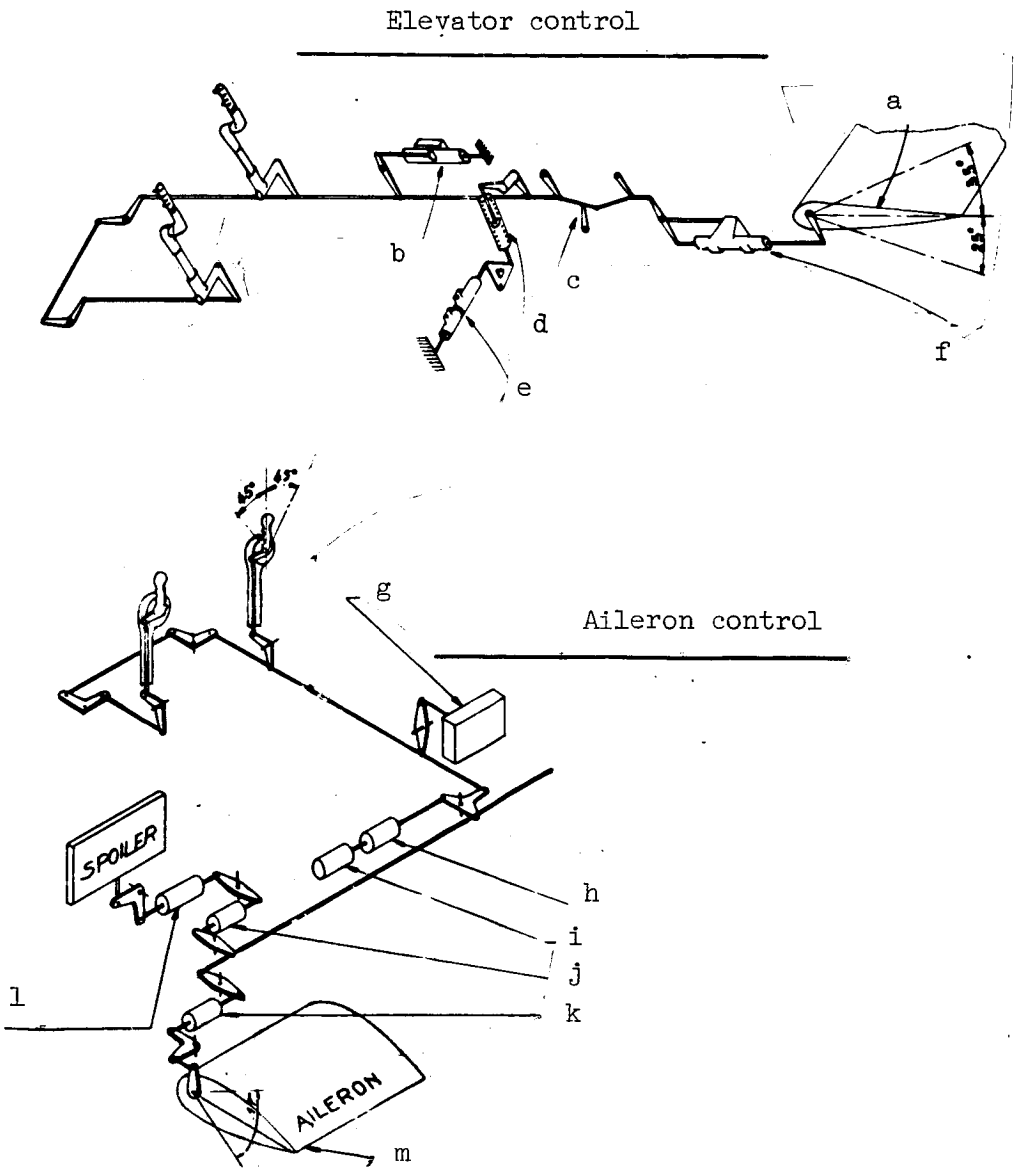

Figure 8. Schematic views of elevator and aileron controls. a, Elevator; b, G restitution Oscar set; c, nonlinear reduction mechanism; d, artificial force device; e, force trim jack; f, servocontrol; g, main propeller pitch control box; h, aileron artificial force device; i, force trim jack; j, spoiler clutch; k, aileron servocontrol; l, spoiler servocontrol; m, aileron deflection (flaps closed).

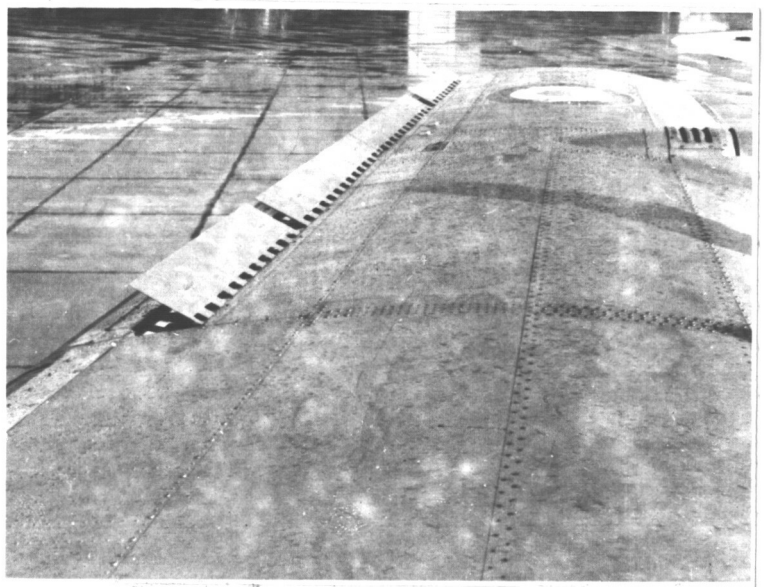

a

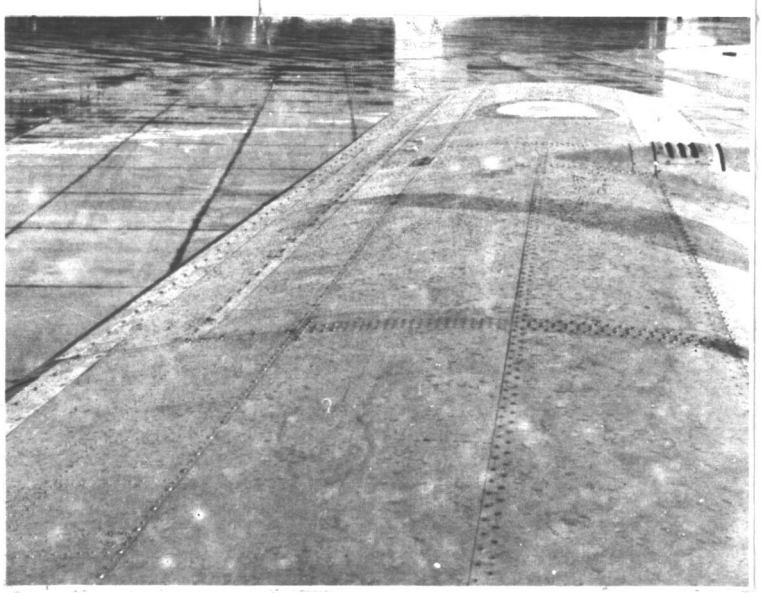

b

Figure 9. Spoilers.
a, In the open position; b, in the closed position.

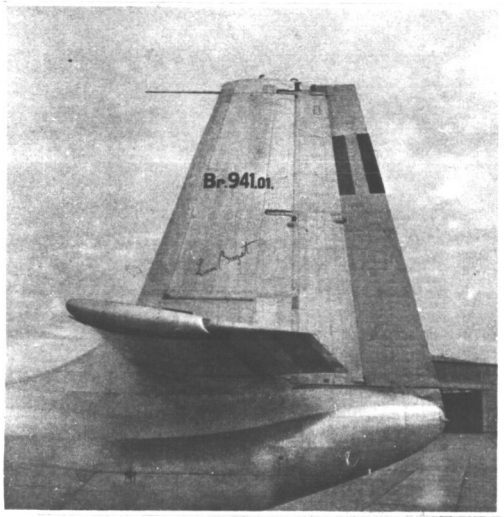

Rudder in neutral

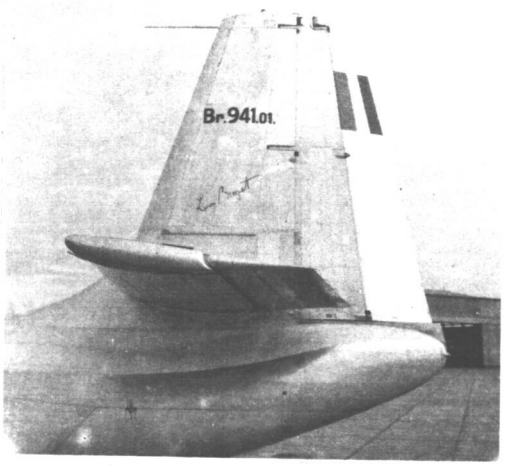

Rudder to the right,
main flap blocked

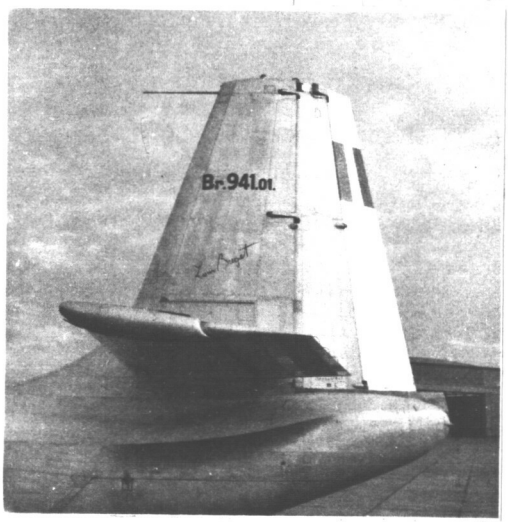

Rudder to the right,
free main flap

Figure 10. Tail fin.

Elevator in neutral

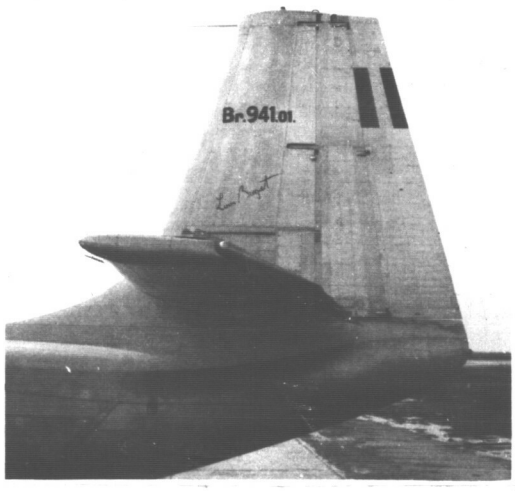

Elevator in nose down position

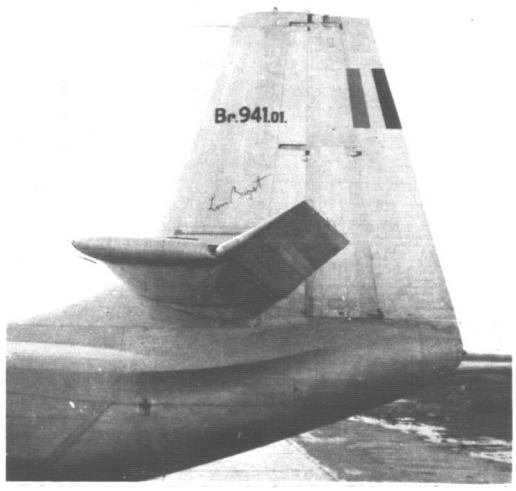

Elevator in nose up position

Figure 11. Elevators

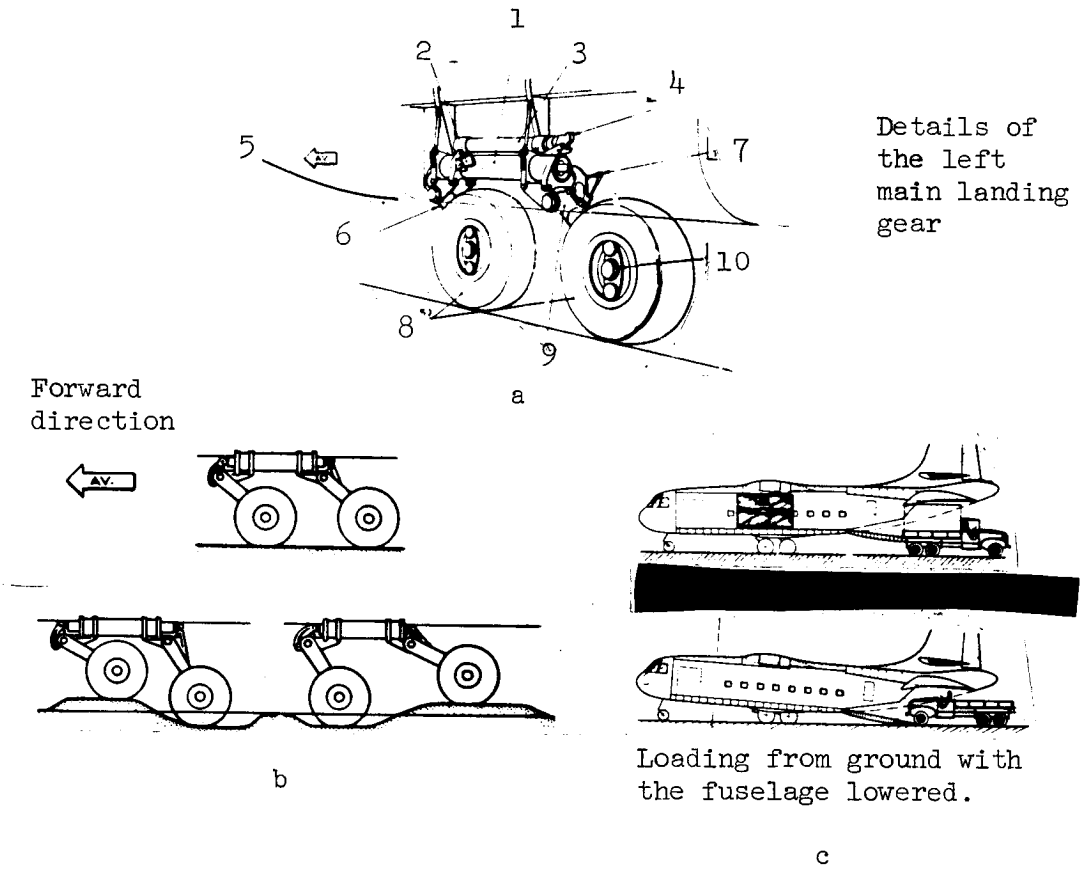

Figure 12. Schematic views of the main landing gear.

a, Principle of operation and loading: 1, jack damper; 2, forward hook-up box; 3, reservoir; 4, rear hook-up box; 5, forward direction; 6, forward torsion bar; 7, hook-up block for gear up position; 8, tires type 14 (950-335); 9, rear torsion bar; 10, Messier-type brake equipped with a Ministop device. b, Action over various surfaces. c, Loading principle.

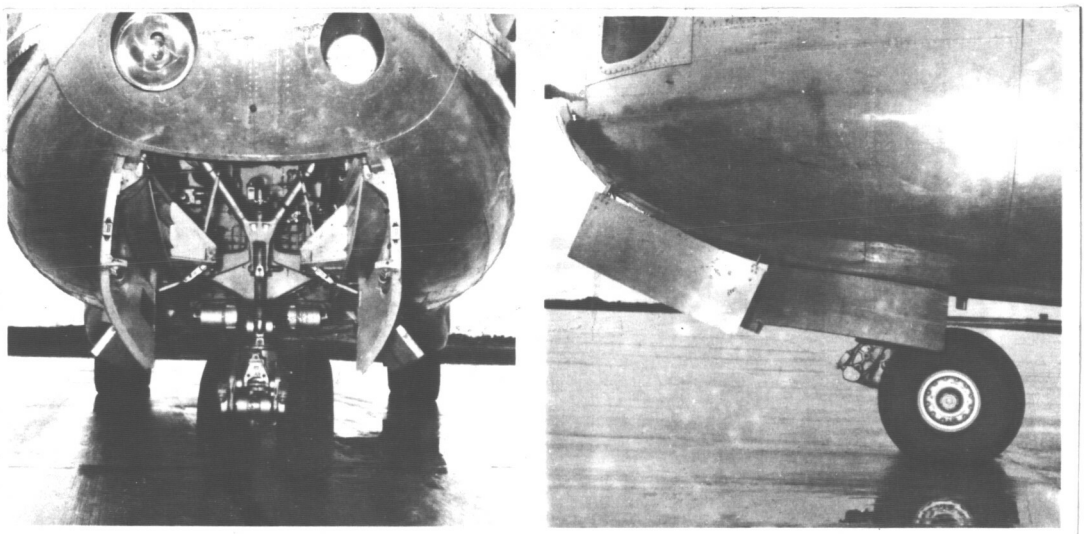

Forward gear

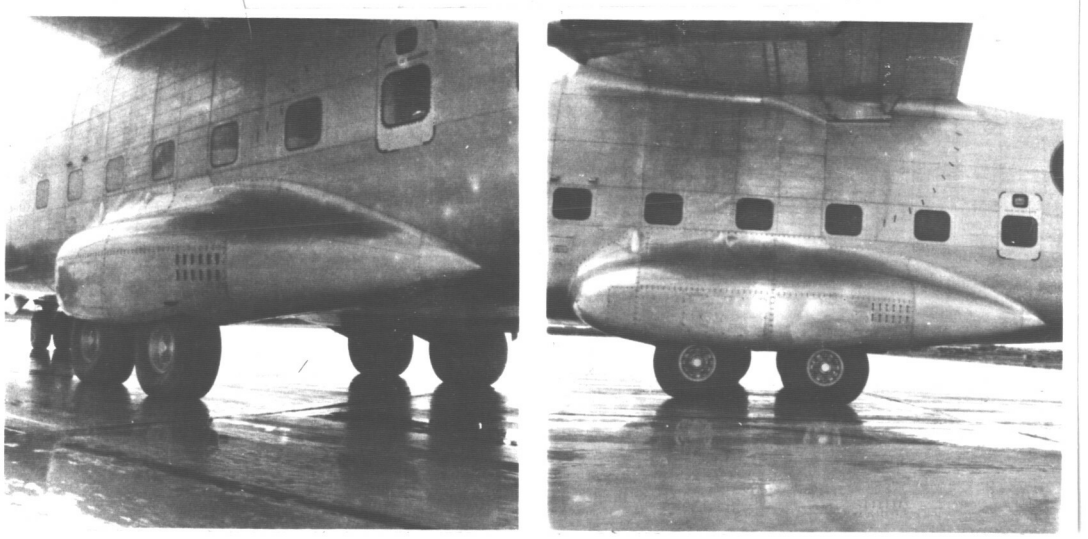

Main gear

Figure 13. Views of the landing gears.

Fuselage horizontal

Fuselage lowered

Figure 14. Loading device.

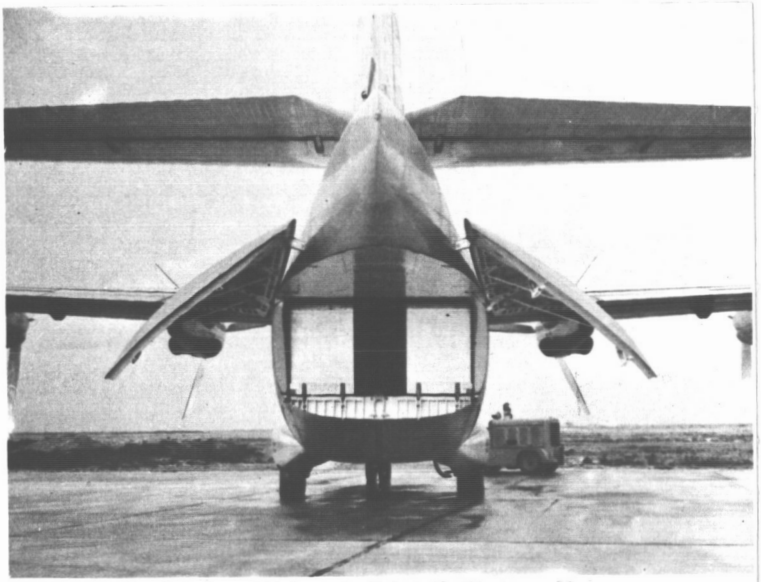

a

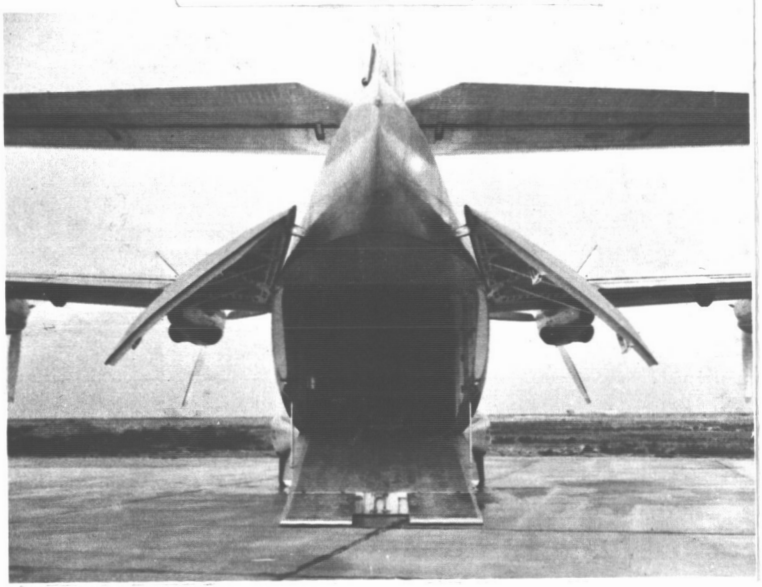

b

Figure 15. Loading, detailed views.

a, Rear doors. Ramp in the stowed position.
b, Access ramp in the down position.

Instrument panel

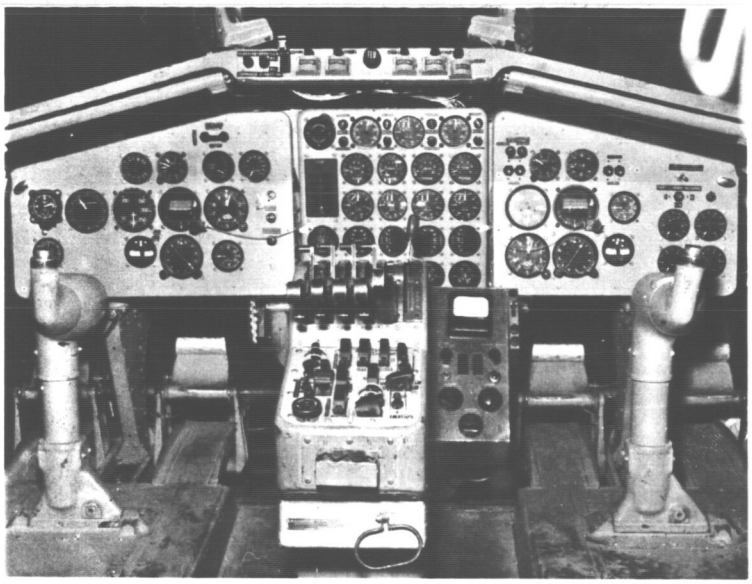

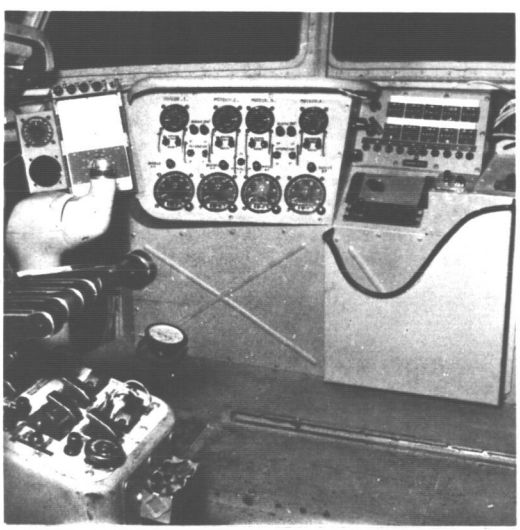

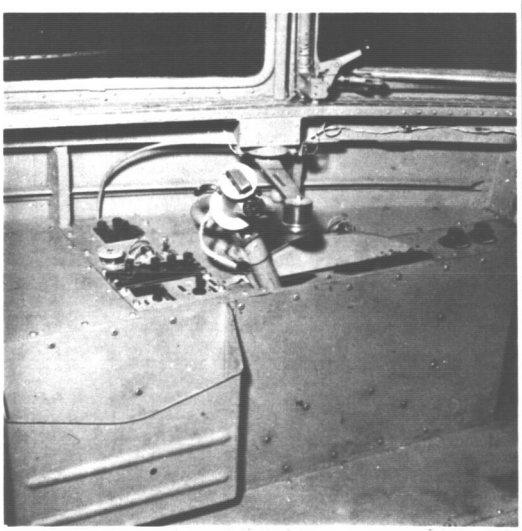

Right seat

Left seat

Figure 16. Cockpit: instrument panel and seats.

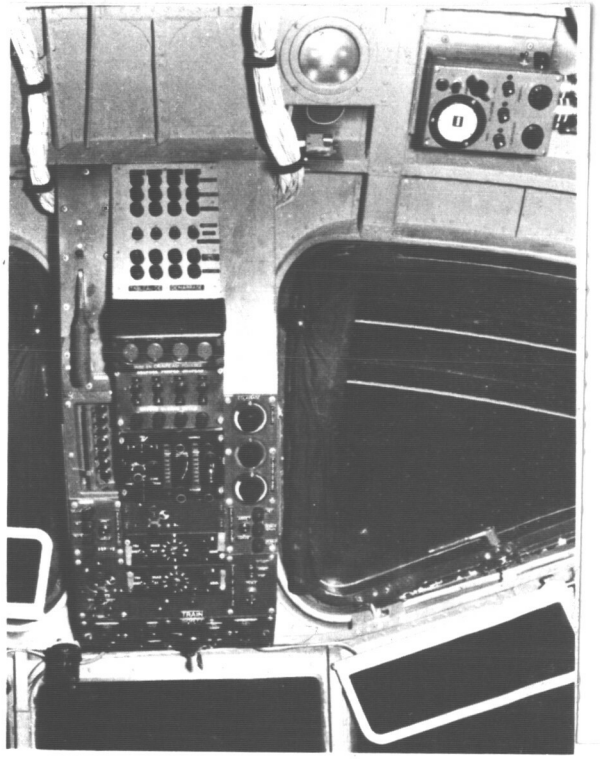

Upper panel, center

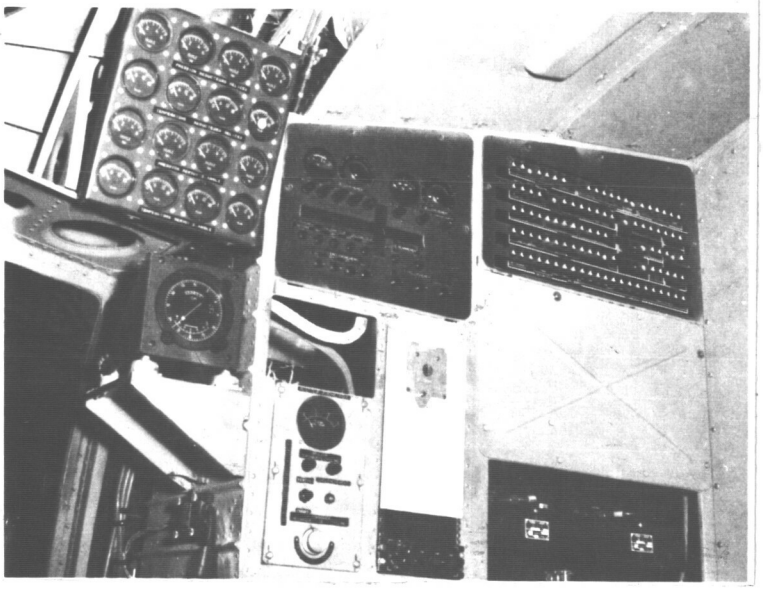

Upper panel, right (flight mechanics position)

Figure 17. Cockpit: Instrument panel and mechanic seat.

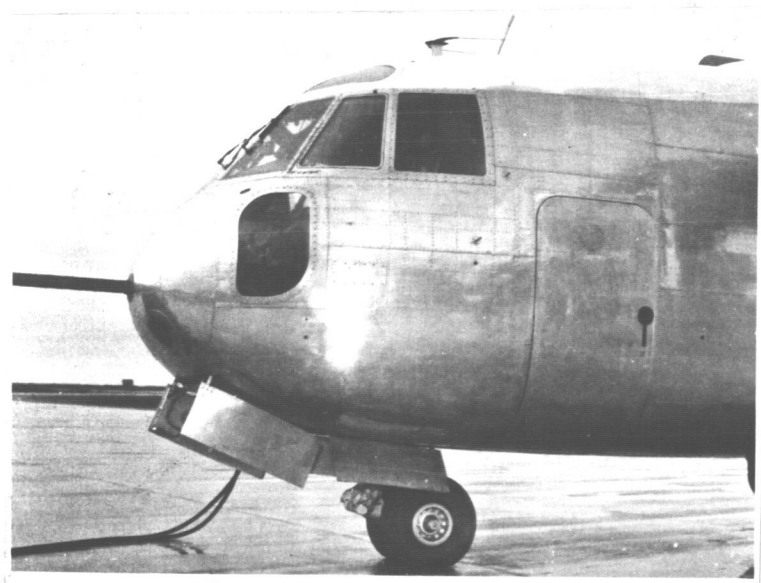

Closed

Open

Figure 18. Access door.

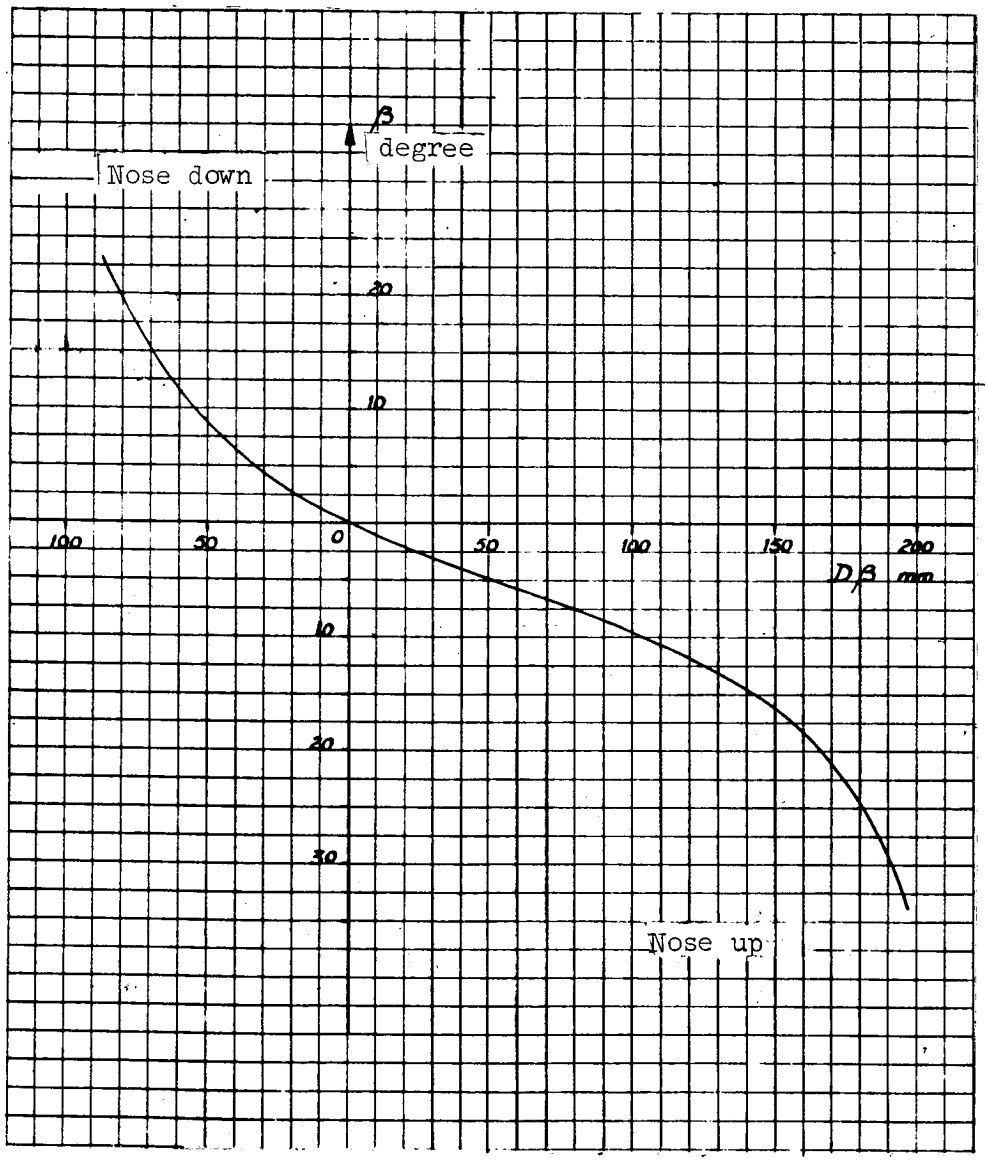

Figure 19. Relation between stick deflection and elevator deflection.

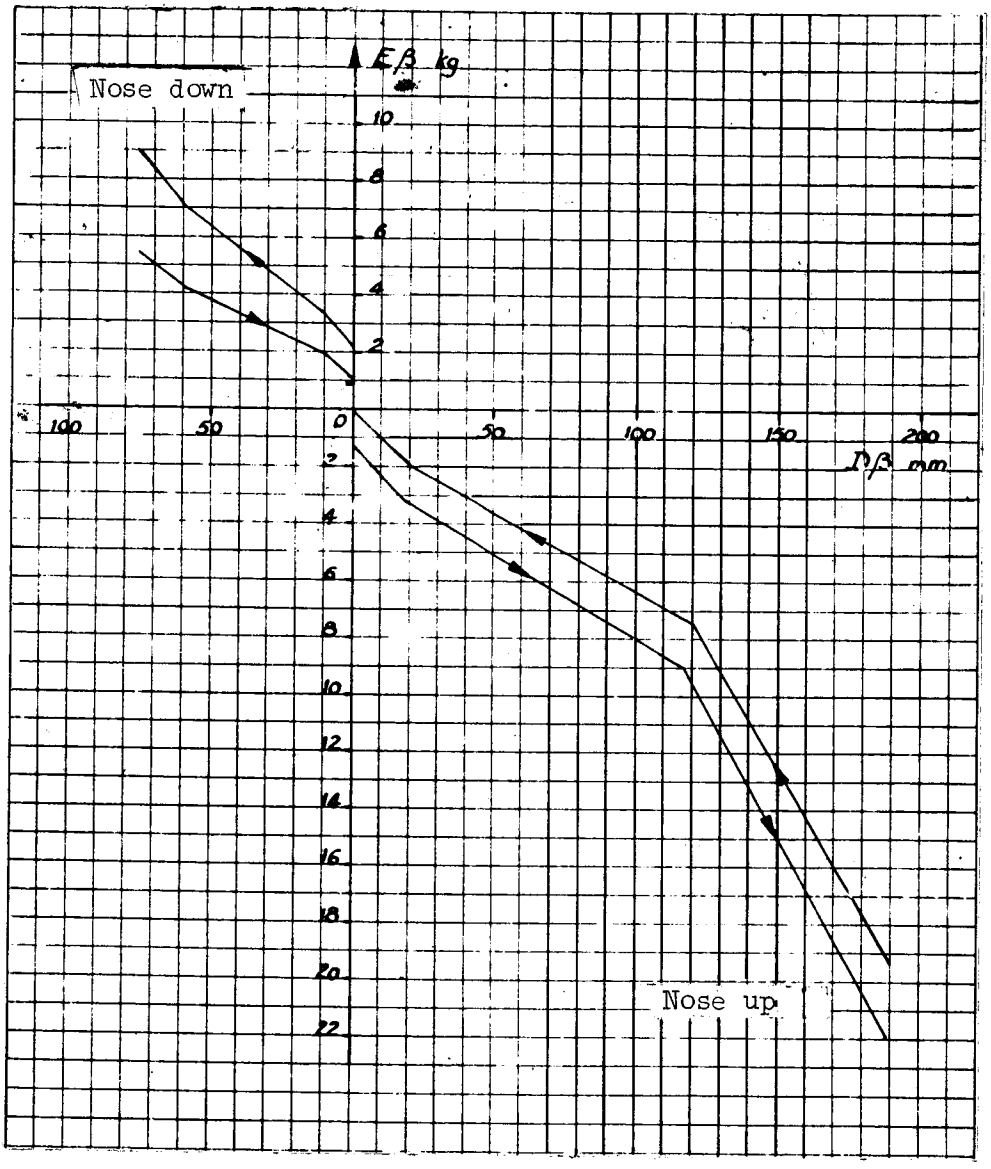

Figure 20. Elevator control forces.

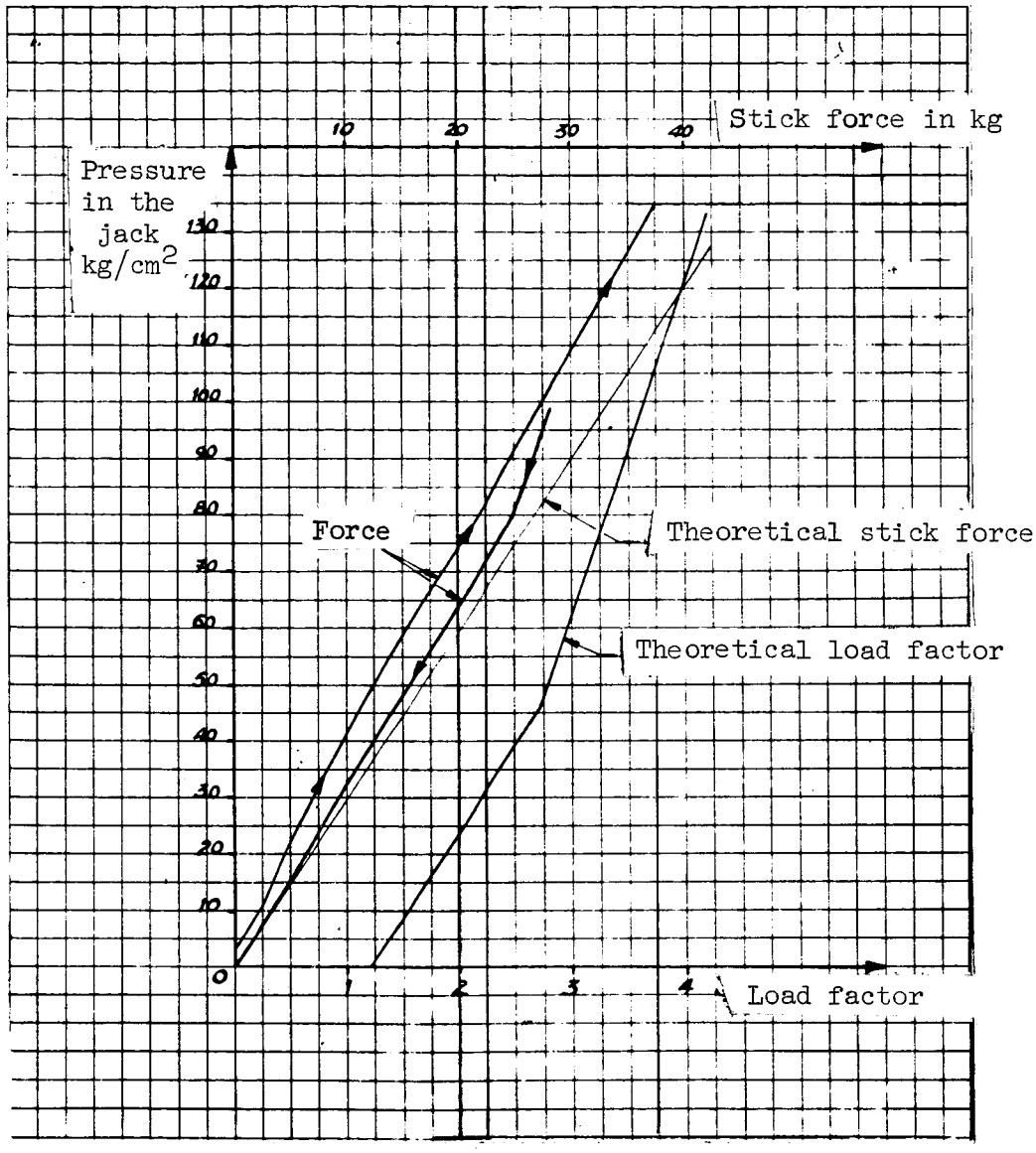

Figure 21. Elevator Oscar valve adjustment curves.

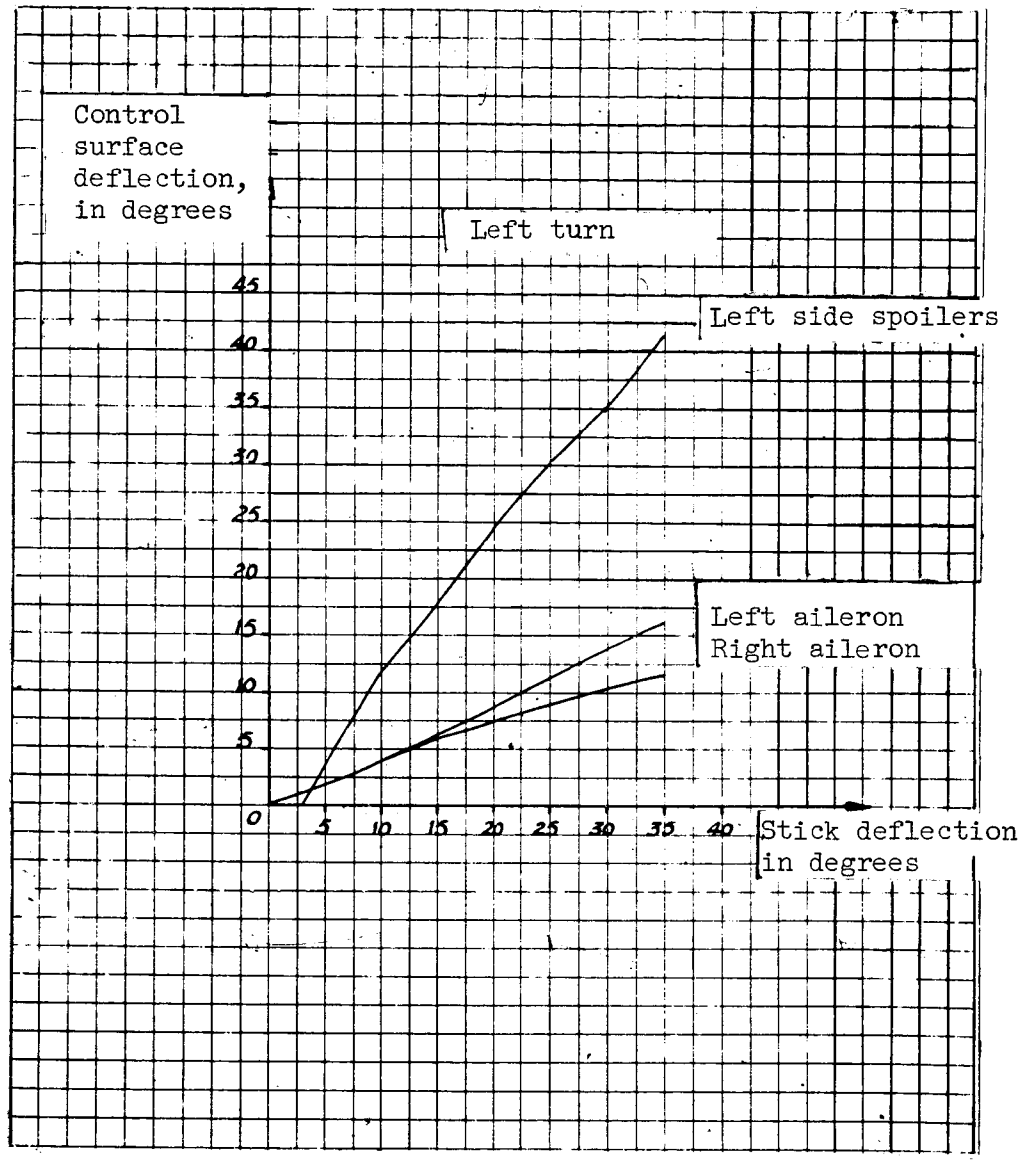

Figure 22. Aileron and spoiler deflection variations.

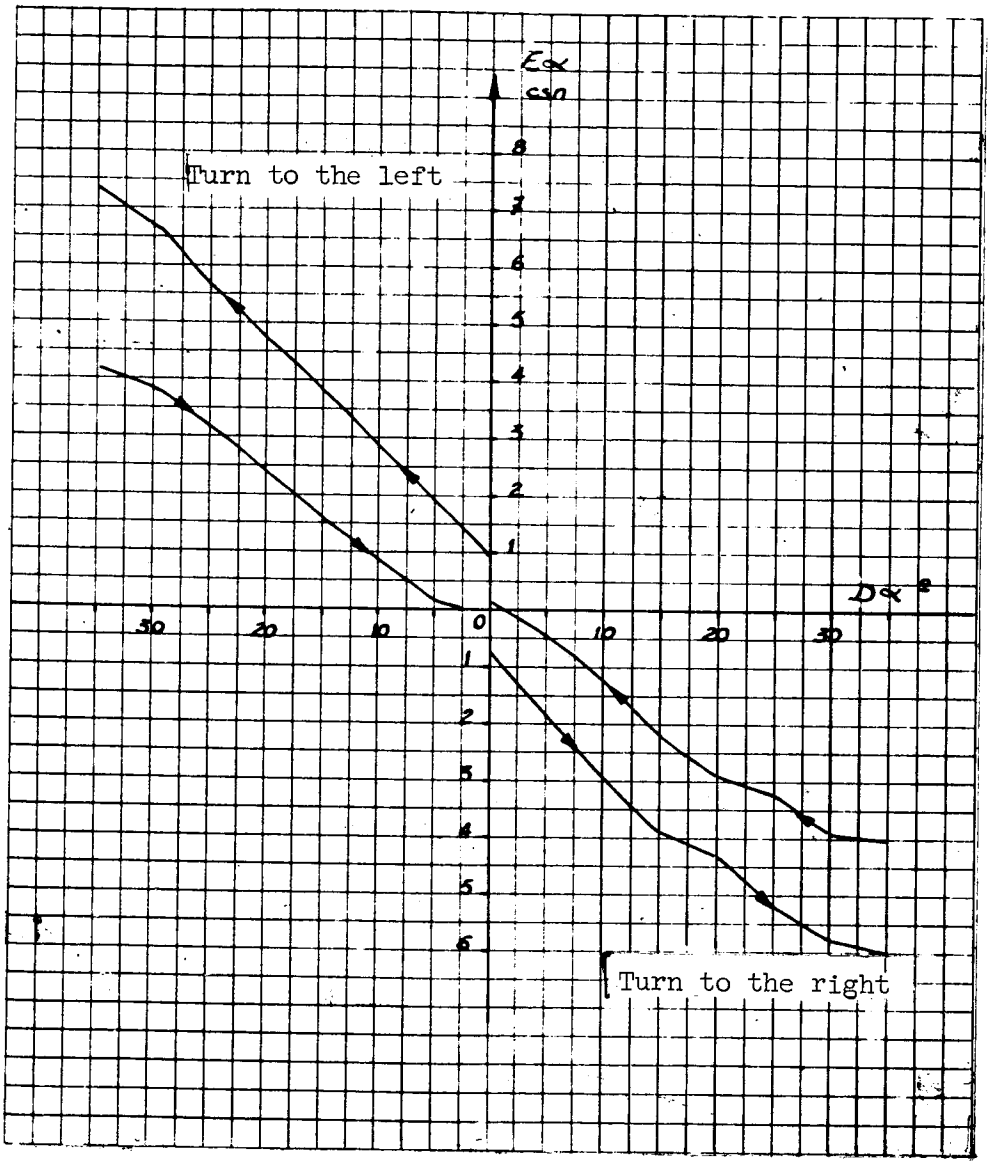

Figure 23. Aileron control forces.

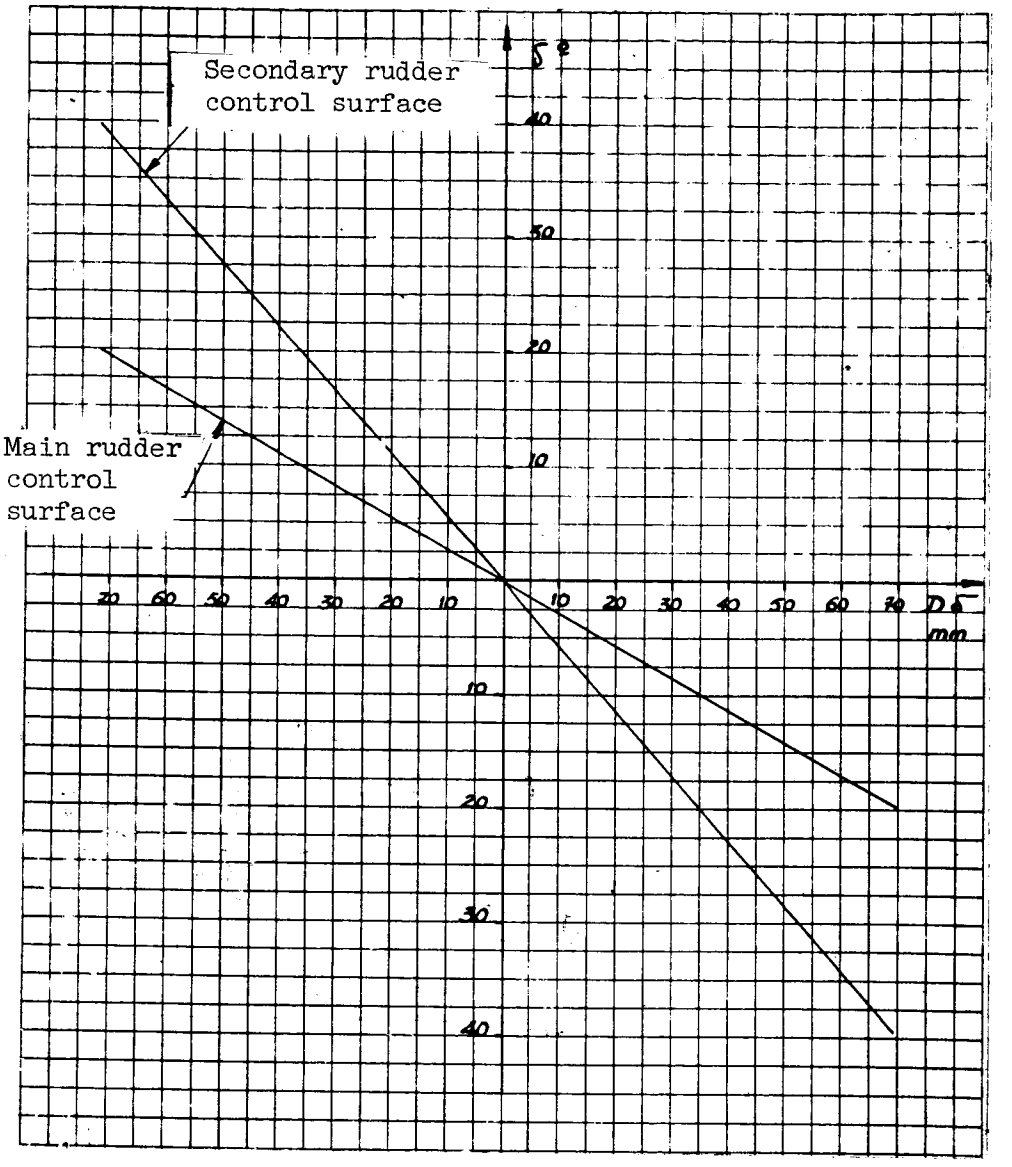

Figure 24. Relation between rudder control and rudder.

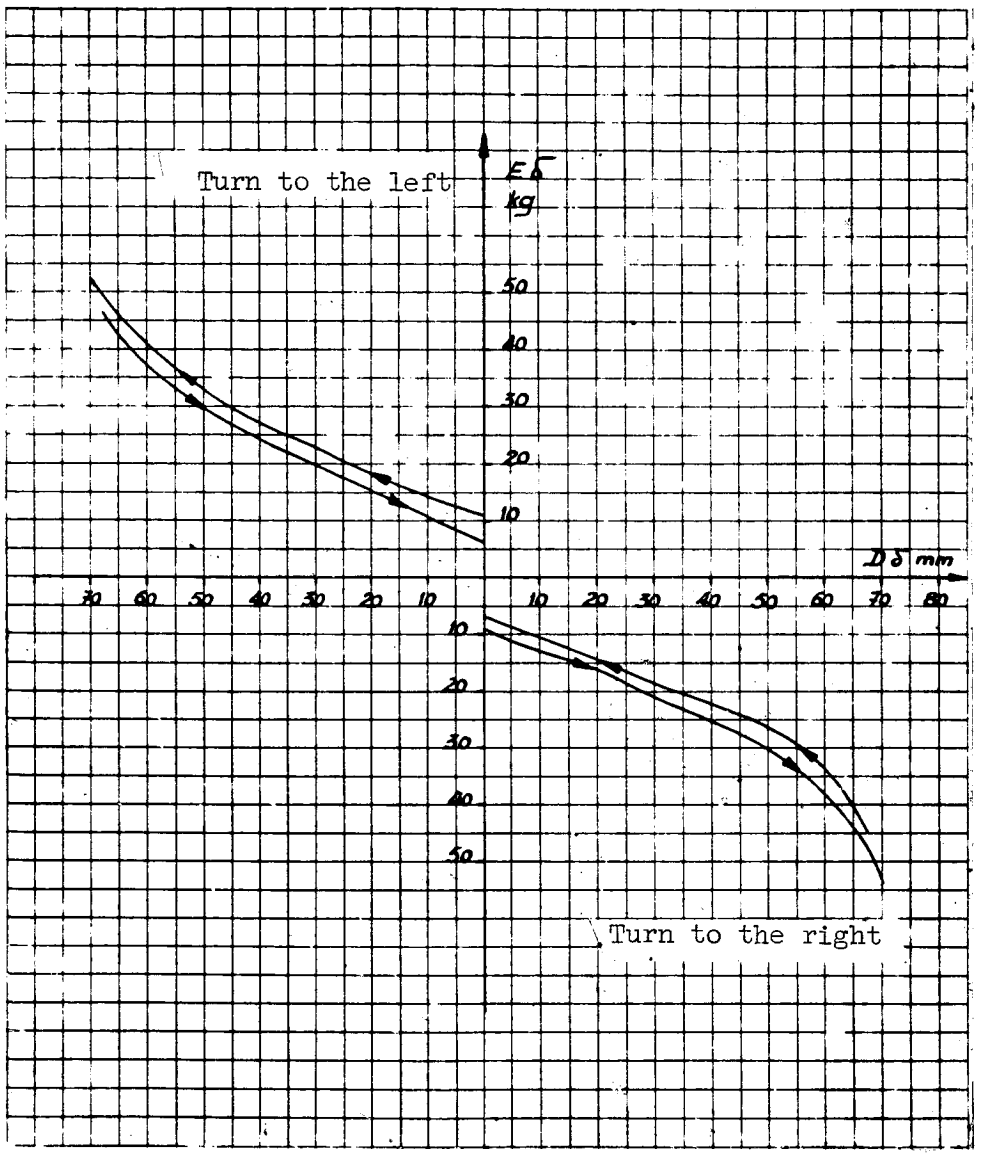

Figure 25. Rudder control forces.

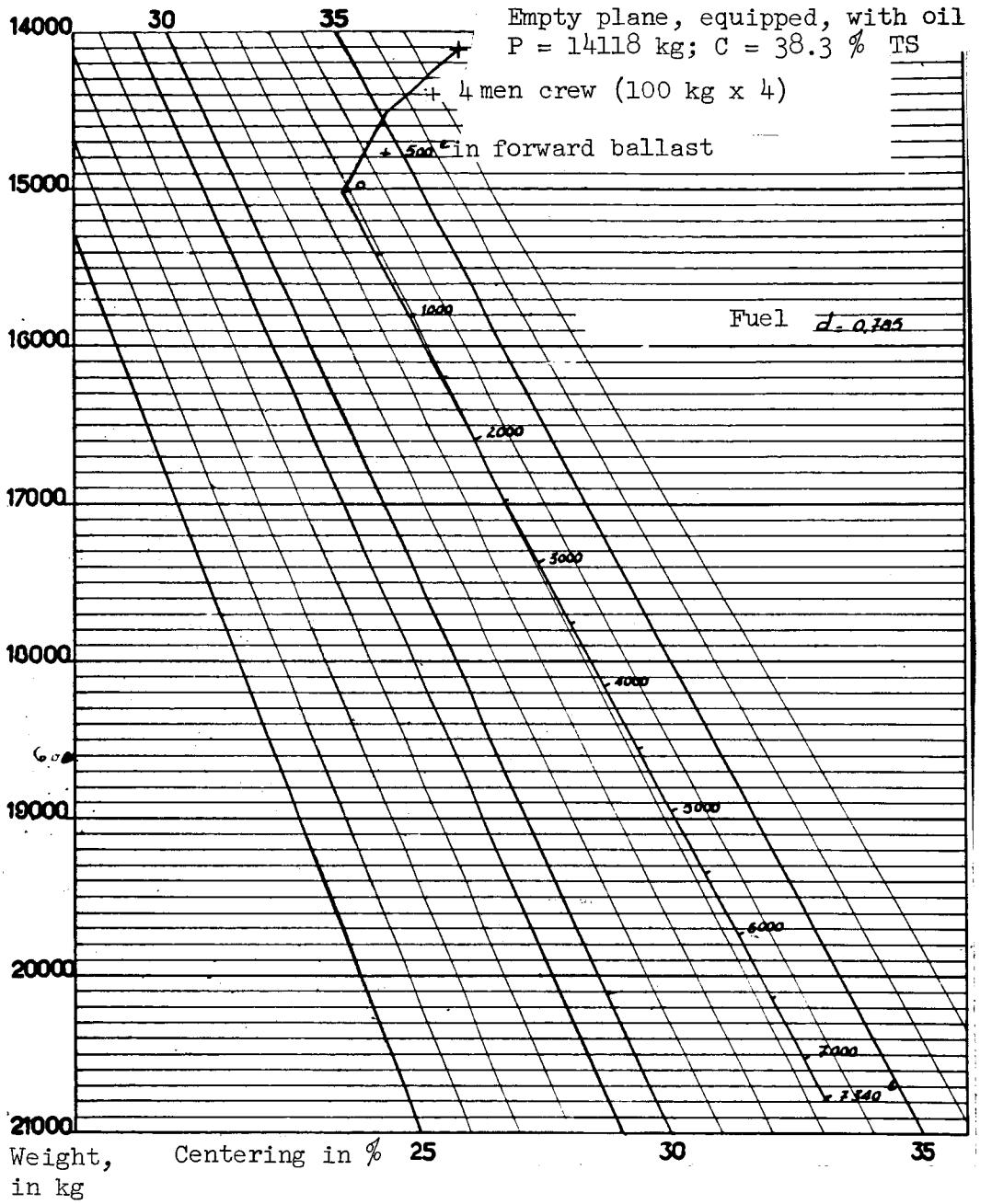

Figure 26. Centrogram.

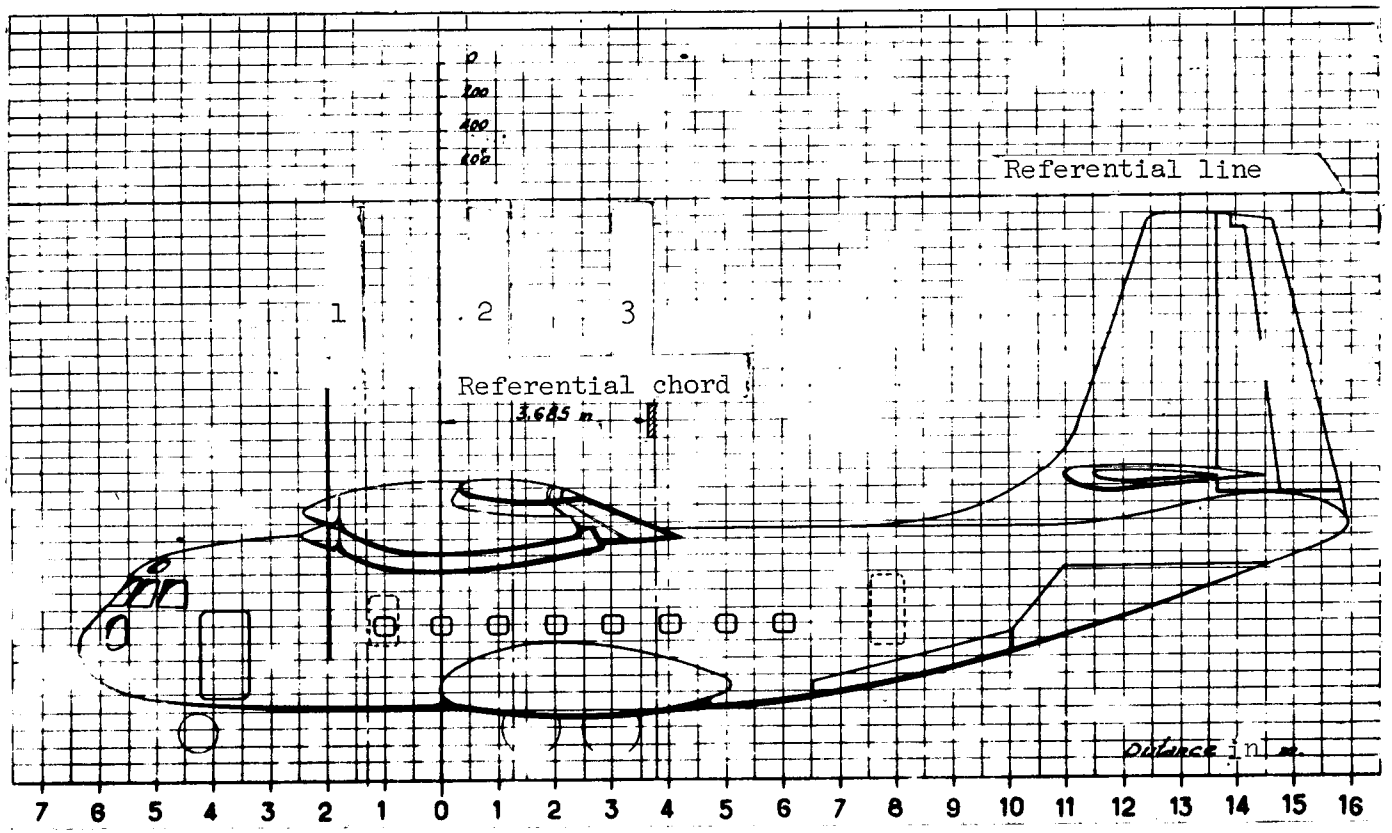

Figure 27. Center calculation.
1, 2 and 3, forward, central and rear ballast, respectively.

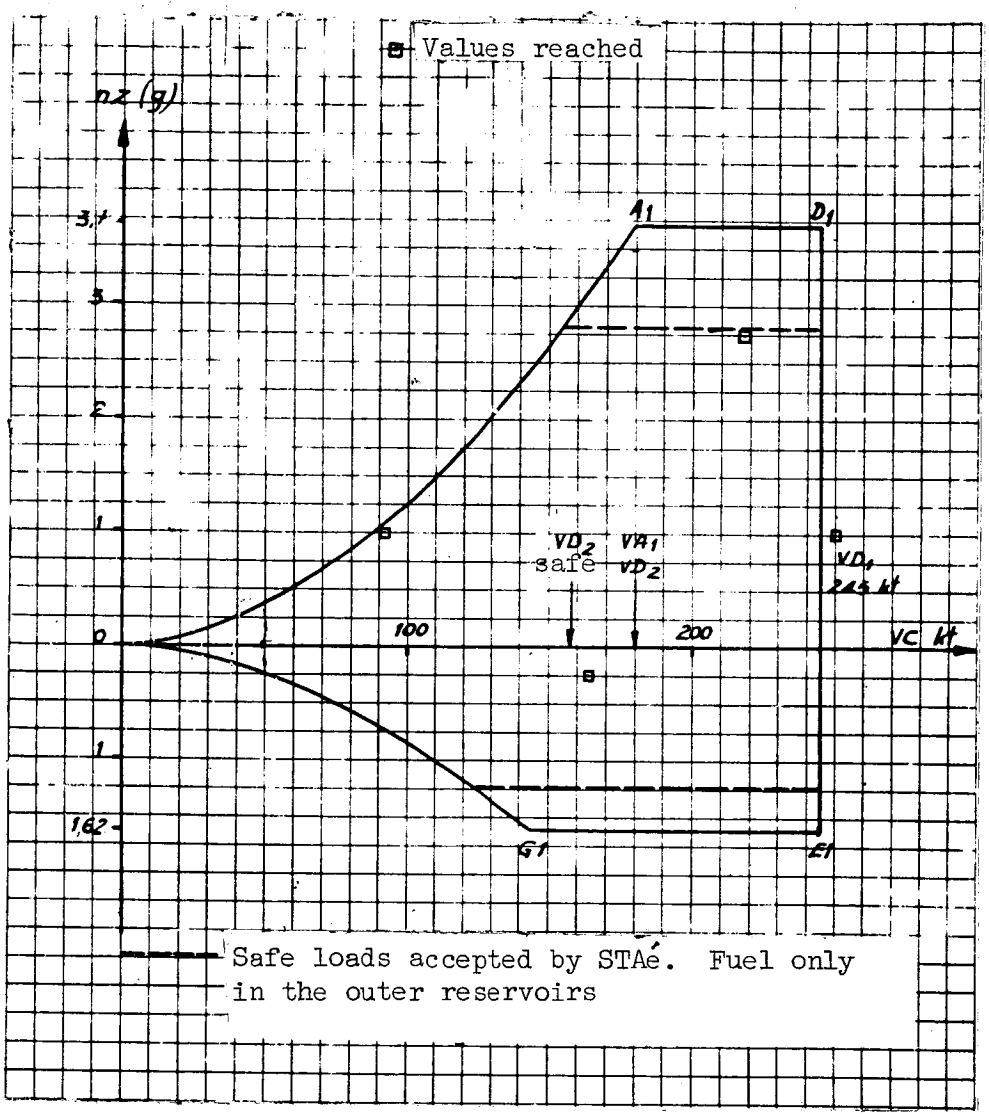

Figure 28. Case D_1.

(for 19,050 kg weight)

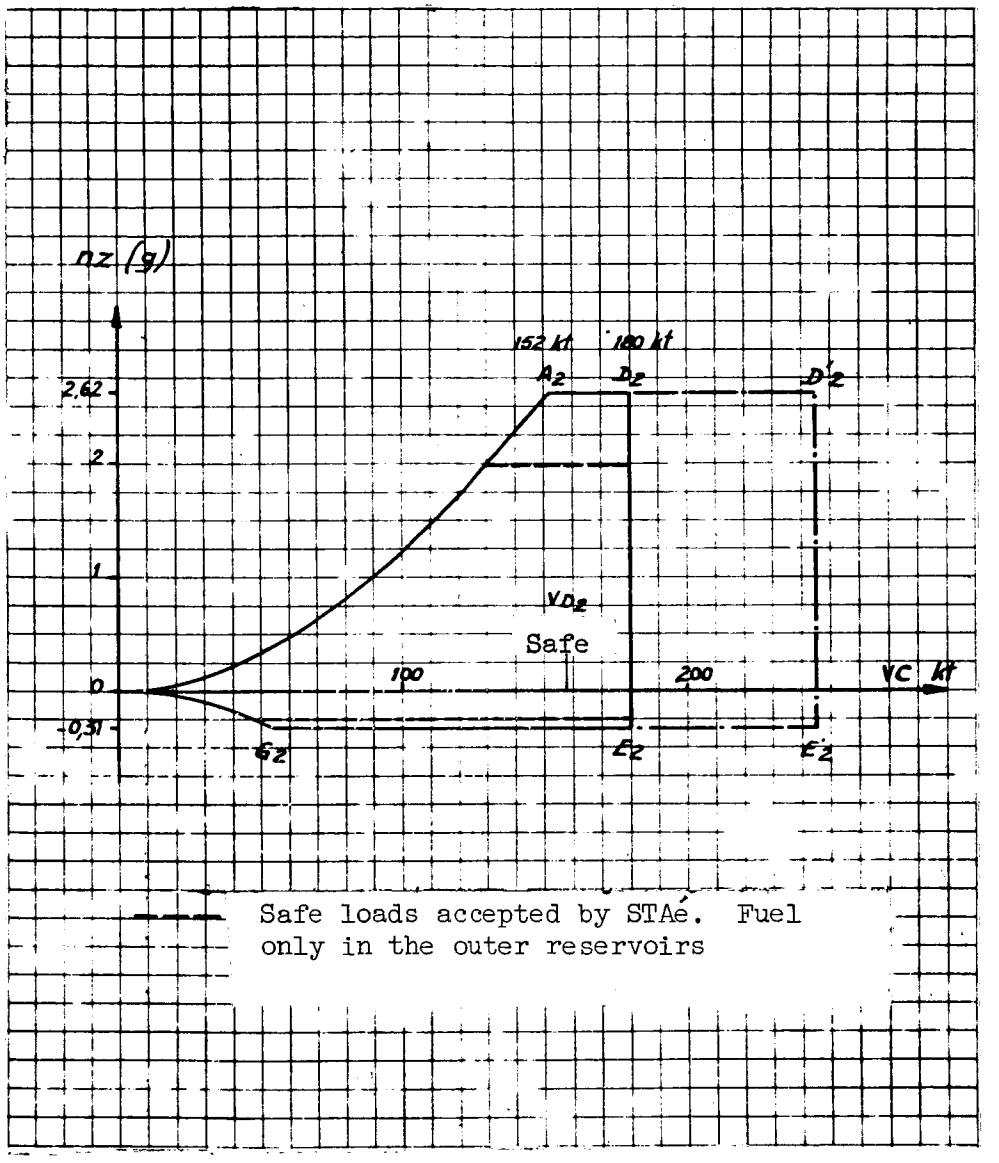

Figure 29. Case D_2.

(for 19,050 kg weight)

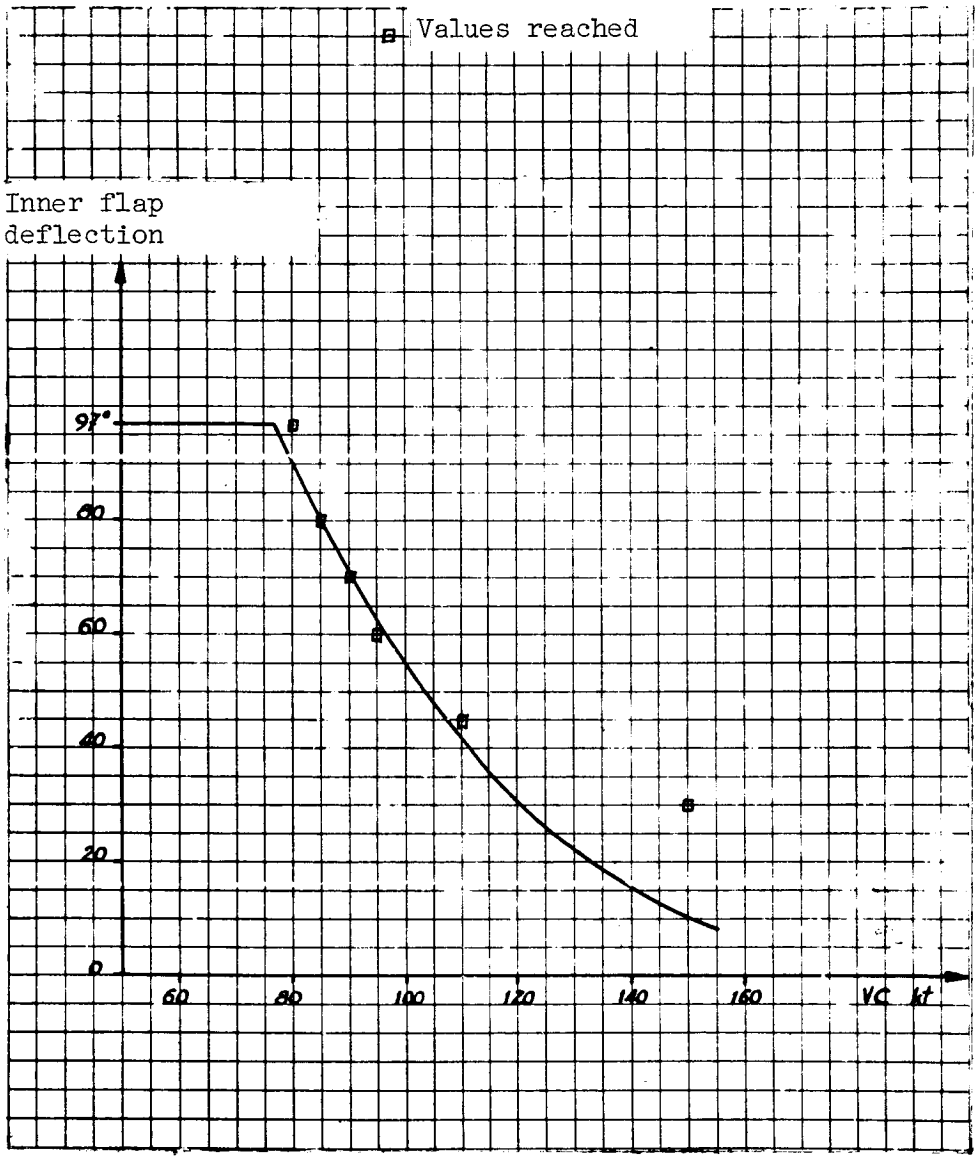

Figure 30. Inner flap deflection limit as a function of Vc.

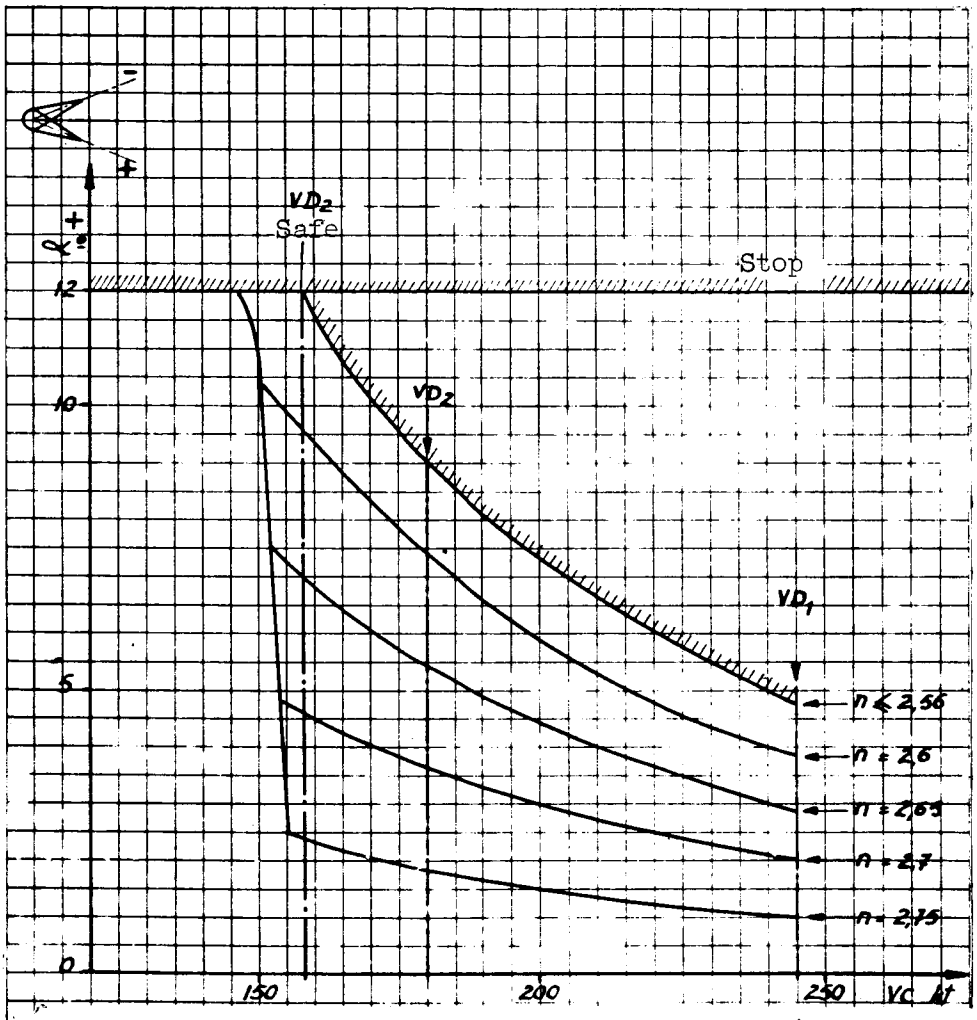

Note: The aileron servo controls 2 x 3000 kg (2 bodies at P = 210 kg/cm^2 permit to have complete deflection for all Vc.

Figure 31. Aileron deflection limits as functions of Vc and of the loading factor. (For 19,050 kg weight, safe loads+)

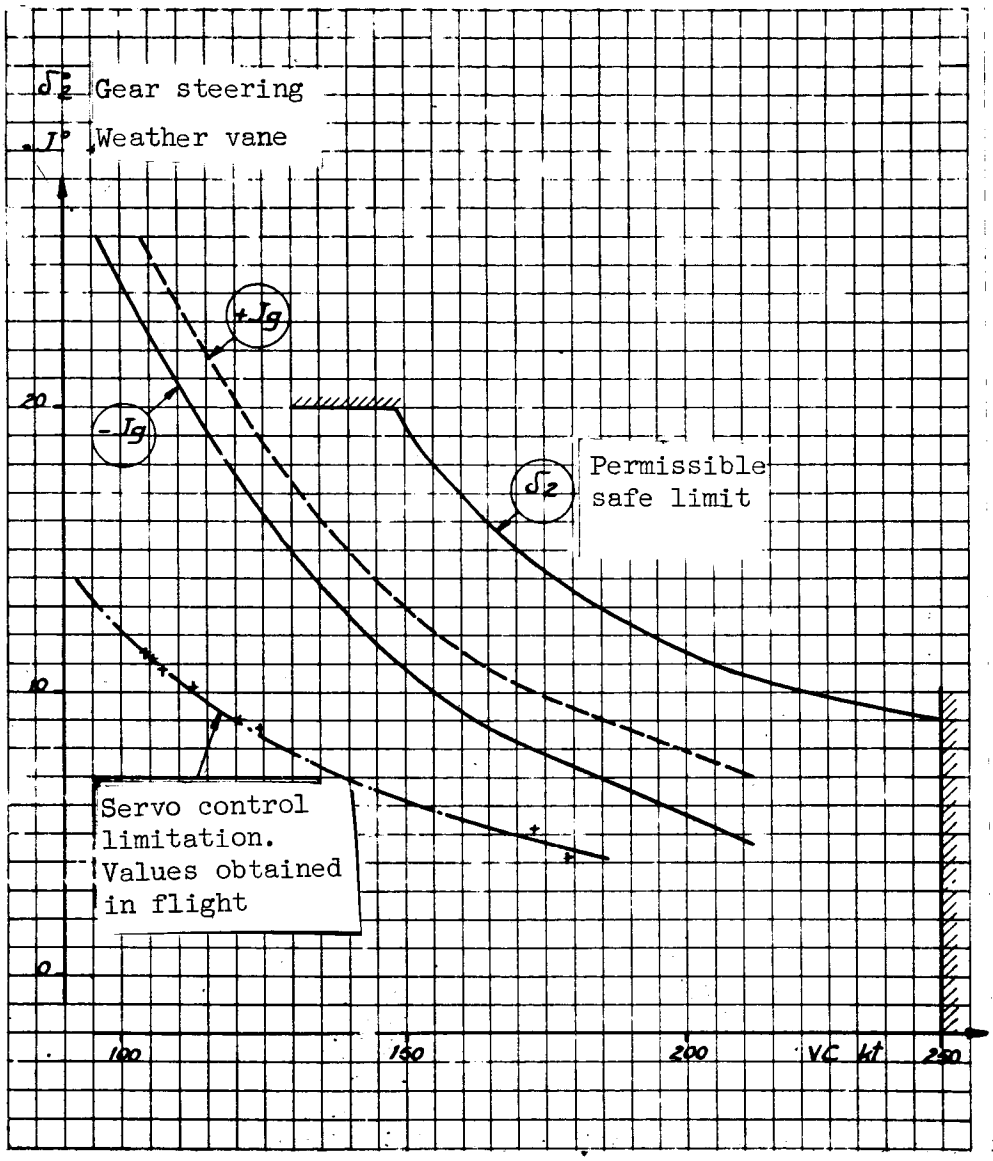

Figure 32. Safe lateral limits.
(In skidding - In rudder deflection.)

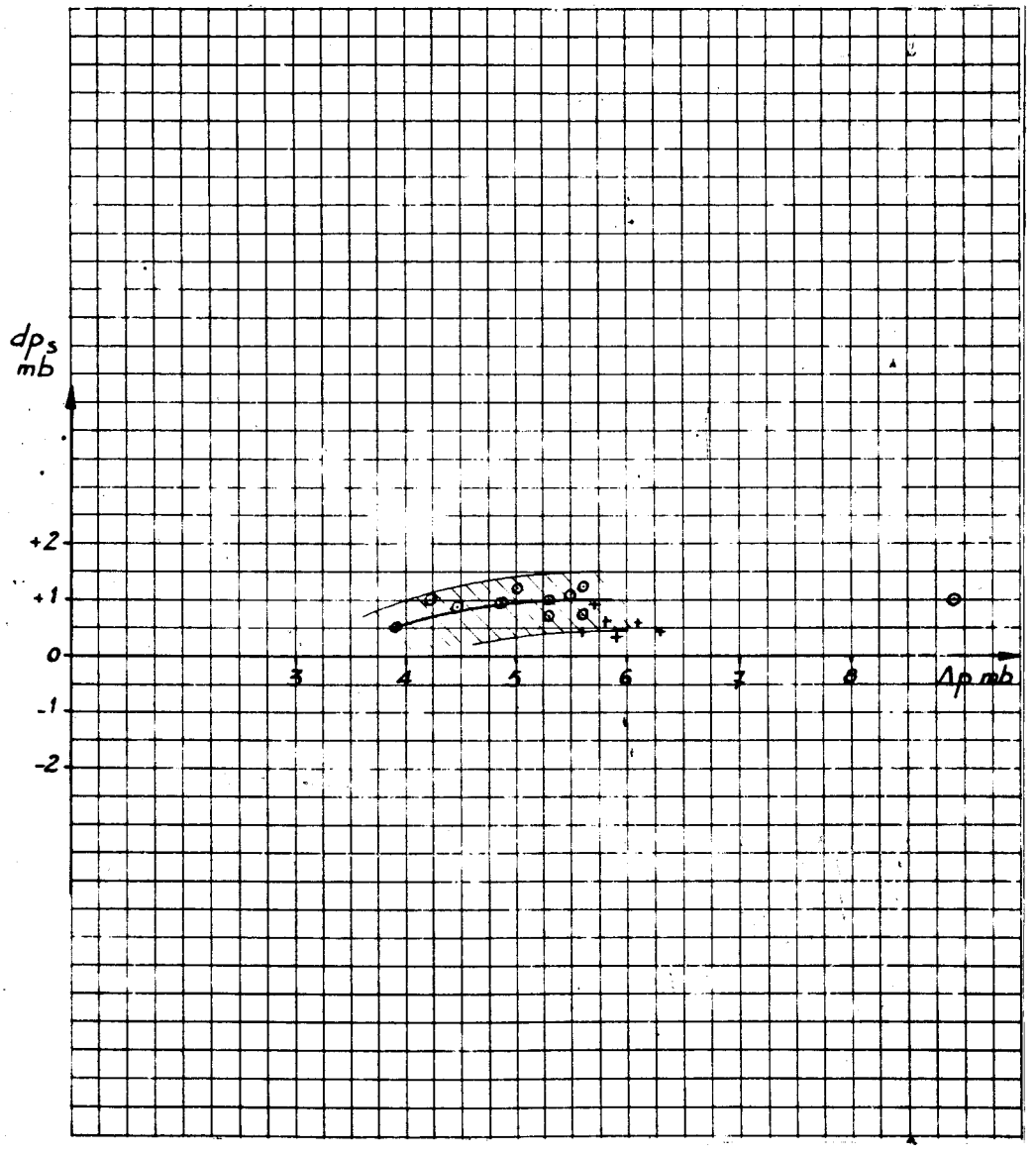

Figure 33. Anemometer calibration in landing configuration.

o Antenna calibration by the velocity measurement method
+ Antenna calibration by the method of "passes at the tower"
Boom antenna - TS.VS configuration. Average blowings

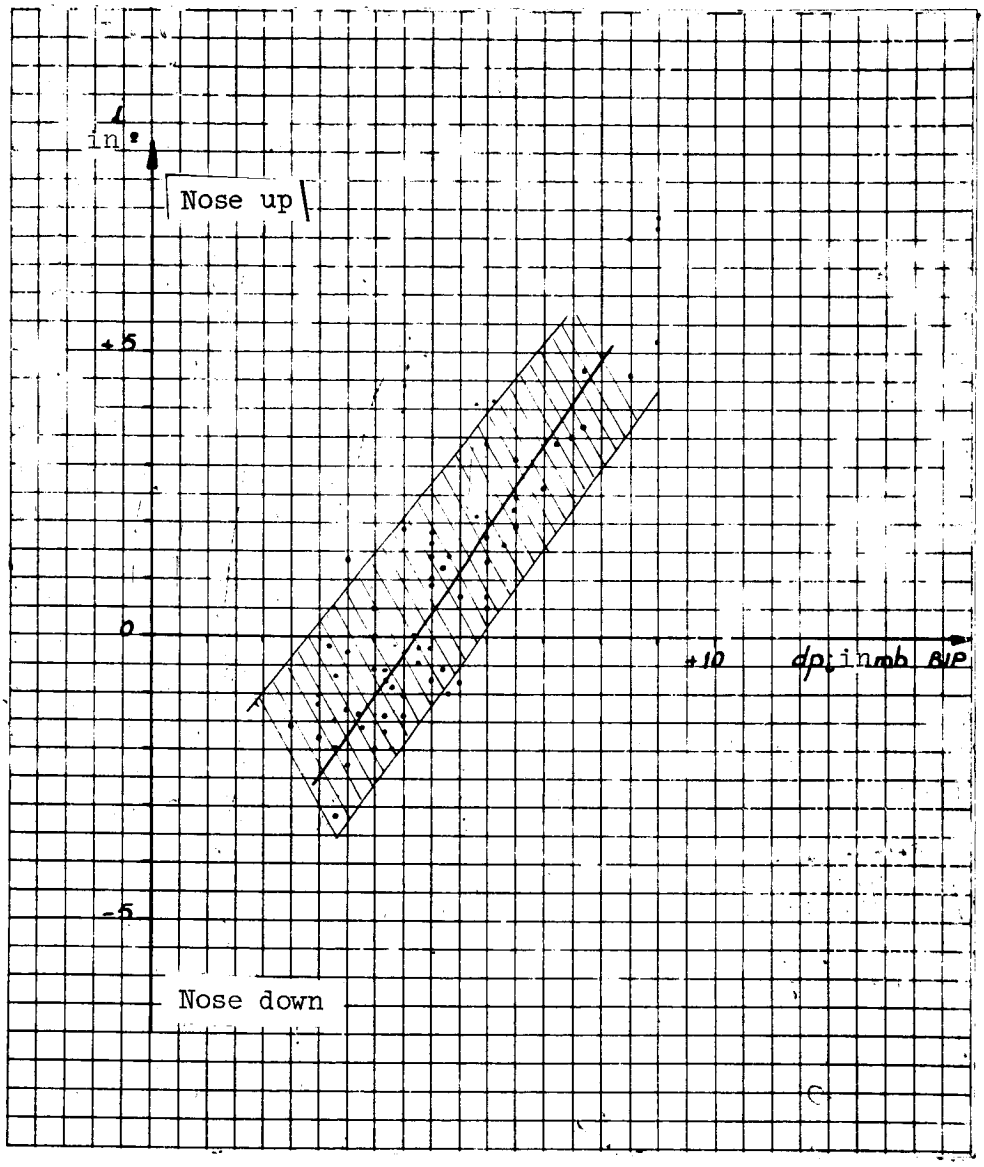

Figure 34. Pitch calibration in landing configuration.

(i true = f(dpi) pressure probe (BIP); low velocities; flaps at 97°; landing gear deployed.)

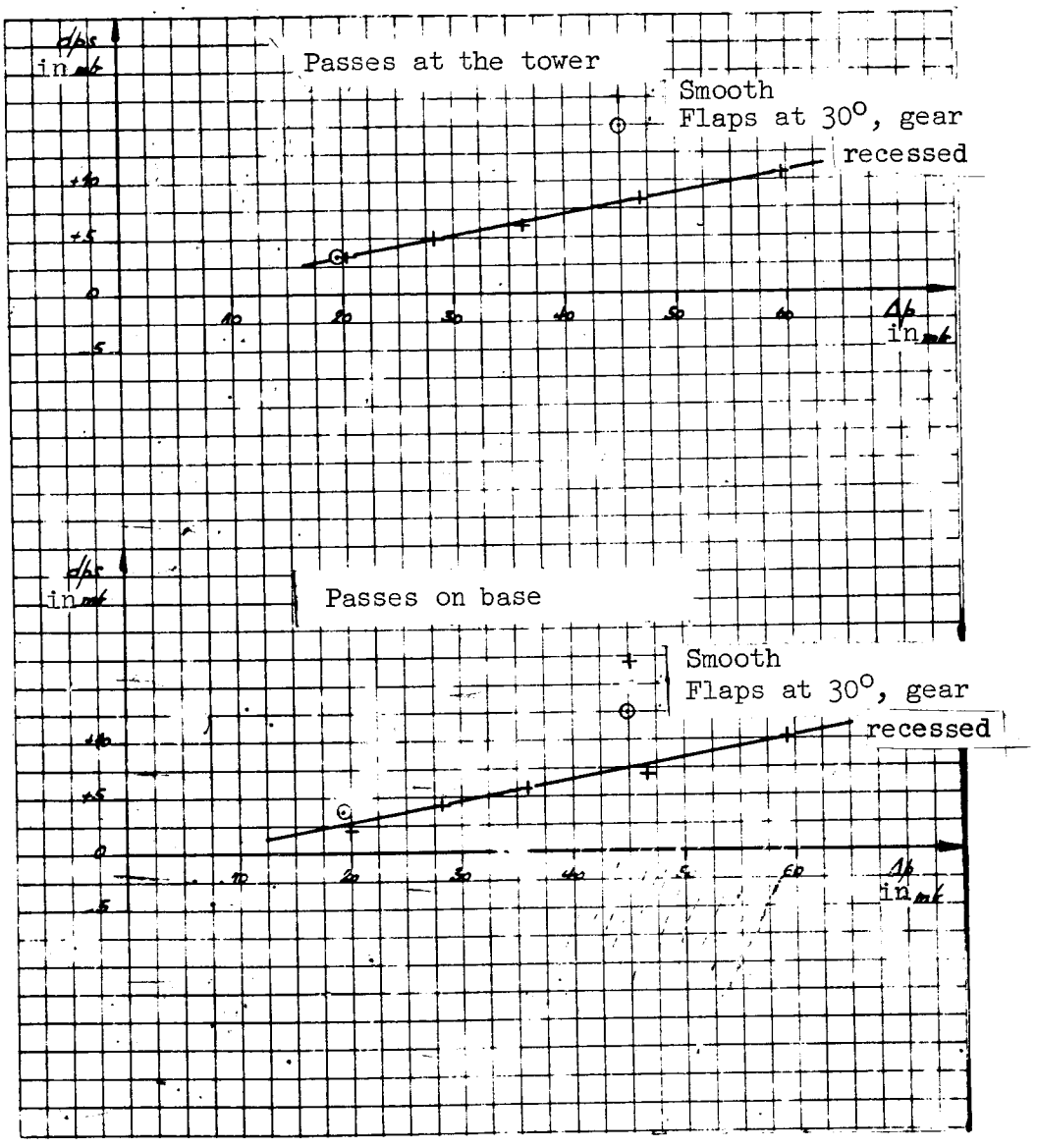

Figure 35. Boom antenna calibration.

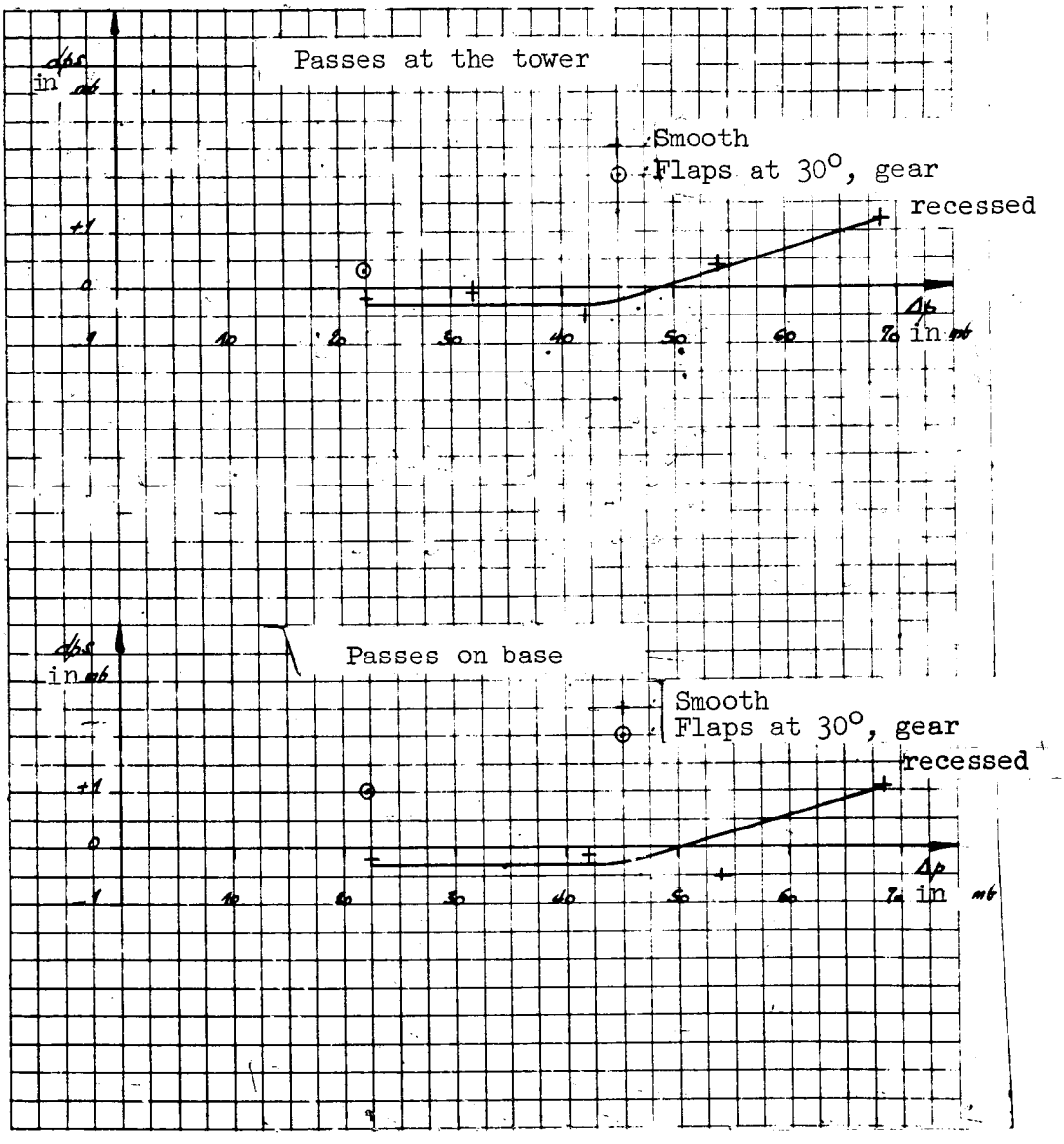

Figure 36. Gerbier antenna calibration.

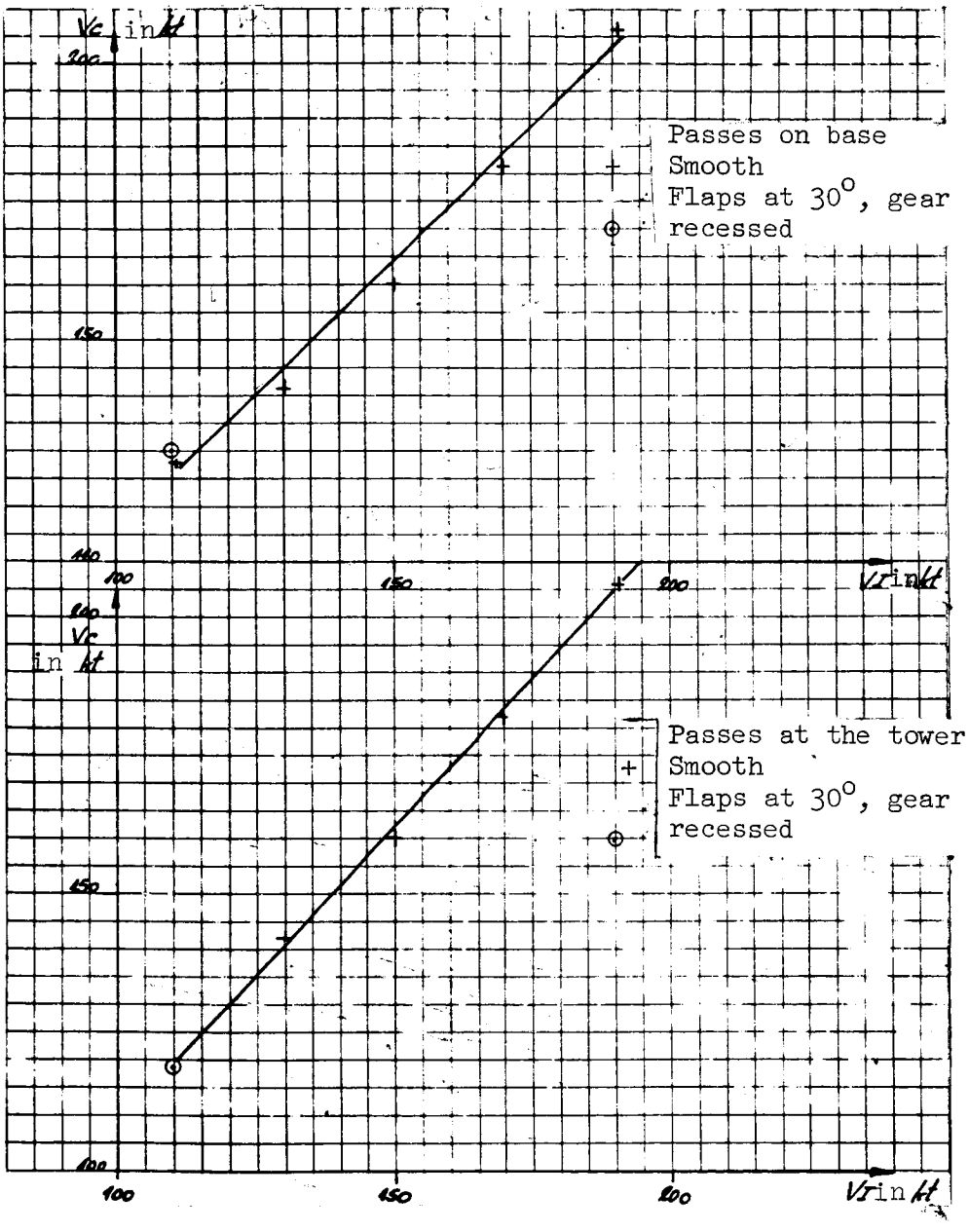

Figure 37. Vc, Vi calibration curves for the boom antenna.

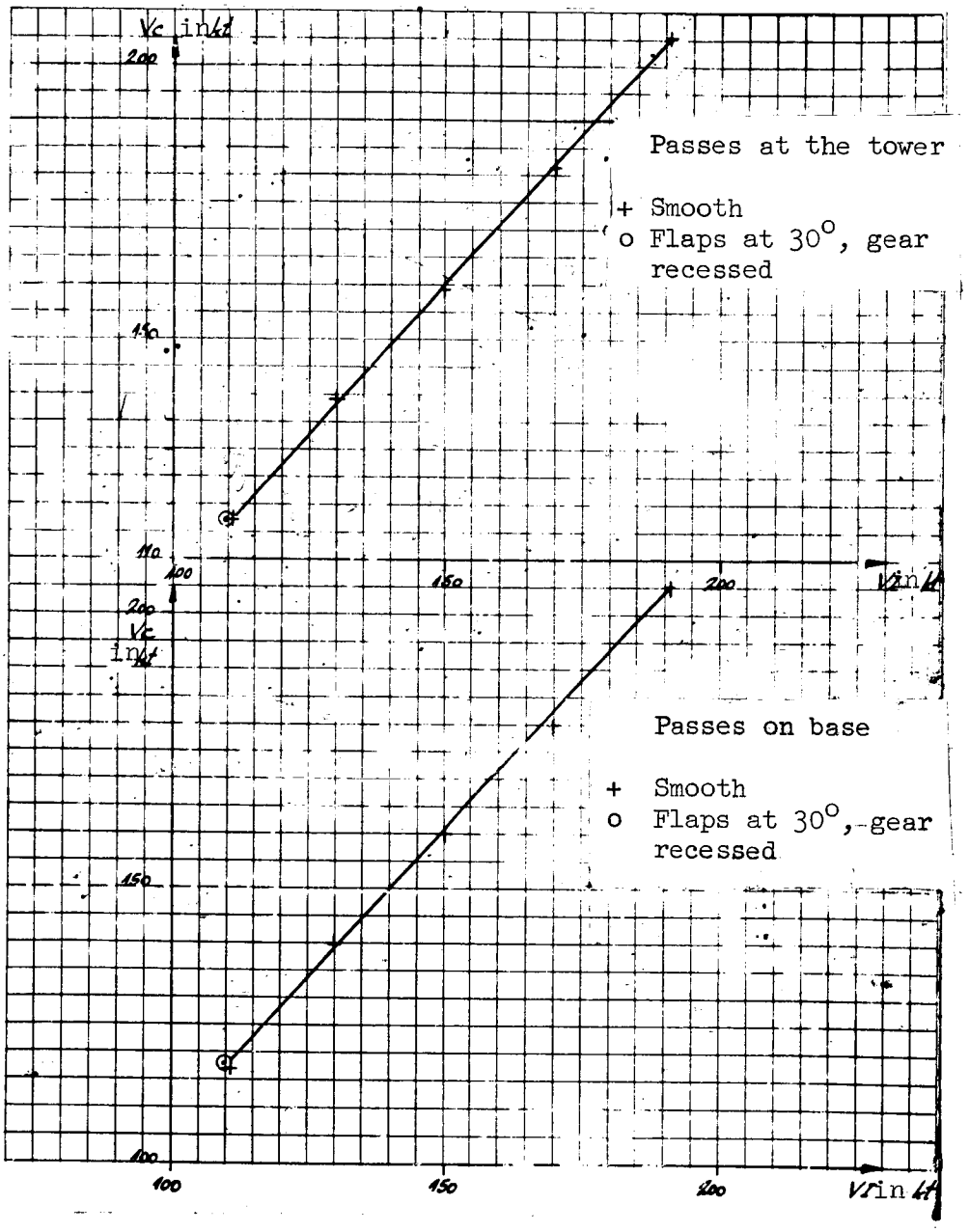

Figure 38. Vc, Vi calibration curves for the Gerbier antenna.

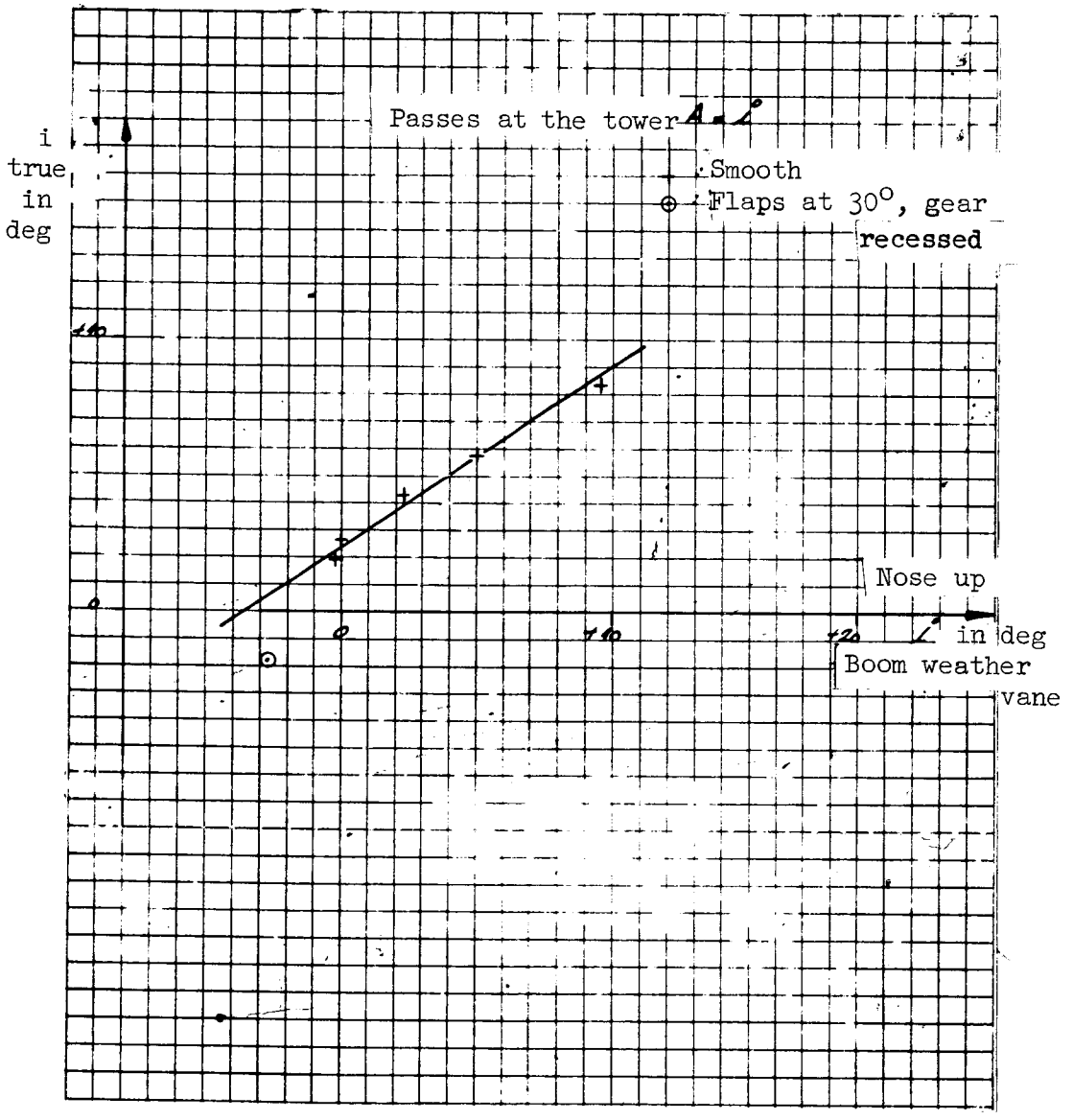

Figure 39. Weather vane pitch calibration.

$i_{true} = f(i_{boom\ weather\ vane})$.

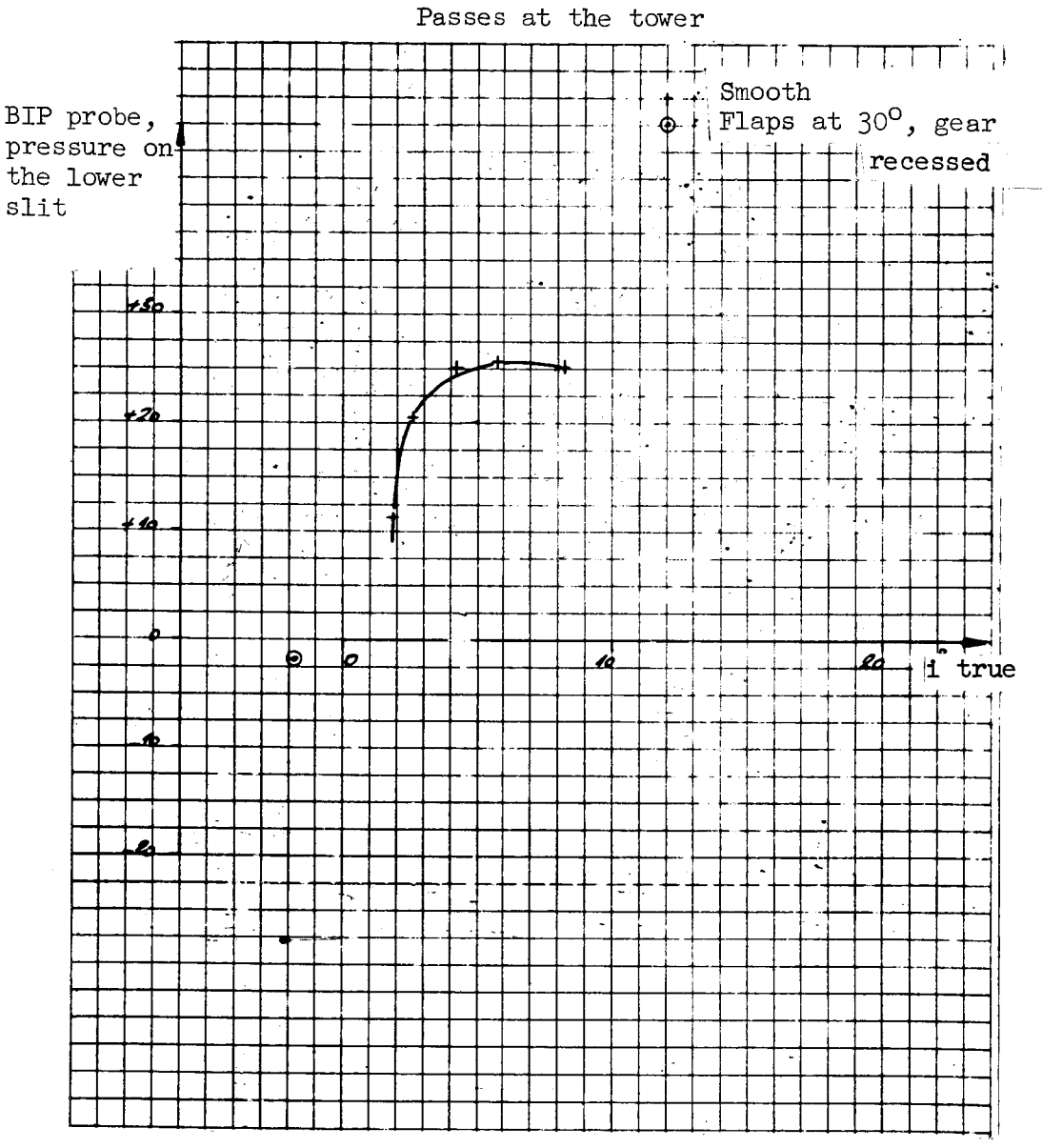

Figure 40. BIP probe calibration.

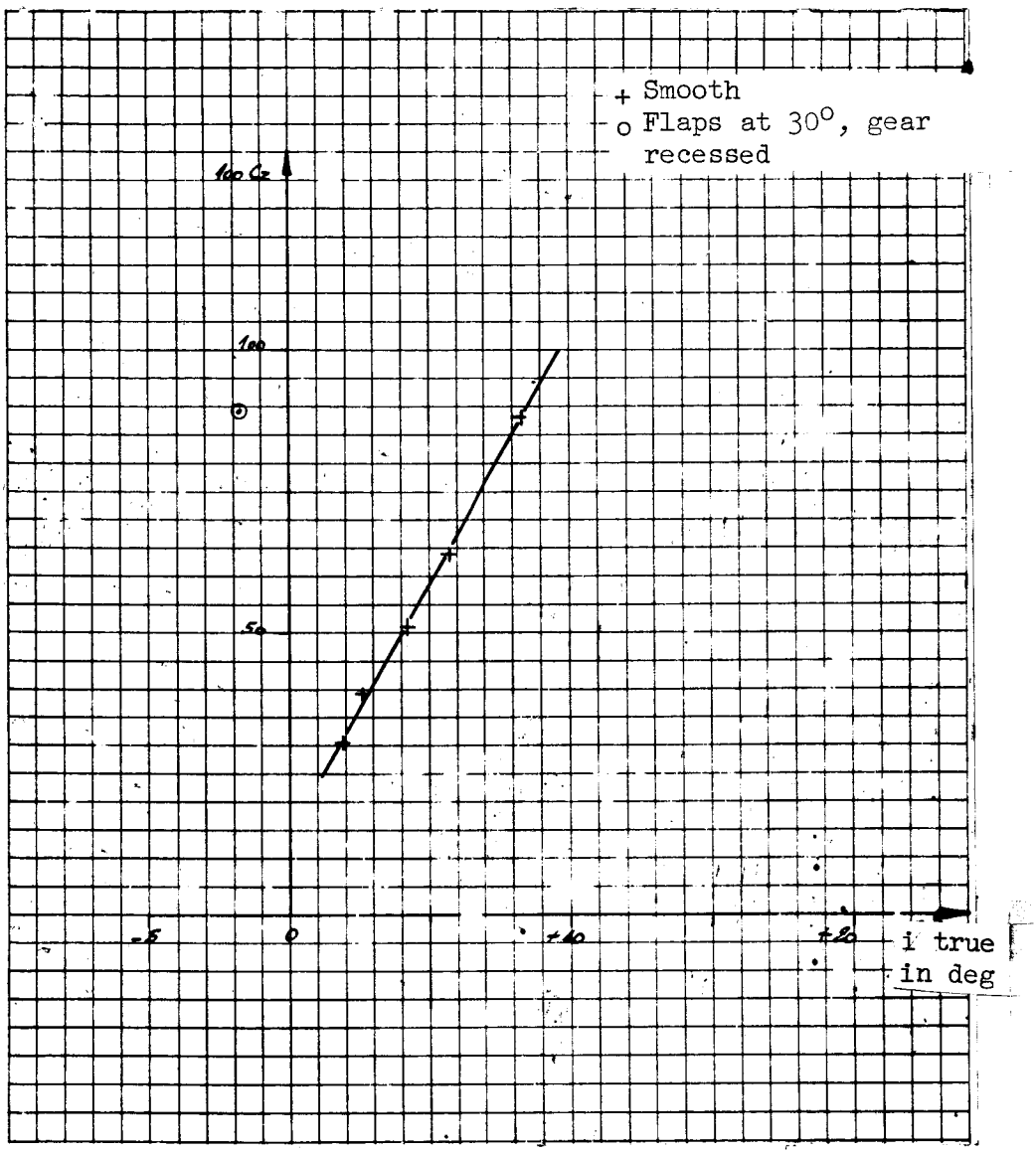

Figure 41. Cruising powered polar diagram.
100 Cz = f(i).

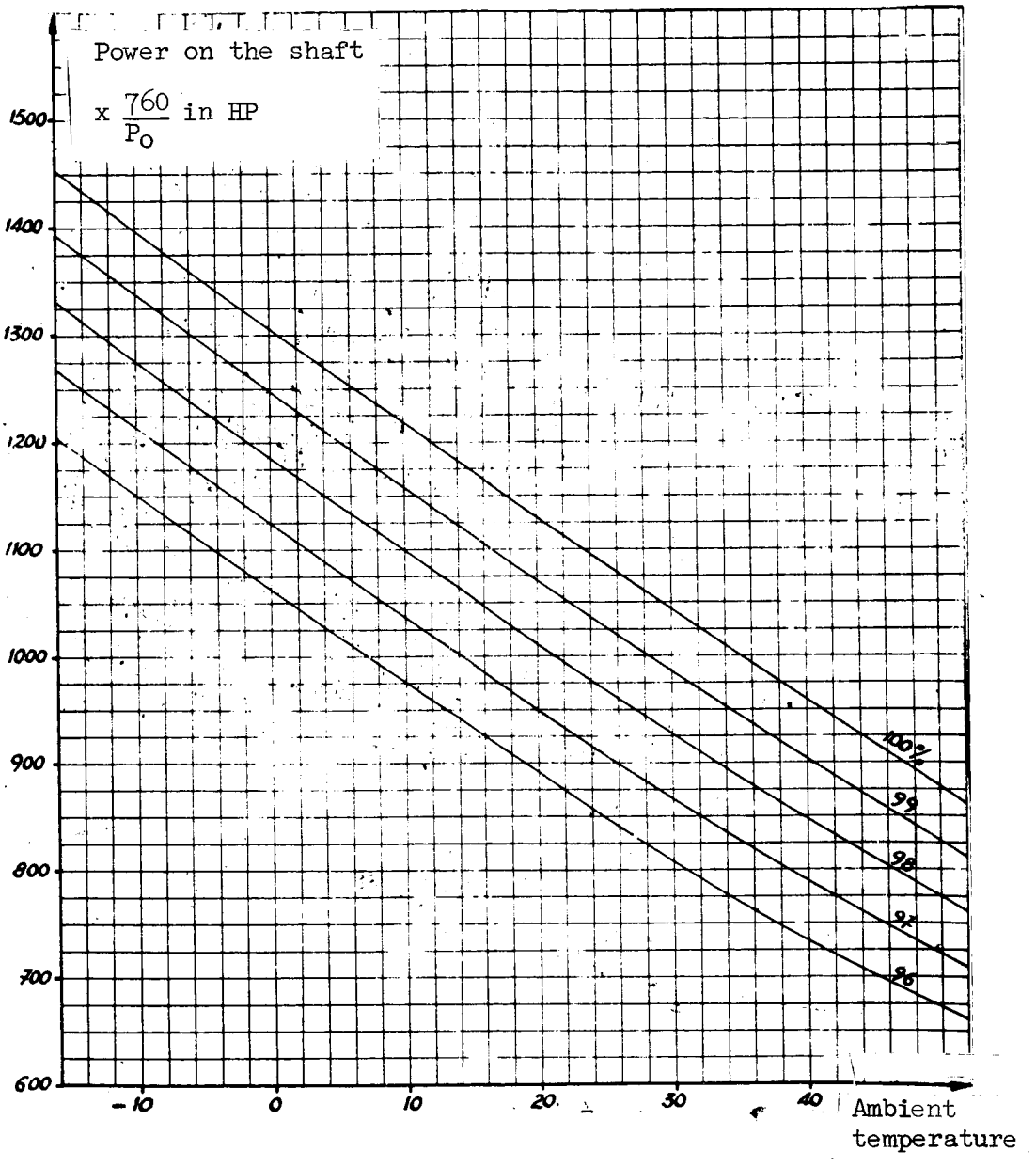

Figure 42. Calculation of the shaft power.
(Output at 6000 rpm.)

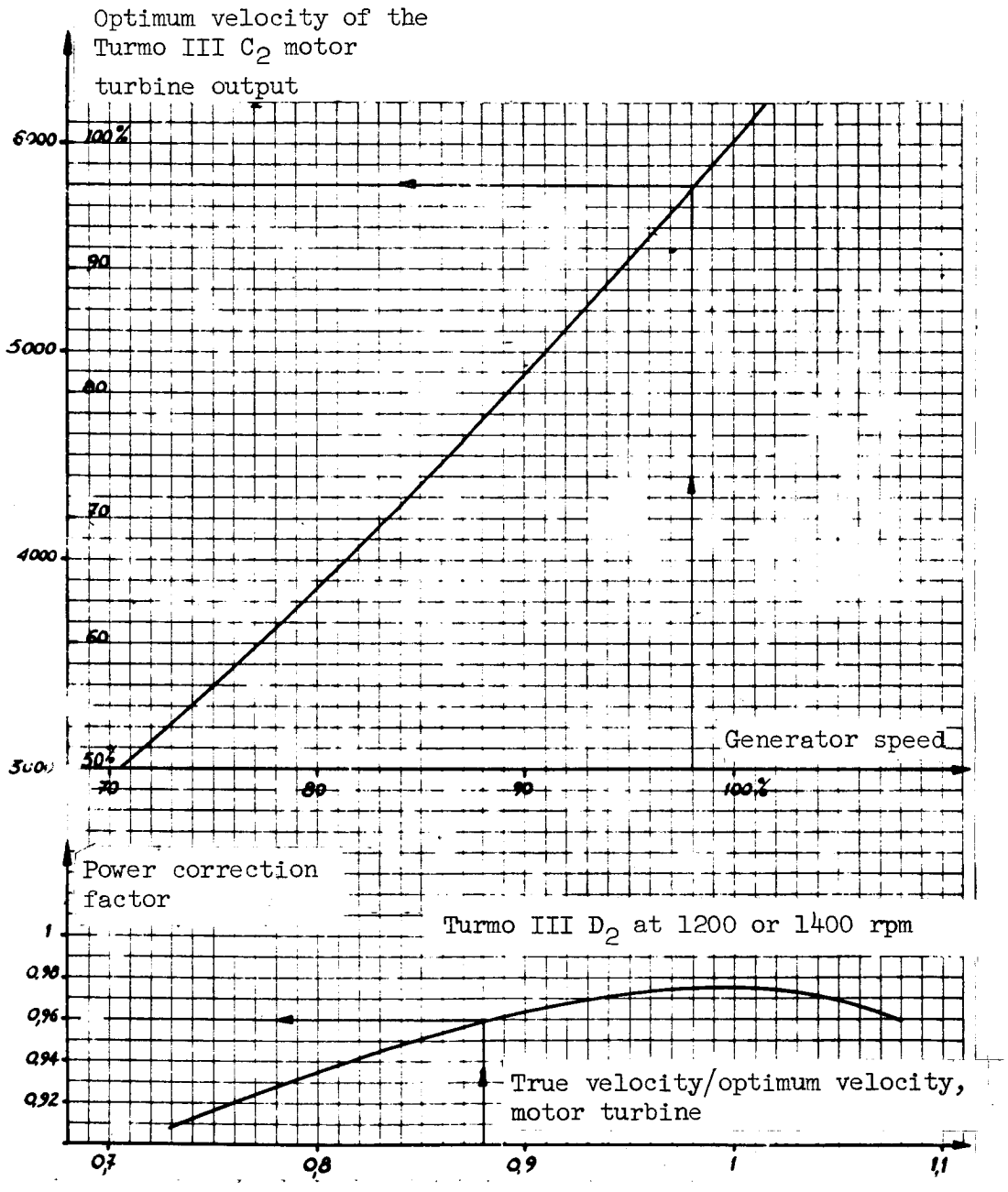

Figure 43. Propeller power, correction due to the forward reducing gear losses.

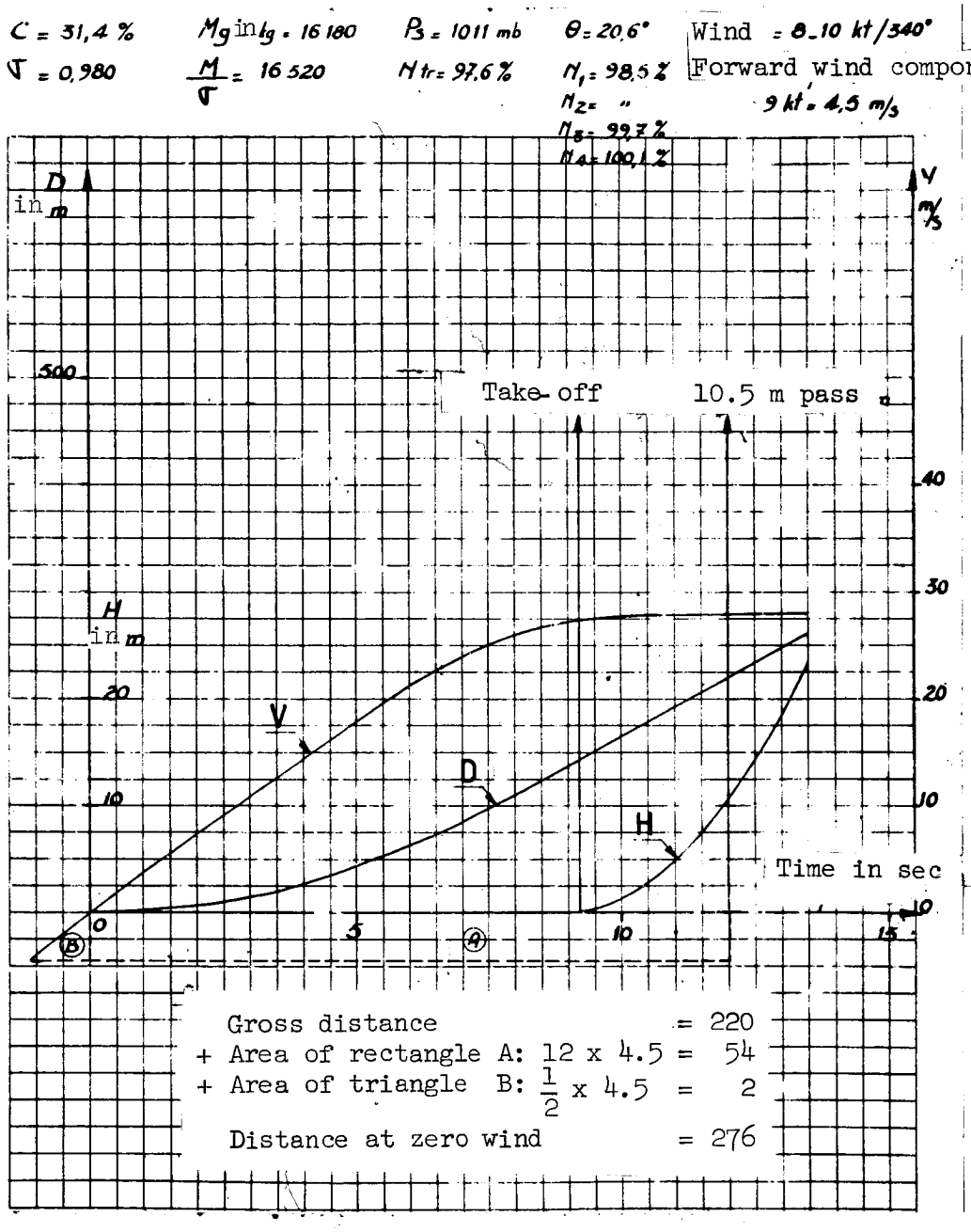

Figure 44. Zero wind transcription of a take-off under nose wind.

(Flight of 20 September 1962; Take-off No. 6 from strip No. 340.)

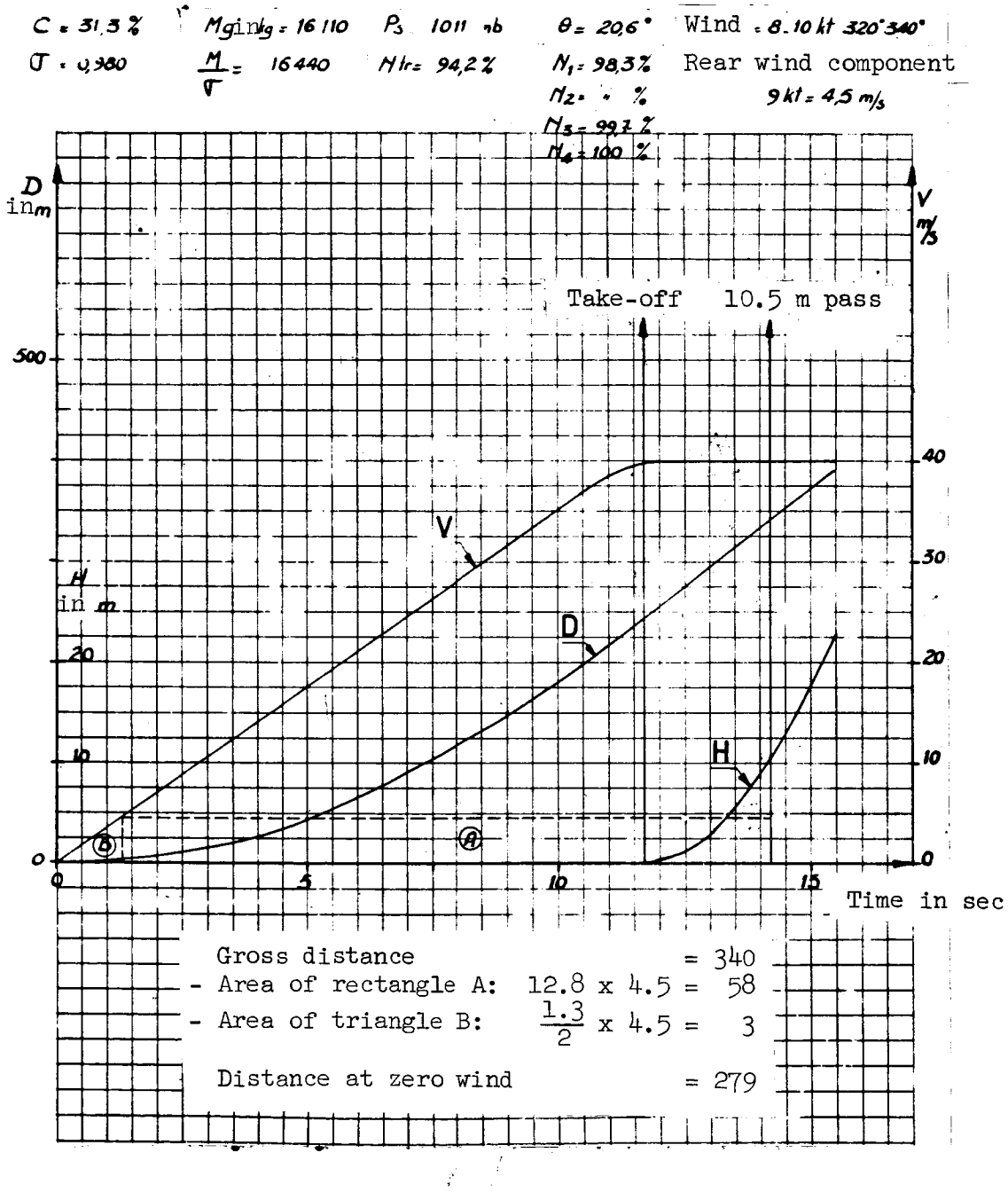

Figure 45. Zero wind transcription of a take-off under tail wind.

(Flight of 20 September 1962; take-off No. 7 from strip No. 160.)

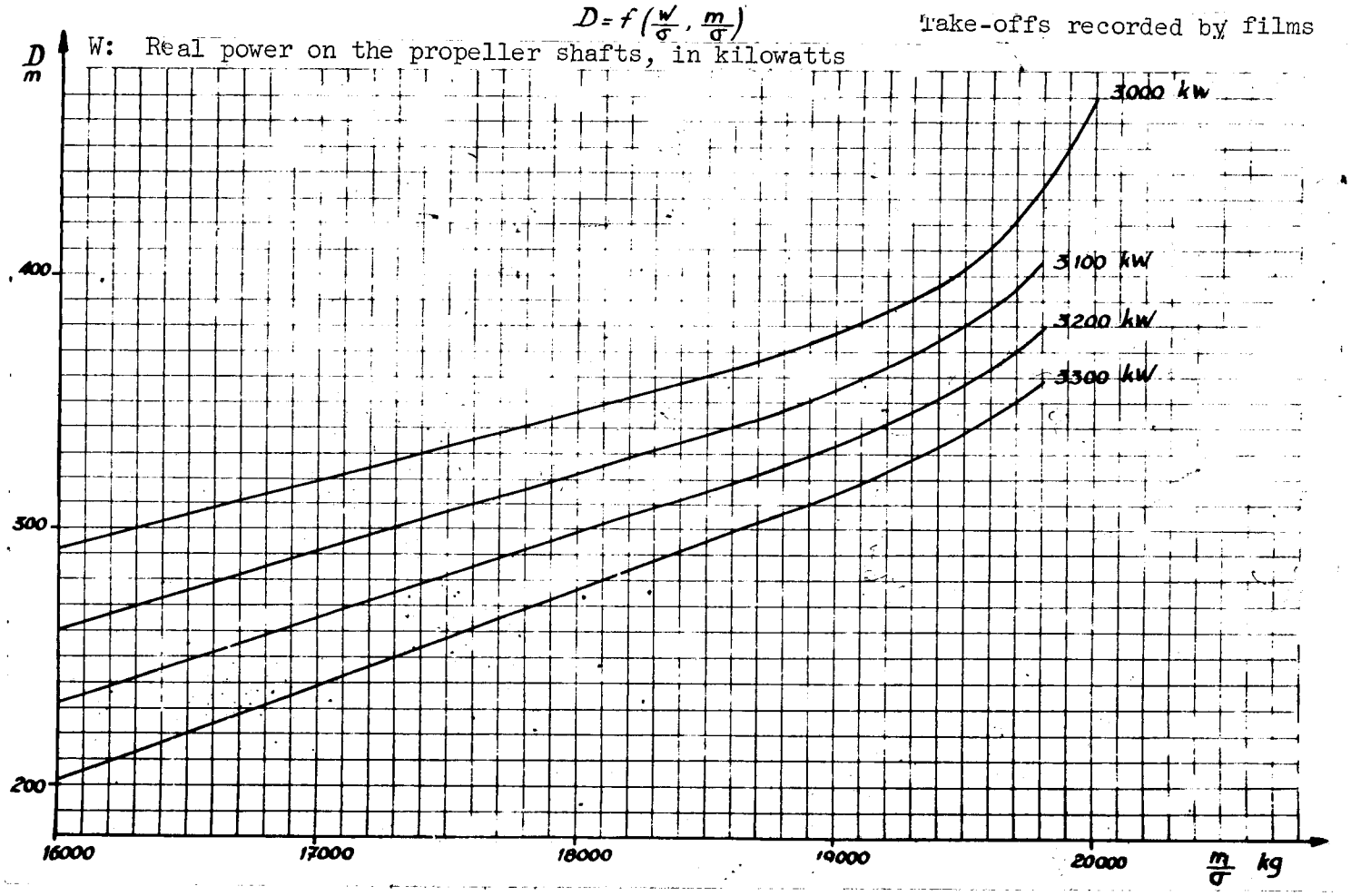

Figure 46. Take-off performance: distance required to go over a 10.5 m obstacle at take-off.

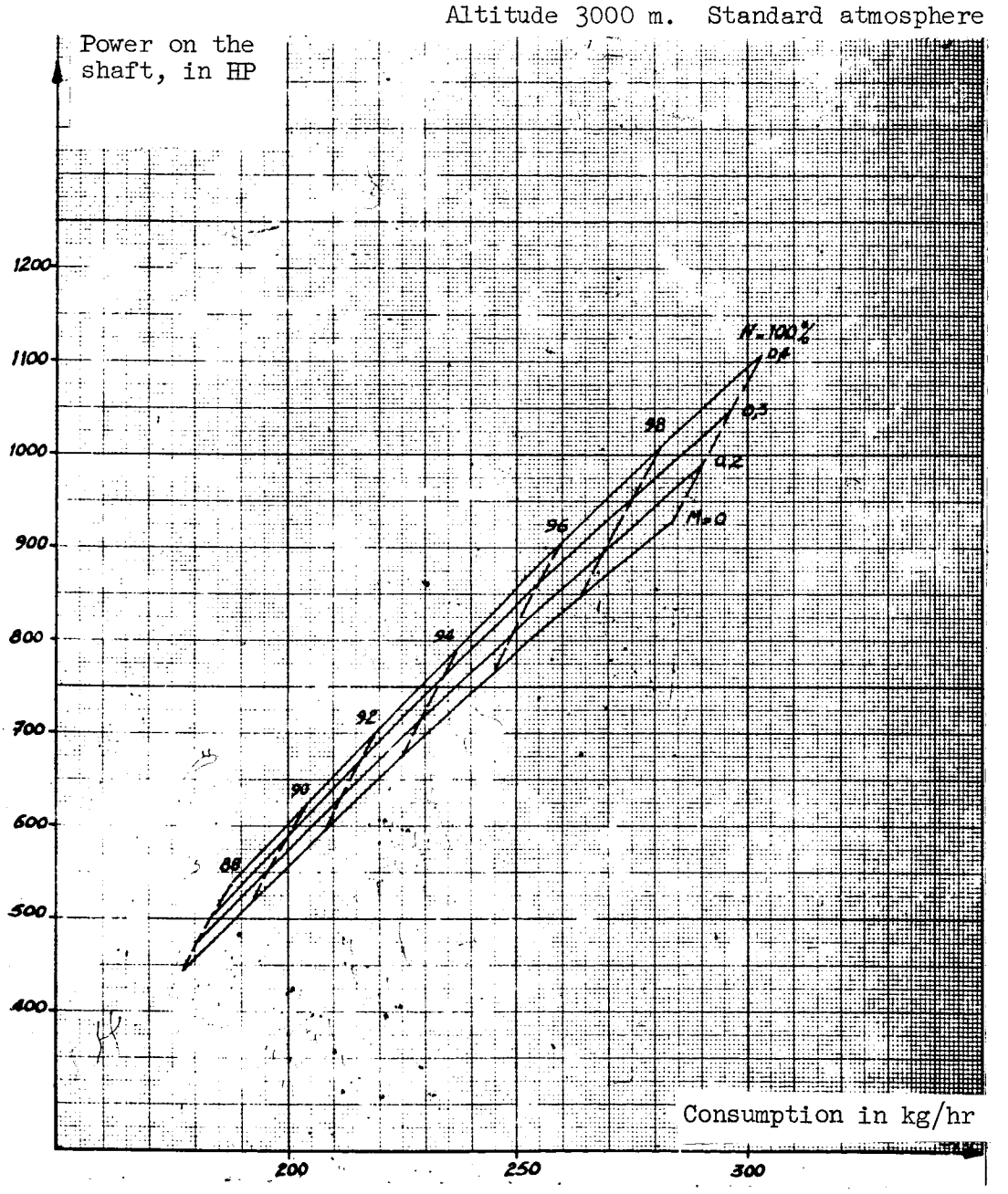

Figure 47. Turmo III D engine cruising power.

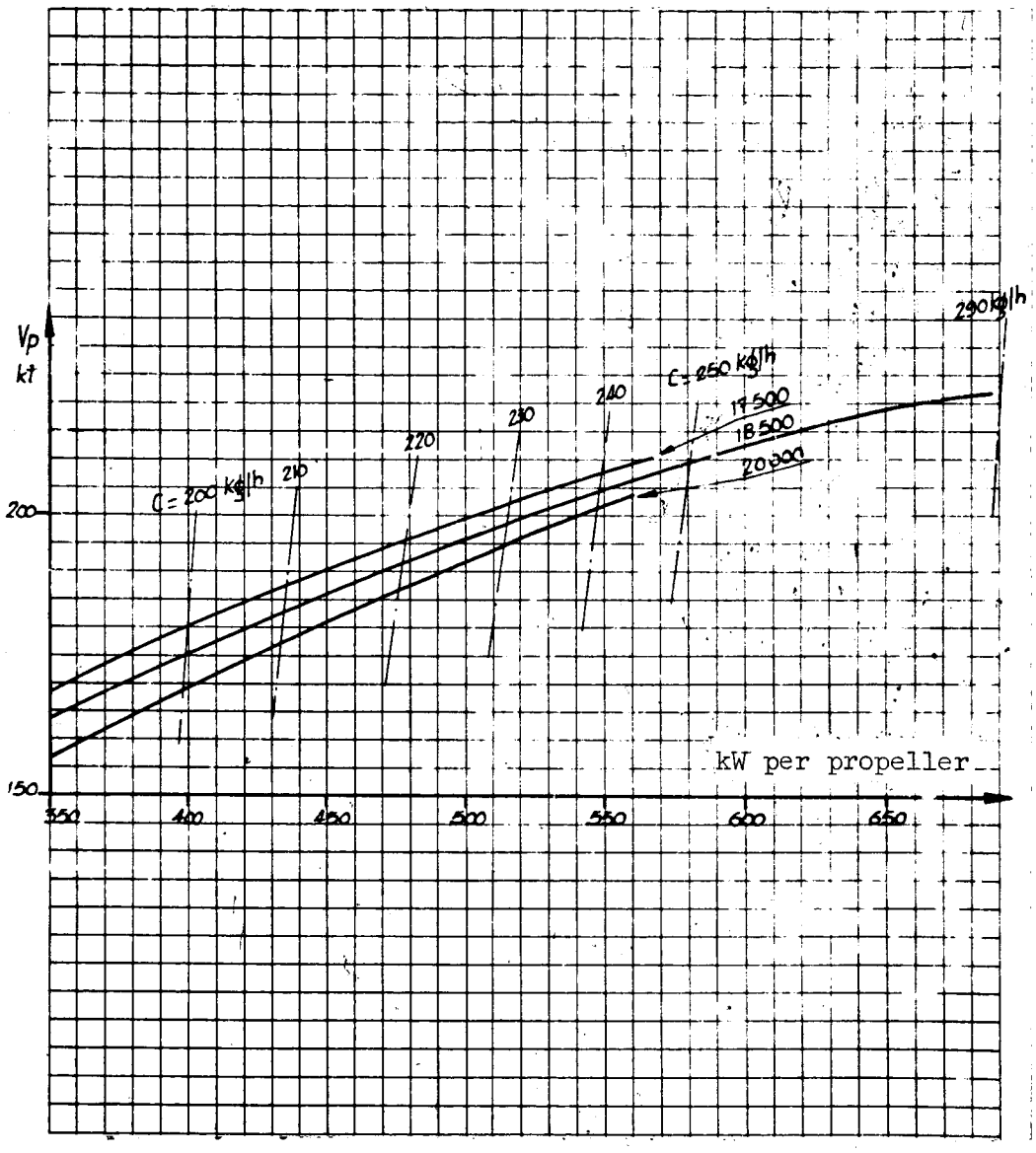

Figure 48. Cruising performance levels.
(Zp = 10,000 ft; standard atmosphere.)

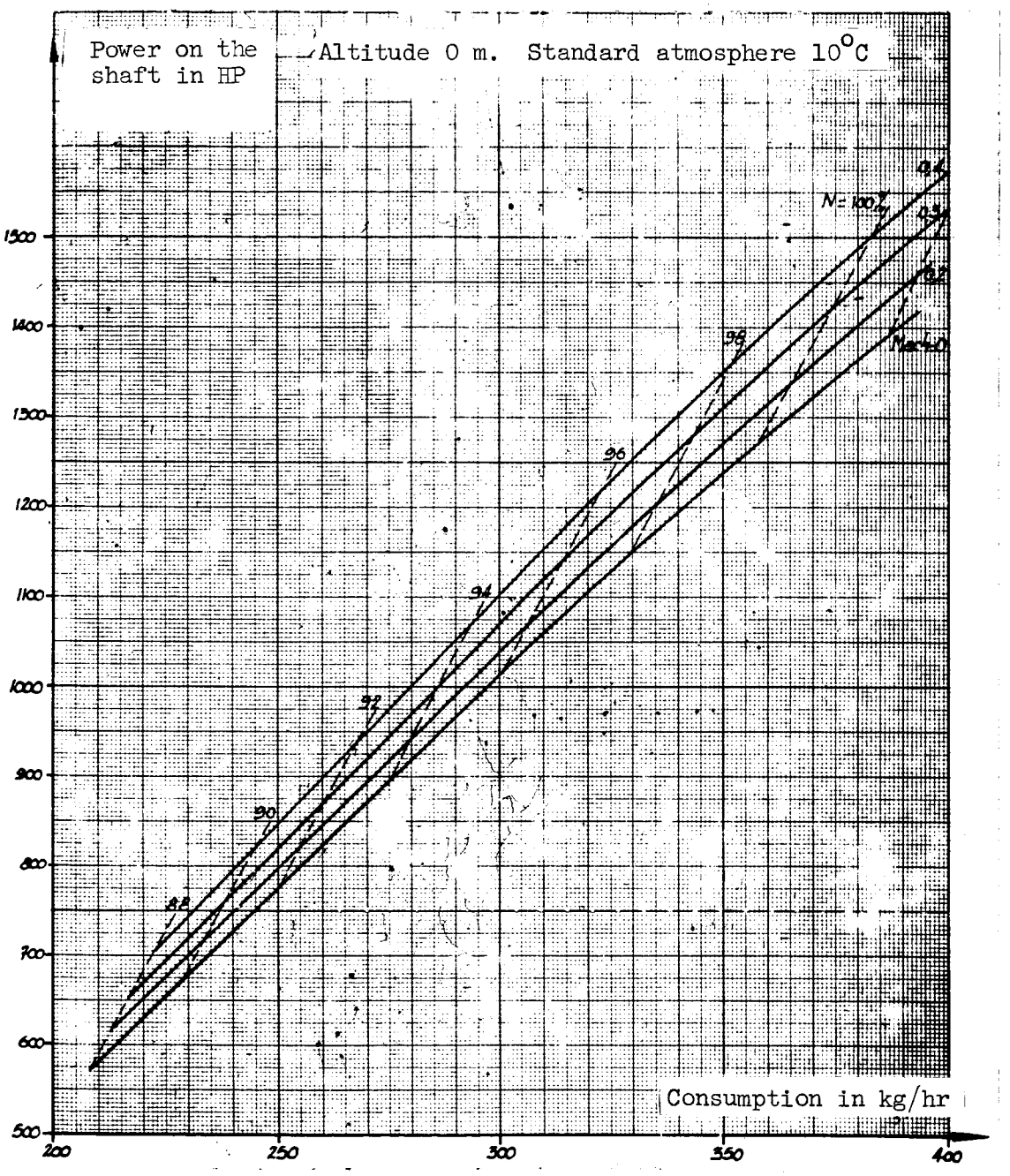

Figure 49. Grounded Turmo III D engine power.

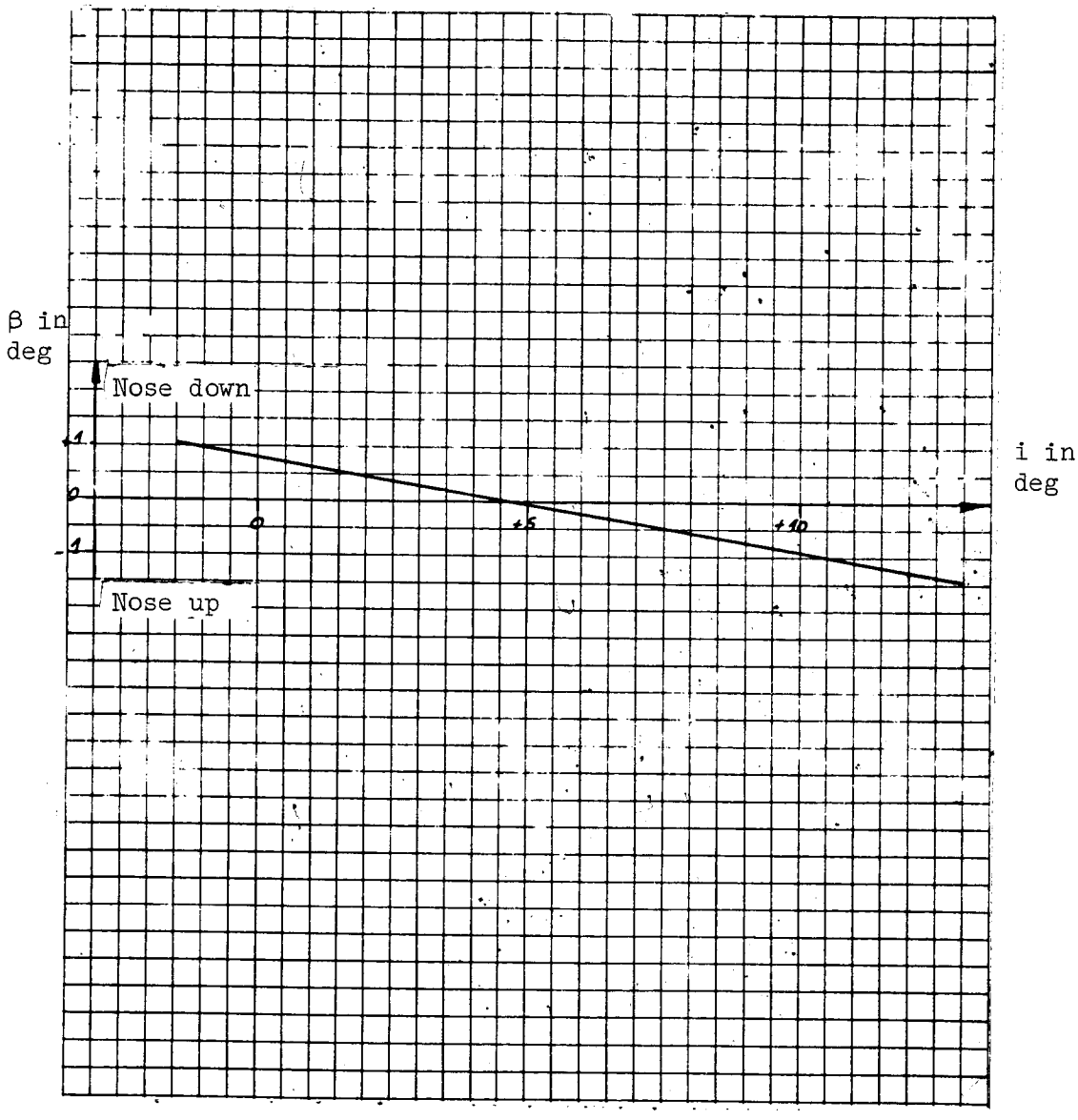

Figure 50. Static longitudinal stability in take-off configuration.

(C = 33%; Landing gear deployed; flaps at 43°; N_G 97%.)

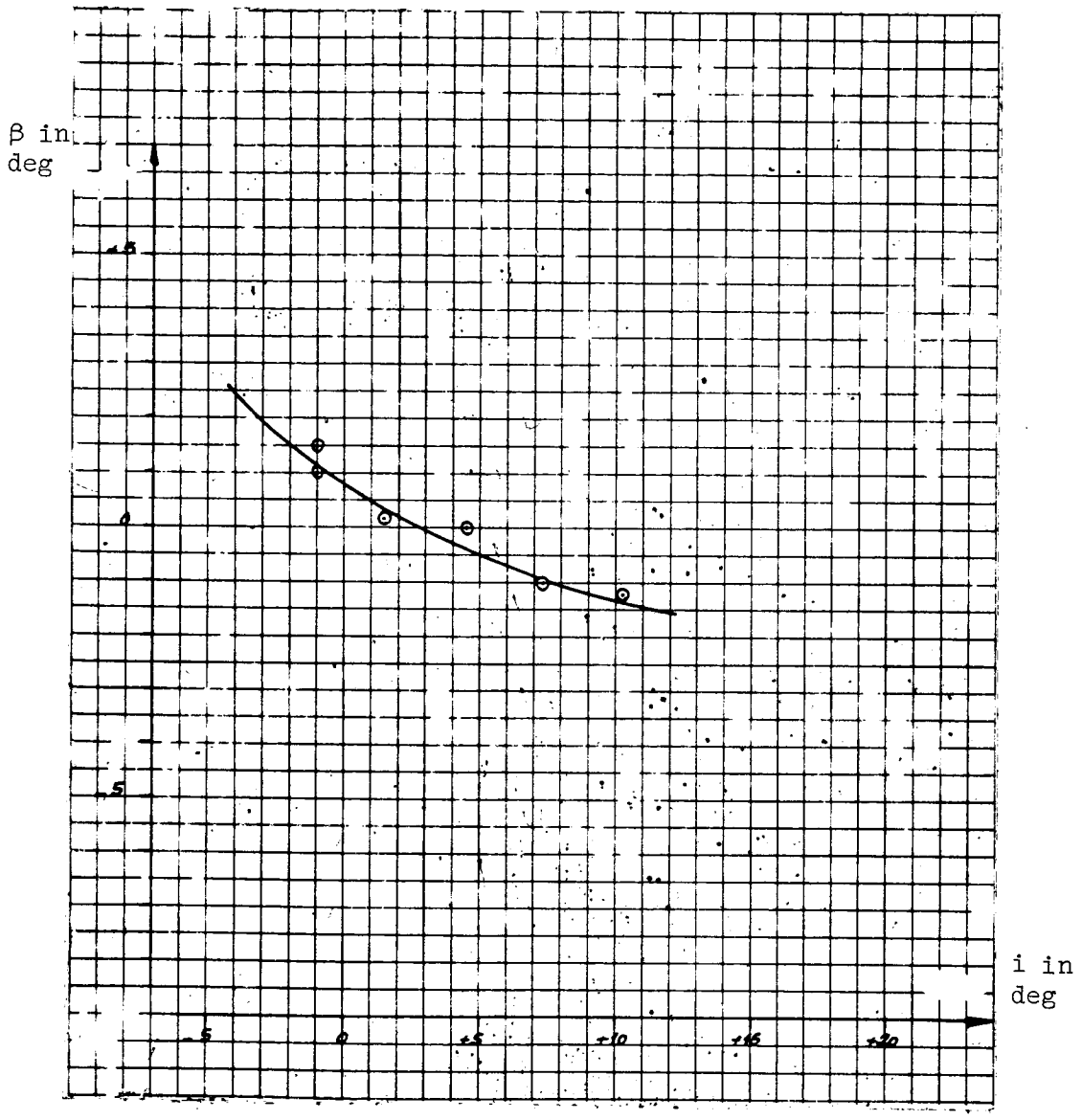

Figure 51. Static longitudinal stability in ascension configuration.

(Landing gear recessed; flaps at 30°; N_G 96.2%; β_e 4°; Zp: 2000 ft; C = 33%.)

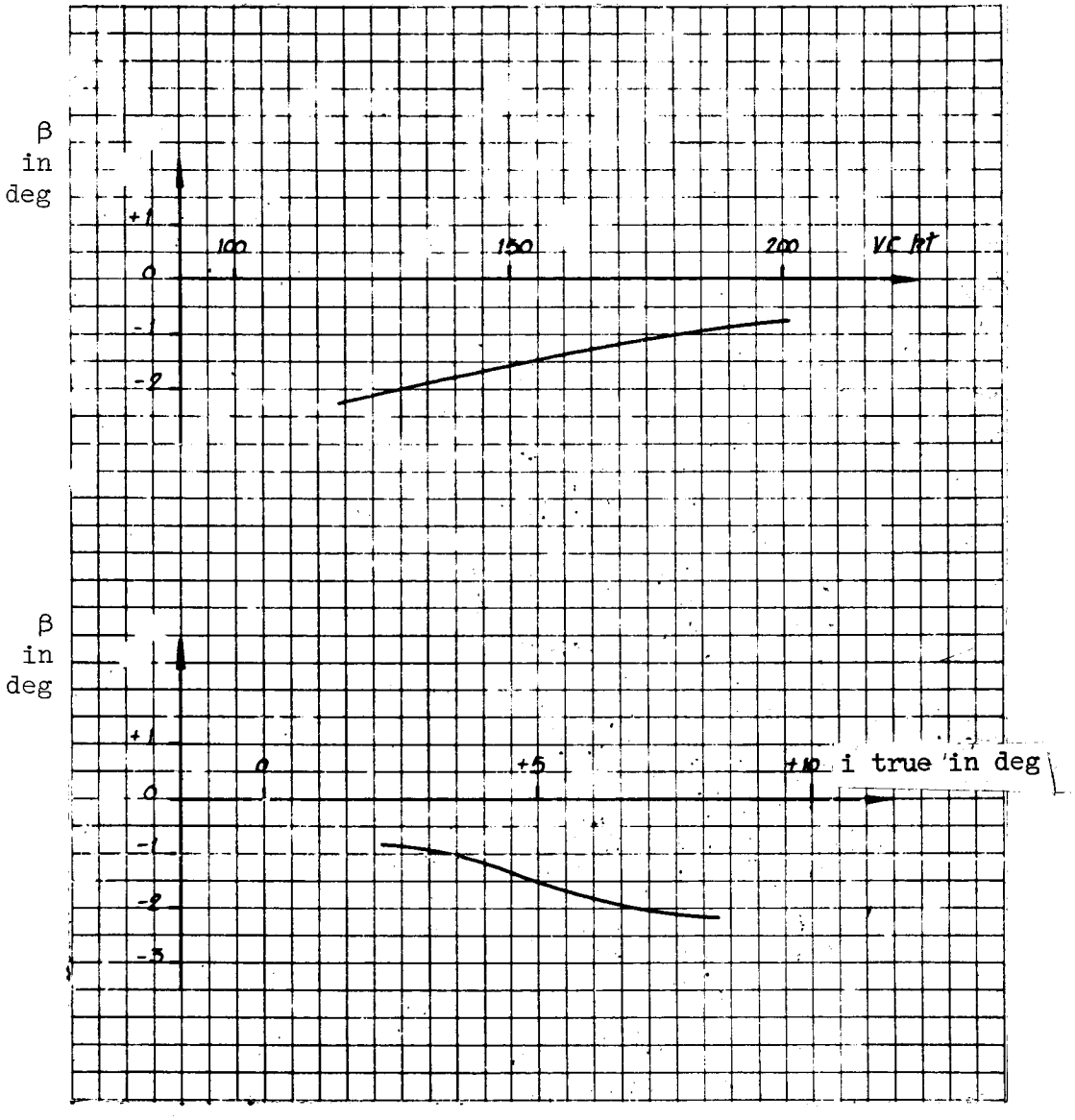

Figure 52. Static longitudinal stability in cruising configuration. (C = 33%; Zp 4500 ft; β_e = 3°.)

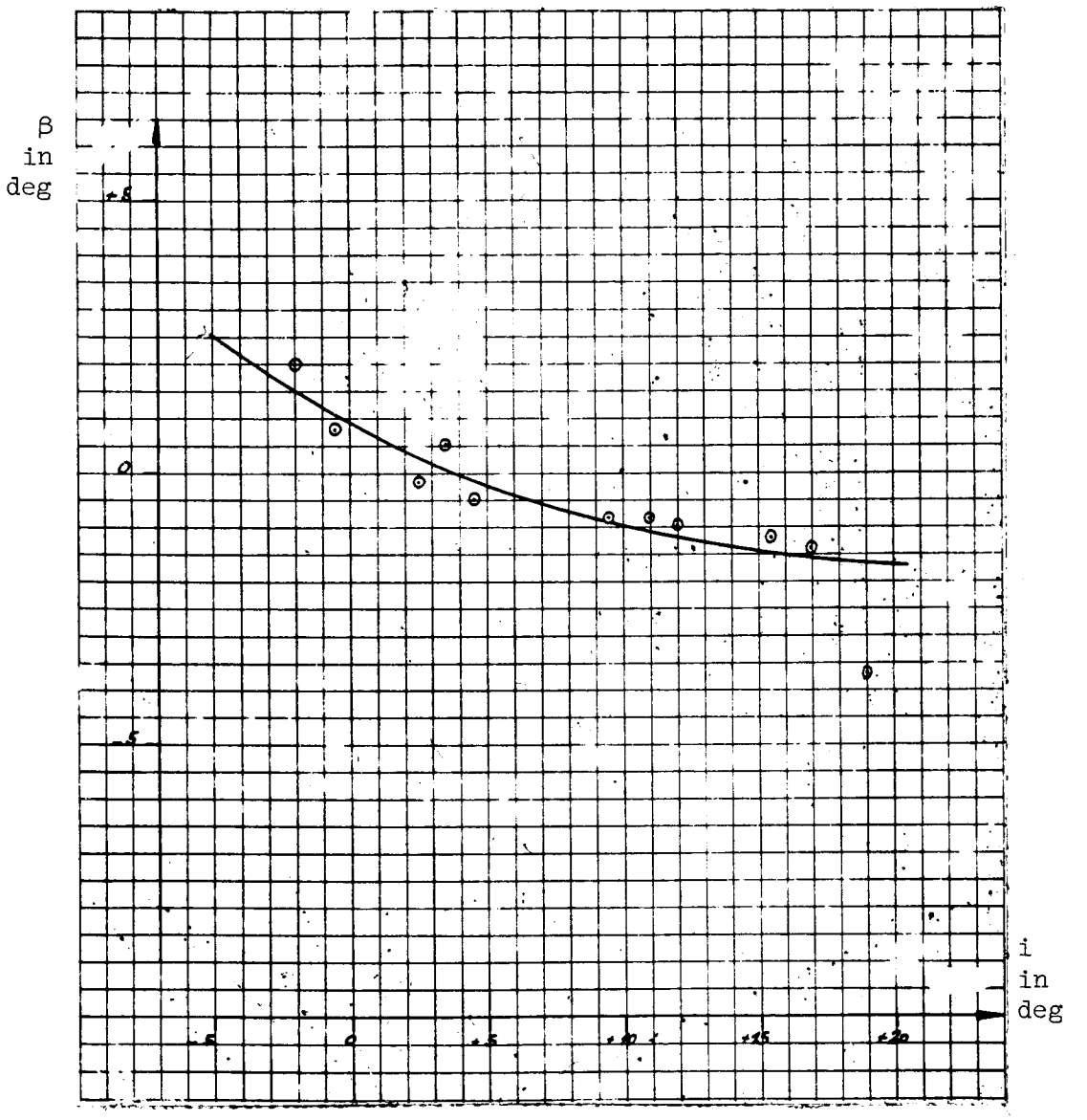

Figure 53. Static longitudinal stability in landing configuration. C = 33%.

(Landing gear deployed; flaps at 97°; N_G 89%; β_e 7.5°; Zp: 2000 ft.)

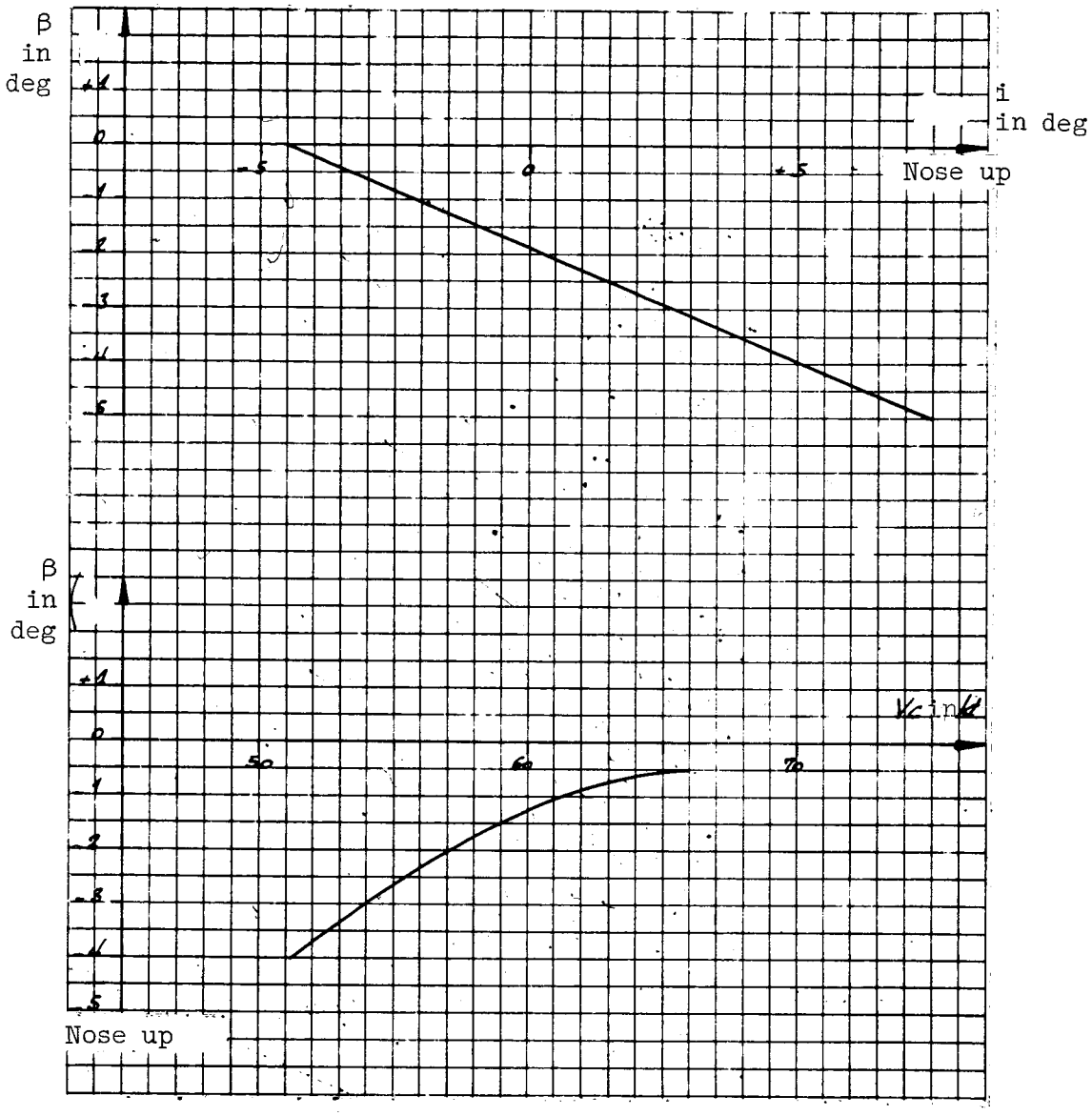

Figure 54. Static longitudinal stability in landing configuration. C = 27%.

(Landing gear deployed; flaps at 97°; N_G 89.9%; Zp average: 1700 ft.)

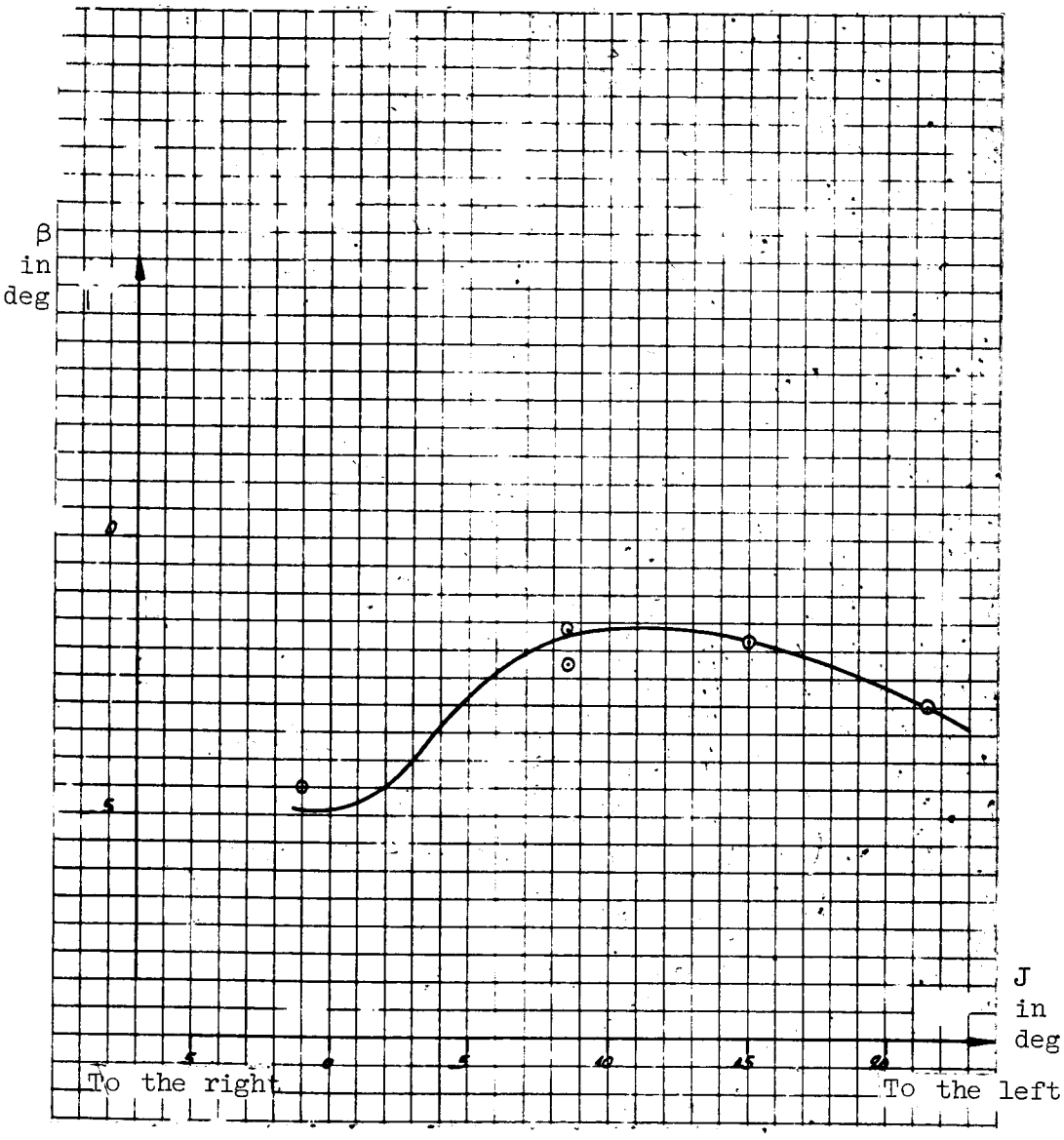

Figure 55. Influence of skidding on the static longitudinal stability.

(Landing gear deployed; flaps at 97°; N_G 89.2%; β_e 7.5°; C = 33%; i average: 20°; Zp 2000 ft.)

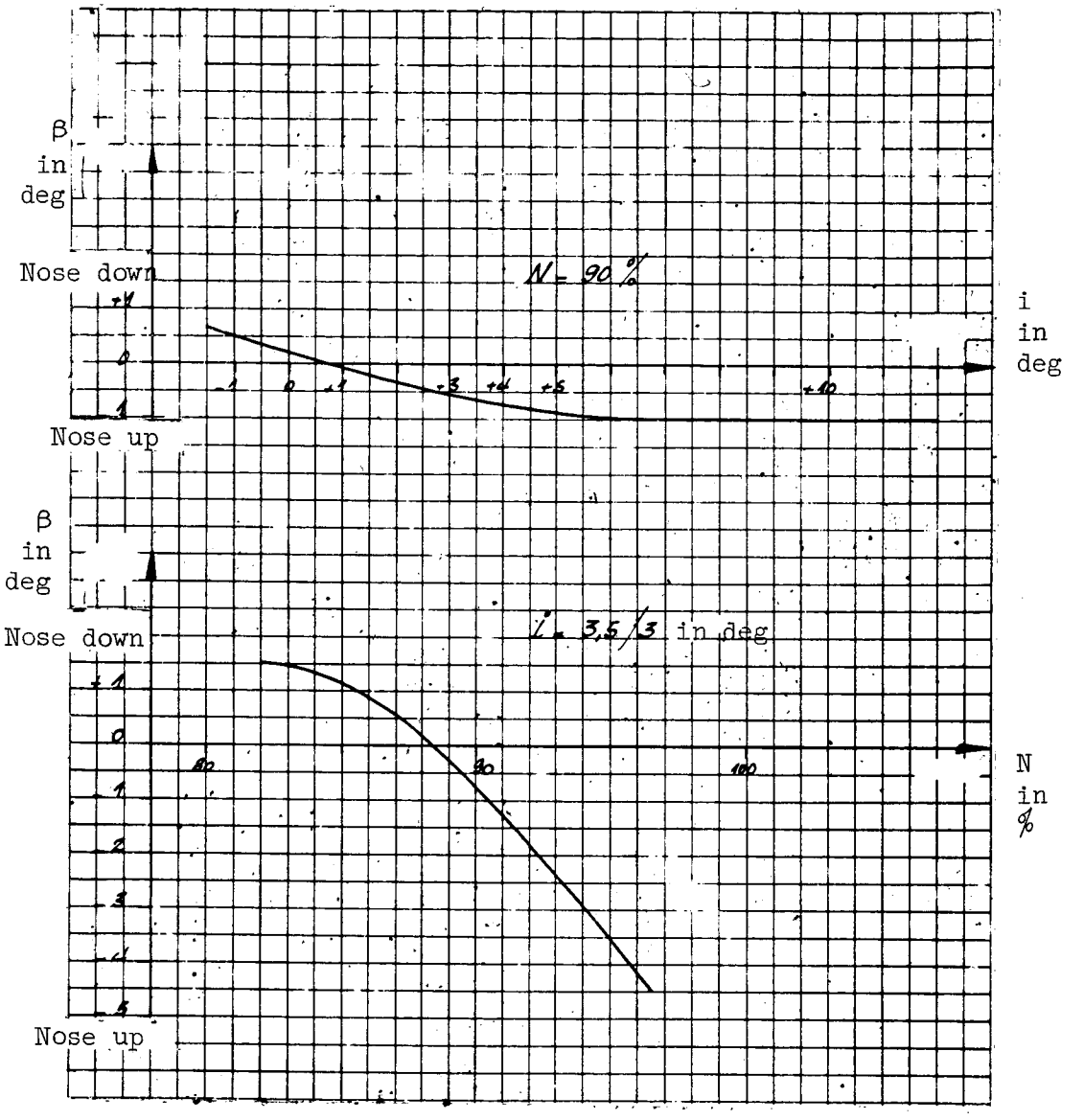

Figure 56. Influence of the blowing on the longitudinal stability.

(Landing gear deployed; flaps at 98°; C = 33%.)

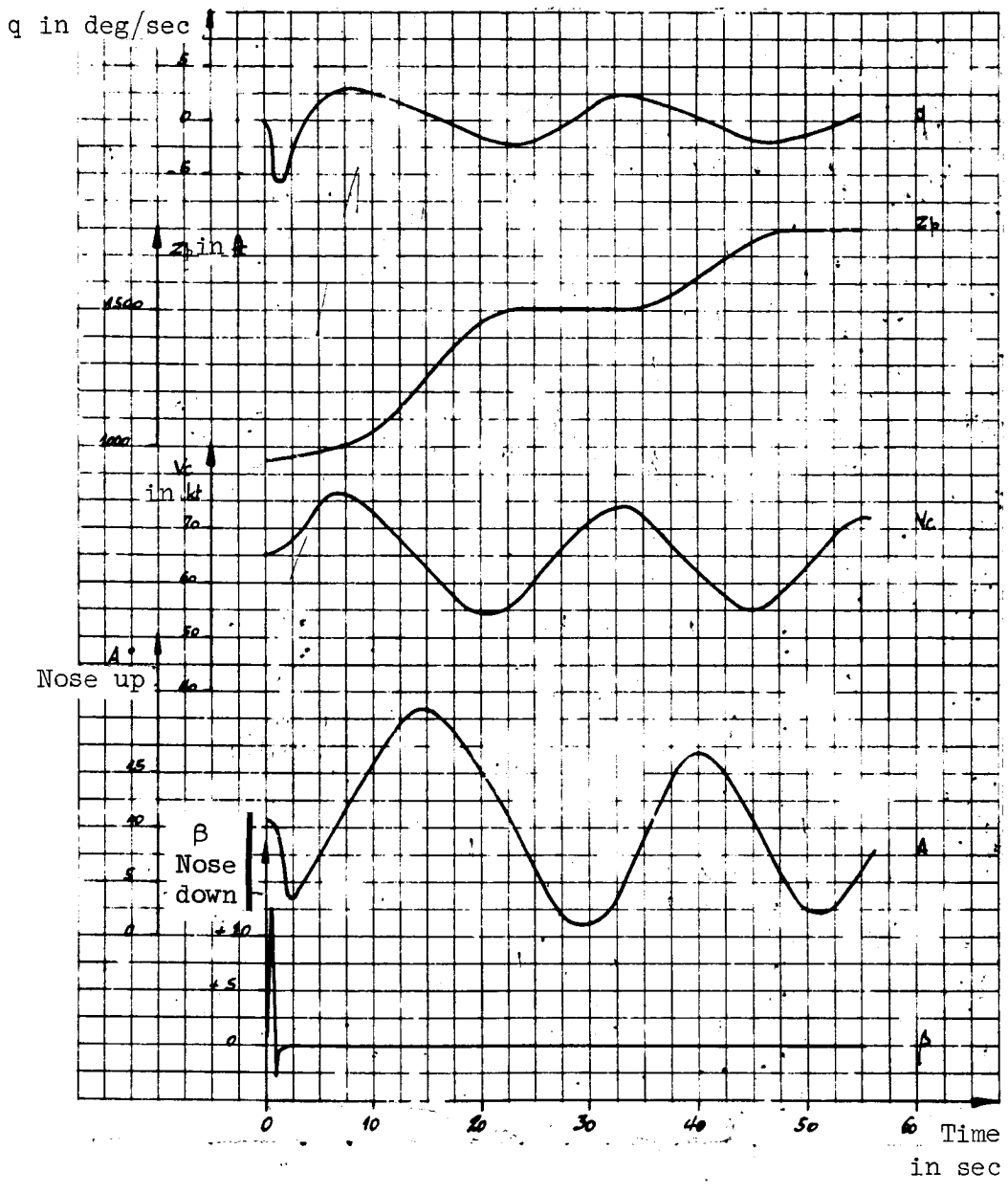

Figure 57. Longitudinal dynamics at take-off. Phugoid. (Landing gear deployed; Flaps at 43°; N_G 97%; C = 33%.)

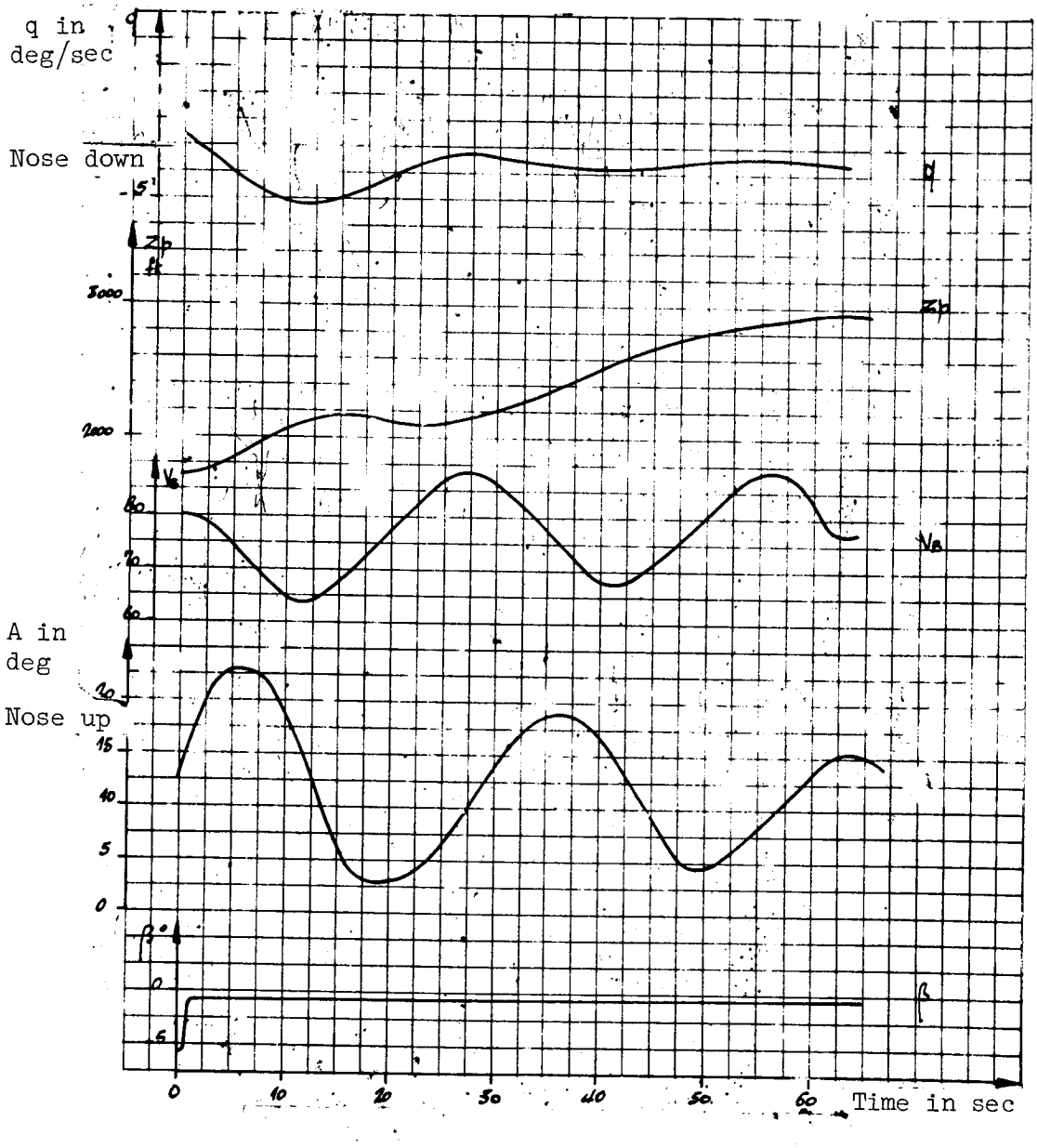

Figure 58. Longitudinal dynamics in ascension. Phugoid. (Landing gear recessed; flaps at 30°; N_G 96.2%; C = 33%.)

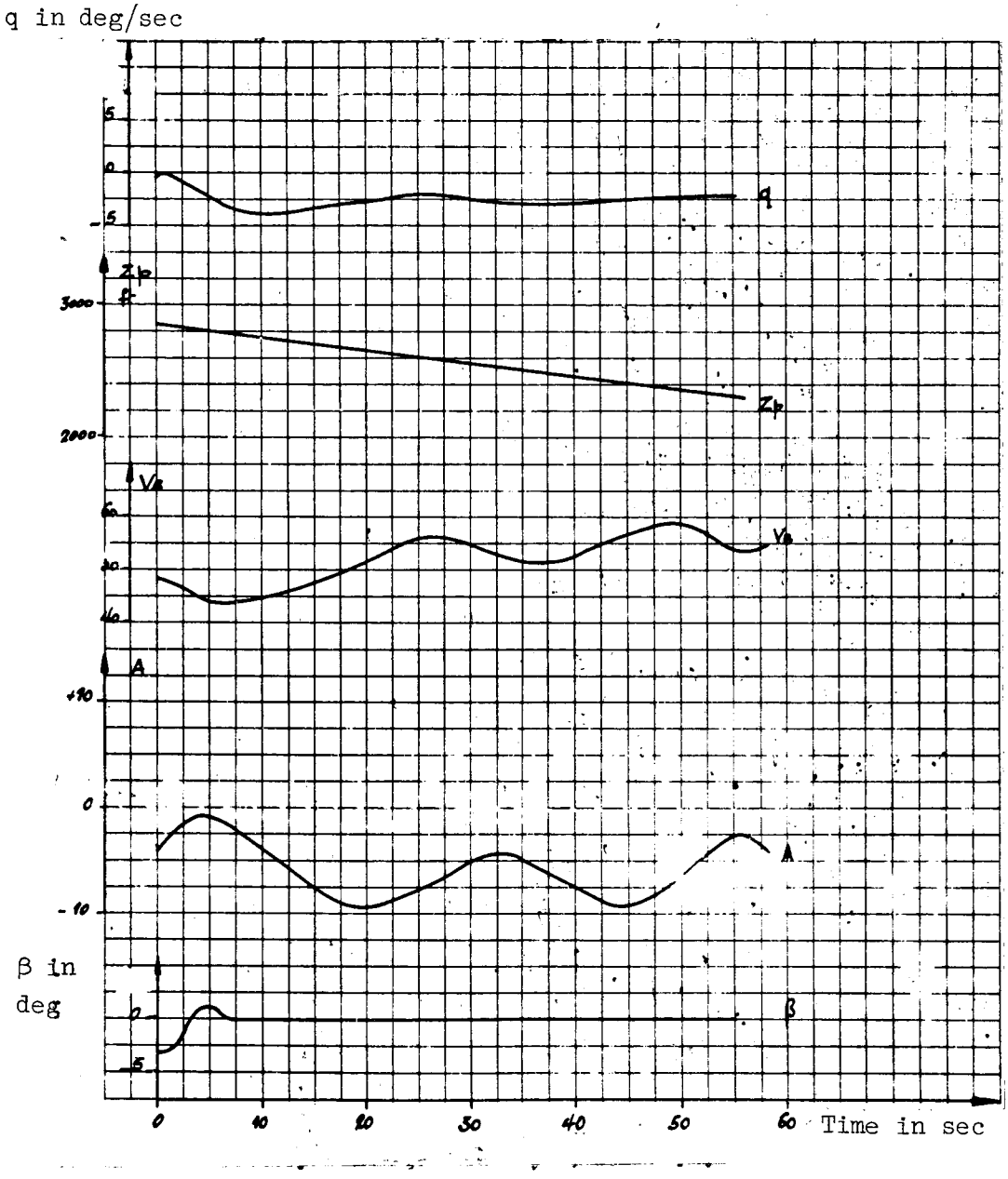

Figure 59. Longitudinal dynamics at landing. Phugoid. (Landing gear deployed; flaps at 97°; N_G 89.4%; C = 33%.)

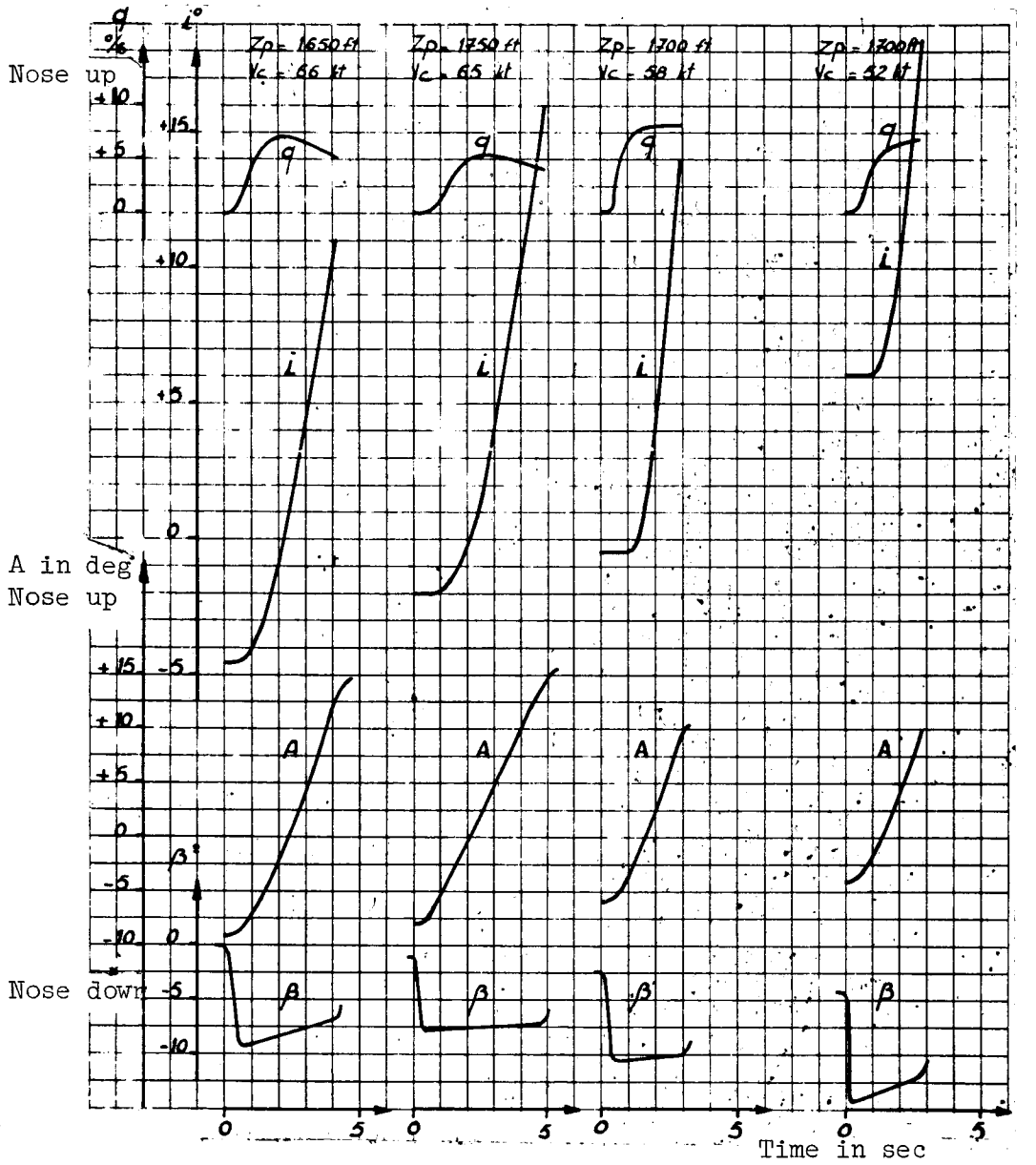

Figure 60. Influence of the starting pitch on the elevator efficiency. 27% center fore.

(Landing gear deployed; flaps at 97°; N_G = 89.8%.)

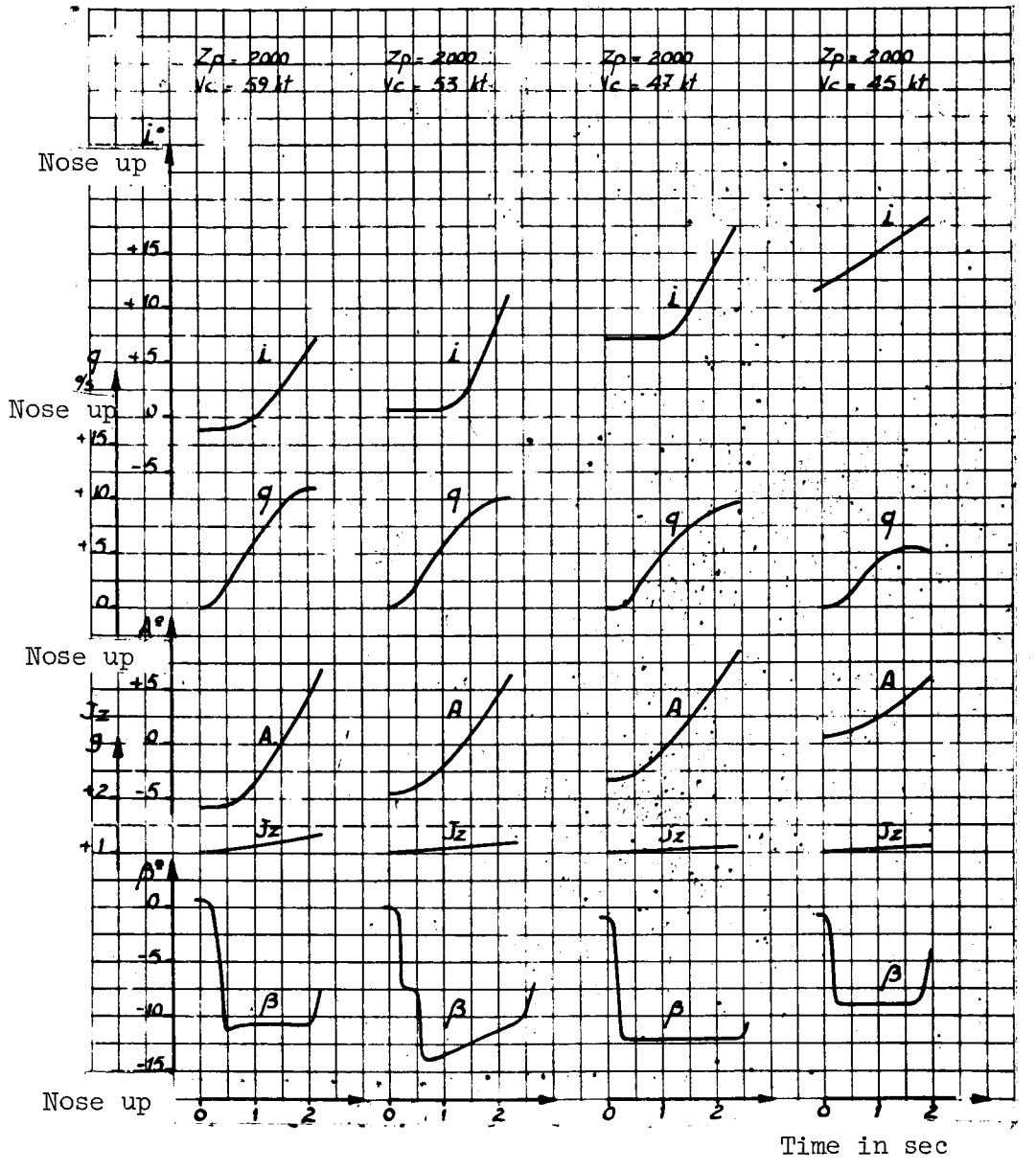

Figure 61. Influence of the starting pitch on the elevator efficiency. 33% center aft.

(Landing gear deployed; flaps at 98°; N_G = 90%.)

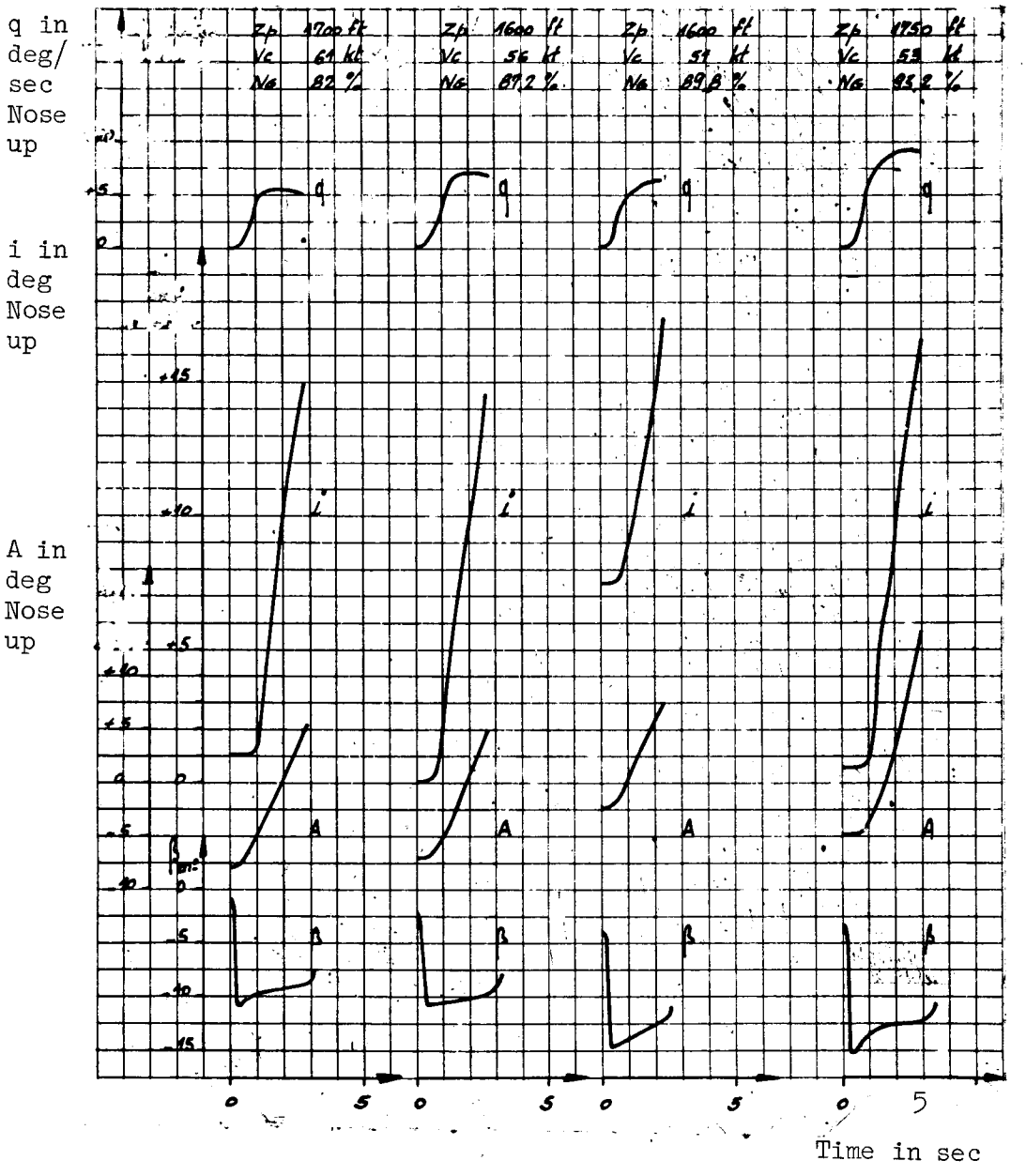

Figure 62. Influence of the blowing pitch on the elevator efficiency. 27% center fore.

(Landing gear deployed; flaps at 97°.)

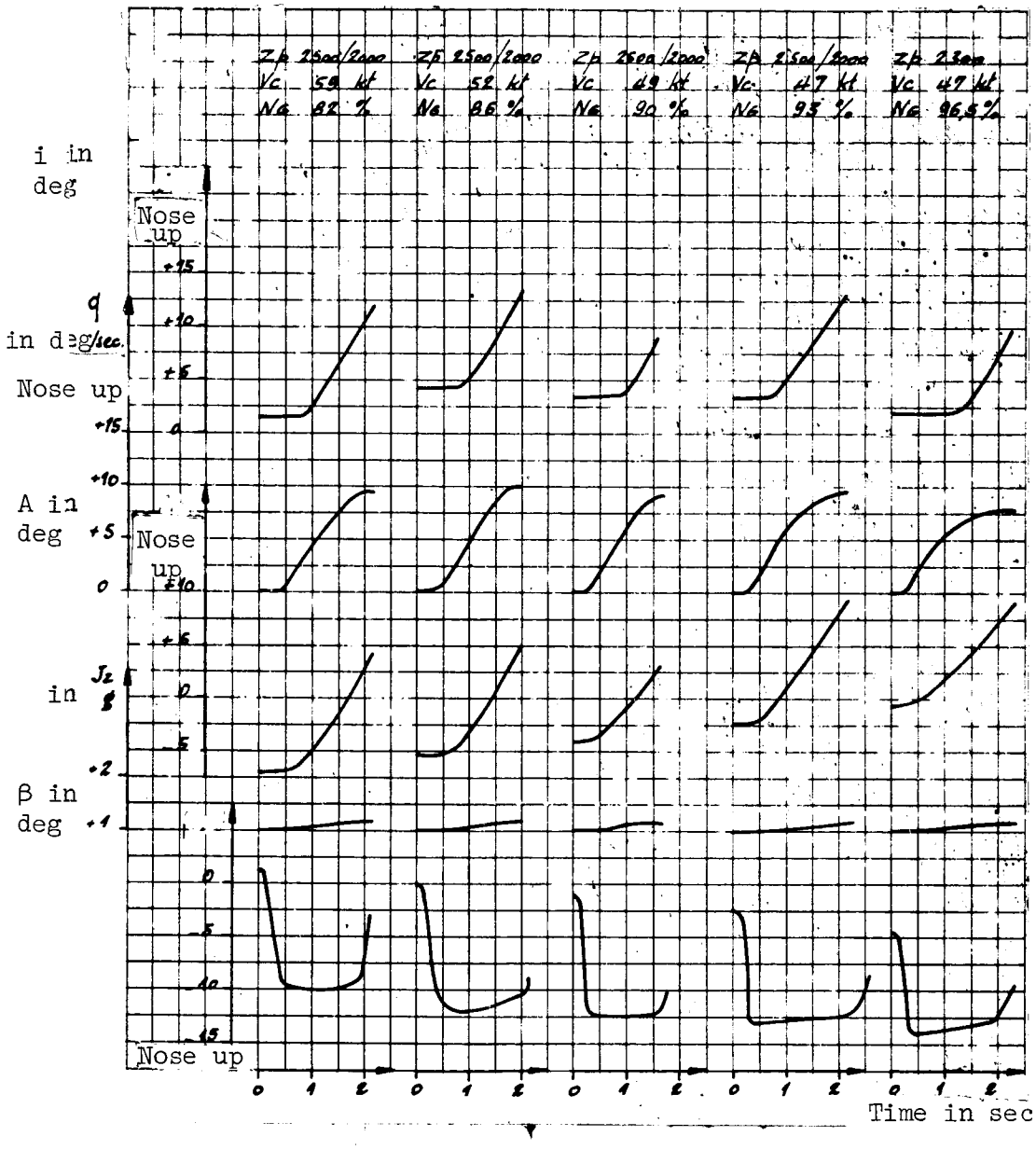

Figure 63. Influence of the blowing pitch on the elevator efficiency. 33% center aft.

(Landing gear deployed; flaps at 98°.)

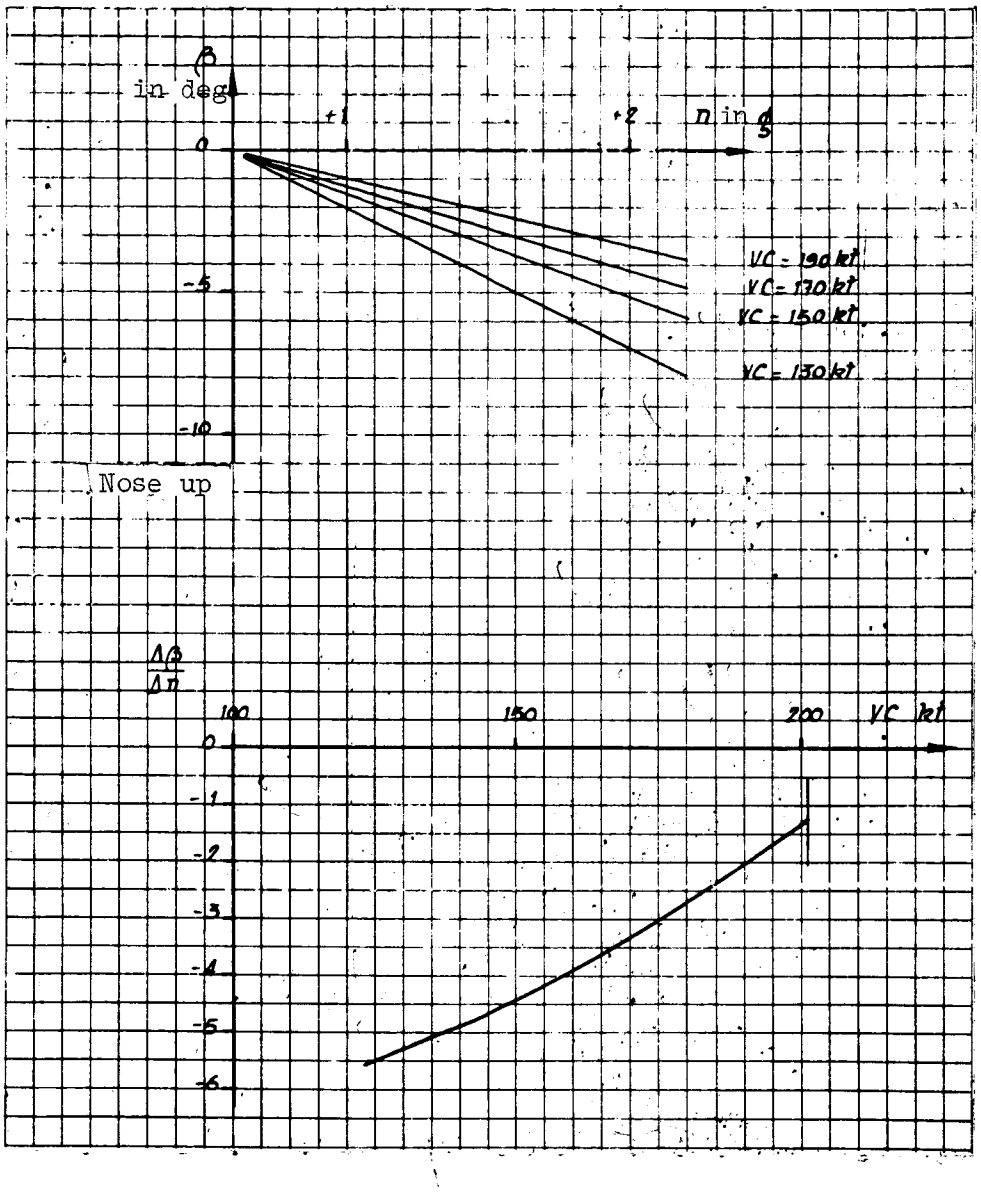

Figure 64. Efficiency of the elevator. g displacement.

(C = 33%; Zp: 4800 ft.)

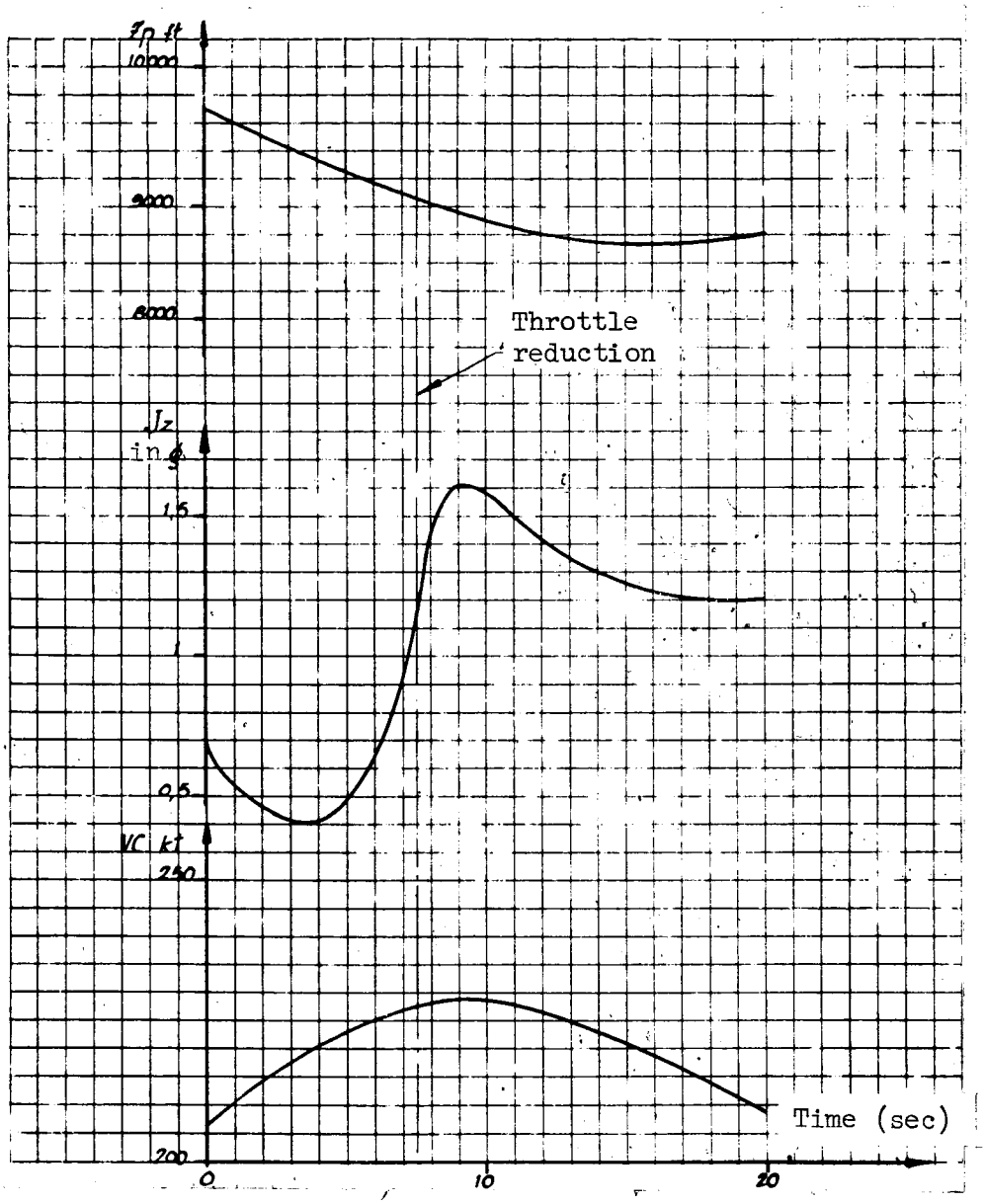

Figure 65. Efficiency of the elevator. Start of nose down maneuver.

(Smooth configuration; starting N_G: 98.7%; C = 33%.)

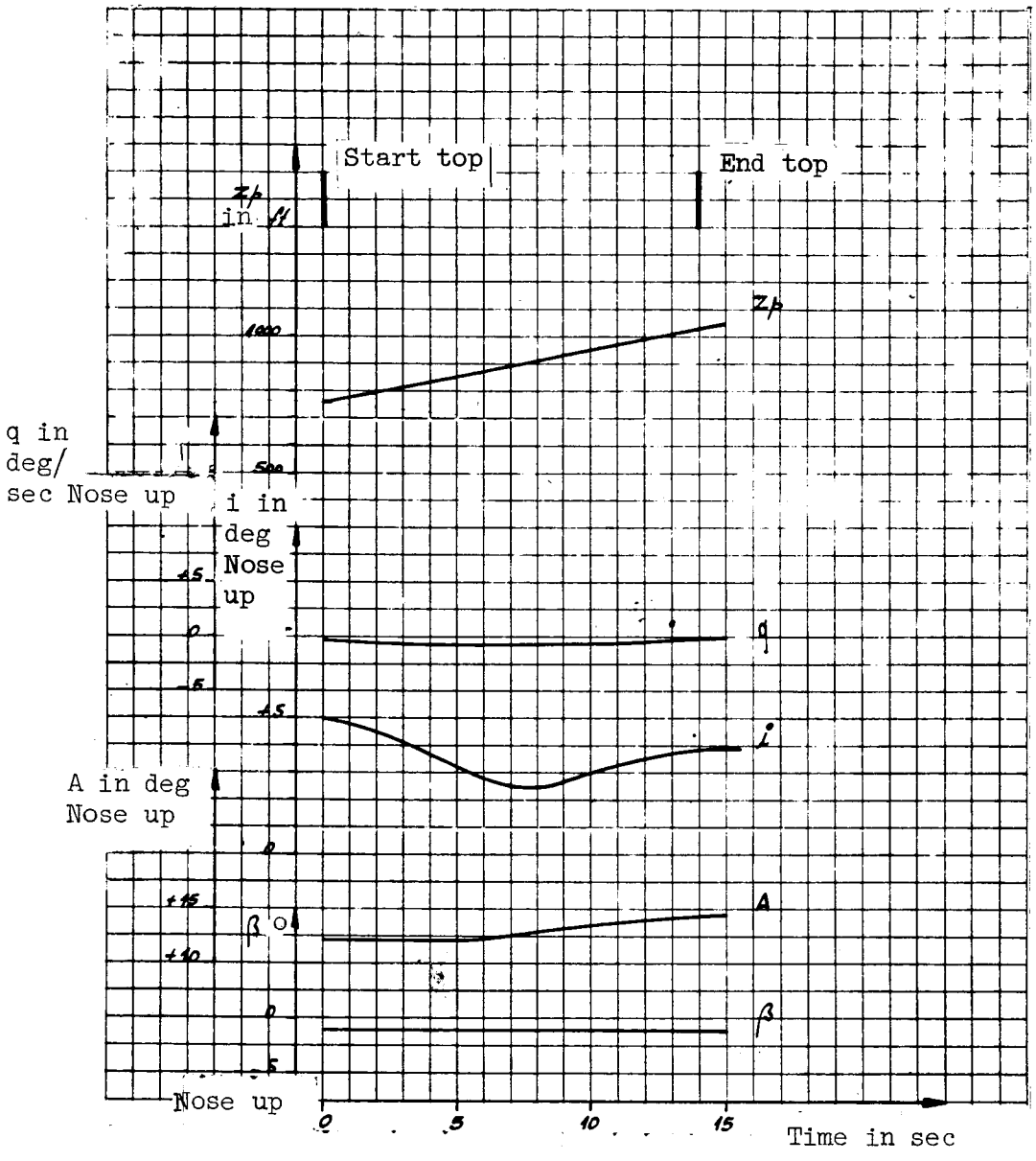

Figure 66. Response to configuration changes. Landing gear recession. Take-off configuration. Center aft: 33%.

(Flaps at 44°; N_G: 96.3%; V_c: 65 kt.)

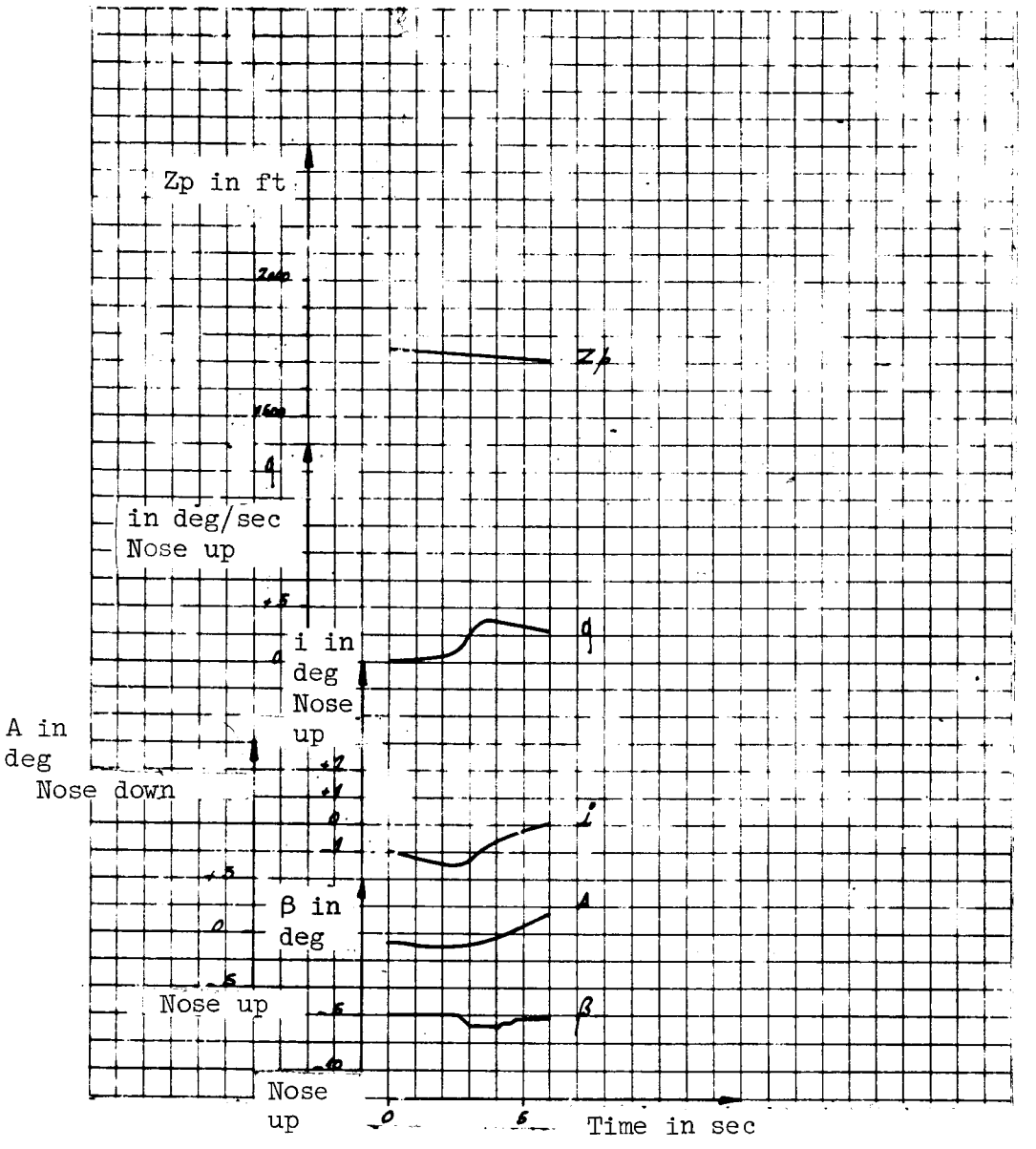

Figure 67. Response to configuration changes. Landing gear deployment. Center aft: 27%.

(Flaps at 30.5°; N_G: 88.4%; V_c: 102 kt.)

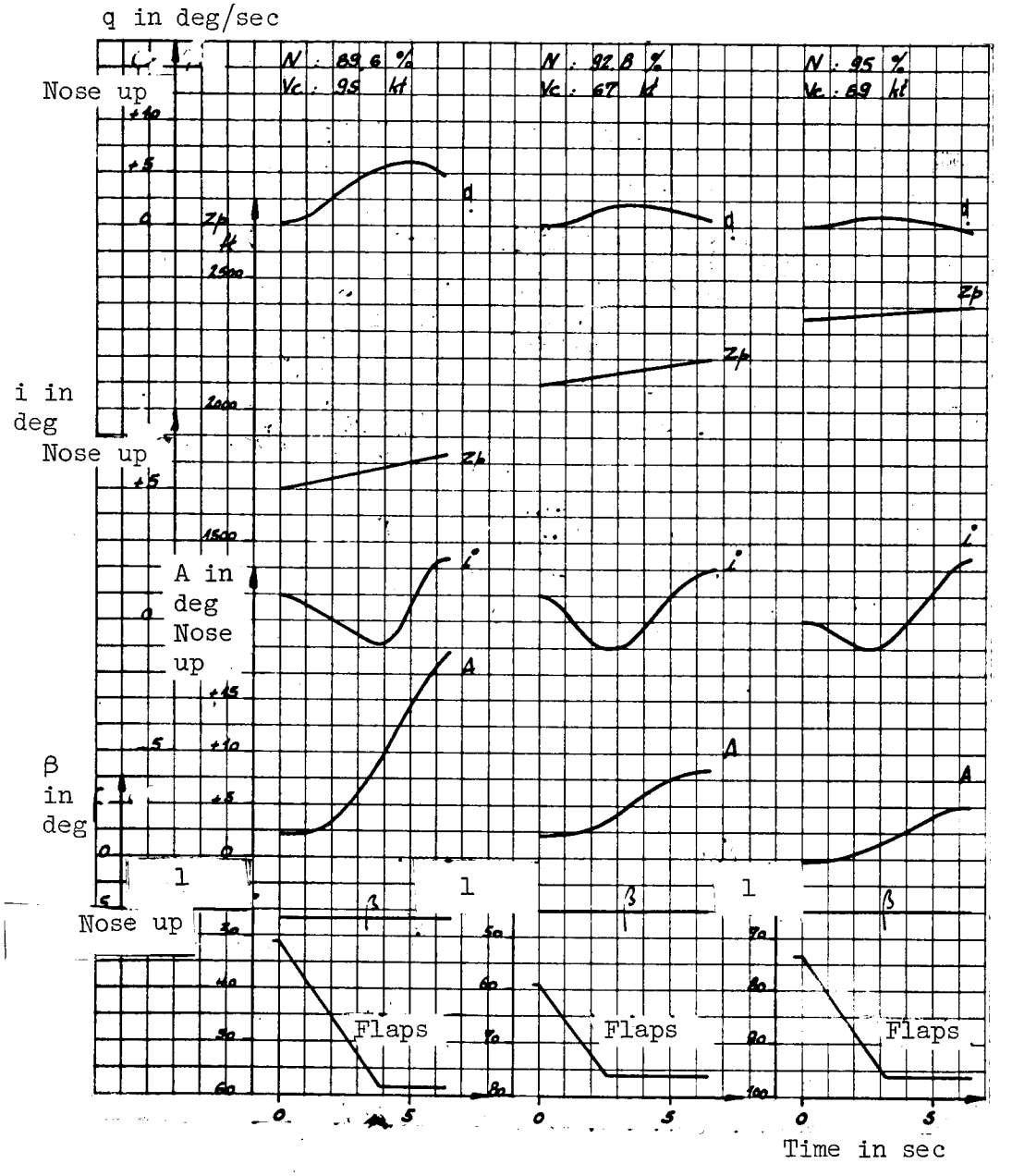

Figure 68. Response to configuration changes. Flaps out. 27% center fore.

l, Flap position in degrees.

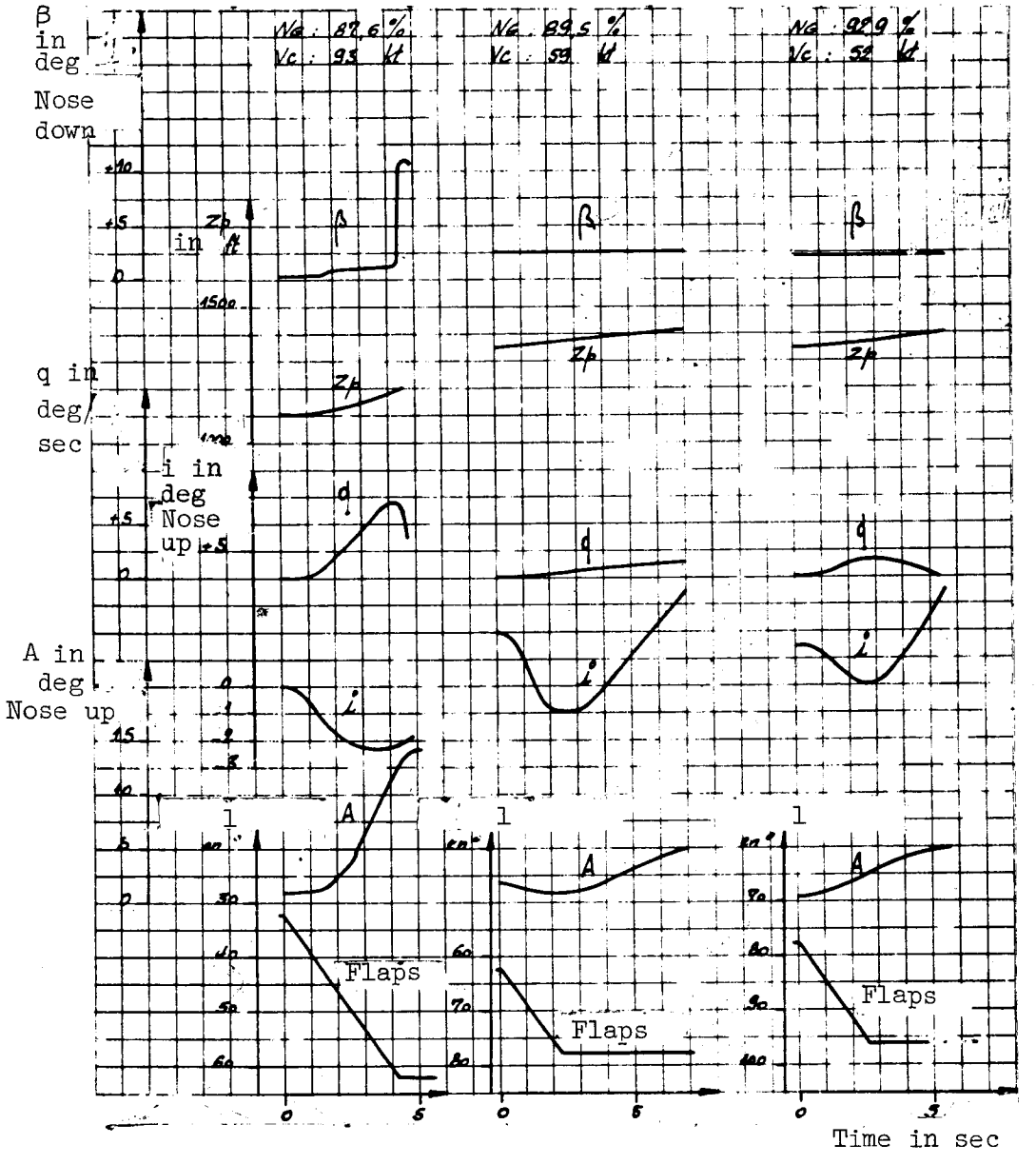

Figure 69. Response to configuration changes. Flaps out. 33% center aft.

l, Flap position in degrees.

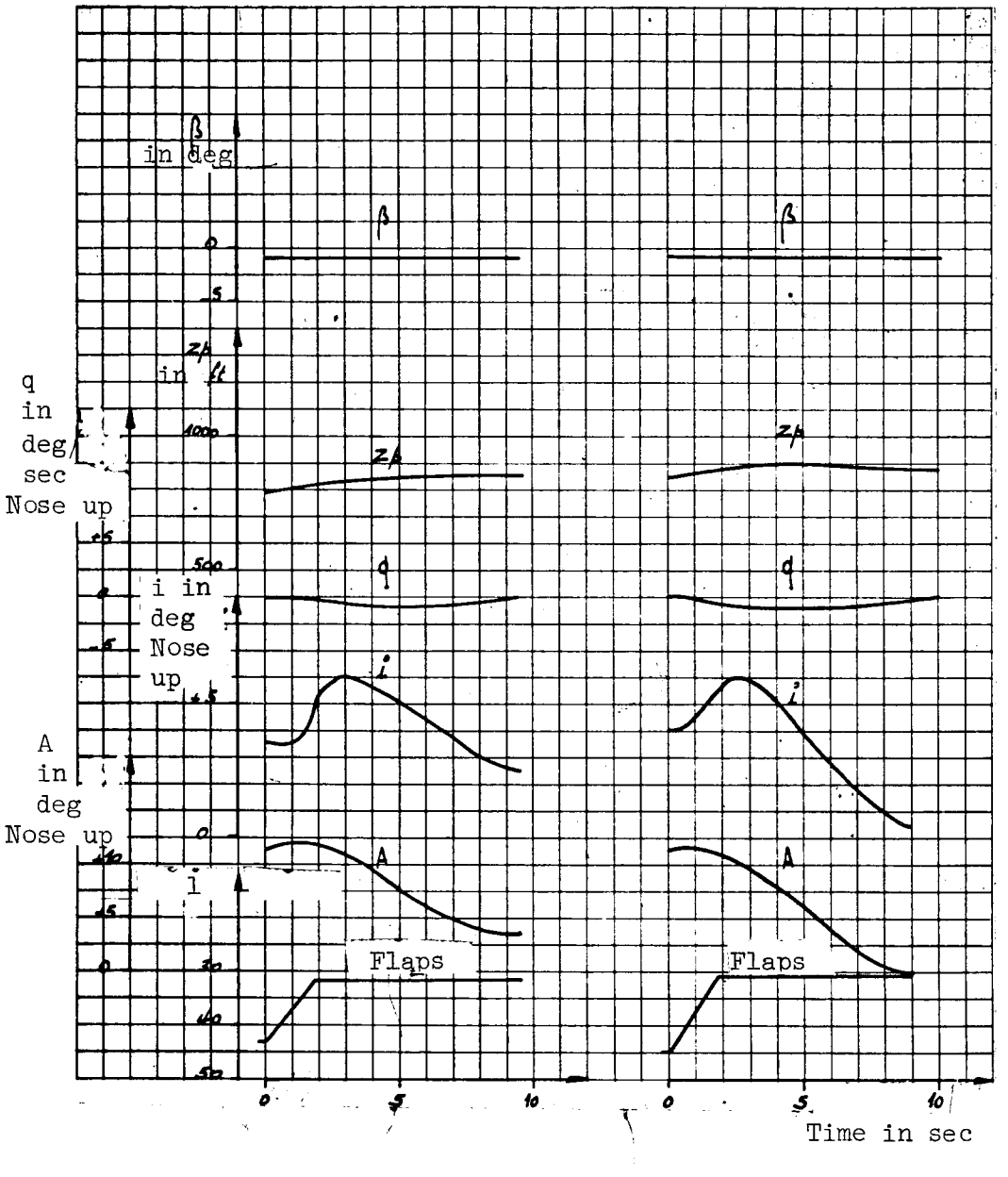

Figure 70. Response to configuration changes. Flaps recessed. Strong blowing. Center aft: 33%.

(Landing gear recessed; N_G: 96.8%; Vc = 65 kt.)

l, Flap position in degrees.

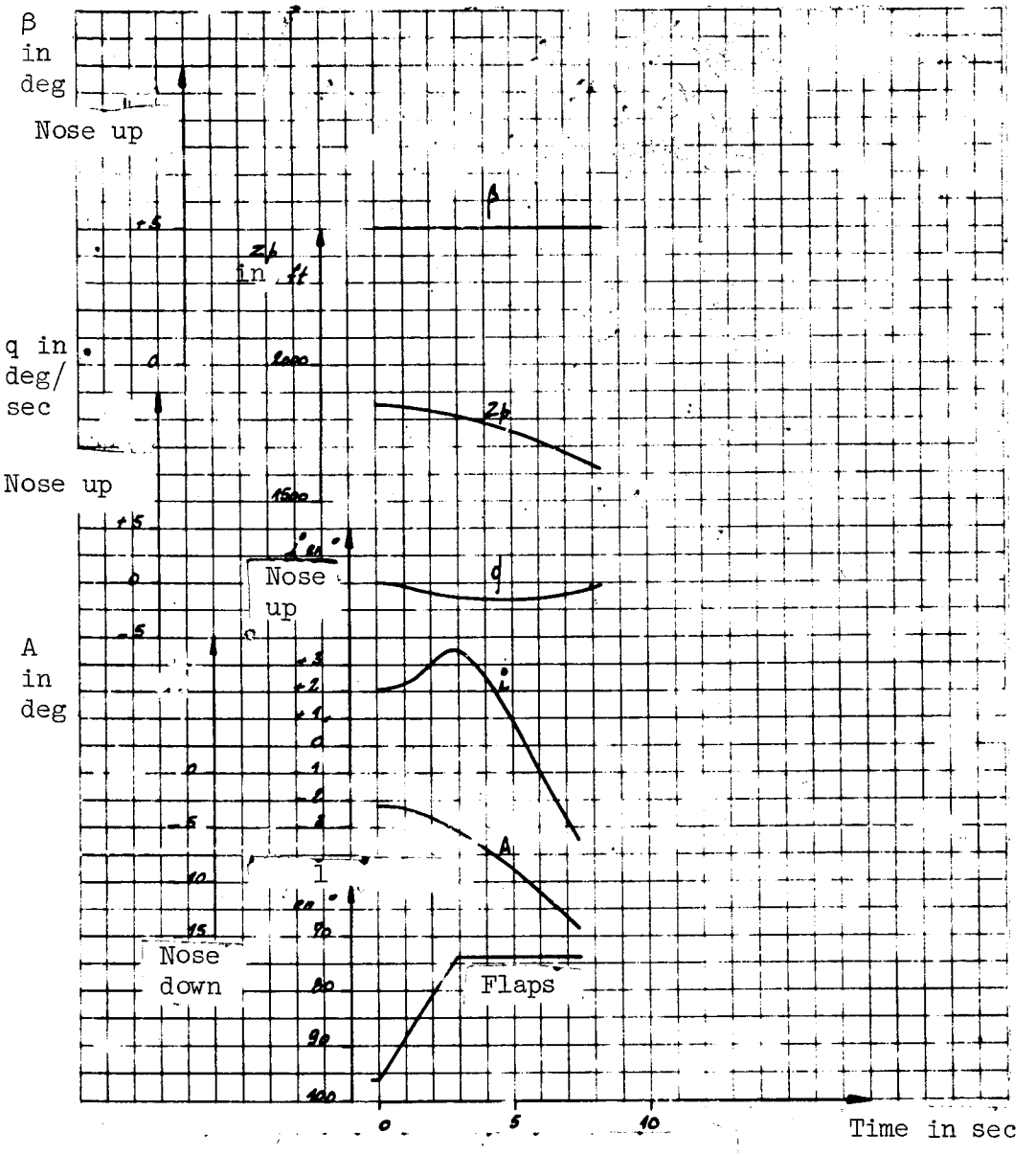

Figure 71. Response to configuration changes. Flaps recessed. Medium blowing. Center aft: 33%.

(Landing gear deployed; N_G: 88%; Vc: 50 kt.)

1, Flap position in degrees.

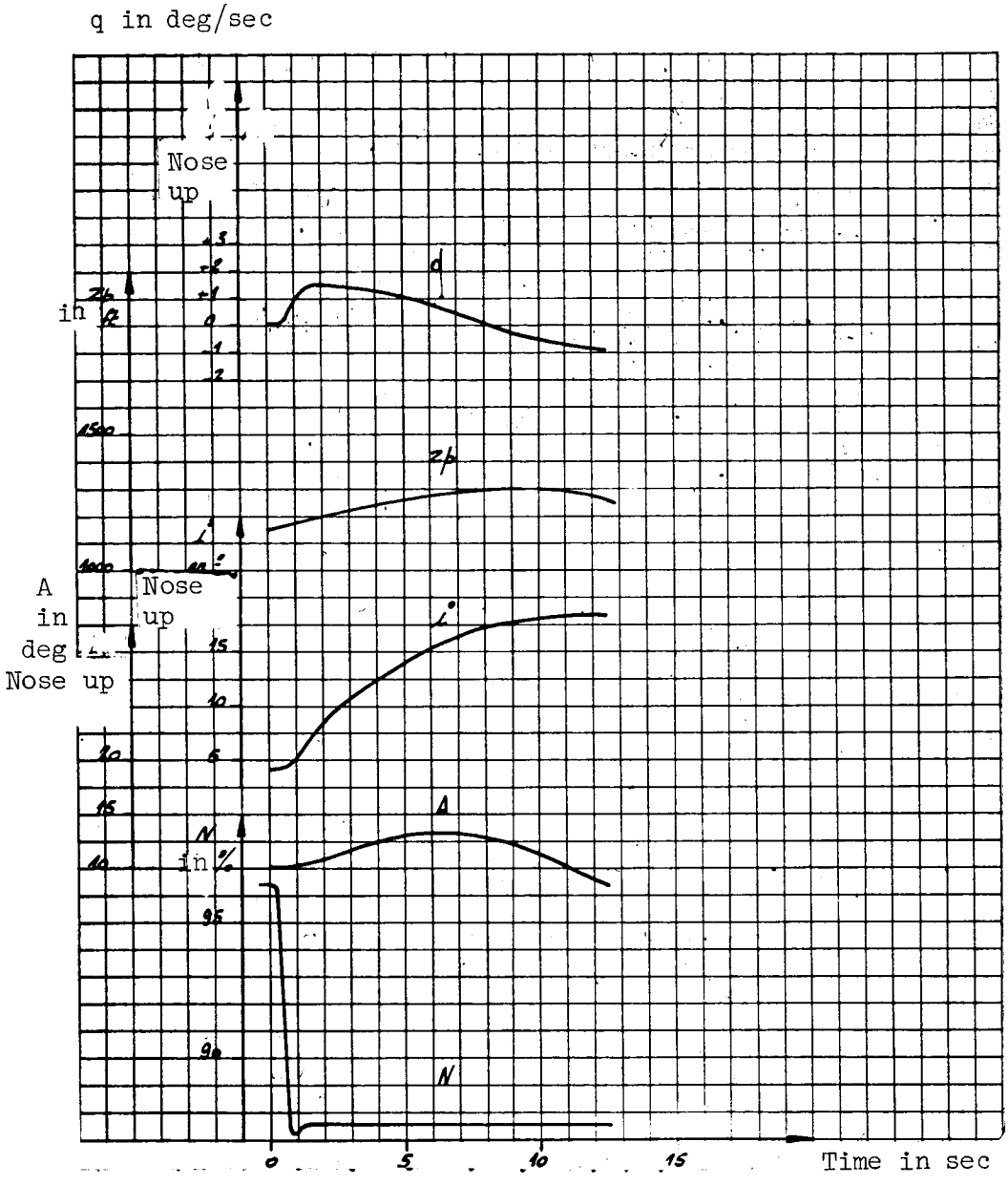

Figure 72. Response to configuration changes. Throttle reduction at take-off. Center aft: 33%.

(Landing gear deployed; flaps at 43°; Vc: 67 kt.)

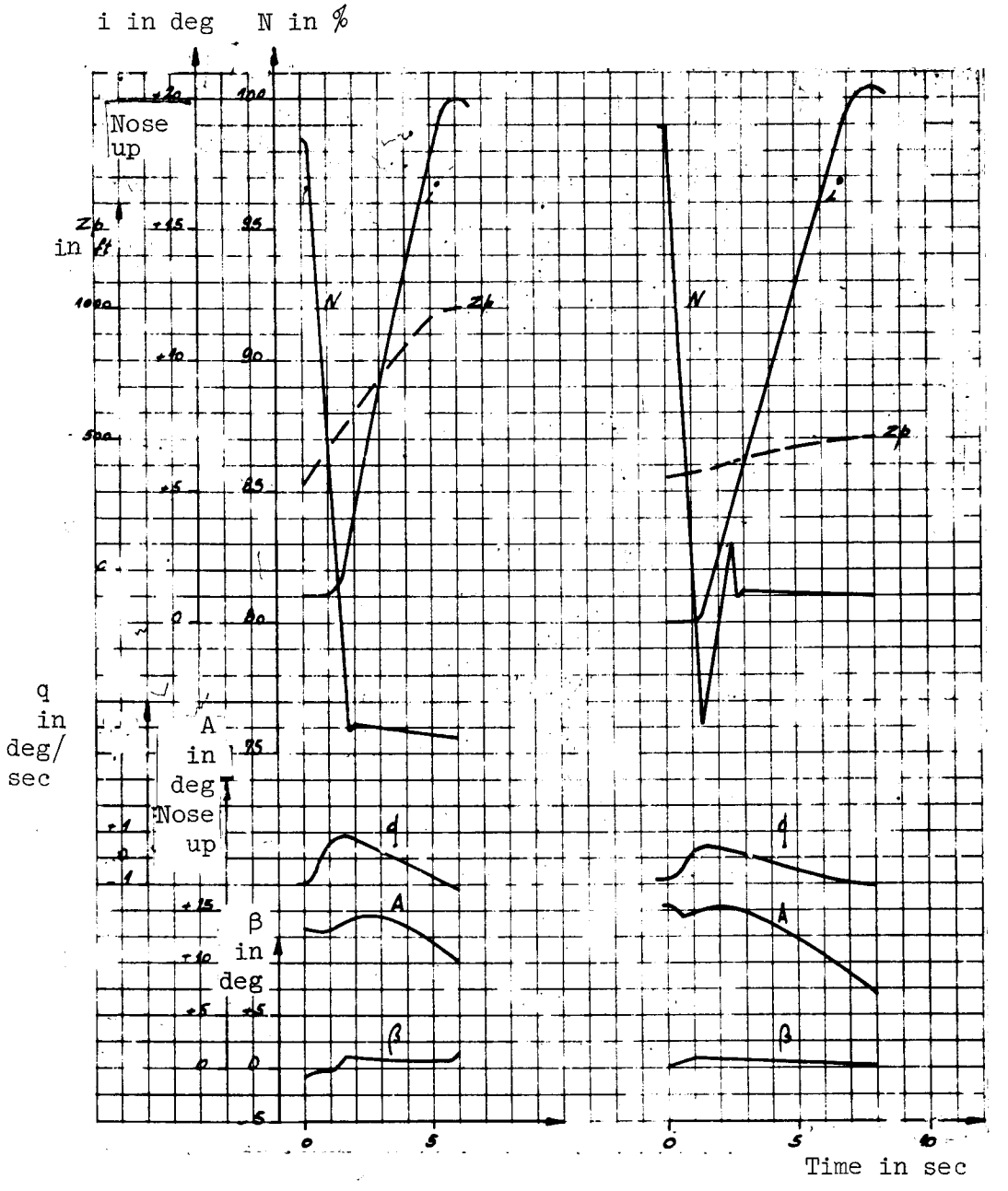

Figure 73. Response to configuration changes. Throttle reduction at take-off. Center aft: 33%.

(Landing gear recessed; flaps at 44°; Vc: 67 kt.)

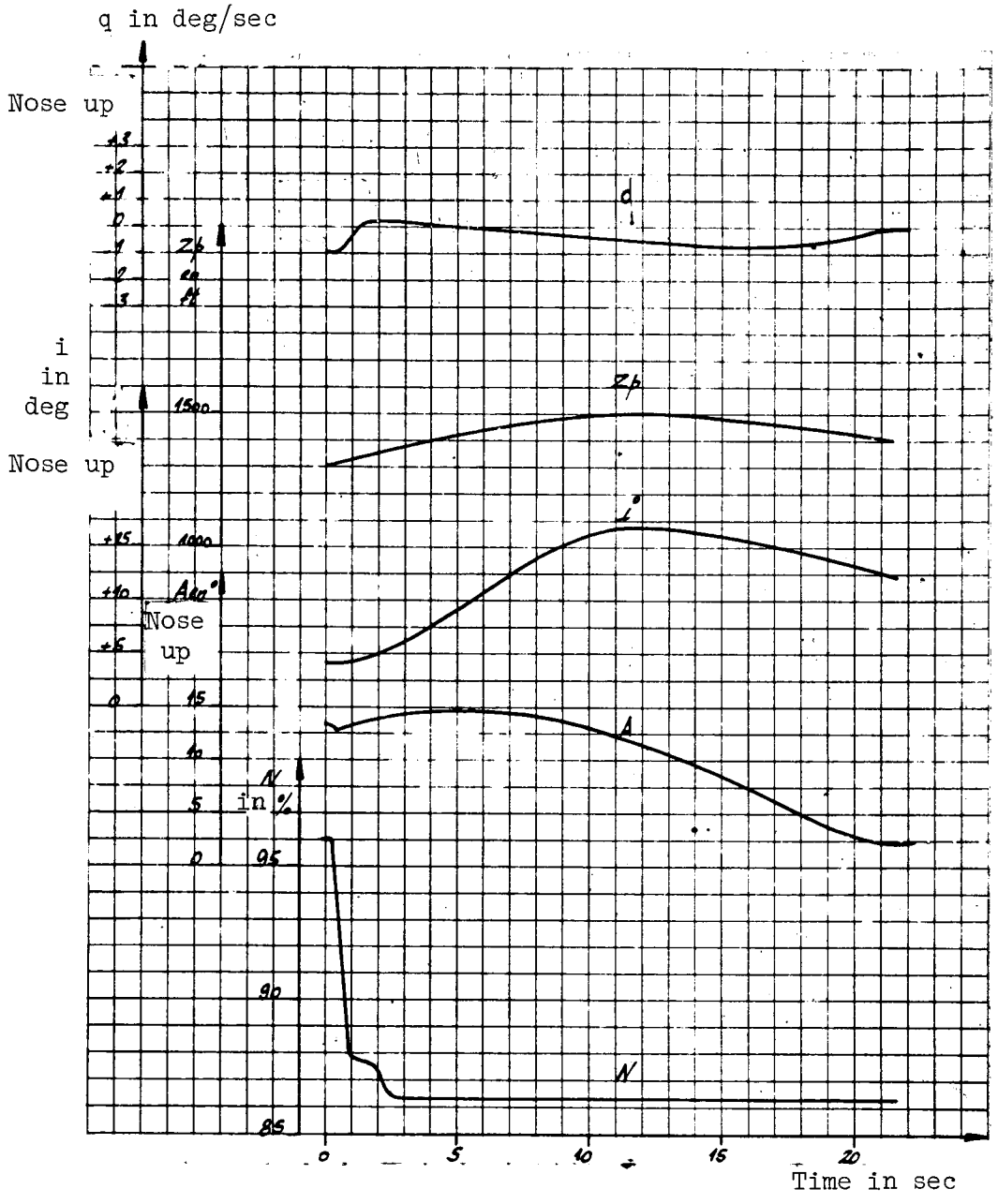

Figure 74. Response to configuration changes. Throttle reduction at ascension. Center aft: 33%.

(Landing gear deployed; flaps at 30°; Vc: 76 kt.)

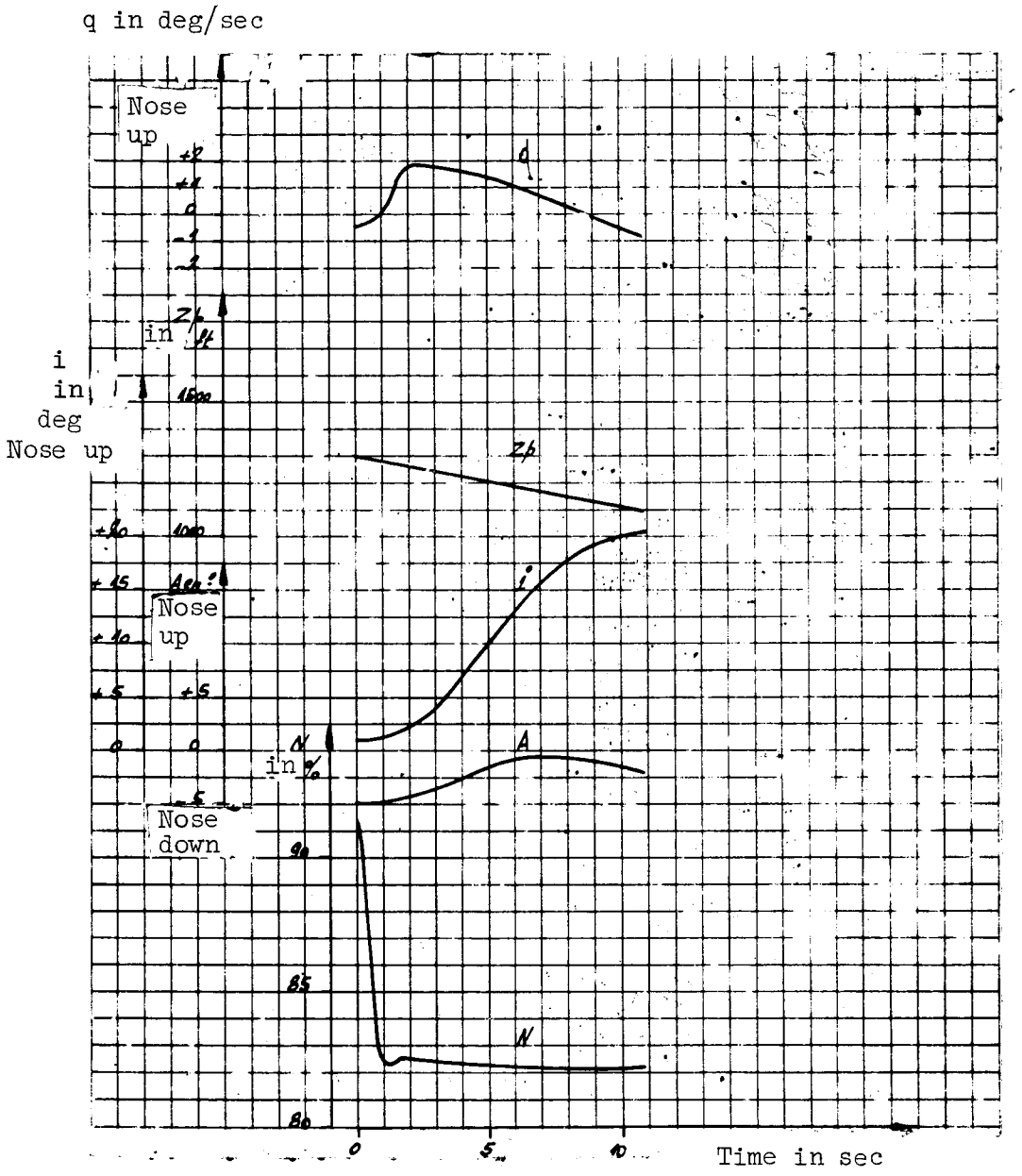

Figure 75. Response to configuration changes. Throttle reduction at landing. Center aft: 33%.

(Landing gear deployed; flaps at 97°; Vc: 49 kt.)

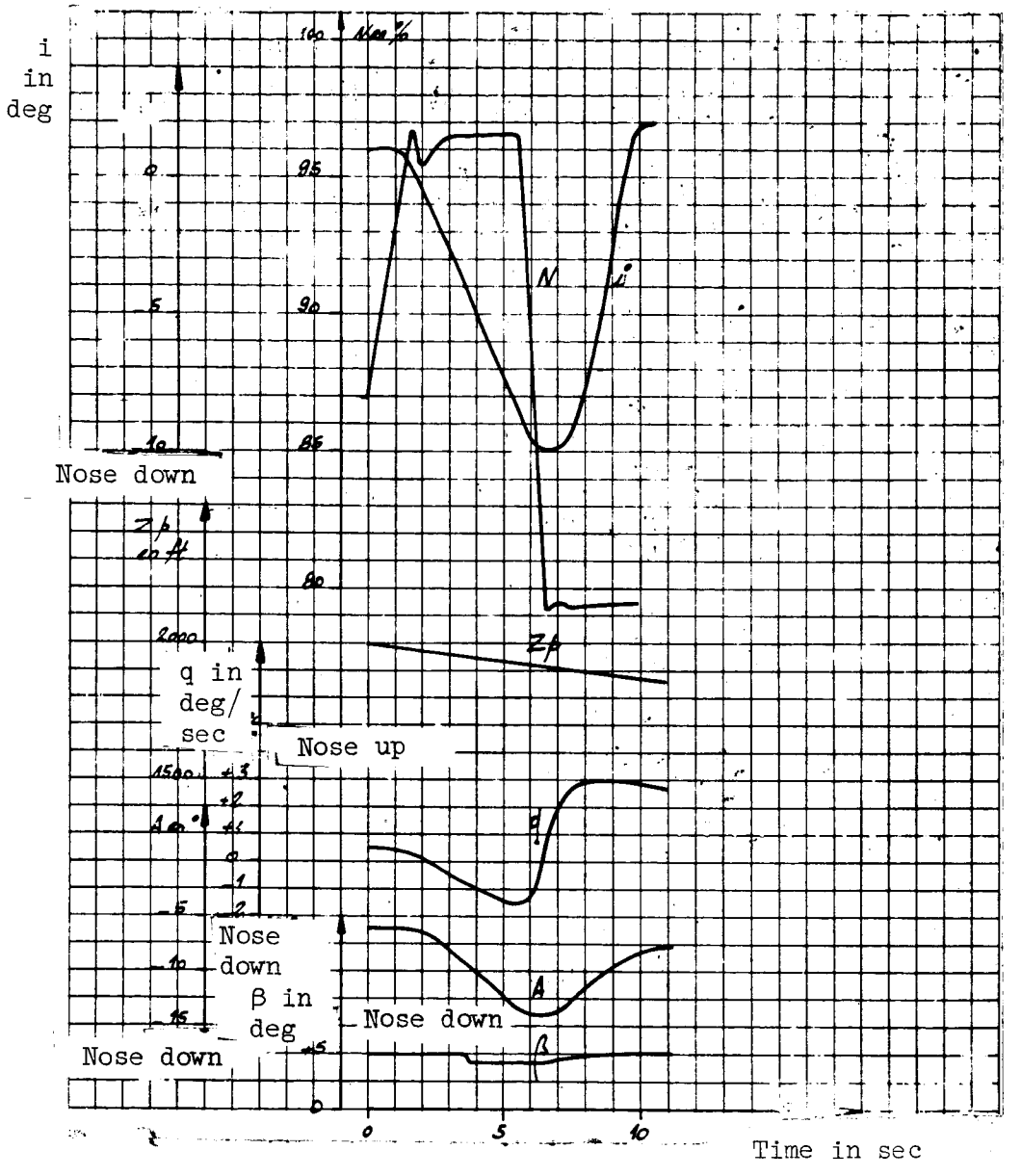

Figure 76. Response to configuration changes. Throttle resumption and reduction. Center aft: 33%.

(Landing gear deployed; flaps at 95.5°; Vc: 52 kt.)

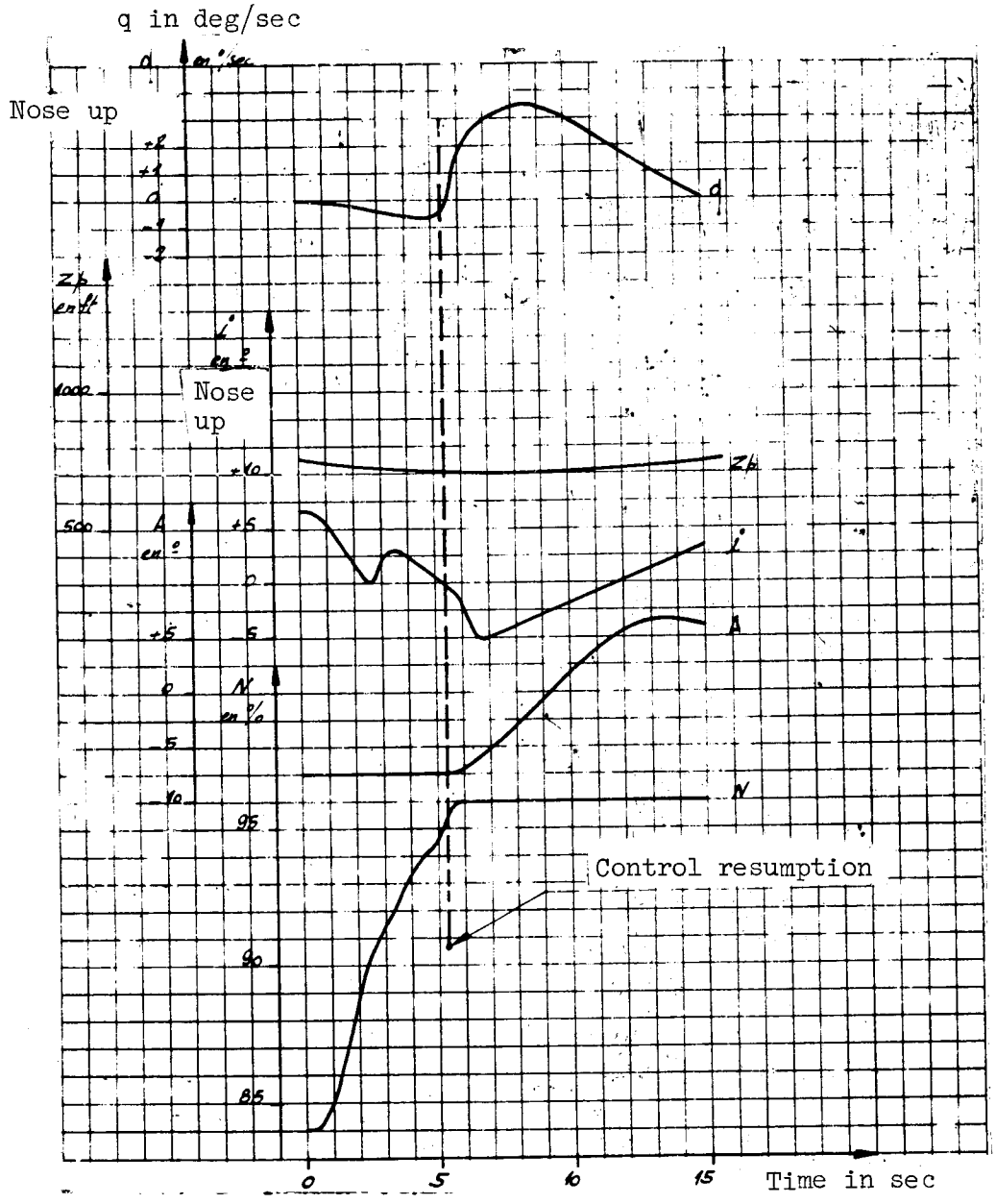

Figure 77. Response to configuration changes. Throttle and control resumptions. Center aft: 33%.

(Landing gear deployed; flaps: 97°; Vc: 55 kt.)

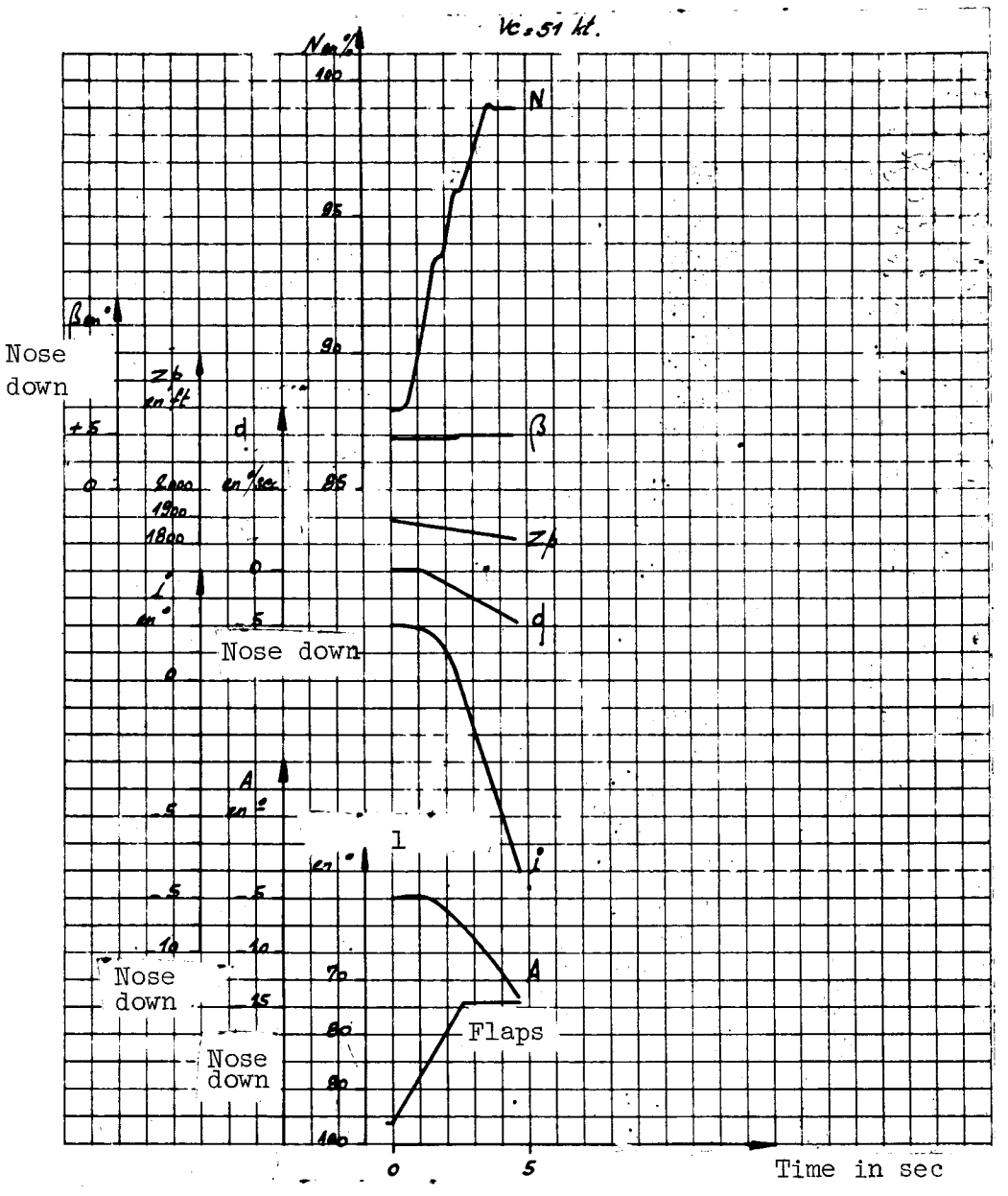

Figure 78. Response to configuration changes. Throttle resumption and simultaneous recession of the flaps. Center aft: 33%.

l, Flaps position in degrees.

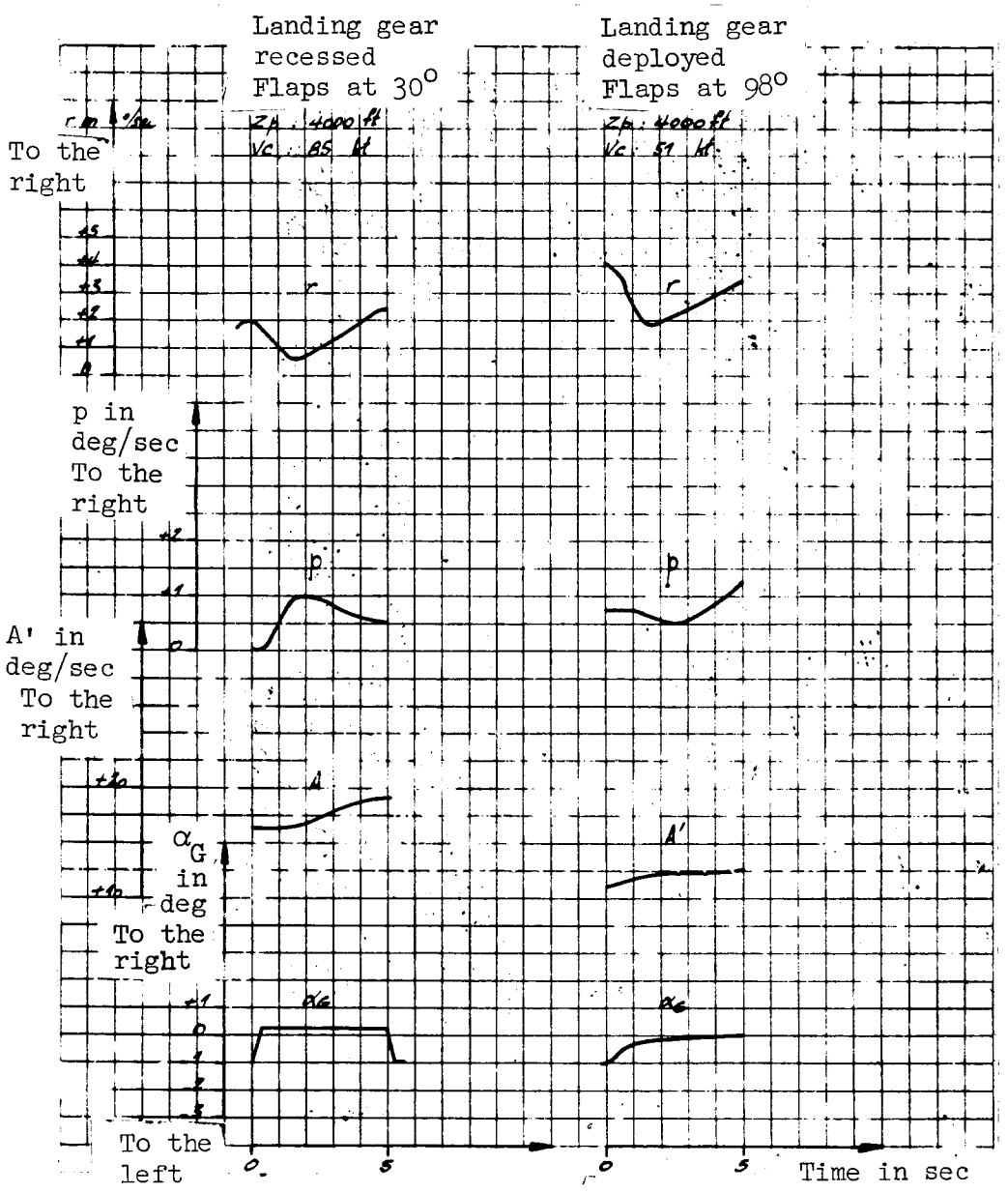

Figure 79. Spiral stability. Release of the stick in controlled turn.

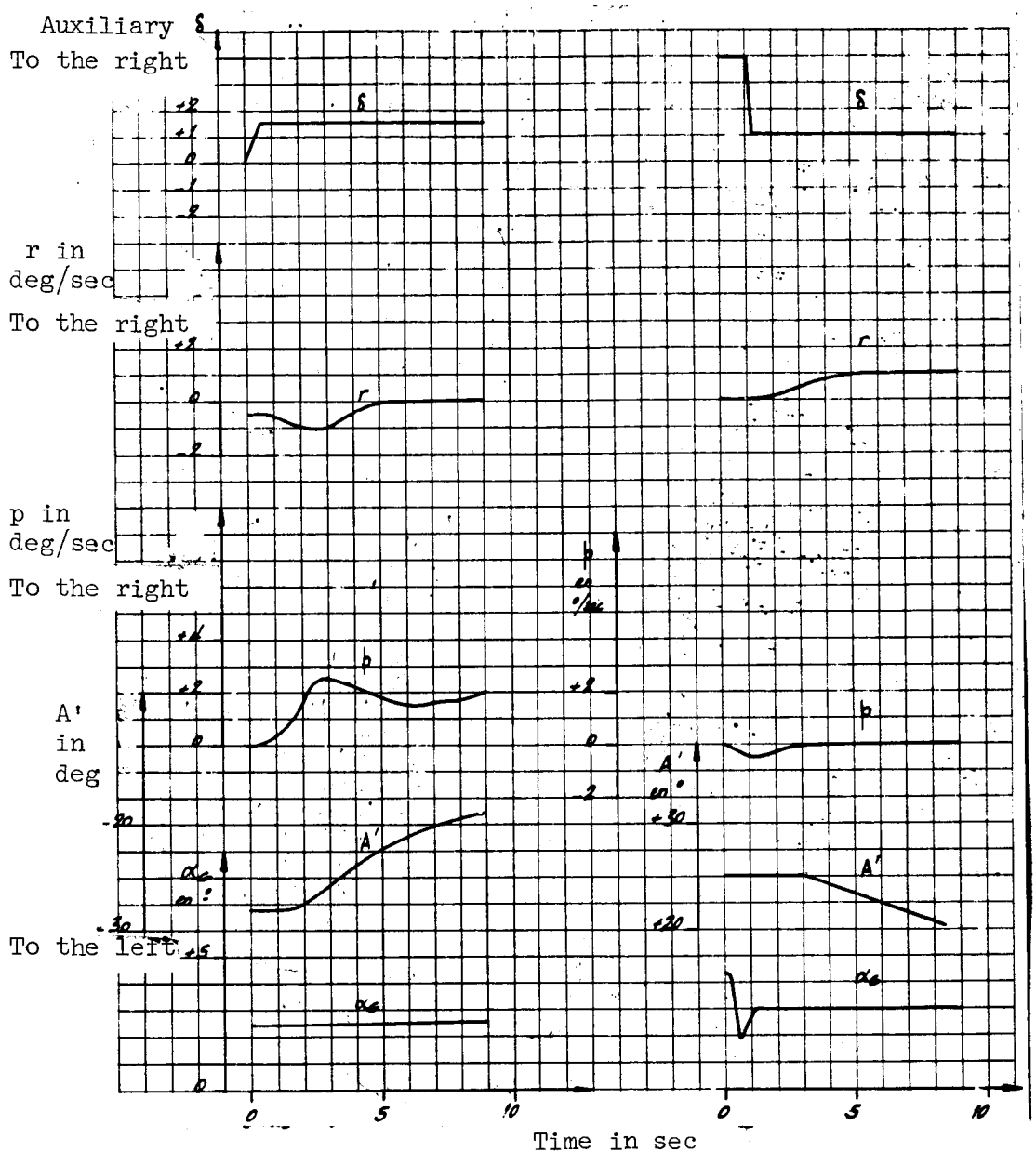

Figure 80. Spiral stability. Release of the stick in cruising turn.

(Smooth configuration; medium Zp = 6300 ft; N = 91.6 %: Vc = 140 kt.)

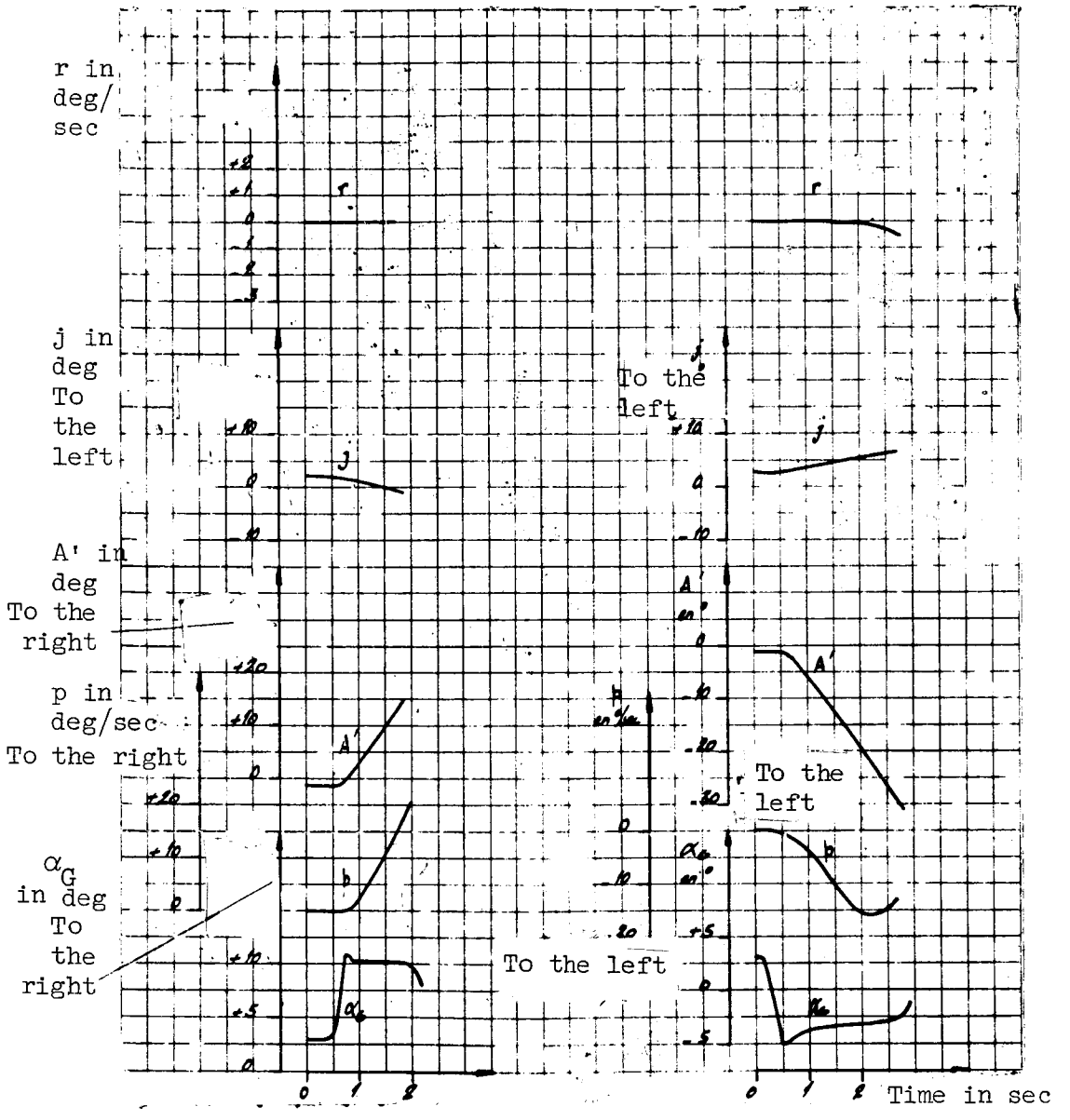

Figure 81. Warping. α square steps. Smooth configuration.

(Medium Zp = 6300 ft; N = 91.6%; Vc = 141 kt.)

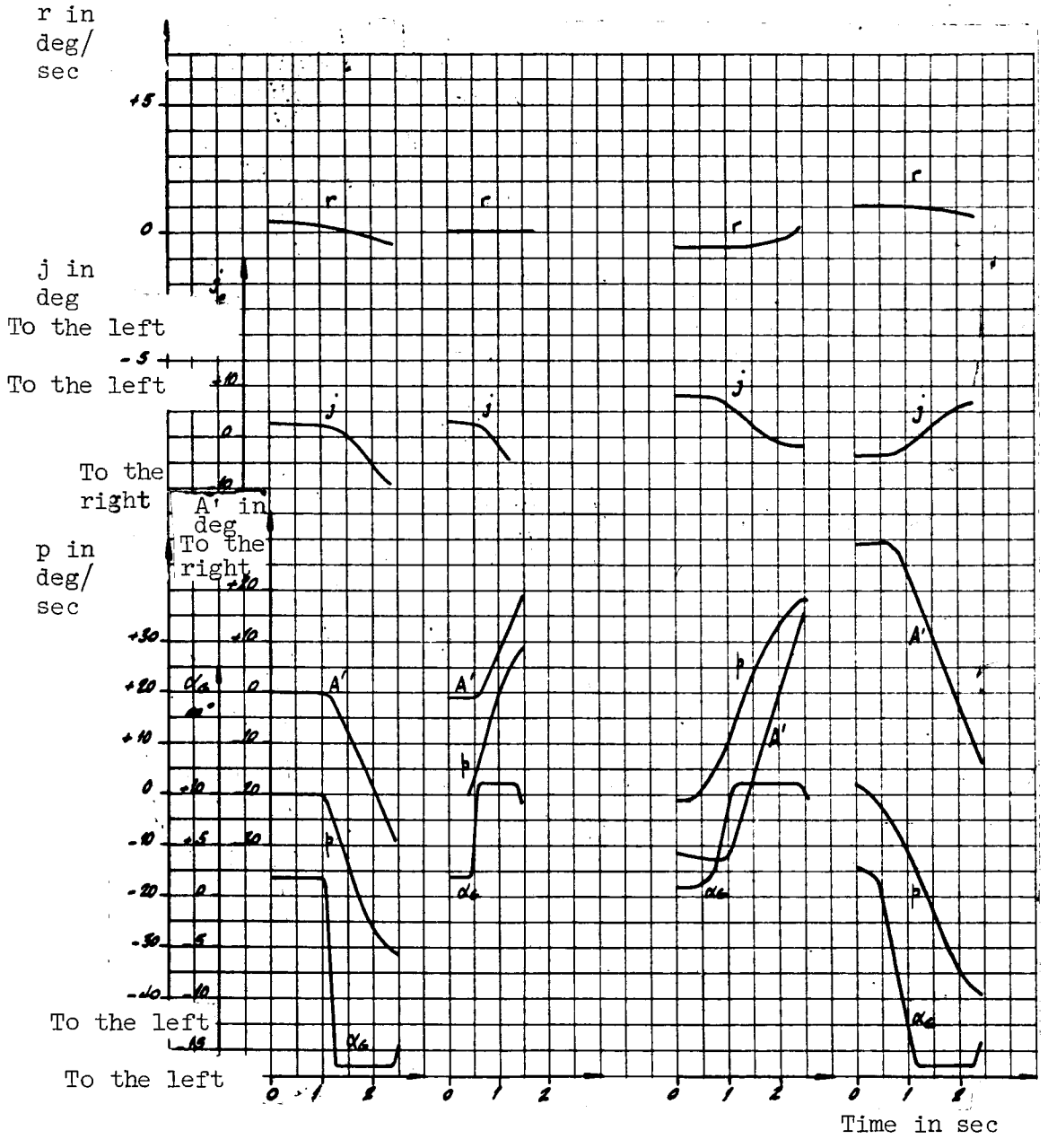

Figure 82. Warping. α square steps. Smooth configuration.

(Medium Zp = 5100 ft; N = 93%; Vc = 140 kt.)

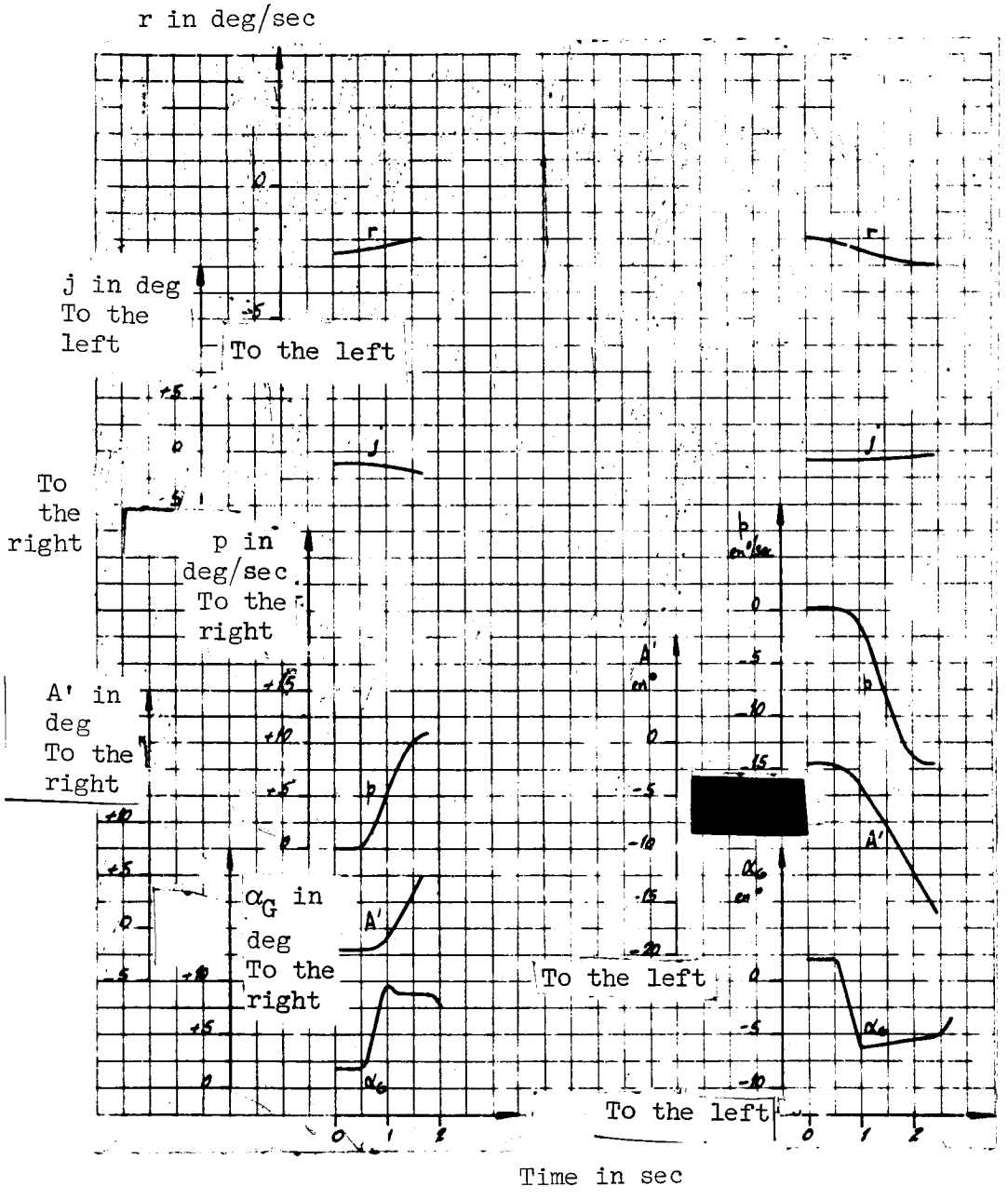

Figure 83. Warping. α_G square steps. Smooth configuration. No differential.

(1/2 deflection; fixed δ_1; Zp = 2500 ft; N = 94.3%; Vc = 137 kt.)

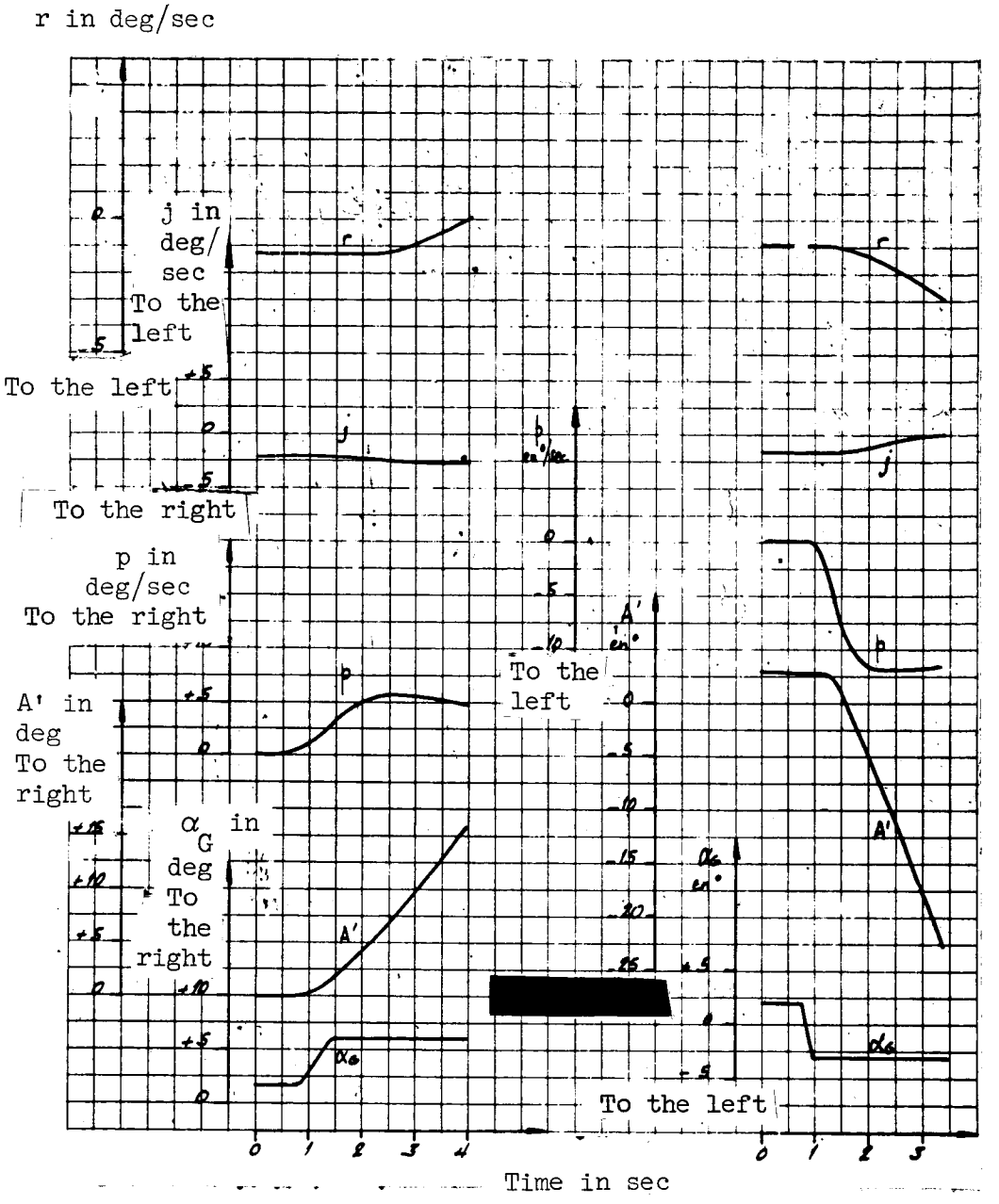

Figure 84. Warping. α square steps. Smooth configuration. No differential.

(Fixed δ_1; Zp = 2850 ft; N = 94.3%; Vc = 172 kt.)

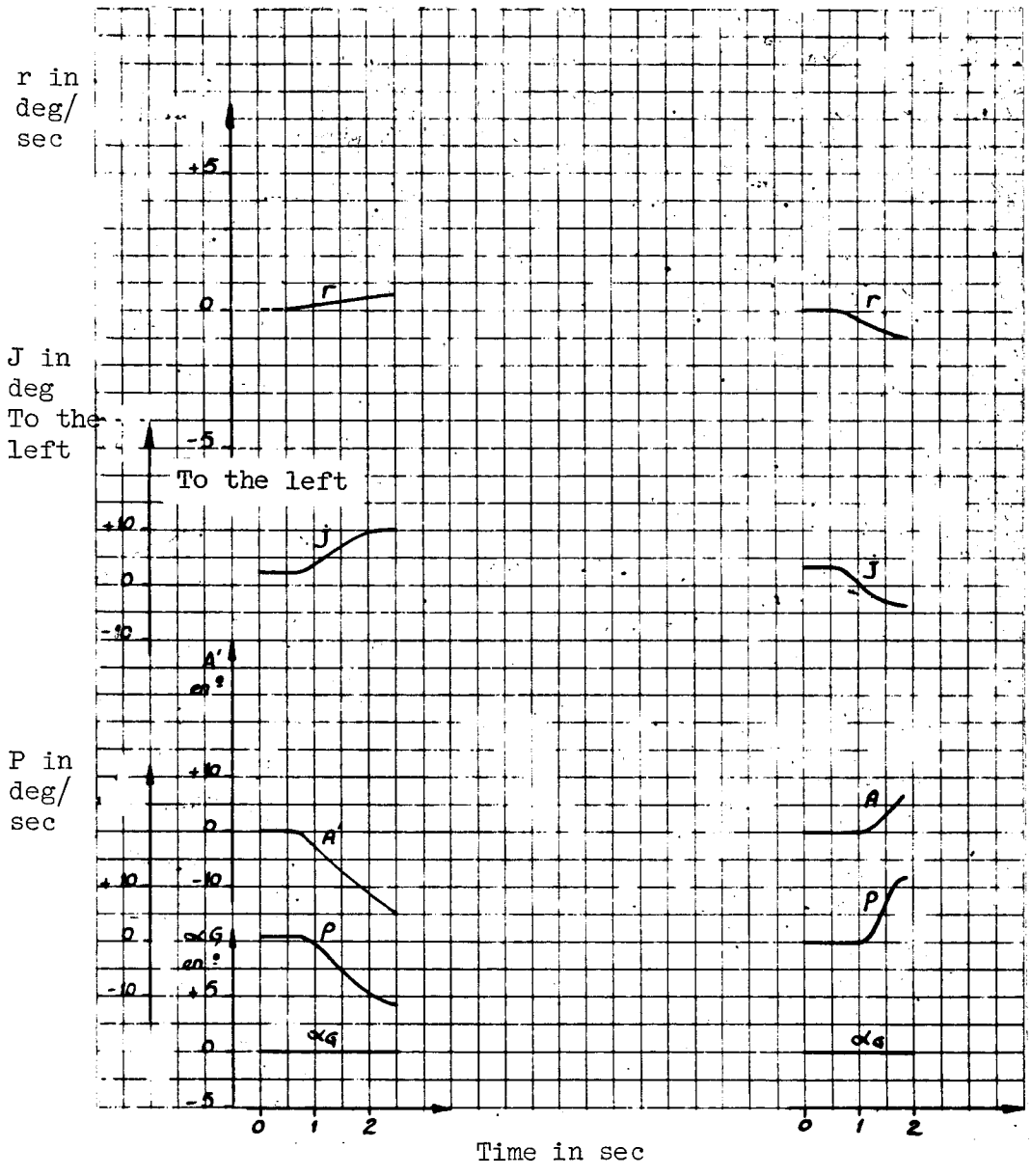

Figure 85. Warping. Fixed ailerons. Cruising configuration.

(Zp = 7000 ft; N = 92.1%; Vc = 123 kt.)

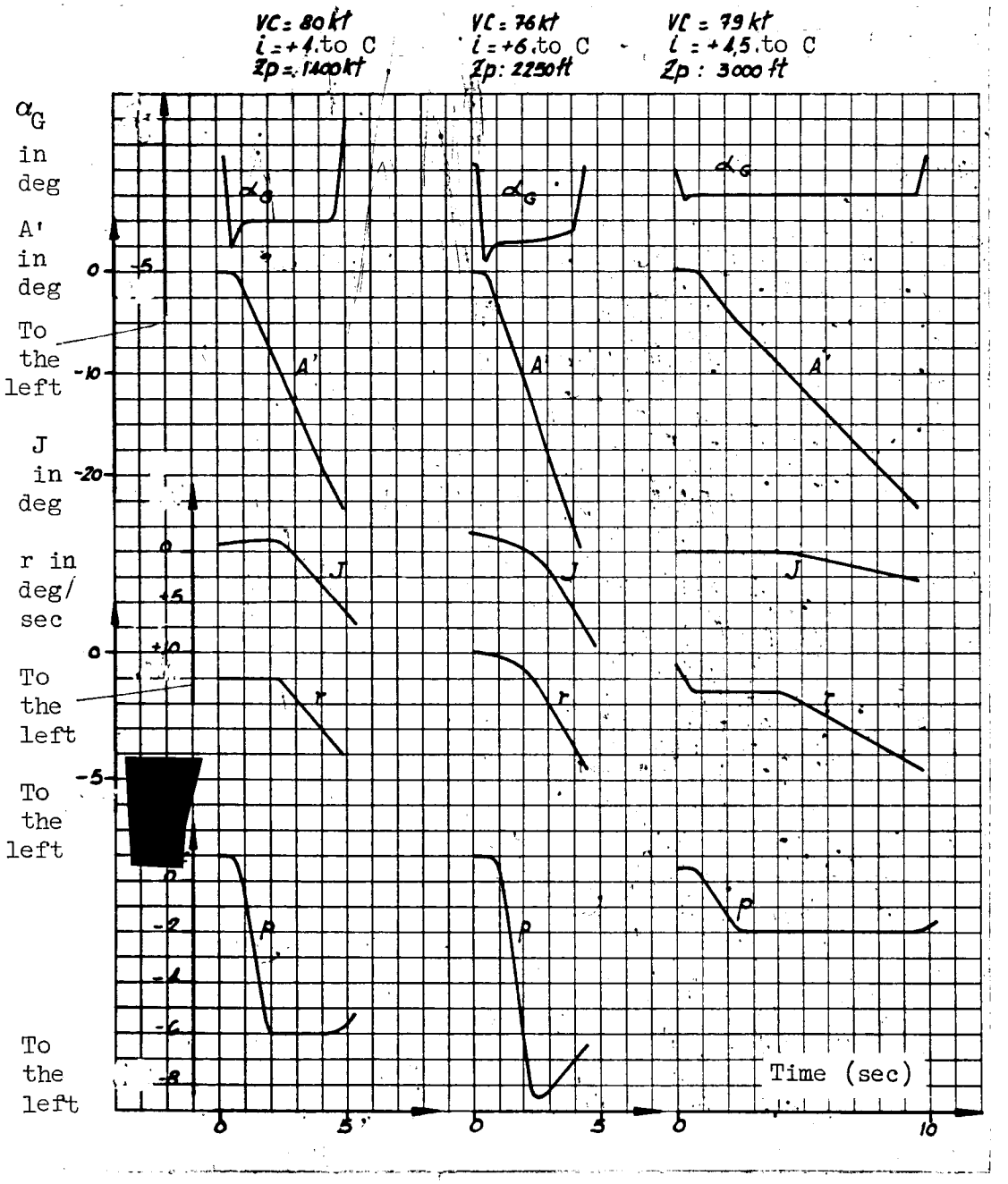

Figure 86. Warping response. Ascension configuration.

(Flaps at 30°; N_G: 96.2%.)

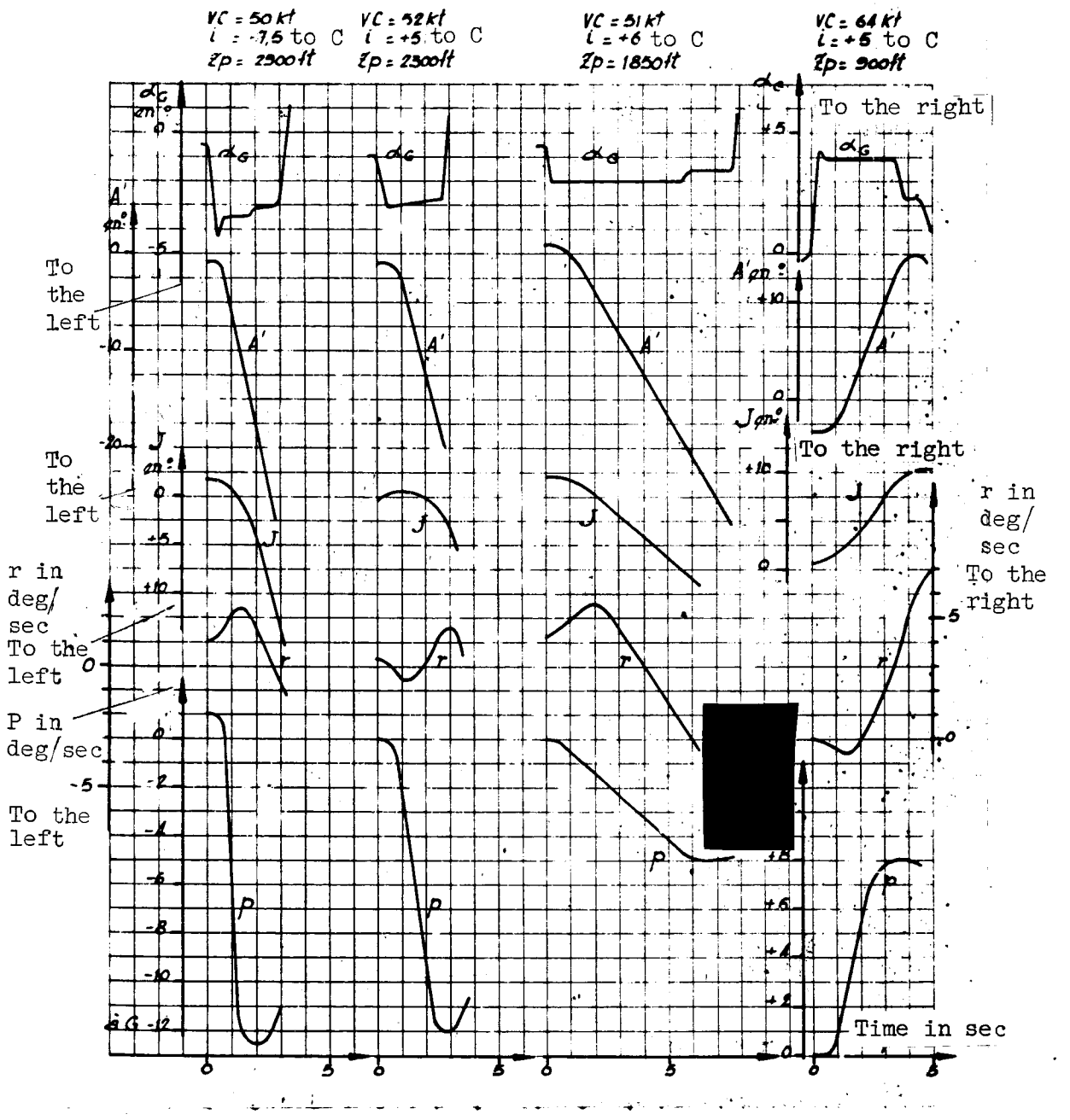

Figure 87. Warping response. Landing with medium blowing configuration.

(Flaps at 97°; N_G = 88.2%.)

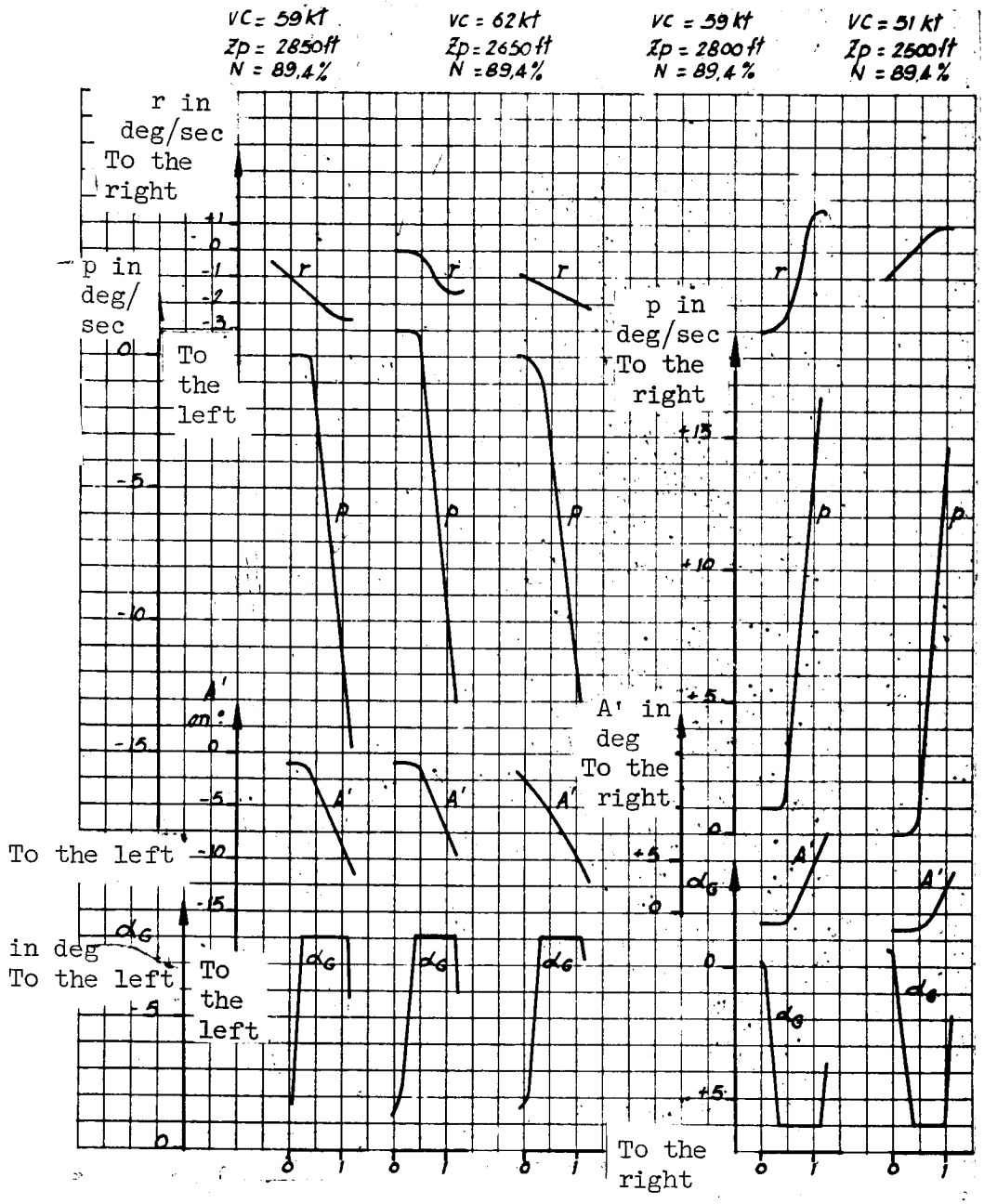

Figure 88. Warping response. Landing with spoilers configuration.

(Flaps: 97%)

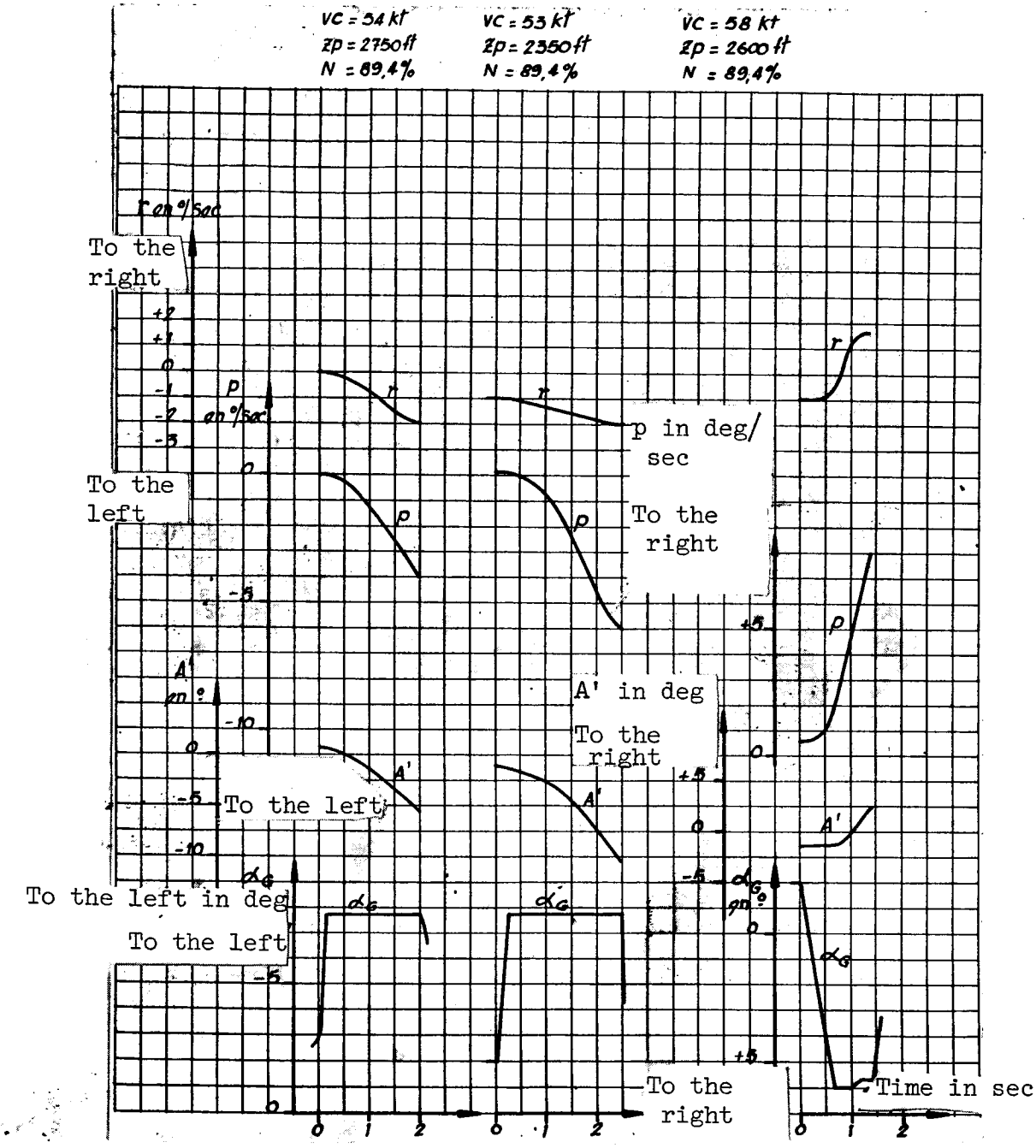

Figure 89. Warping response. Landing without spoilers

(Flaps at 97°)

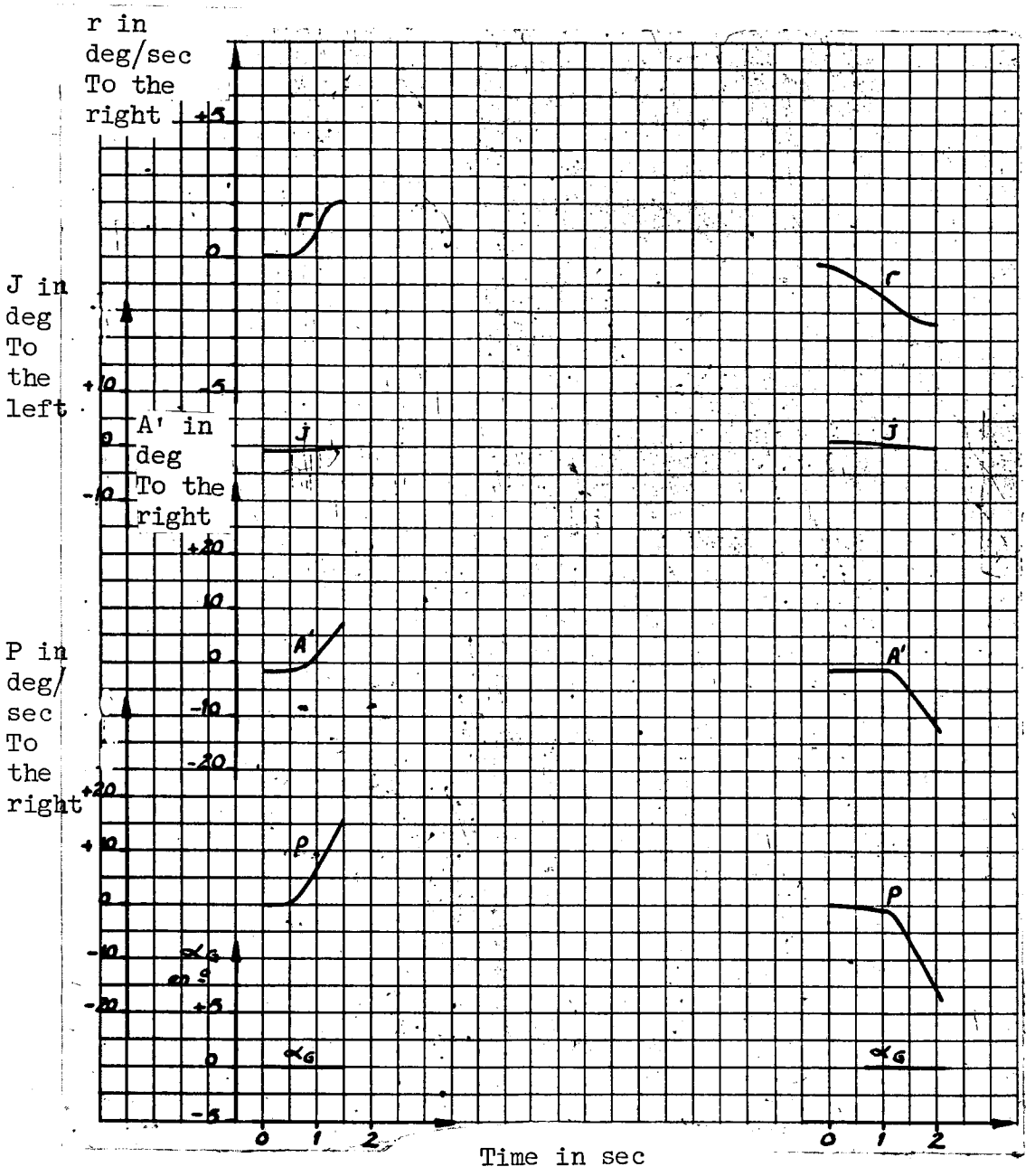

Figure 90. Warping response. Landing with fixed ailerons configuration.

(Flaps at 97°)

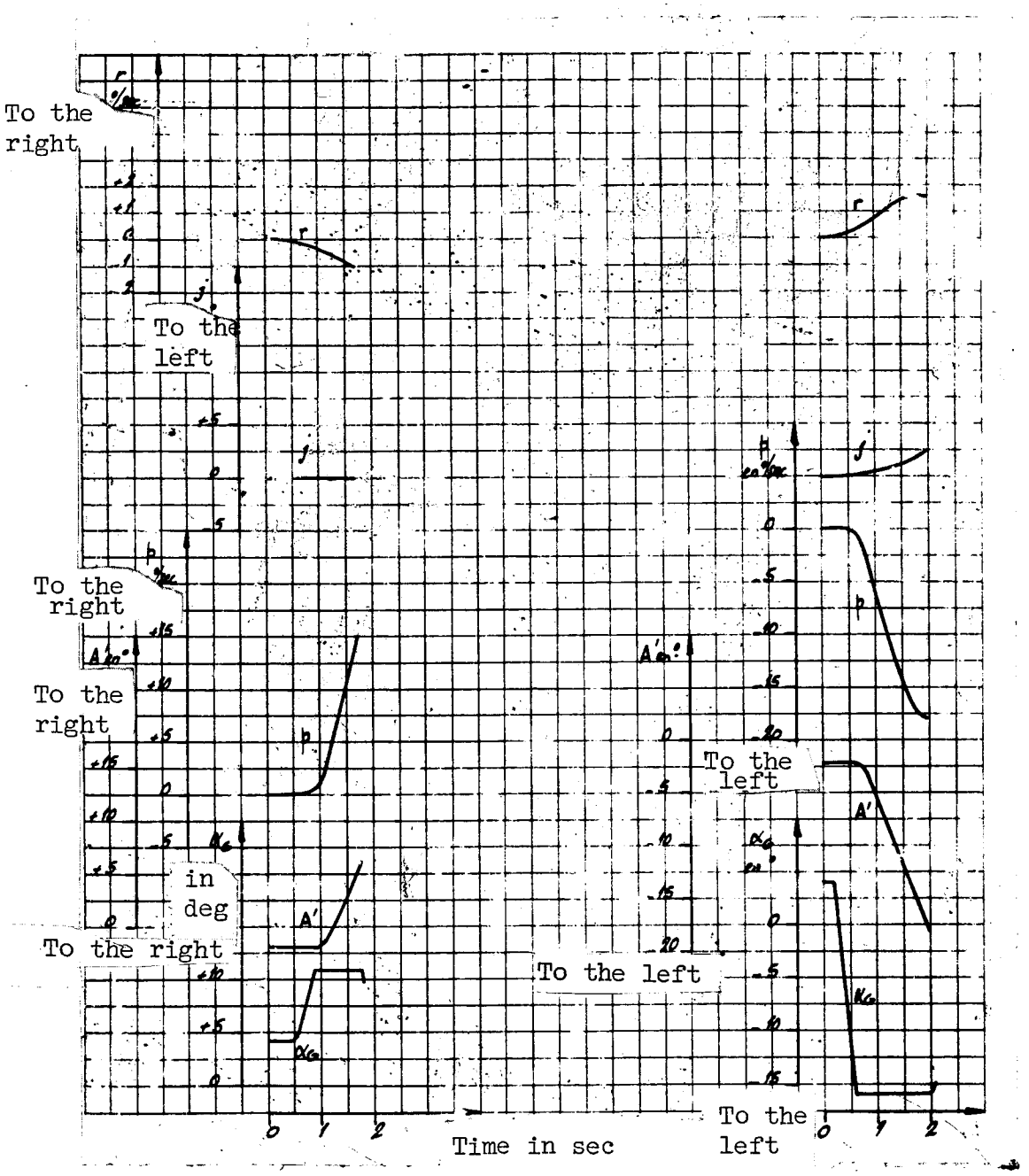

Figure 91. Warping response. Landing with no differential.
α_G square steps.

(Flaps at 97°; Zp: 2200 ft; N = 89.9%; Vc = 62 kt.)

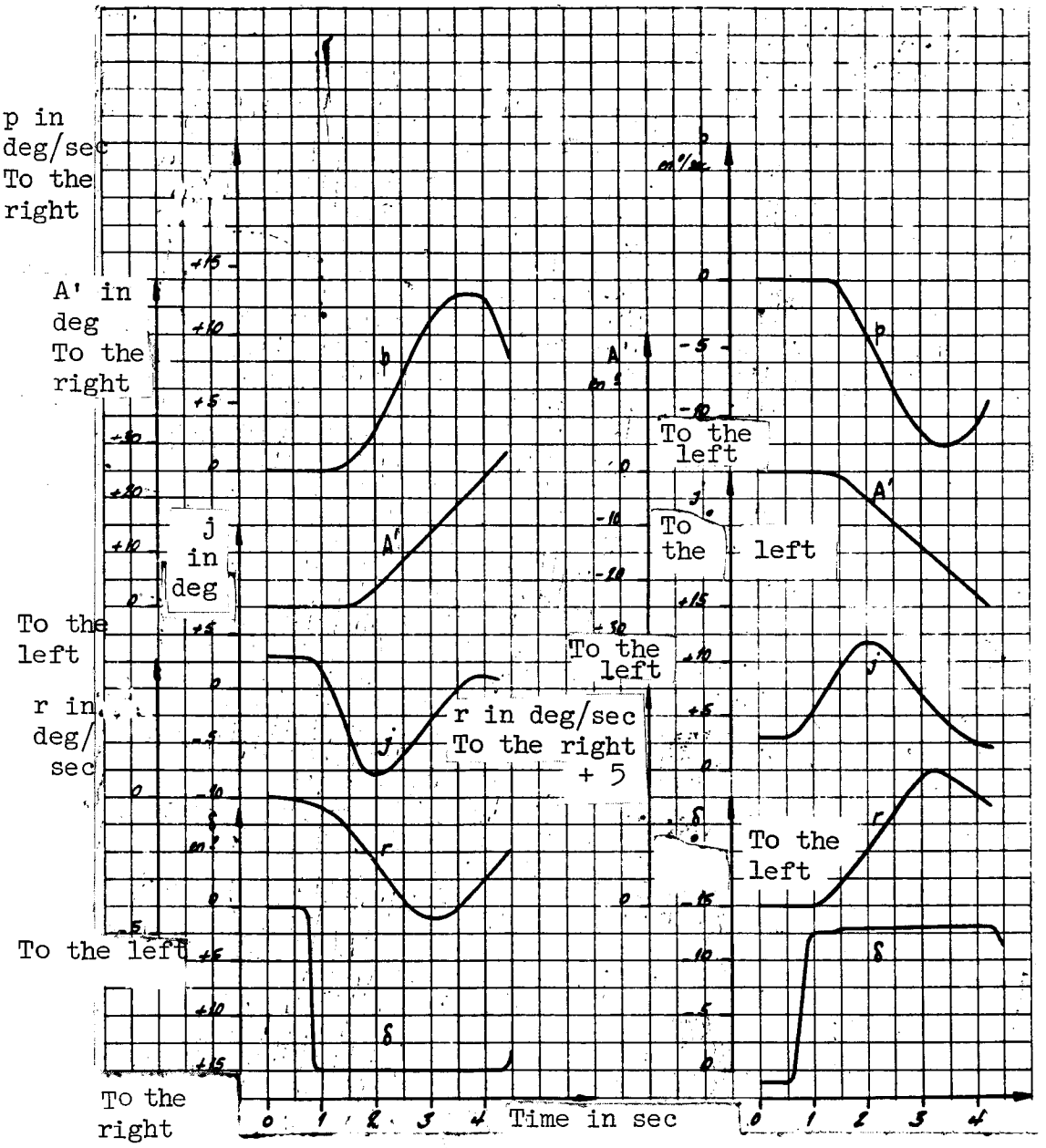

Figure 92. Rudder response. δ_2 square steps. Fixed main flap in smooth configuration.

(Zp = 6150 ft; N = 91.5%; Vc = 143 kt.)

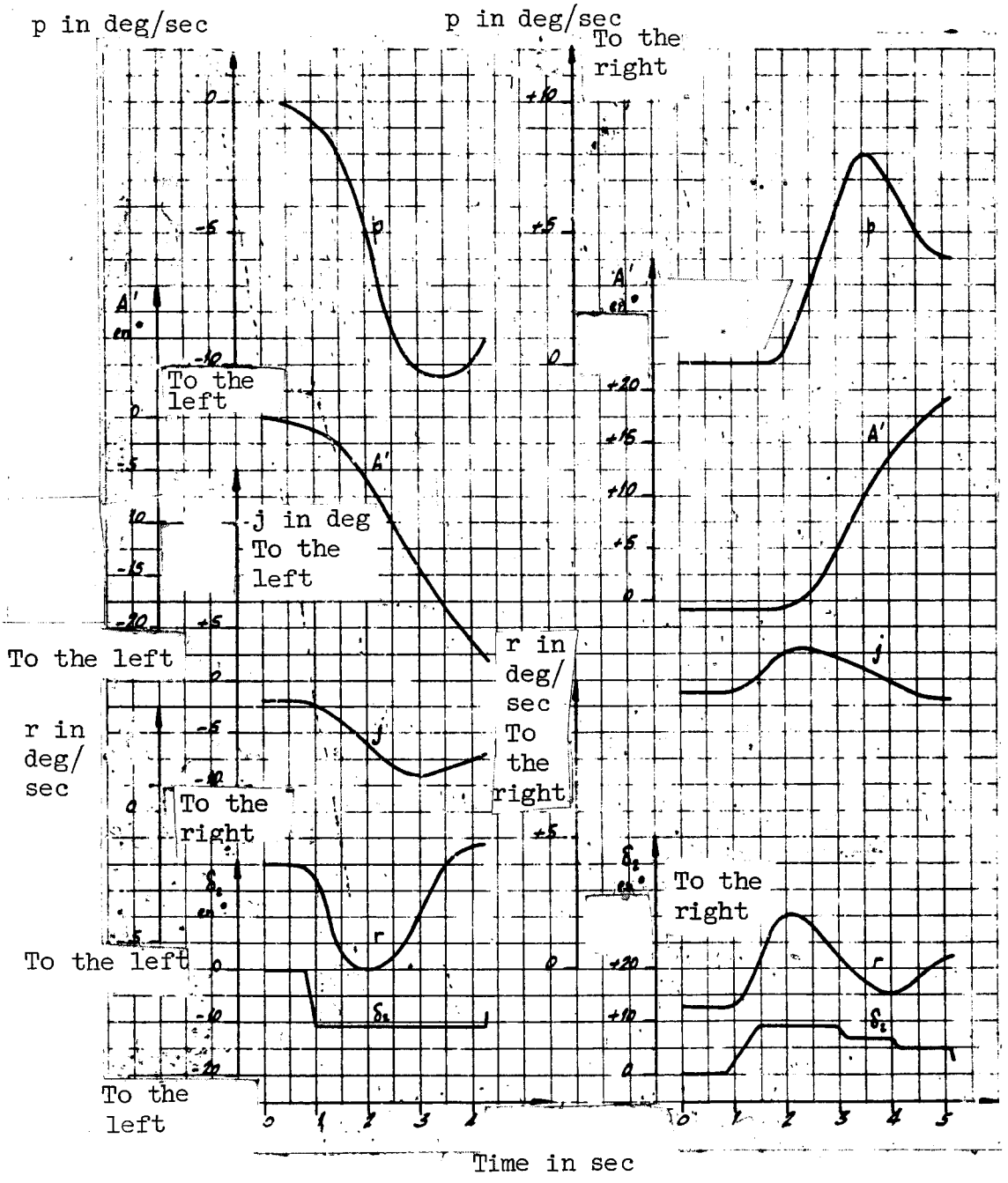

Figure 93. Rudder response. δ_2 square steps. With differential. Smooth configuration.

(Fixed δ_1; Zp = 2900 ft; N = 94.3%; Vc = 142 kt.)

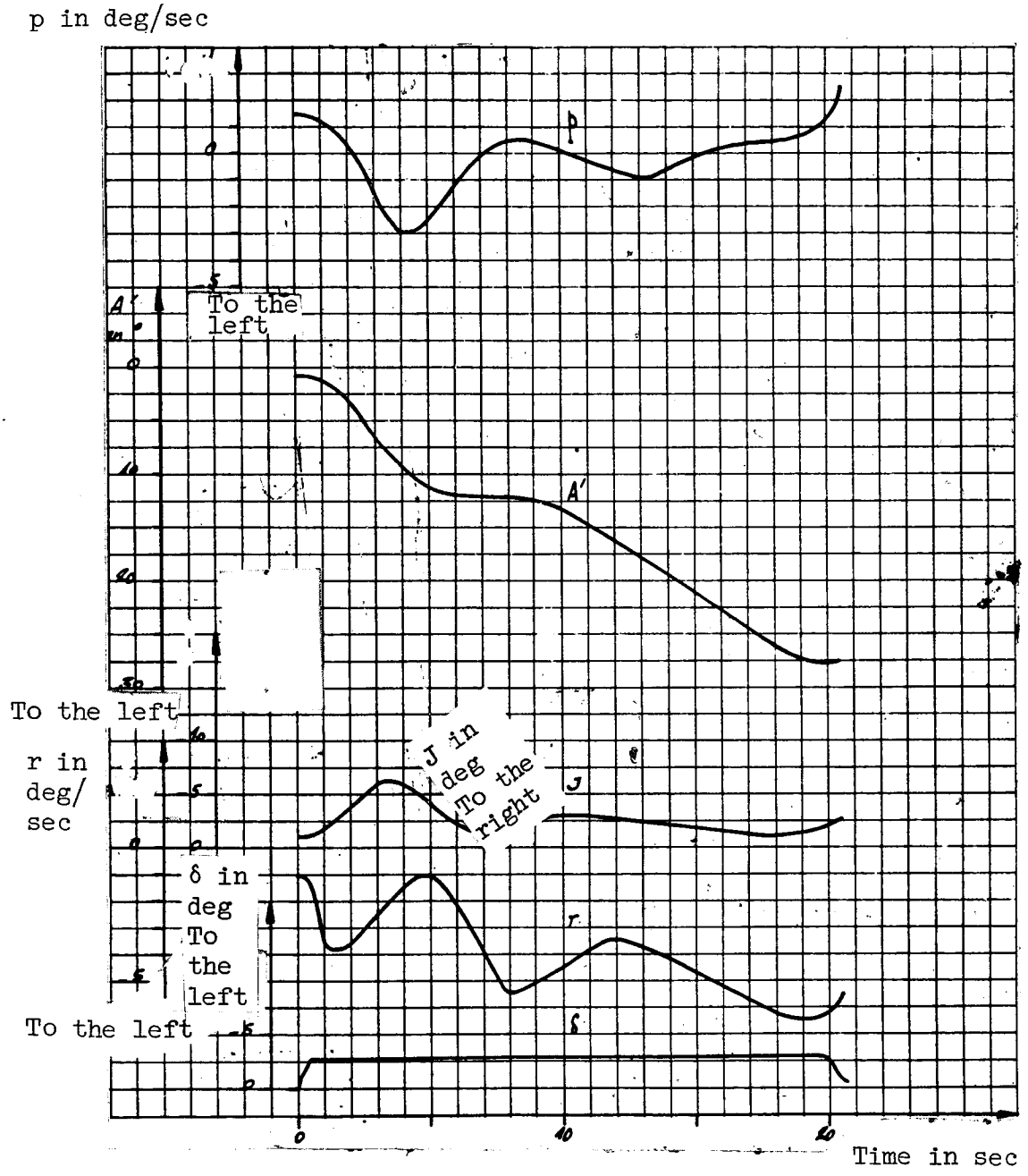

Figure 94. Rudder response to the left. δ square steps. Ascension configuration.

(Flaps at 30°; N_G 96%.)

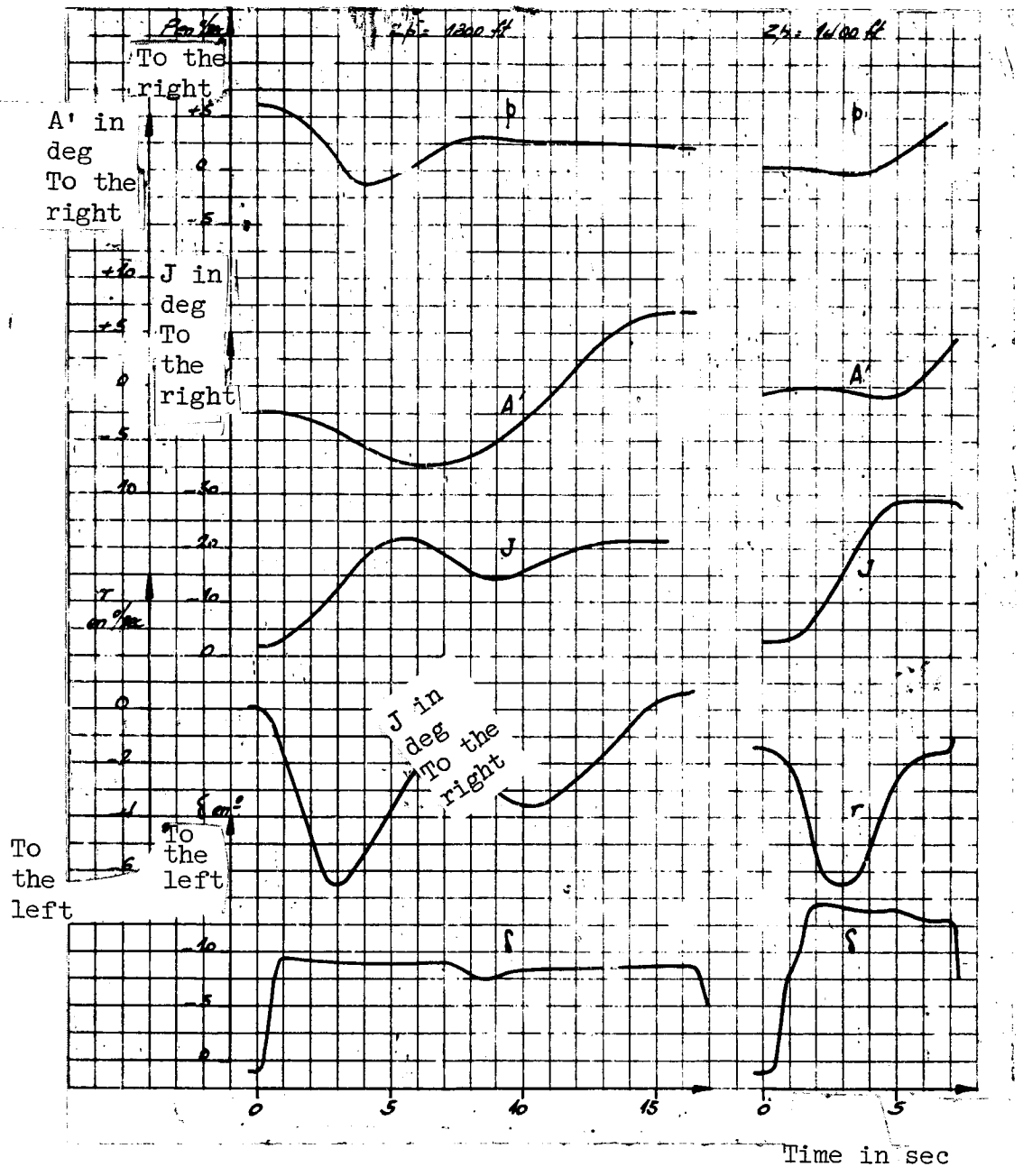

Figure 95. Rudder response. Steps to the left. Strong blowing. Landing configuration.

(Flaps at 97°; N_G 90%; Vc 55 kt.)

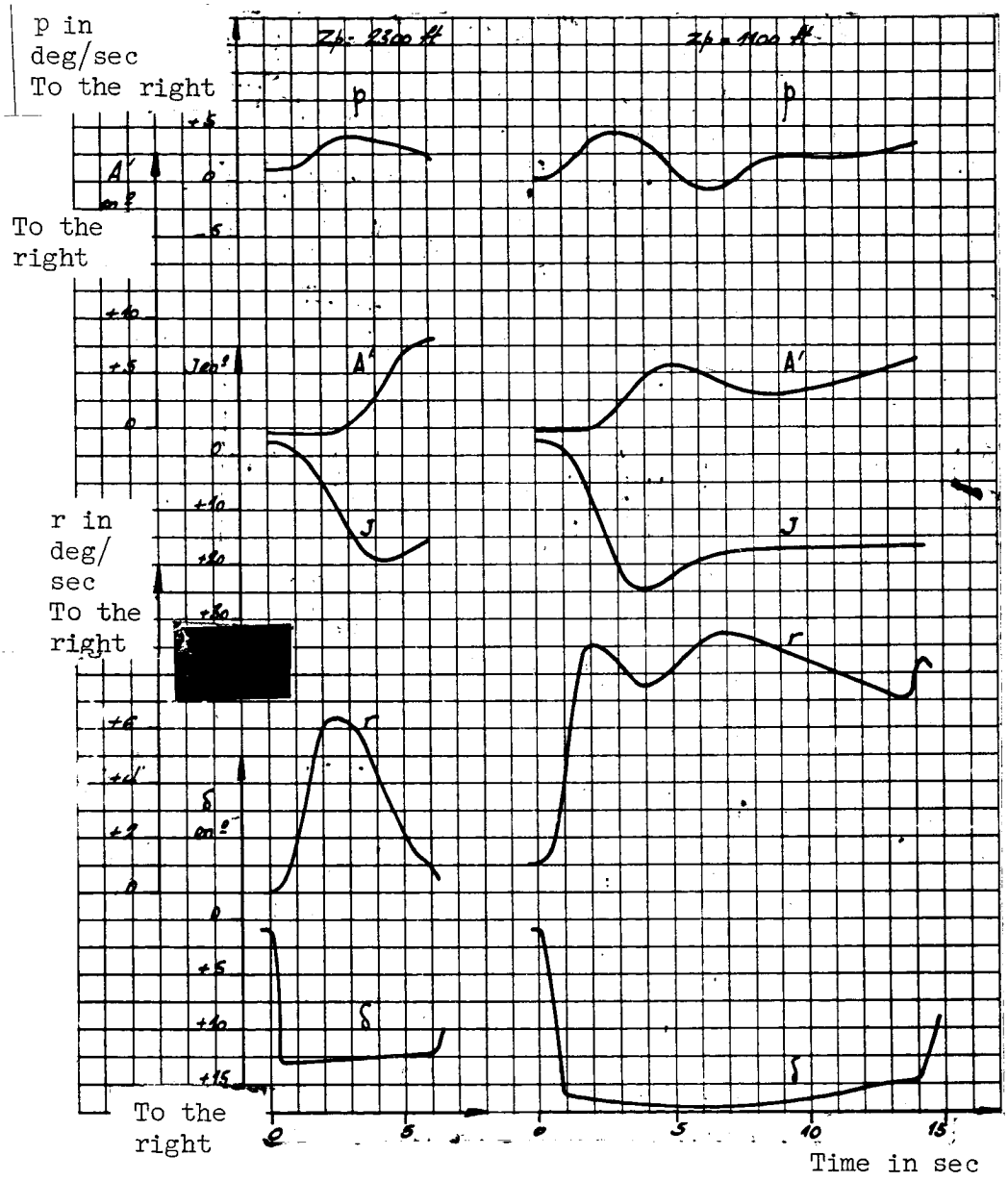

Figure 96. Rudder response. Steps to the right. Strong blowing. Landing configuration.

(Flaps at 97°; N_G 90%; Vc 55 kt.)

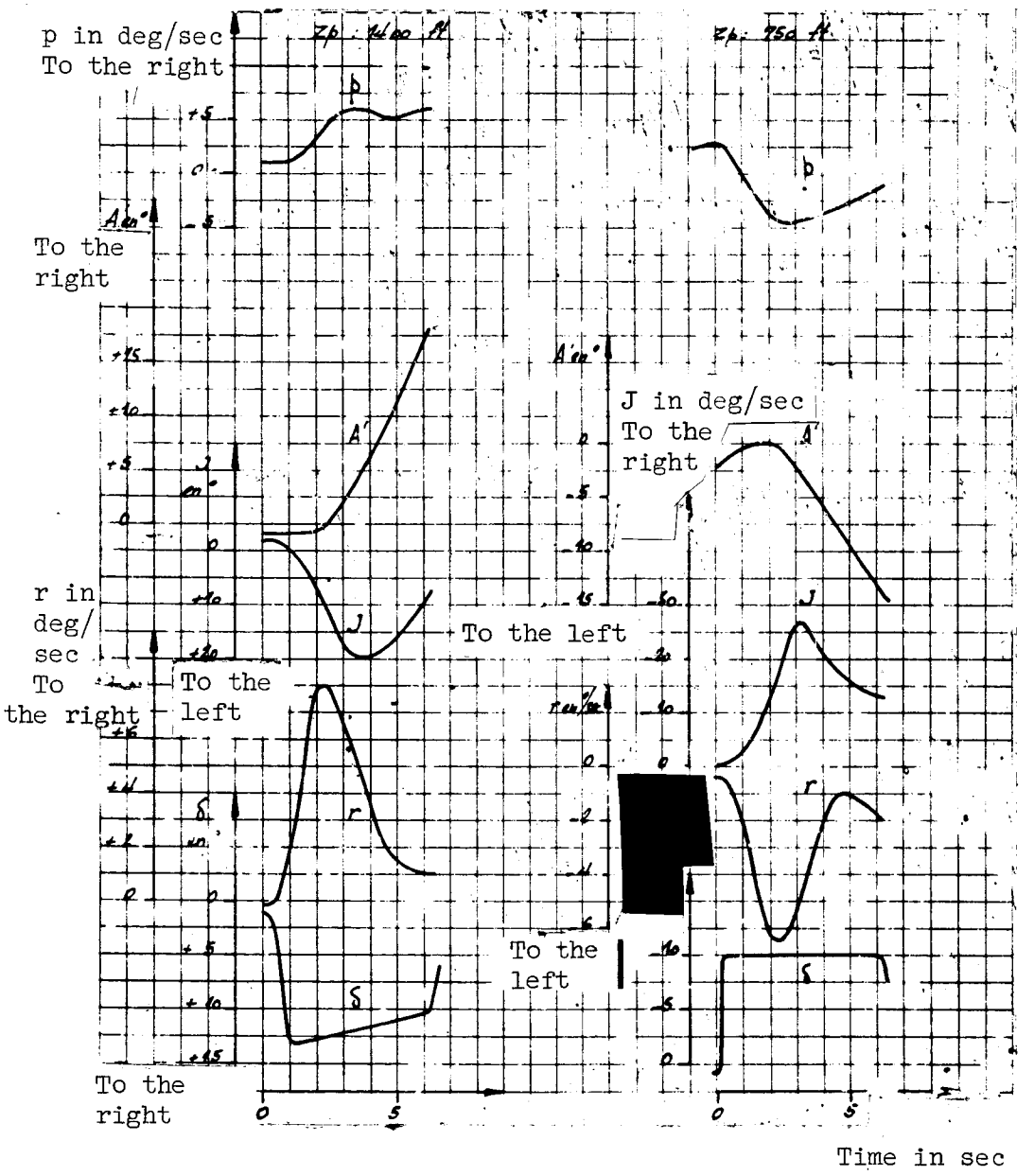

Figure 97. Rudder response. Both steps. Weak blowing. Landing configuration.

(Flaps at 97°; N_G 83%; Vc: 58 kt.)

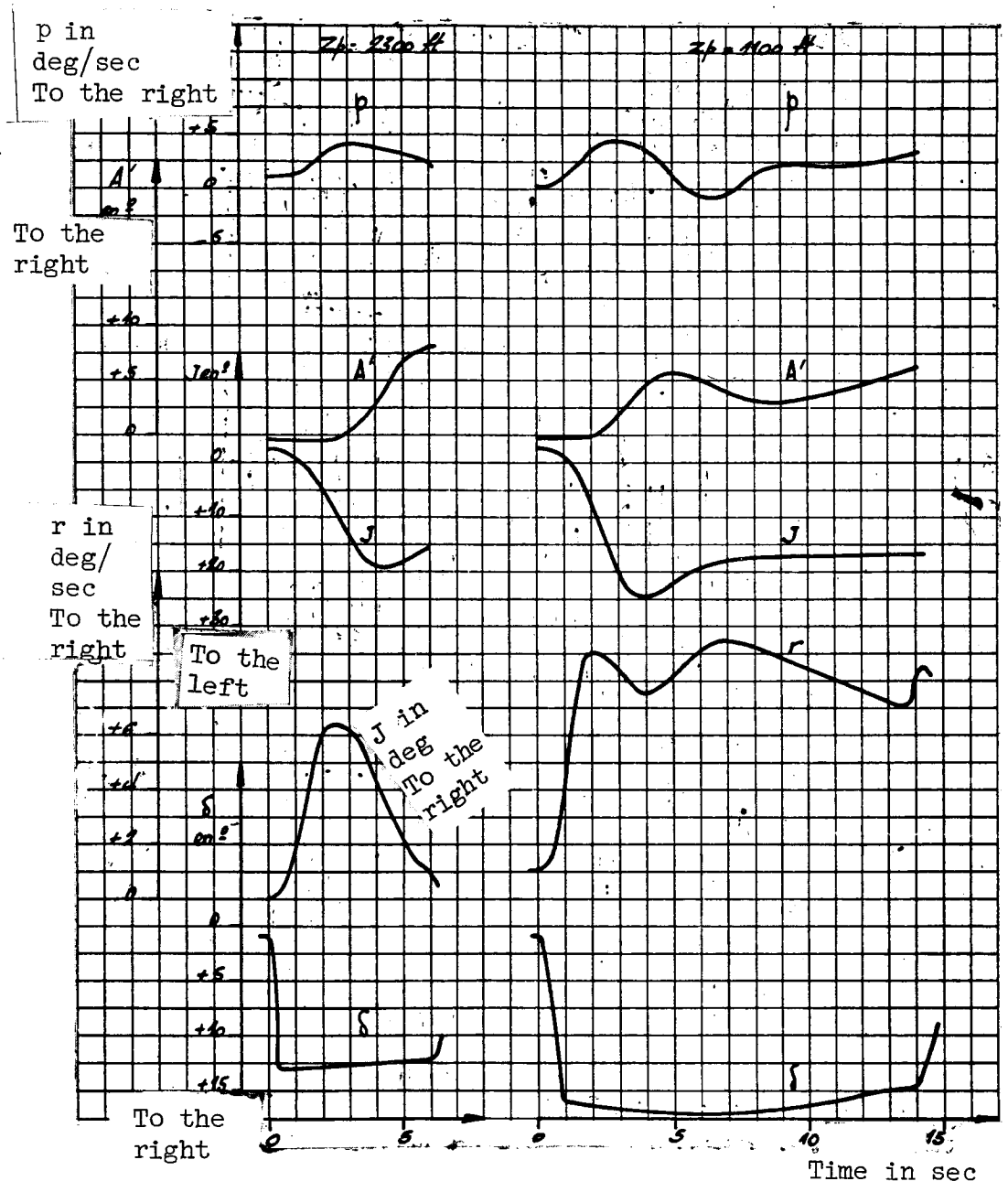

Figure 96. Rudder response. Steps to the right. Strong blowing. Landing configuration.

(Flaps at 97°; N_G 90%; Vc 55 kt.)

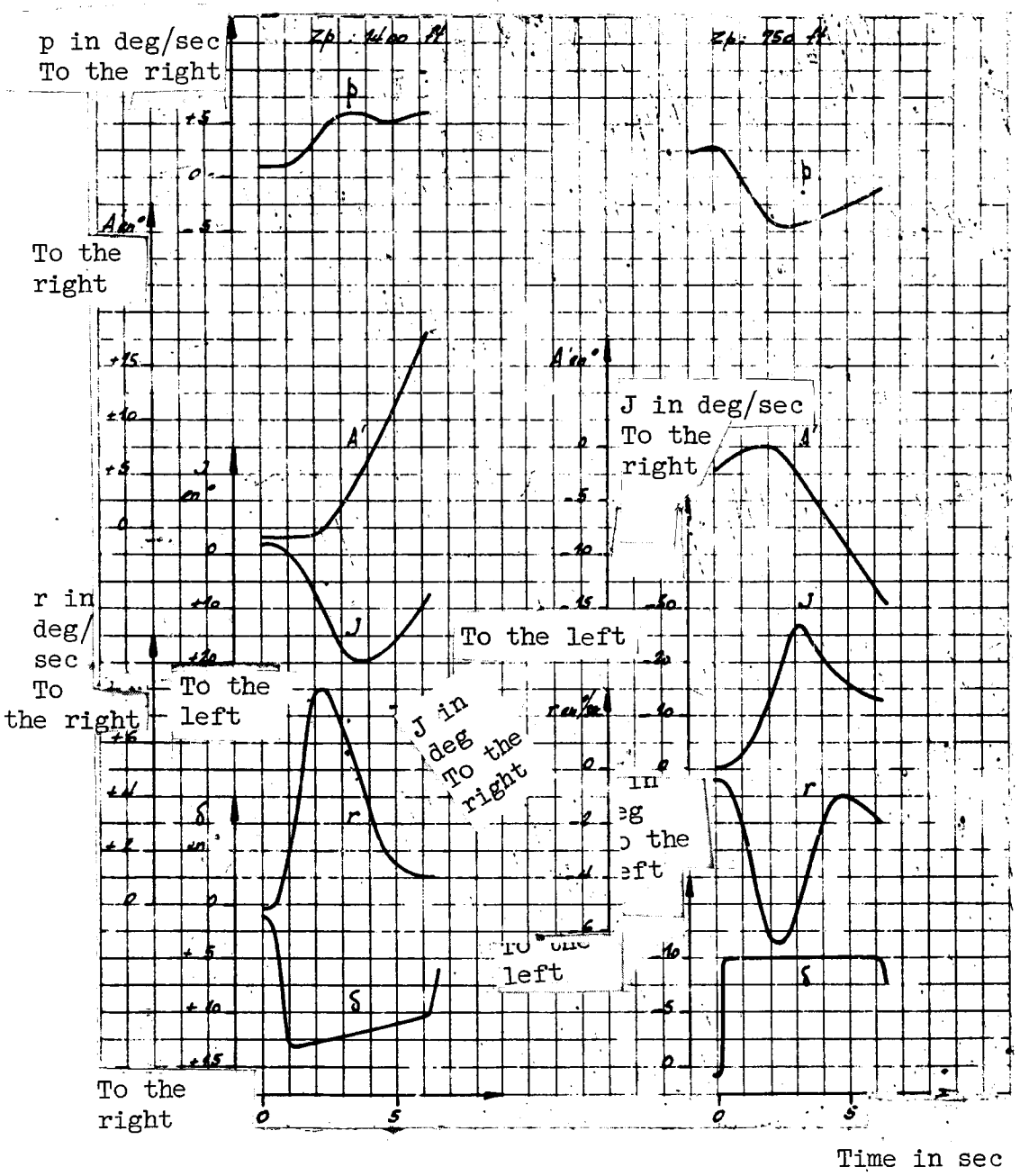

Figure 97. Rudder response. Both steps. Weak blowing. Landing configuration.

(Flaps at 97°; N_G 83%; Vc: 58 kt.)

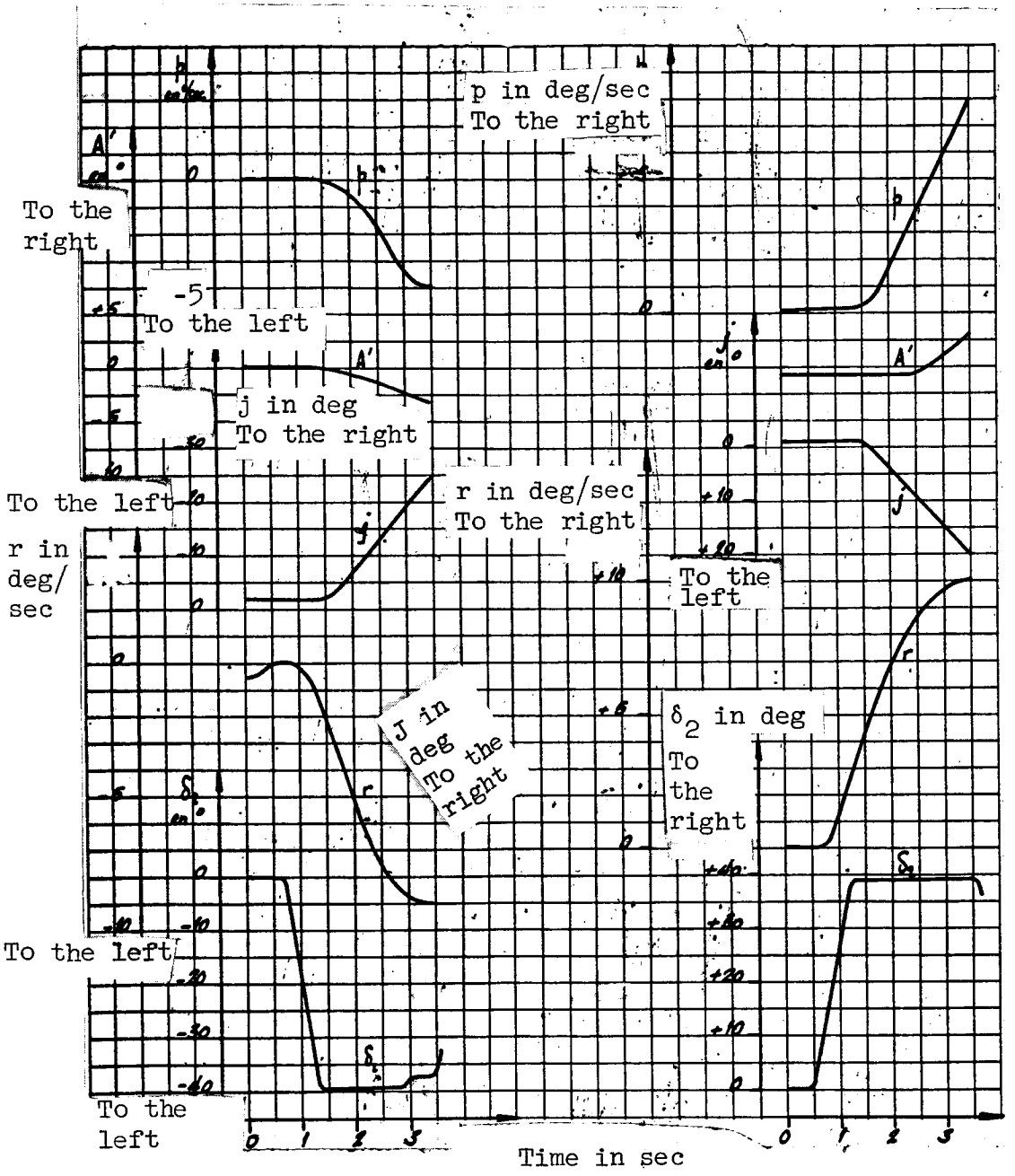

Figure 98. Rudder response. With differential. δ_2 square steps. Landing configuration. Main flap free.

(Flaps at 97°; Zp: 1900 ft; N = 89%; Vc = 59 kt.)

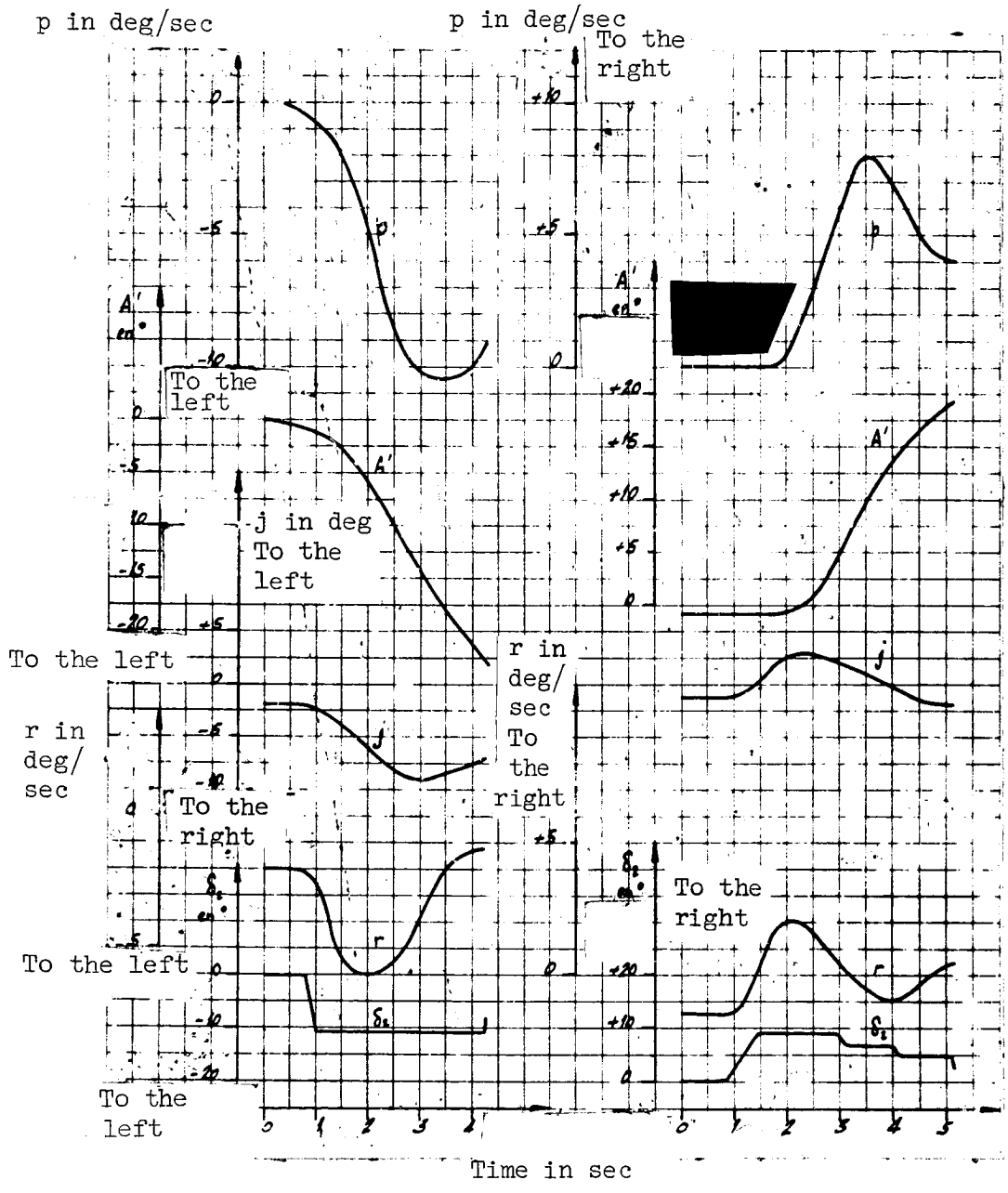

Figure 93. Rudder response. δ_2 square steps. With differential. Smooth configuration.

(Fixed δ_1; Zp = 2900 ft; N = 94.3%; Vc = 142 kt.)

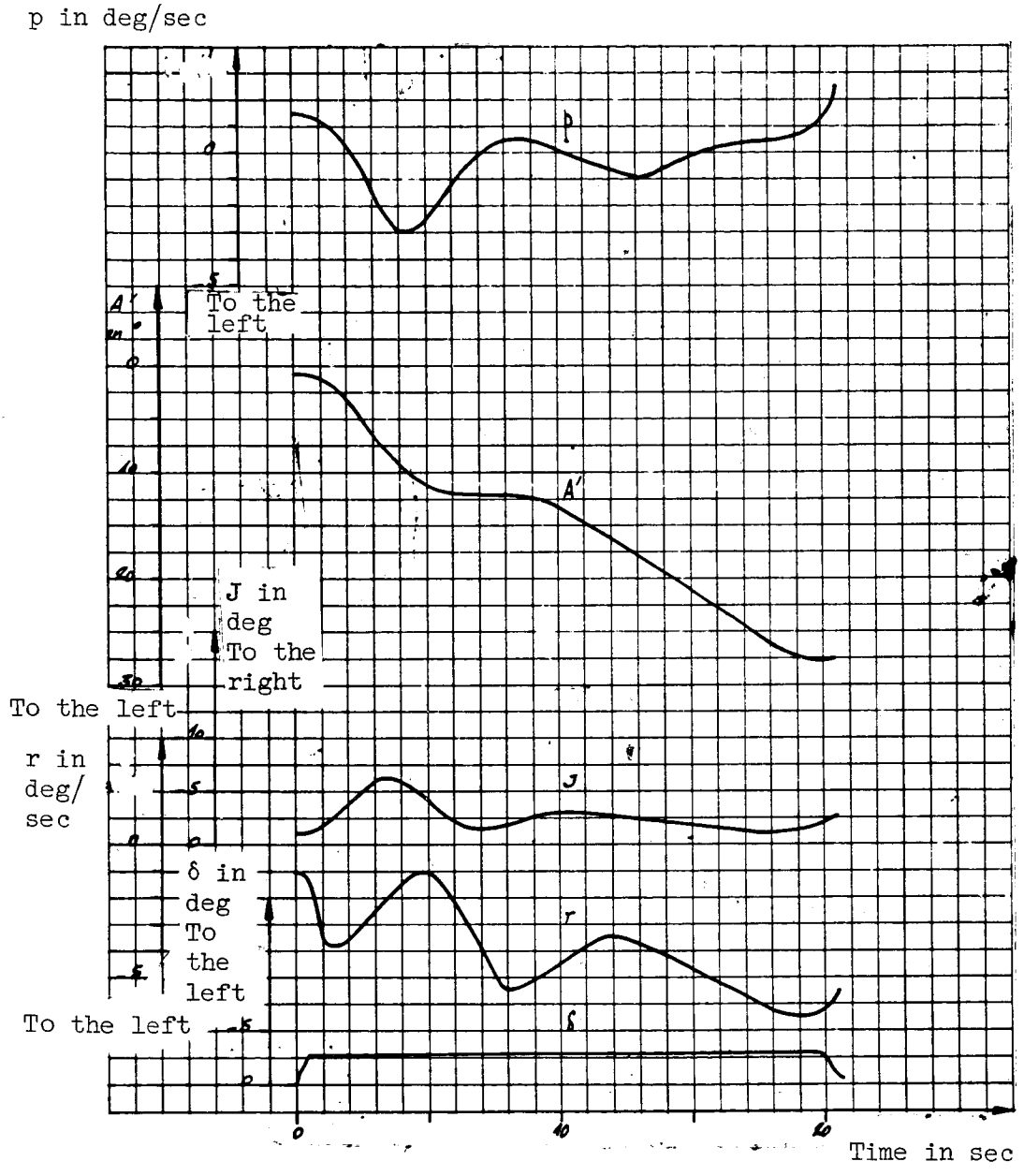

Figure 94. Rudder response to the left. δ square steps. Ascension configuration.

(Flaps at 30°; N_G 96%.)

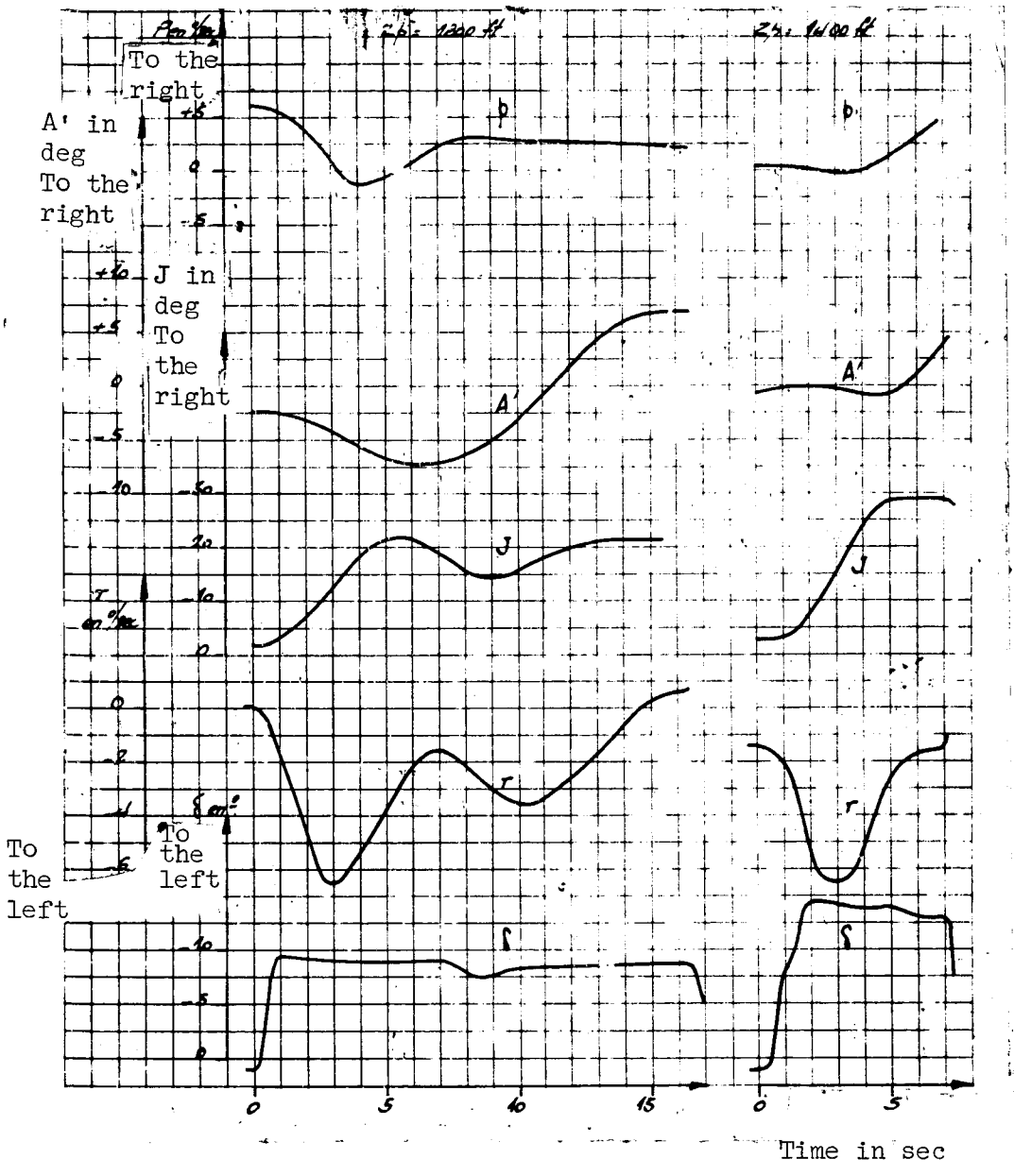

Figure 95. Rudder response. Steps to the left. Strong blowing. Landing configuration.

(Flaps at 97°; N_G 90%; Vc 55 kt.)

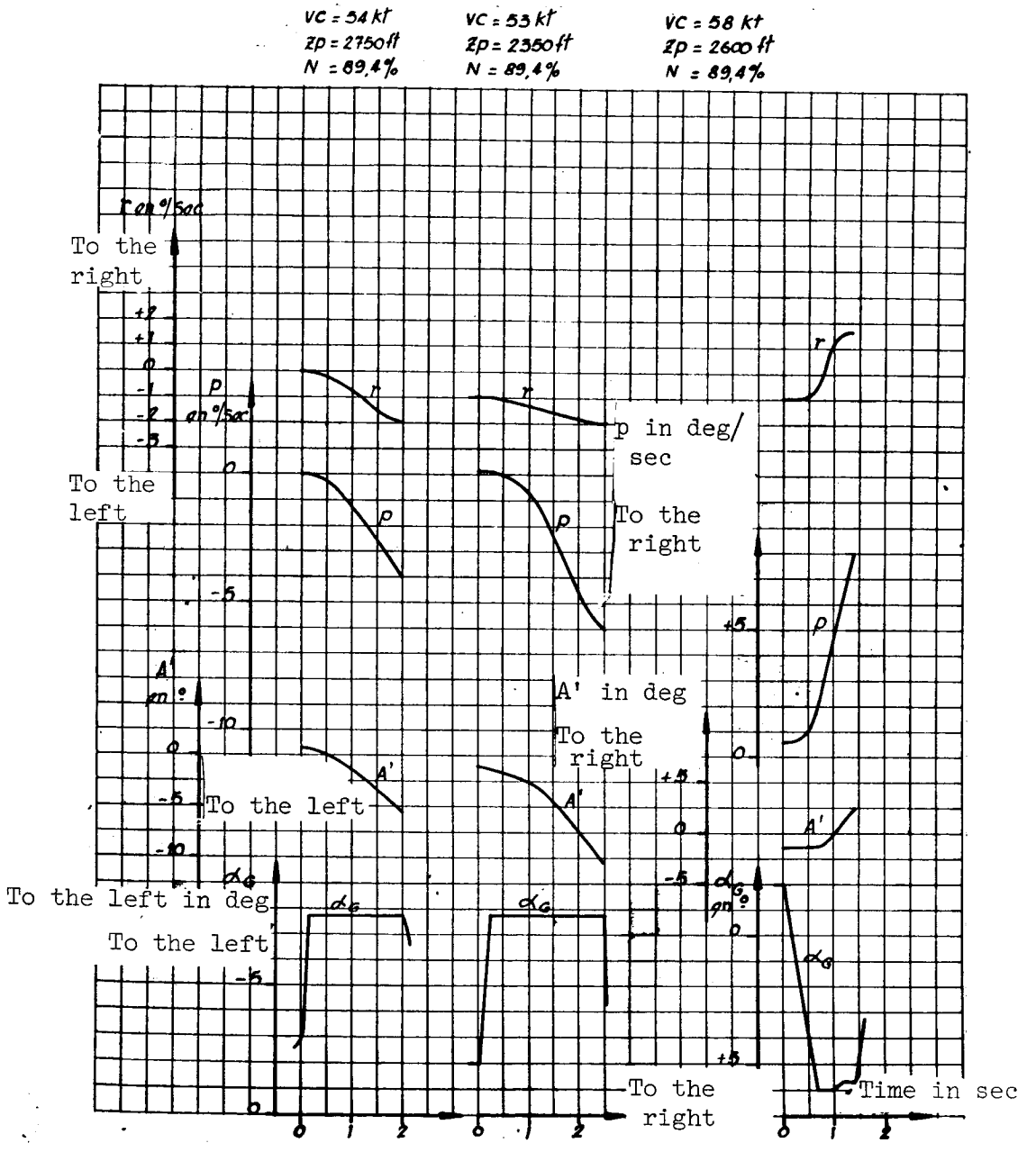

Figure 89. Warping response. Landing without spoilers [redacted]

(Flaps at 97°)

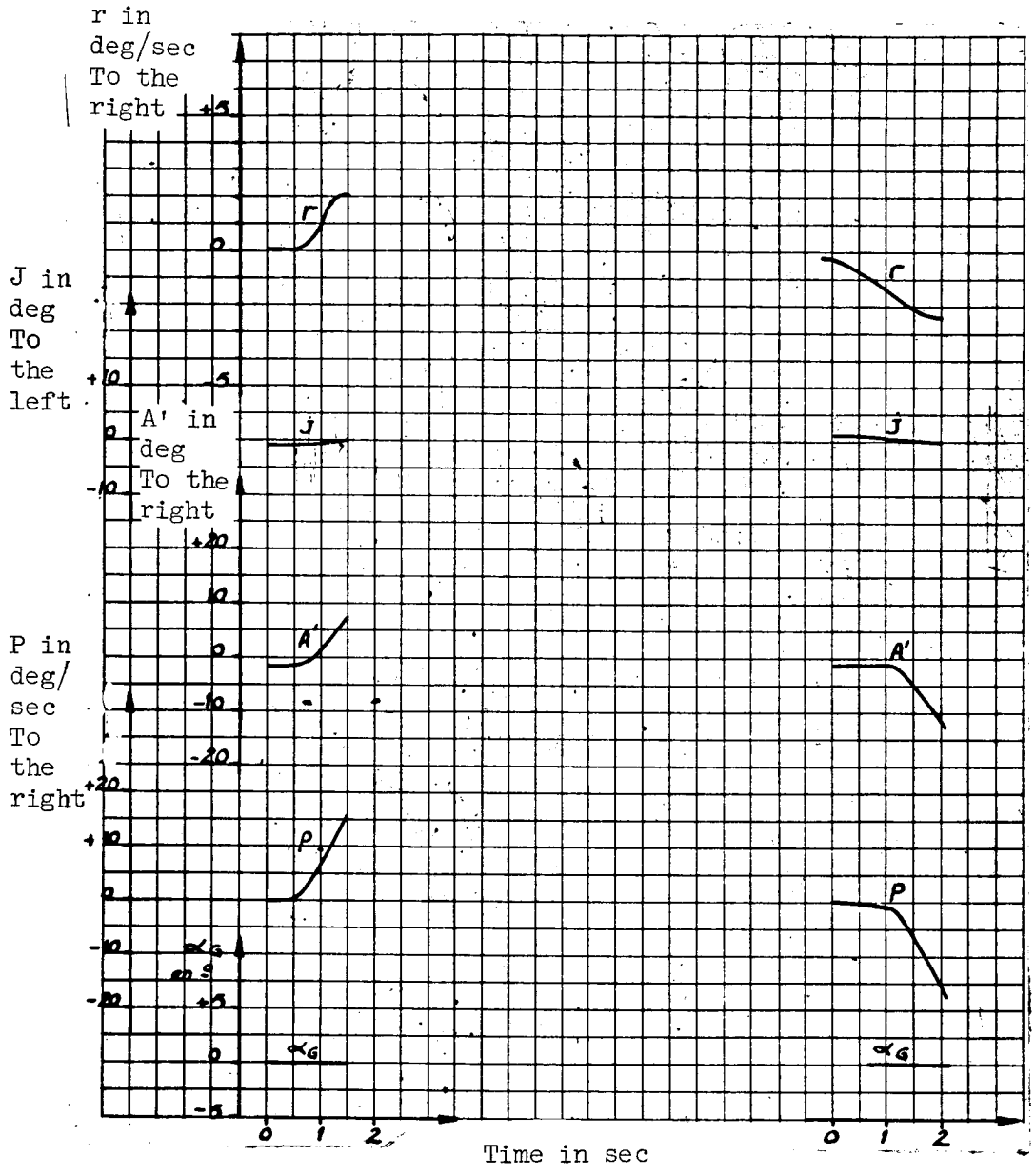

Figure 90. Warping response. Landing with fixed ailerons configuration.

(Flaps at 97°)

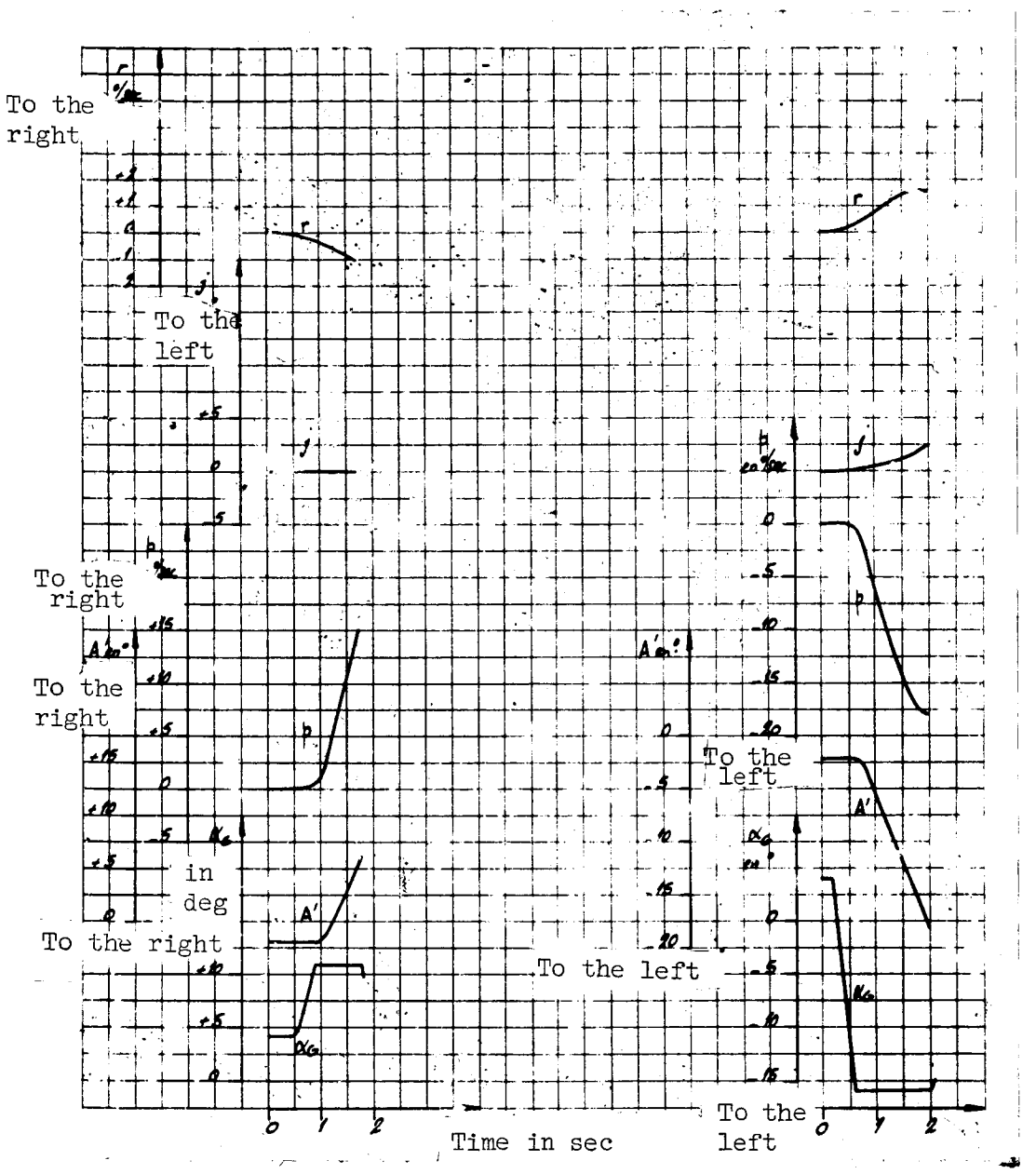

Figure 91. Warping response. Landing with no differential. α_G square steps.

(Flaps at 97°; Zp: 2200 ft; N = 89.9%; Vc = 62 kt.)

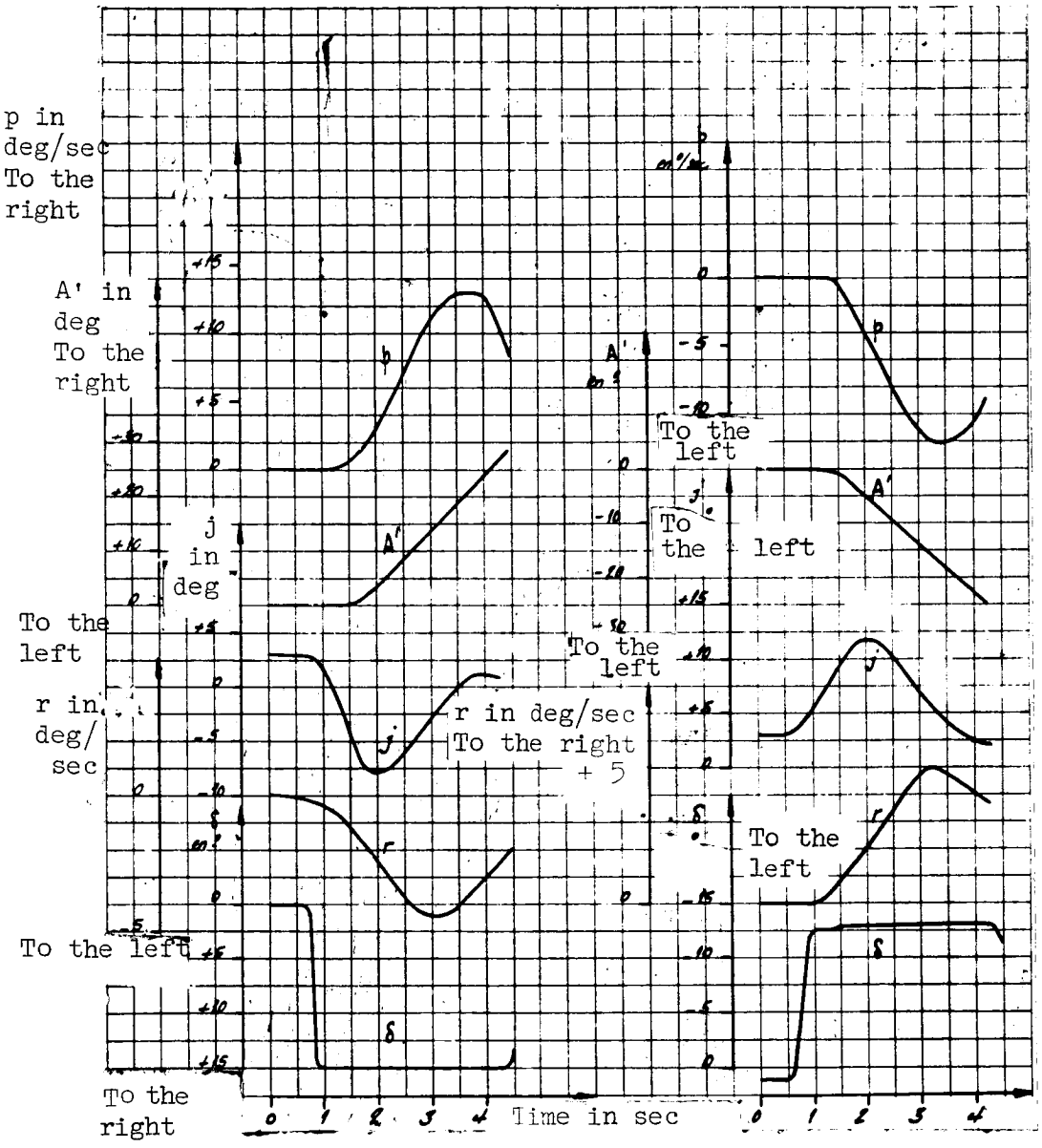

Figure 92. Rudder response. δ_2 square steps. Fixed main flap in smooth configuration.

(Zp = 6150 ft; N = 91.5%; Vc = 143 kt.)

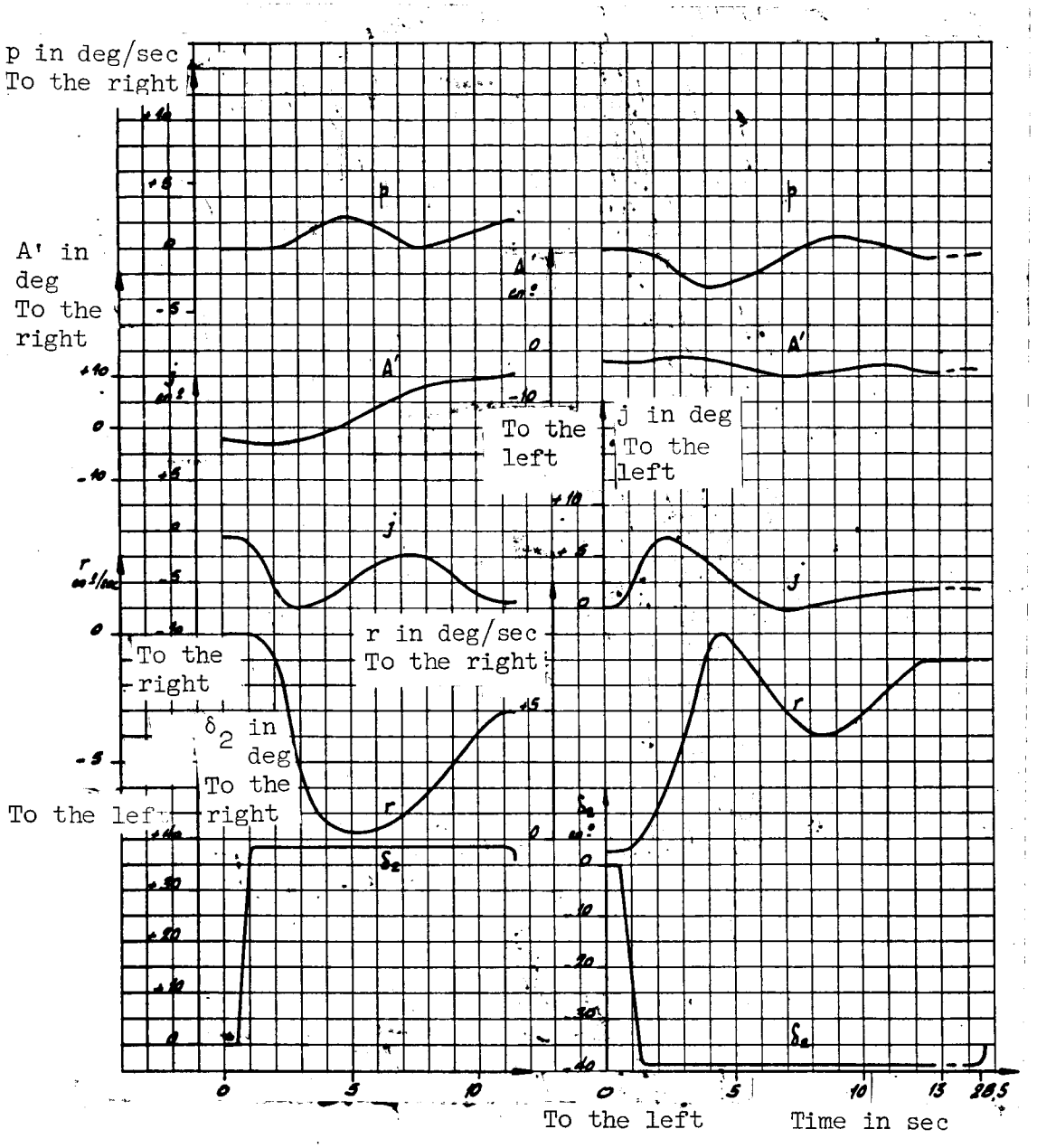

Figure 100. Rudder response. δ_2 square steps. Landing configuration.

(Fixed main δ; flaps at 97°; Zp = 3300 ft; N = 90.4%; Vc = 60 kt.)

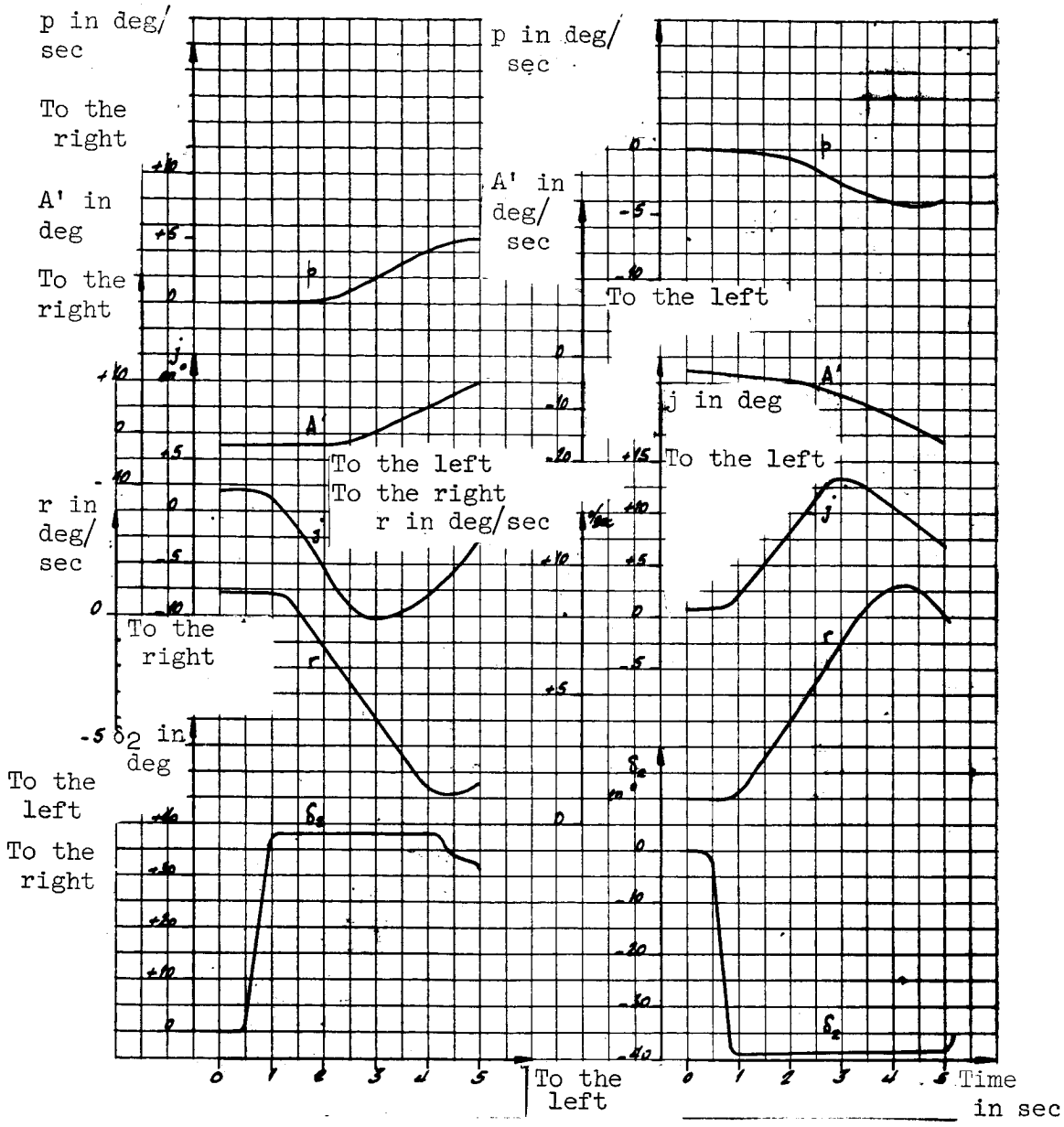

Figure 101. Rudder response. δ_2 square steps. Take-off configuration.

(Fixed main δ; flaps 45°; Zp = 4750; N = 80.9%; Vc = 70 kt.)

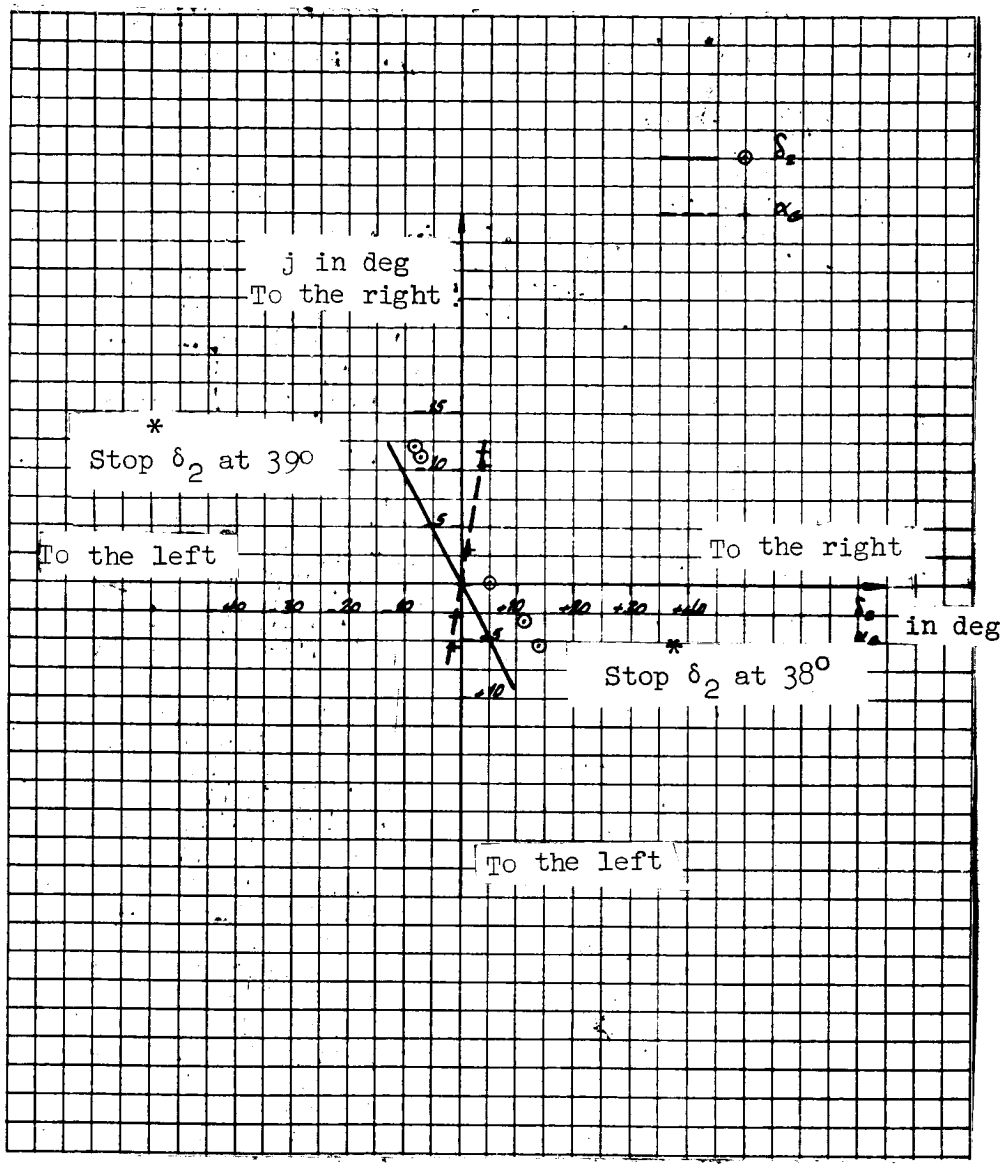

Figure 102. Controls homogeneity. Stabilized-skidded flight.. Smooth configuration.

Fixed main δ; Zp = 6500 ft; N = 90.7%; Vc = 143 kt.

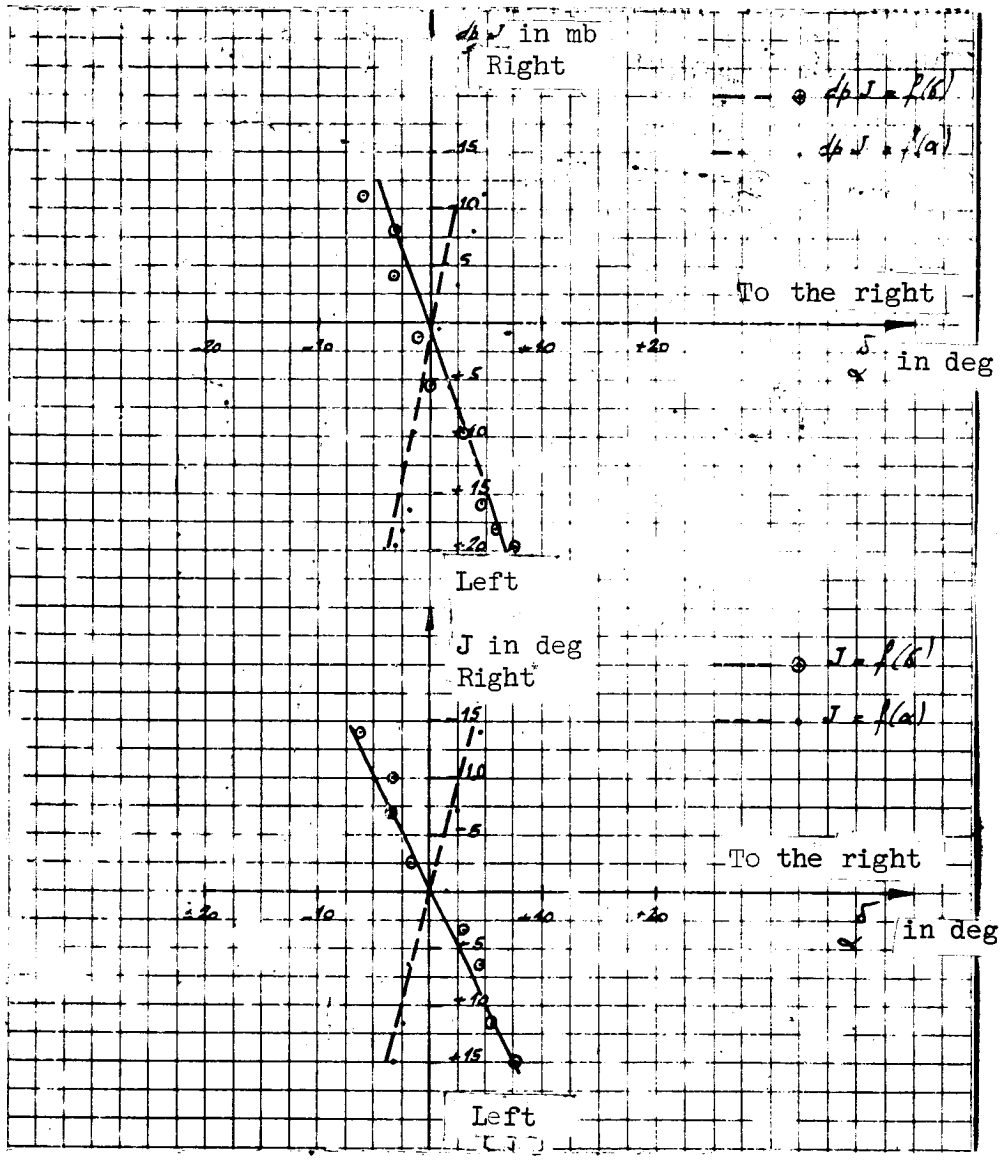

Figure 103. Lateral controls homogeneity. Stabilized-skidded flight. Ascension configuration.

Flaps 30°; N_G = 91.2%.

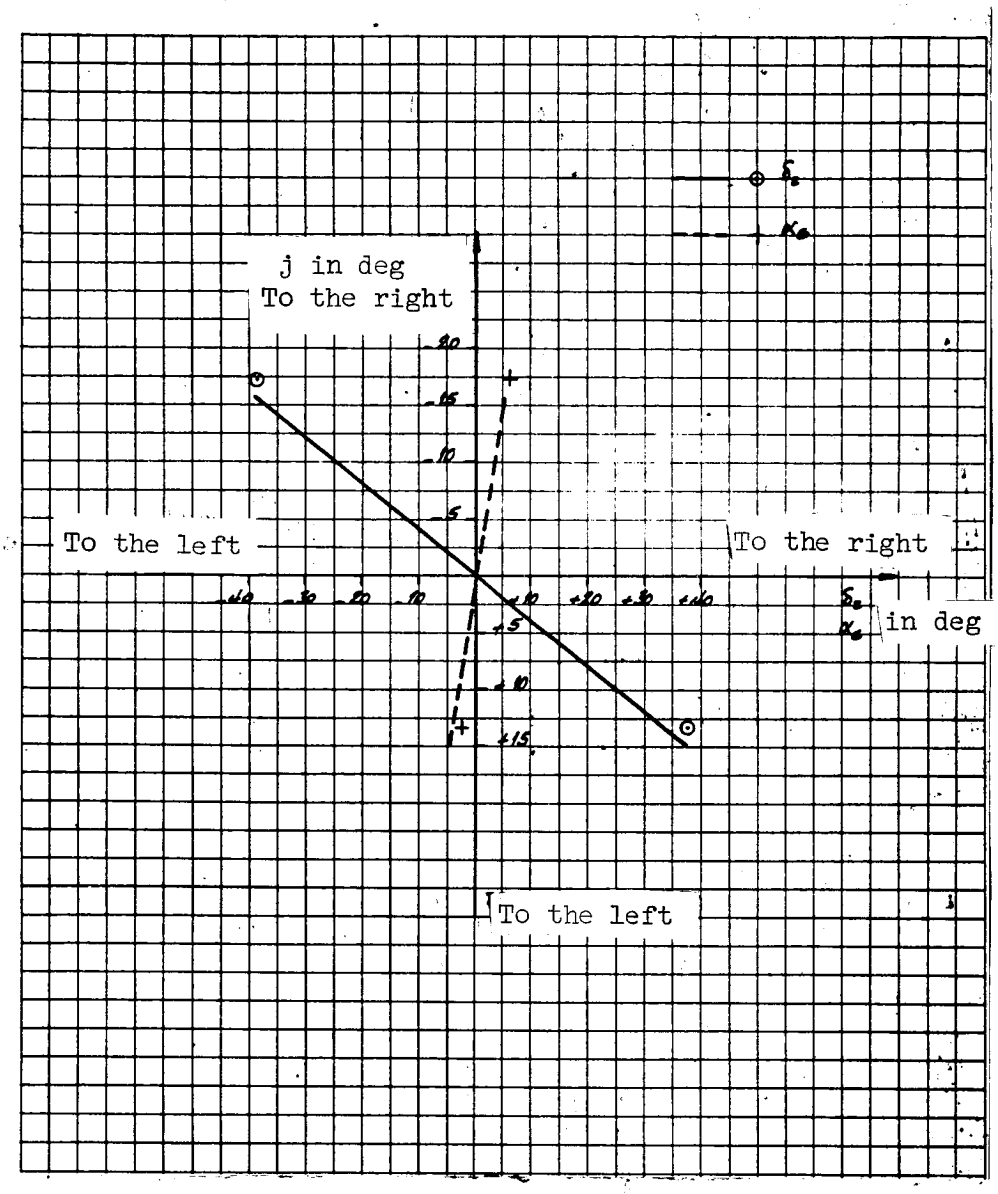

Figure 104. Controls homogeneity. Stabilized-skidded flight. Take-off configuration.

Fixed main δ; flaps 45°; Zp = 5150 ft; N = 80.9%; Vc = 74 kt.

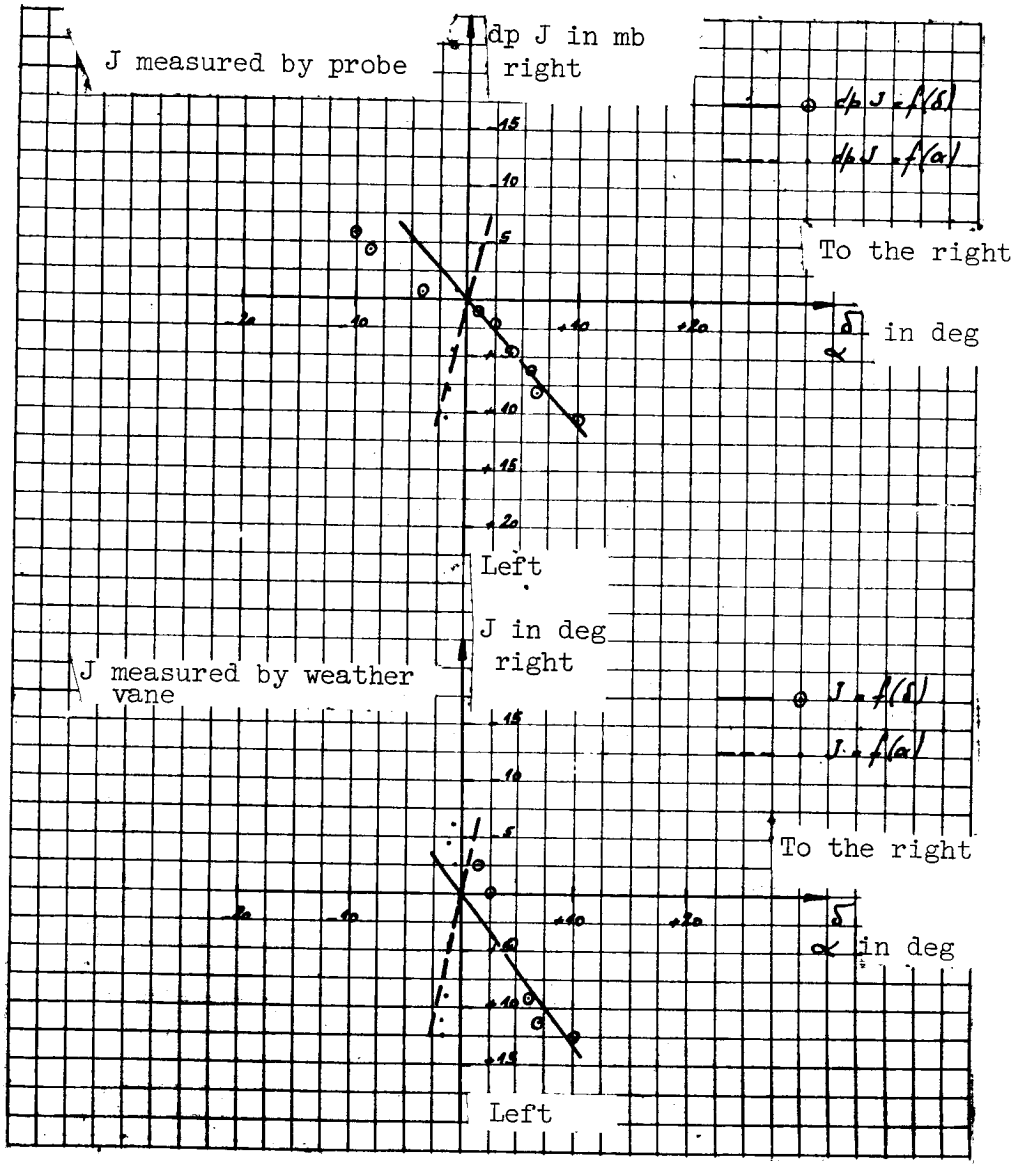

Figure 105. Lateral controls homogeneity. Stabilized-skidded flight. Landing configuration.

Flaps 98°; N_G = 88.9%.

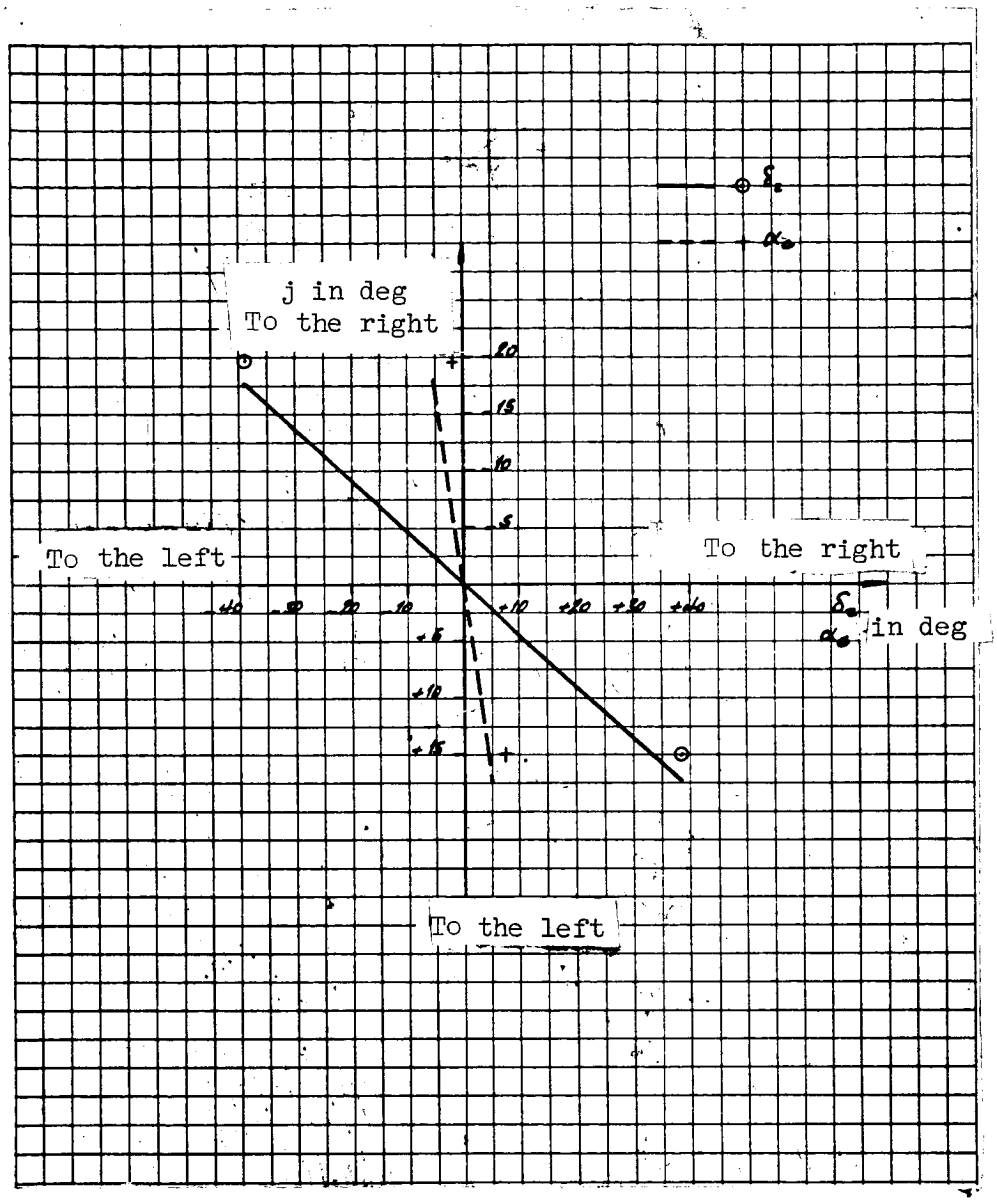

Figure 106. Controls homogeneity. Stabilized-skidded flight.

Fixed main δ; landing gear recessed; flaps 97° Zp = 4350 ft; N = 90.4%; Vc = 60 kt.

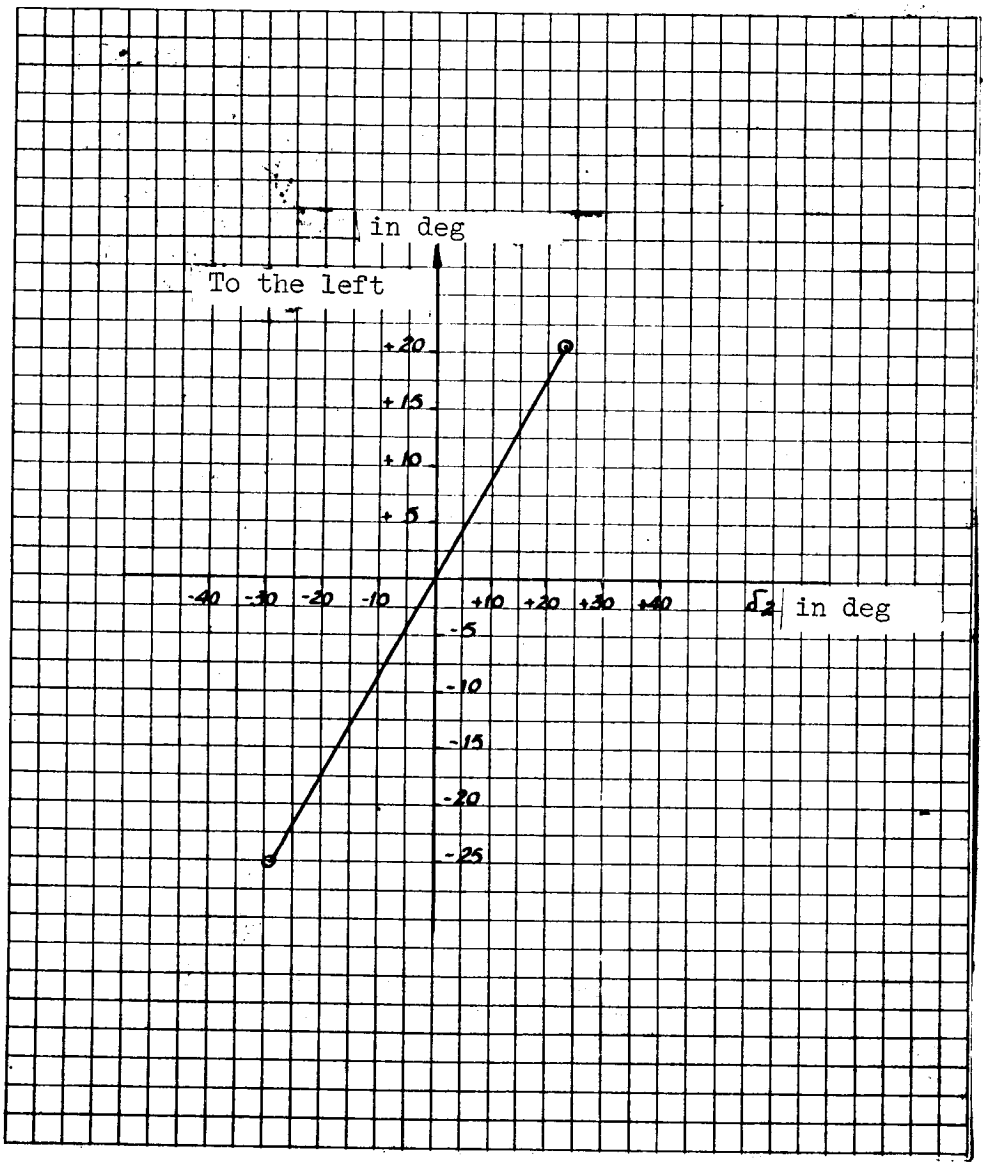

Figure 107. Lateral controls homogeneity. Stabilized-skidded flight. Landing configuration with fixed ailerons.

Flaps 98°; N_G = 90%.

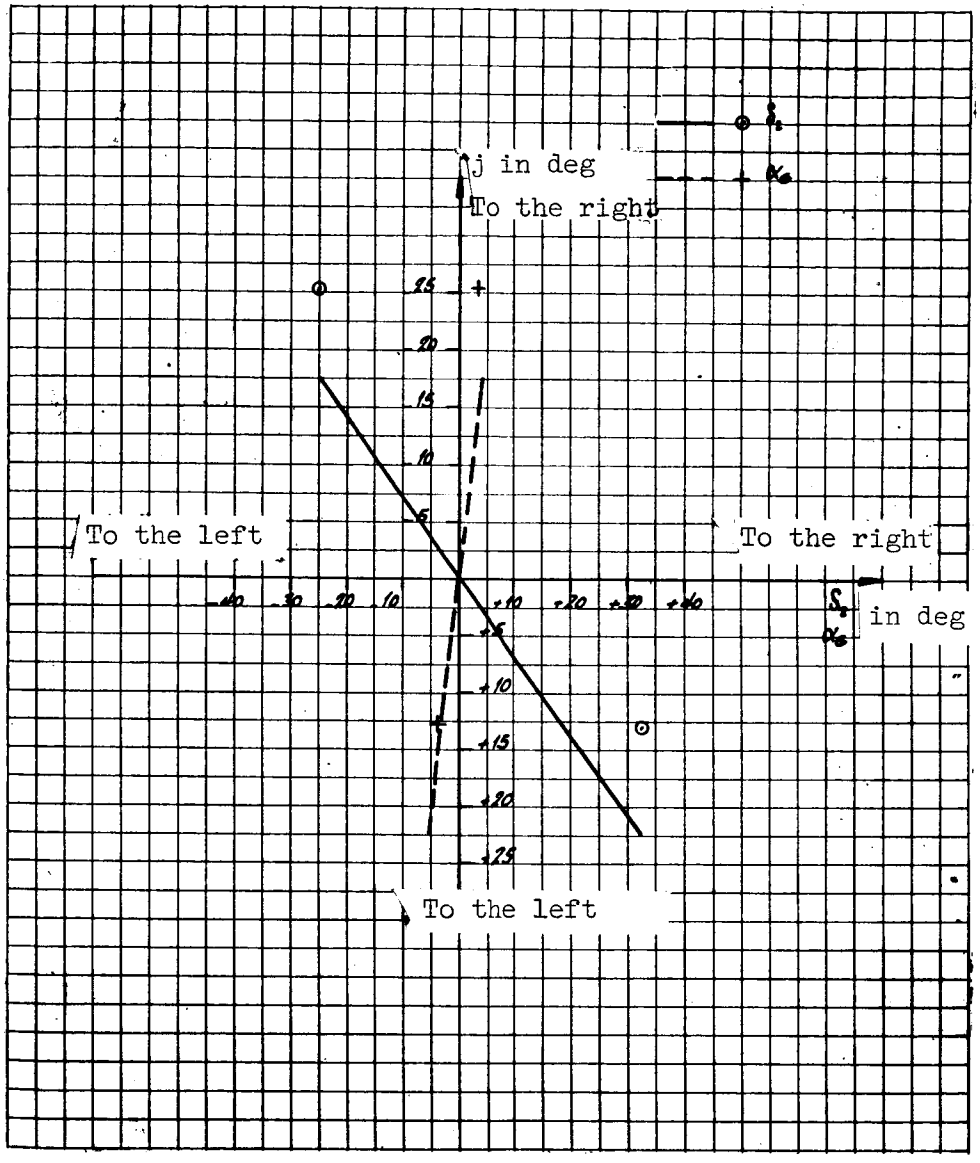

Figure 108. Controls homogeneity. Landing configuration. Rudder differential.

Flaps: 97°; Zp = 1150 ft; N = 91.6%; Vc = 60 kt.

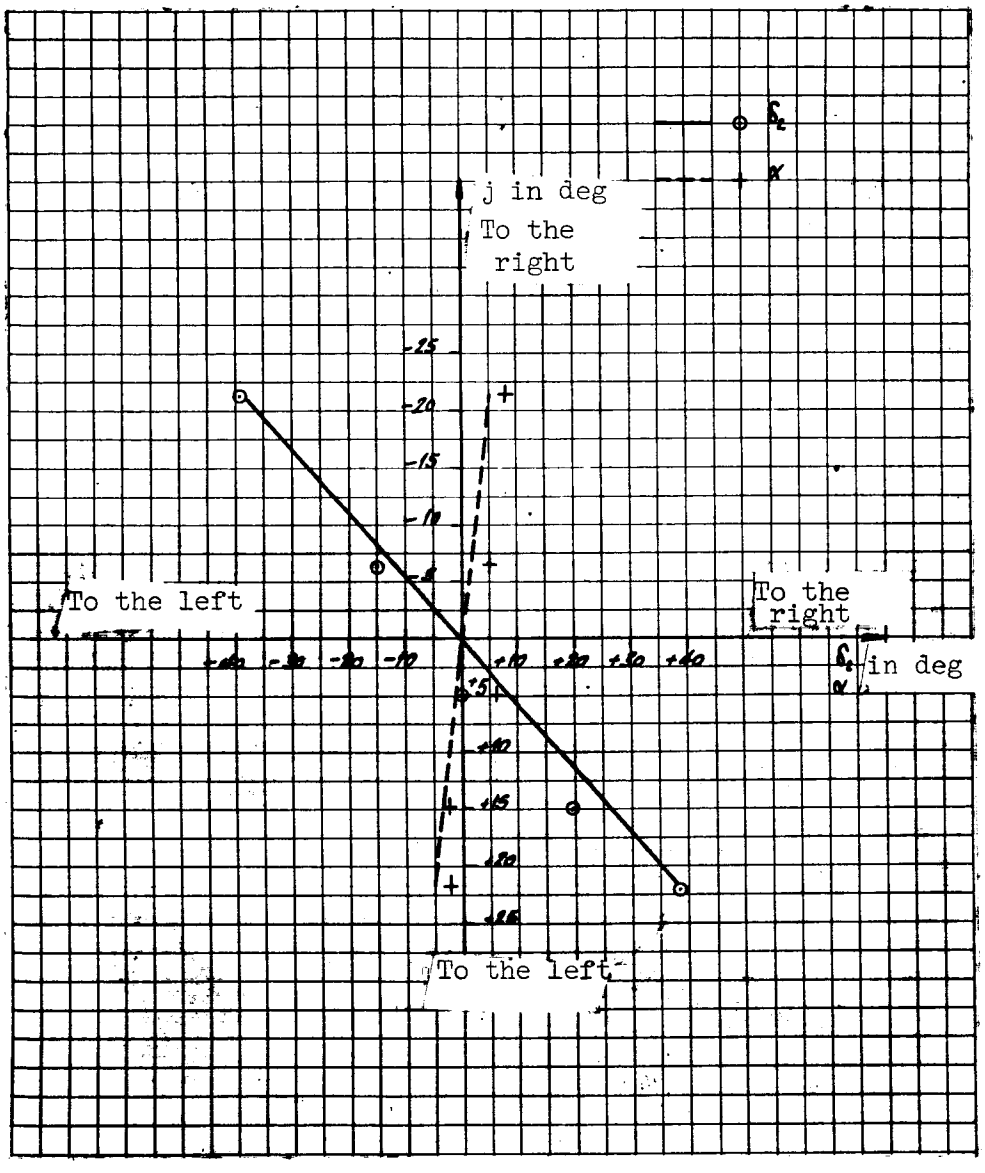

Figure 109. Controls homogeneity. Landing configuration. Rudder differential.

Fixed δ_1; flaps: 97°; N_G = 90%.

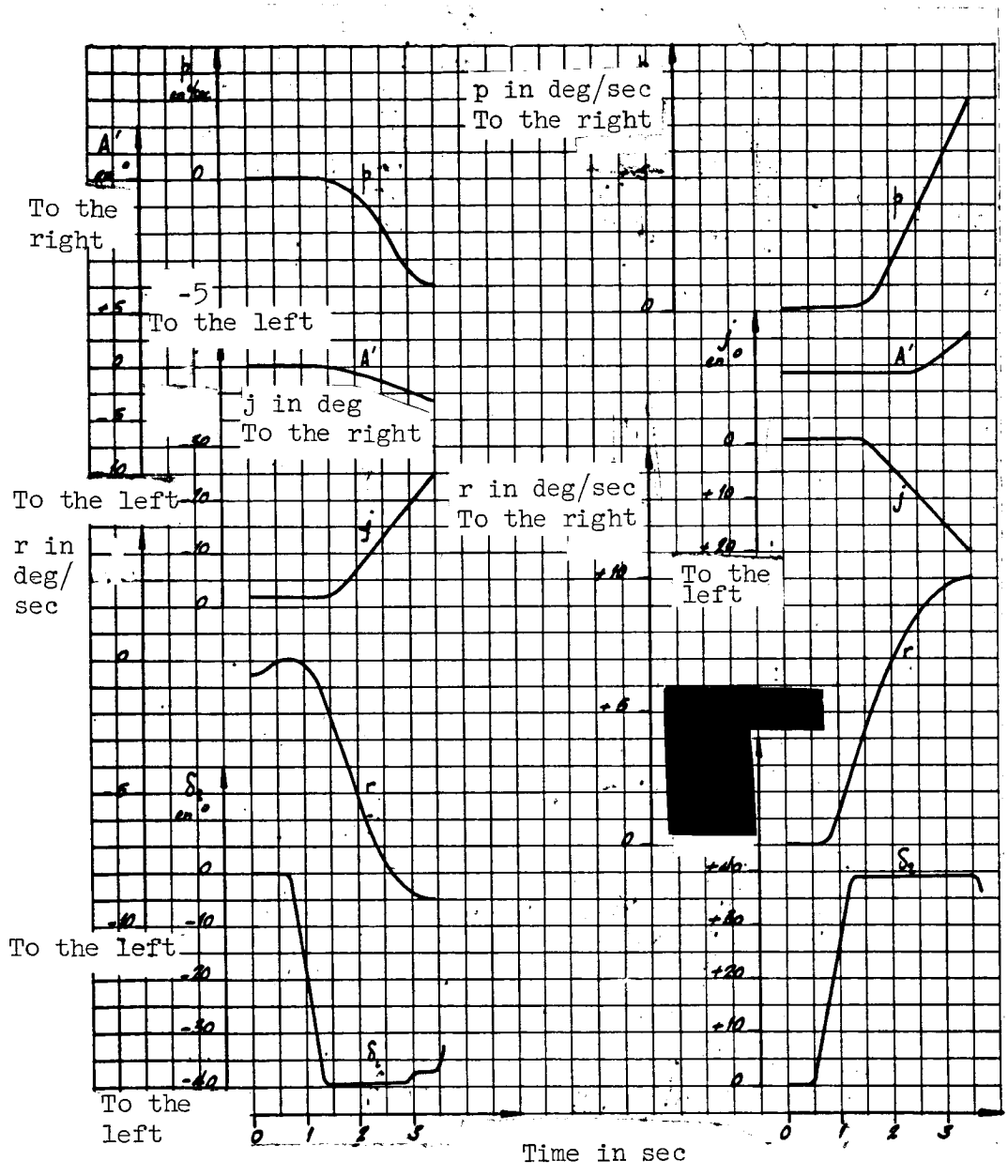

Figure 98. Rudder response. With differential. δ_2 square steps. Landing configuration. Main flap free.

(Flaps at 97°; Zp: 1900 ft; N = 89%; Vc = 59 kt.)

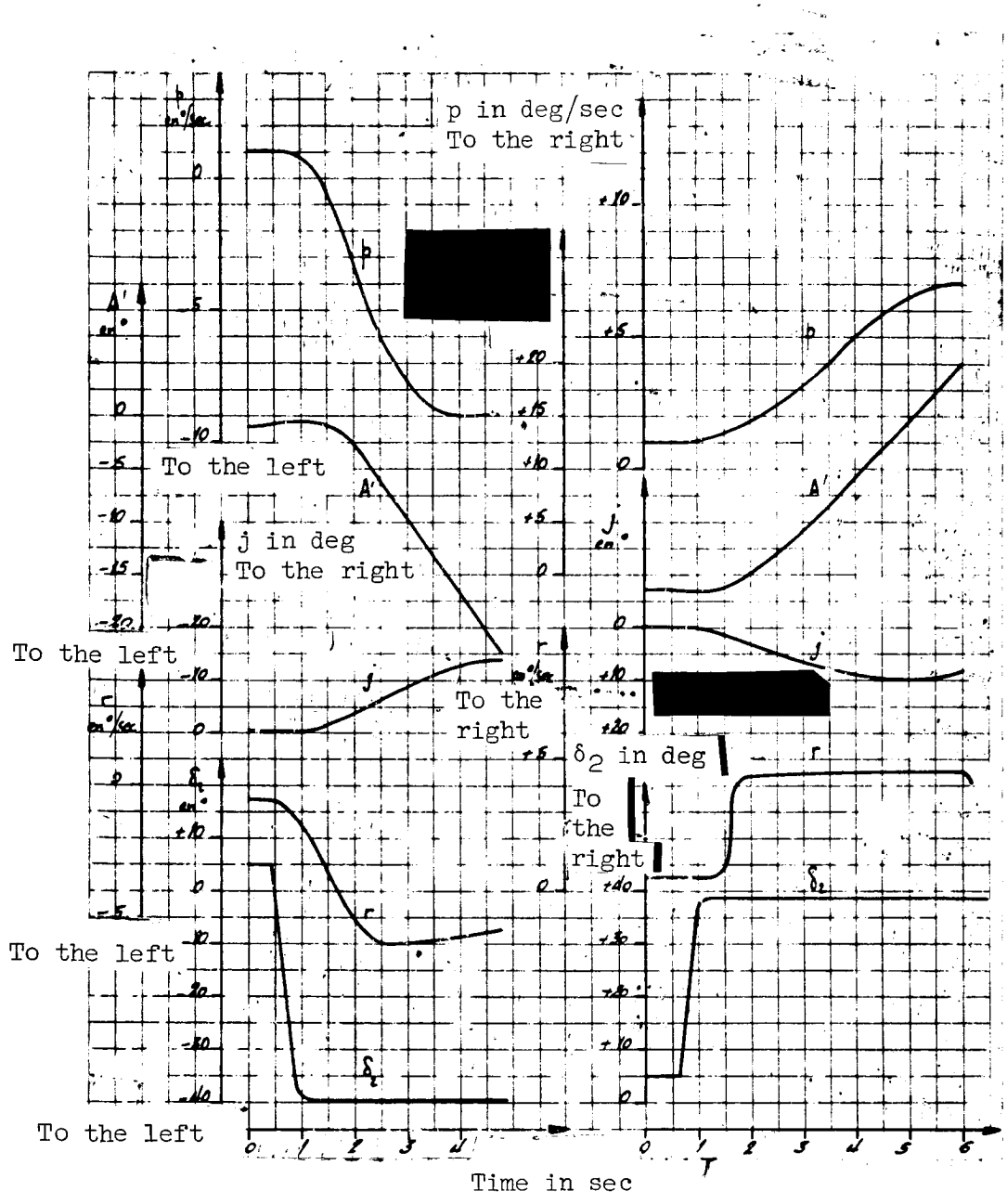

Figure 99. Rudder response. With differential. δ_2 square steps. Landing configuration.

(Fixed δ_1; flaps at 97°; Zp 1900 ft; N = 89.6%; Vc = 59 kt.)